A Thesis

Entitled

The Effects of Polyelectrolytic Agents on the Viability, Phenotype, and Mineralization of Osteoblast-like Cells

By

Katherine L. Dziak

Submitted as partial fulfillment of the requirements for

The Master of Science in Bioengineering

_____
Advisor: Ozan Akkus, PhD

_____
Committee Member: Vijay Goel, PhD

_____
Committee Member: Ronald Fournier, PhD

_____
Committee Member: Cora Lind, PhD

_____
Graduate School

The University of Toledo

December 2005

An Abstract of

The Effects of Polyelectrolytic Agents on the Viability, Phenotype, and Mineralization of Osteoblast-like Cells

By

Katherine L. Dziak

Submitted as partial fulfillment of the requirements for

The Master of Science in Bioengineering

The University of Toledo

December 2005

Studies have shown that the mechanical properties of bone, as a composite material, depend on the mineralization, crystallinity, molecular structure, and arrangement of the mineral crystals with the collagen matrix. [1,2] Knowing that the strength of any composite material is intimately affected by the size and shape of reinforcing inclusions, it can be proposed that the material level mechanical function of bone tissue can be altered by modifying the size and/or

shape of carbonated hydroxyapatite crystals. [3,4] Polyelectrolytes (negatively and positively charged macromolecules) have been shown to alter the nucleation, growth, and the resulting morphology of mineral crystals in solution by limiting growth on specific crystal faces. [5-8] Some of these polyelectrolytes are in peptide form and possess biocompatible properties. *Therefore, polyelectrolytes carry the potential of being administered in vivo with the intention of modulating bone's mechnical function by way of tailoring crystal geometry and size.* This study assessed biocompatibility of polyelectrolytic agents on osteoblast-like cells as well as the capability of polyelectrolytic agents to alter crystal properties in bone nodules formed *in vitro*. It was hypothesized that collagen production would not be altered, but the viability and genetic expression will differ with polyelectrolyte treatment. Furthermore, it is hypothesized that the size and shape of crystals will also differ with polyelectrolyte treatment.

Primary bone marrow stromal cells were isolated from neonatal rat femurs and osteoblast-like phenotype was induced with 10 nM dexamethasone. The culture media was supplemented with 10 mM β-glycerol phosphate and 50μg/mL ascorbic acid to initiate mineralization. After subculturing and growing cells to confluence, cultures were grown for 21 days before the final evaluation. Osteoblast-like cells were treated with five types of polyelectrolytes (9 wells per treatment group): polystyrene sulfonate (PSS) (7.85μg/well/day), poly-L-glutamic acid (PLG) (101.39μg/well/day), poly-L-lysine (PLL) (1.71μg/well/day), and poly-L-aspartic acid (PLA) (0.183μg/well/day) and sodium citrate (SC) (5.5μg/well/day)

to alter the properties of mineral crystals. Control cultures (9 wells) were similarly induced for mineralization but were not treated with any polyelectrolyte. Non-mineralizing cell culture characteristics were evaluated using digital photography, Sircol Soluble Collagen Assay Kit, ALP Staining Kit, and RT-PCR. Mineral crystal characteristics were evaluated by Raman spectroscopy and x-ray diffraction (XRD). Vickers microhardness of the mineralized nodules was also assessed. General MANOVA was used to test for the significance of non-mineralizing data by comparing dosage, treatment, and time. Significant differences in non-mineralizing data and all mineralizing data were evaluated using one-way ANOVA and Tukey's *post hoc* test was used to test for the significance of the difference between treatment groups. Significance was set at $p<0.05$ and the borderline significance was set at $0.05<p<0.1$.

Genetic expression was not notably changed by any polyelectrolyte treatment. PLG, PLL, and SC generated significantly less collagen production per cell than control cultures. PSS treated cultures had low cell viability, substantially smaller nodules and the resulting crystals had extremely poor crystallinity, to an extent that no discernible XRD patterns were generated. The type-B carbonate content was elevated with the administration of PLA, PLL and PSS, indicating that these polyelectrolytes facilitated the substitution of carbonate ions in place of phosphate ions within the crystal lattice. XRD analysis revealed that PLA treated crystals were about 10% longer along the 002 plane. Microhardness of the

mineralized bone nodules was not significantly altered by any of the polyelectrolyte treatments.

The current study has demonstrated that while polyelectrolytes are biocompatible, administration at certain concentrations can affect the geometry and stoichiometry of mineral crystals grown under *in vitro* conditions. The effect varied between polyelectrolytes, with PSS treatment yielding the most amorphous crystal structure with higher carbonate substitution. PLL and PLG treatment caused higher carbonate substitutions within the mineral crystals, probably by facilitating the diffusion of carbonate ions in the vicinity of growing mineral crystals. Polyelectrolytes may affect the crystal growth directly by binding on crystal surfaces or indirectly by affecting cellular activity. The results of this preliminary study indicated that polyelectrolytes are biocompatible and can selectively alter carbonated hydroxyapatite crystal size, morphology, and stoichiometry *in vitro*.

Acknowledgements

This work was funded by NSF CAREER-0449188 and the University of Toledo's research action fund. I would like to thank Dr. Ozan Akkus, my family, friends, and co-workers for their continued generous assistance, support, insights, and patience. I would like to especially thank Dr. Akkus; through your guidance, focus, and knowledge, I have learned to be more critical of my own work and always be aware of the next steps. You have set an unmatched example on how to become a better researcher and scientist. Thanks also to my co-workers who were always there to provide insight and lend a helping hand or word of encouragement. Specifically to Nick Wasserman who initially wrote the Raman Spectral analysis software which I used in my data analysis and used as the basis for my custom written XRD pattern analysis software. Special thanks to Dr. Scott Molitor for providing specimen for cell harvesting, Dr. Douglas Leaman for assistance with RT-PCR, and Dr. Cora Lind who taught me everything I know about x-ray diffraction. I would also like to thank Shane Searles for his assistance in sample preparation. Dan, without you, I would not have pursued my Masters degree. Thank you for your understanding, support, and encouragement. To my family and friends, your confidence and encouragement helped me obtain this goal, thanks.

Table of Contents

List of Figures

List of Tables

Chapter 1: Introduction

1.1 Bone Anatomy and Physiology

Bone is the connective tissue that forms the major portion of the skeleton in vertebrates. It is a nanocomposite material that is dense, semirigid, porous, and calcified. There are two main types of bone, cancellous and cortical. Cancellous bone accounts for approximately 20% of the skeletal mass. [9] It forms a network of plates and rods termed trabecula that is located in the inner portion of the ends of the bone, epiphysis and metaphysis. Cortical bone, which is much denser than cancellous bone, accounts for the other 80% of the skeletal mass. [9] It is located as a thin layer on the epiphysis and metaphysis and is the principle component of the shaft (aka diaphysis) of the long bones. It functions to support and protect the skeleton. Surrounding the cortical bone is a layer of fibrous connective tissue and an inner cellular or cambium layer of undifferentiated cells, the periosteum. Within the diaphysis is located a marrow cavity, which is lined by a thin layer of cells termed the endosteum.

Bone is composed of primarily extracellular matrix (ECM). The ECM is approximately 65% mineral crystal and 35% organic material with a small amount of cells and water. [9] The mineral crystals are primarily hydroxyapatite, $Ca_{10}(PO_4)_6(OH)_2$, which can contain impurities of sodium, magnesium, and

strontium for the calcium, carbonate for the phosphate, and fluoride and chloride for the hydroxyl. [9,10] It was found that newly formed mineral has a low Ca/P ratio with low carbonate impurities; whereas, mature mineral has a Ca/P ratio of about 1.66 with increased carbonate impurities. [10] The organic matrix is 90% collagen and 10% various non-collagenous proteins, which include osteocalcin, alkaline phosphatase, osteonectin, osteopontin, and bone sialoprotein. [9,10]

Various cells within the bone are responsible for producing and maintaining the mineral and organic matrix. These cells include osteoclasts, osteoblasts, osteocytes, bone-lining cells, precursor cells, bone marrow cells, and the immune regulatory system.

Osteoclasts, derived from haematopoeitic marrow cells, are multinucleated giant cells whose primary function is resorption of bone. They are located on surface cavities of bone where they create an enclosed environment with a pH of about 3.5. The low pH functions to dissolve bone mineral. [9,10] Their lifespan is up to 7 weeks, at which time they migrate to the marrow space and undergo apoptosis leaving behind a cavity in the bone surface. [9]

Osteoblasts are plump, cubiodal cells which cover the surface of the bone and are derived from mesenchymal progenitors. Their primary function is to form bone; they achieve bone formation by synthesis and secretion of unmineralized bone matrix, calcification and resorption of bone, and regulation of calcium and

phosphate in and out of bone. Osteoblasts arise from the marrow stroma. Differentiation is thought to be under the control of core-binding factor-α1 (Cbfa1), a transcription factor. [9,10] The formation of bone is regulated by osteoblasts into two stages, matrix formation and mineralization. Matrix formation precedes mineralization by about 10 to 15 days. The matrix is primarily type I collagen organized into a nanocomposite structure. Mineralization occurs in the gaps between the collagen fibers. Alkaline phosphatase, a key protein in mineralization, cleaves the phosphate from molecules in the extracellular fluid. The phosphate ions can then be used in the formation of the hydroxyapatite crystals. [9,10]

Other noncollagenous proteins important in bone formation by osteoblasts during the mineralization stages include osteocalcin (aka bone-Gla protein) whose distribution is restricted to calcified tissue. [10] Bone sialoprotein, a phosphorylated glycoprotein, has a high capacity to bind calcium. [10] Sialoprotein I (aka osteopontin) is typically found at the mineralization front and ectopic sites of calcification. [10] It has been found to be essential for mineralization and crystal growth. [10] Osteonectin is another glycoprotein that has a high affinity for calcium and type I collagen. [10] The primary function is in orientation and growth of mineral crystals. [10]

Once osteoblasts become quiescent after completing mineralization, they are in a resting state where they are termed bone-lining cells. Bone-lining cells are

flattened, thin, and elongated. Osteoblasts that have become embedding within their own matrix are termed osteocytes. Osteocytes are the most abundant cell type. They function to stabilize bone mineral, detect microdamage, and influence adaptive modeling and remodeling in response to the amount and distribution of strain within bone tissue.

Many growth factors have been found to interact with the various cell types to induce varied responses. The work is on-going to determine how these growth factors influence bone homeostasis, and at what level they are present *in vivo*. Some of the growth factors include insulin and insulin-like growth factors, epidermal growth factor, transforming growth factor α and β, platelet derived growth factor, acidic and basic fibroblastic growth factor, interleukin-1, tumor necrosis factor, and more. [10]

1.2 Polyelectrolytes

Polyelectrolytes are long-chain molecules that have many ionizable sites and are arranged in either a linear open conformation or folded tertiary conformation. [11] Naturally occurring polyelectrolytes are found in various noncollagenous bone proteins such as osteocalcin, osteonectin, and bone sialoprotein. [8] Both the acidic and basic groups in these proteins have a role in binding proteins to hydroxyapatite. [8] Synthetic polyelectrolytes, including polystyrene sulfonate (PSS), poly-L-glutamic acid (PLG), poly-L-lysine (PLL), poly-L-aspartic acid

(PLA), and sodium citrate (SC), have been used as multilayer films in various biomedical applications. [7]

PLG and PLA have been shown to selectively alter the hydroxyapatite crystal morphology *in vitro*. [5,6] The PLA and PLG treated crystals were up to 20% thicker than the controls. [5] Furthermore, it has been shown that polyelectrolytes, including PLL, PGA, and PSS, will modulate nucleation and crystal growth *in vitro* depending on the concentration. [5-8] At low concentrations, crystal growth is induced by concentrating Ca^{2+} and PO_4^- in the vicinity of the crystal surface, and the shape is tailored since polyelectrolytes are coating certain faces of the crystal; whereas, at high concentrations, crystal growth is inhibited by polyelectrolytes completely covering the crystal, not allowing for any transport of ions to the crystal surface (see Figure 1.01). [6,7]

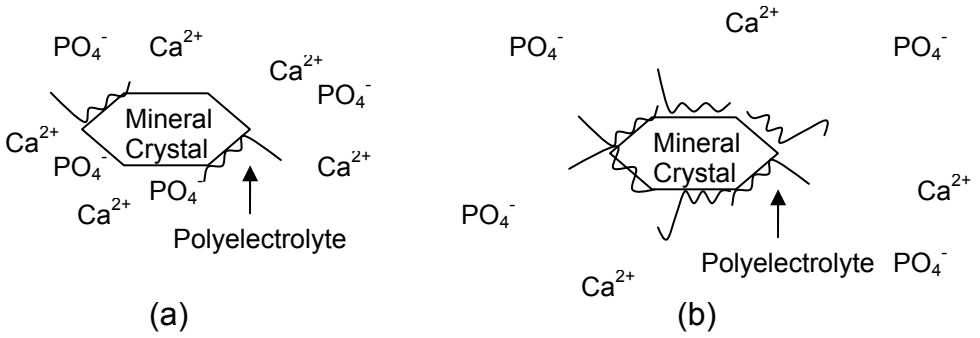

Figure 1.01: Polyelectrolyte concentration influences the interaction with mineral crystals. (a) Polyelectrolytes at low concentrations result in tailoring the mineral crystal by covering selected areas of the surface; whereas, (b) polyelectrolytes at high concentration inhibit crystal growth by completely covering the surface.

Five polyelectrolytes are being investigated in this study, including PLA, PLG, and PSS, which are anionic, and PLL and SC, which are cationic (see Table 1.01 for their monomeric structures).

Table 1.01: The molecular structure of investigated polyelectrolytes.

Polyelectrolyte	Monomeric Structure	Charge
Poly-L-Aspartic Acid (PLA)	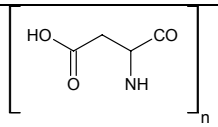	Anionic
Poly-L-Glutamic Acid (PGA)	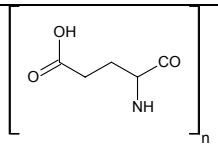	Anionic
Poly-L Lysine (PLL)	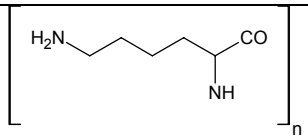	Cationic
Polystyrene Sulfonate (PSS)	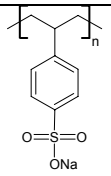	Anionic
Sodium Citrate Dihydrate (SC)	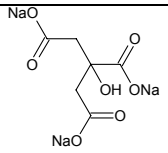	Cationic

1.3 Osteoporosis

Osteoporosis, "a disease characterized by low bone mass and structural deterioration of bone tissue, leading to bone fragility and an increased susceptibility to fractures of the hip, spine, and wrist," affects more than 10 million Americans; of these, 8 million are female. [12,13] Post menopausal women

have a 50% chance of suffering from an osteoporotic fracture during the remainder of her life, whereas 60 year old males have a 25% chance. [12-14] Another 34 million Americans have low bone mass, an early warning sign of osteoporosis. [12,13] The disease is costing hospitals and nursing homes over $14 billion annually. [12,13] Identifying and treating osteoporosis is crucial since it is asymptomatic; typically the first outward symptom of osteoporosis is a fracture. [14] It has been found that effective treatment can reduce the risk of fracture by nearly half. [14]

As noted earlier, osteoblasts are the bone cells responsible for formation of new bone; whereas the osteoclasts are the bone cells responsible for resorption of bone. Osteoporosis is caused by an imbalance in the remodeling of bone caused by overactivity of the osteoclasts. [14-17] Other substances that are thought to affect the balance of remodeling include parathyroid hormone (PTH), prostaglandins, growth factors, acidosis, corticosteroids, calcium, vitamin D, estrogen, transcription factors, and proteins. [14-17]

Currently, the only way to screen for osteoporosis is to use a dual energy x-ray absorptiometry (DXA) scan to obtain the bone mineral density. [14] Although this measurement strongly correlates to bone strength, the rate of bone turnover, geometry, microarchitecture, and mineralization also contribute significantly to bone strength. [16,17]

The treatments for osteoporosis typically aim to decrease resorption of bone by osteoclasts; however, some treatments are targeting the formation of bone by osteoblasts. The anti-resorptive drugs include estrogen, calcitonin, selective estrogen receptor modulators (SERMs), and bisphosphonates. [14-16,18] Parathyroid hormone (PTH), statins, and fluoride are the current bone formation treatments. [14,15,18]

Estrogen increases BMD; studies regarding fracture risk while taking estrogen indicate vertebral fracture incidence is decreased. [15,18] The exact mechanism by which estrogen decreases bone resorption is unknown. Furthermore, estrogen has been shown to increase the risk for uterine and breast cancer while decreasing the risk for cardiovascular disease and possibly Alzhemier's disease. [15,18] SERMs have similar benefits as estrogen but do not have the negative side effects [15,18]. Raloxifene, a currently available SERM, has been shown to reduce vertebral fractures and slightly increase BMD. [14,15,18] Tamoxifen, another SERM, has been shown to have stimulatory effects to the uterus; therefore, it is not approved for treatment. [18] Lasofoxifene, a more potent SERM which is in clinical trials, shows similar effects as raloxifene. [15]

Calcitonin is a hormonal inhibitor of bone resorption and acts by decreasing the formation and attachment of osteoclasts to bone. [15,18] It is given in subcutaneous injections or as a nasal spray. [18] Calcitonin has been shown to

increase vertebral BMD and decrease the incidence of vertebral fractures. [14,15,18]

Bisphosphonates inhibit bone resorption by targeting osteoclast recruitment, differentiation, action, and apoptosis. [15,18] Alendronate and risedronate, both bisphophonates, have been shown to decrease the incidence of both vertebral and non-vertebral fractures while increasing the BMD. [15,16,18] Although anti-resorptive treatments have been shown to decrease incidence of fractures, the gain in bone formation is typically minimal since osteoblastic activity is not stimulated.

Parathyroid hormone (PTH) has a dual effect depending on the way it is administered. [18,19] When it is continuously administered, PTH leads to bone resorption since the G-protein coupled receptors stimulated become tolerant due to feedback mechanisms. [19] However, when PTH is administered intermittently, the feedback mechanism is not activated, allowing for an increase of secondary messengers leading to increased bone formation. [19] It has been shown to reduce the incidence of both vertebral and non-vertebral fractures and increase spinal BMD. [15,18,19]

Statins are a class of drugs initially used to reduce serum cholesterol levels. [15,20] It was found that statins, including simvastatin, mevastatin, atorvastatin,

lovastatin, and cerivastatin, also stimulate bone formation by increasing the expression of bone morphogenic protein 2 (BMP-2). [15,20]

Fluoride has also been used to treat osteoporosis. It results in a large increase in spine bone density; however, at high dosage, it has been shown to increase fracture incidence. [14,18] Recently, low dosage fluoride treatment has been investigated. Results have shown increase in BMD and decrease in fracture incidence. [14,18]

1.4 Statement of Purpose

Studies have shown that the mechanical properties of bone, as a composite material, depend on the mineralization, crystallinity, molecular structure, and arrangement of the mineral crystals with the collagen matrix. [1,2] Knowing that the strength of any composite material is intimately affected by the size and shape of reinforcing inclusions, it can be proposed that the material level mechanical function of bone tissue can be altered by modifying the size and/or shape of carbonated hydroxyapatite crystals. [3,4] Within this study, the effects of treating osteoblast-like cells with various polyelectrolytes at different dosage levels will be investigated. The dosage levels are similar to those used during bench top studies by Eanes, Ofir, Furedi-Milhofer, and Romberg. The dosages used in those studies have been shown to alter the nucleation, growth, and the resulting morphology of mineral crystals in solution by limiting growth on specific faces. Therefore, polyelectrolytes carry the potential of being administered *in vivo* with the intention of modulating bone's mechanical function by way of

tailoring crystal geometry and size. This study assessed the capability of polyelectrolytic agents to alter crystal properties in bone nodules formed *in vitro*. It was hypothesized that the size and shape of crystals will differ with polyelectrolyte treatment.

It is hypothesized that in non-mineralizing treatment polyelectrolytes will adversely affect viability and genetic expression while not affecting collagen production of osteoblast-like cells in culture. In mineralizing treatment, osteoblast-like cells in cell culture with polyelectrolytes are hypothesized to alter the carbonated hydroxyapatite crystals by inducing crystallization in a dose dependent manner or altering the shape of the crystals.

Knowing how specific dosages of different polyelectrolytes tailor the mineral crystal size and shape, thus the strength of the bone composite material, polyelectrolytes could be used to treat diseases of the bone which cause either a detrimental increase or decrease (osteoporosis) in bone strength.

1.5 Methods Used to Test Hypothesis

Evaluation of viability was completed using trypan blue staining and cell-counting using a hemocytometer. Phenotypic expression was evaluated using Sircol Soluble Collagen Assay Kit (BioColor Ltd, Newtonabbey, Northern Ireland) to determine collagen production, alkaline phosphatase staining (Sigma-Aldrich, St. Louis, MO) to determine presence of alkaline phosphatase, and semi-quantitative

reverse transcriptase polymerase chain reaction (RT-PCR) to determine the presence of various proteins including alkaline phosphatase, osteocalcin, osteonectin, osteopontin, type I collagen, and GAPDH for normalization of results. Morphological changes were qualitatively monitored using a digital photograph acquisition system attached to a microscope.

Mineralization characteristics were determined by using Raman spectroscopy (Horiba Inc., Edison, NJ) for evaluation of crystallinity and mineral to matrix ratio. Crystal morphology was investigated using x-ray diffraction (PANalytical X'Pert Pro Diffractometer, Natick, MA). Vickers microhardness test was used to determine the hardness of the crystals.

All results were analyzed statistically using a general MANOVA to determine which parameters (dosage, treatment, and/or time) had significant effects. Significance was set at $p<0.05$, and borderline significance was set at $0.05<p<0.1$. Significant and borderline significant results using the general MANOVA were tested using a one-way ANOVA and Tukey's *post hoc* test at a significance level of $p<0.05$ and borderline significance set at $0.05<p<0.1$.

Chapter 2: Materials and Methods

2.1 Cell Culture

Note: Suppliers, catalog numbers, and cost of supplies and chemicals are found in an excel file on a CD-R titled “Katie Stammen – Preliminary Master’s Data and Protocols” in the file D:\Protocols for testing procedures\Reagent List.

The overview of the study design is shown in Figure 2.01. It is a flowchart outlining the main steps accomplished to complete the study. The experimental techniques also indicate the day each was completed and how many wells were tested. In addition, the sample number is indicated where appropriate. Appendix A lists sample assignments regarding what well was tested with what experimental technique. Appendix B contains all detailed experimental methods.

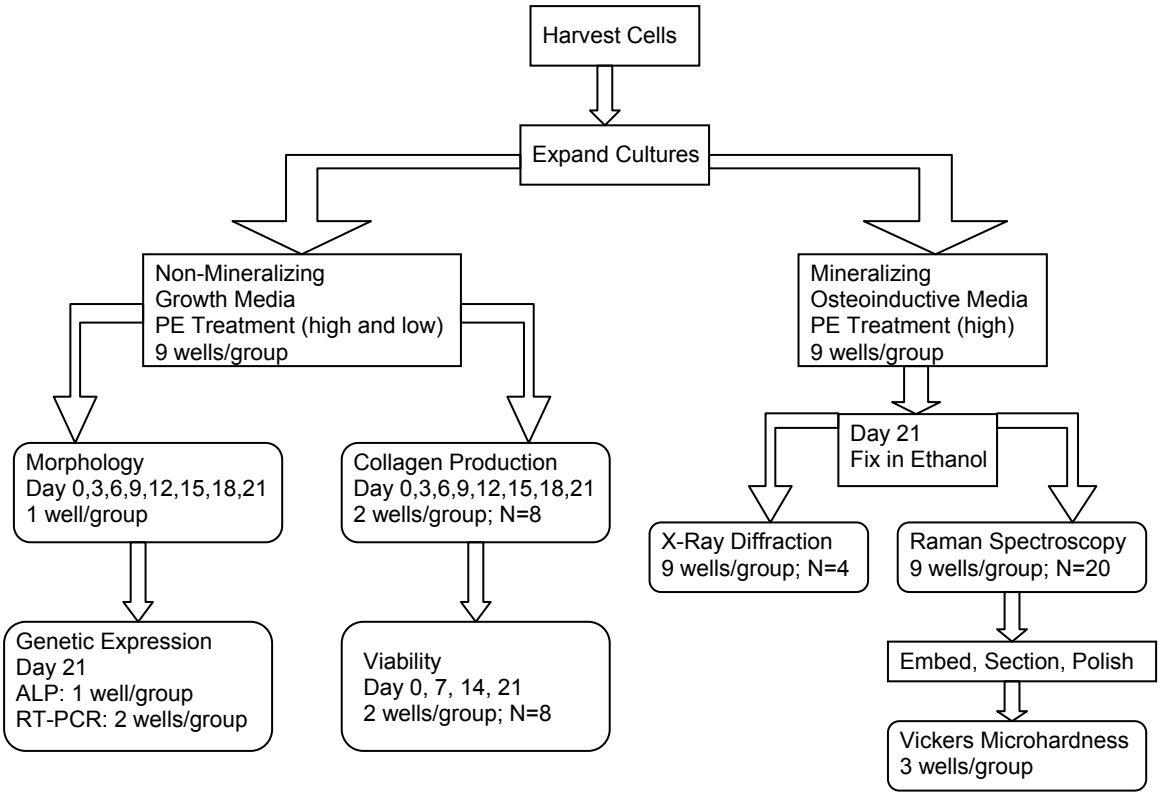

Figure 2.01: Study Design Overview

2.1.1 Harvesting Cells

Primary bone marrow stromal cells are isolated from mixed breed neonatal rats, a generous gift from Dr. Scott Molitor (The University of Toledo, Toledo, OH). The lower limbs are wiped with 70% ethanol to remove stray hairs and clean the area. Using tweezers (Fisher Scientific, Hanover Park, IL), the skin above the femur is lifted and cut using scissors (Fisher Scientific, Hanover Park, IL) to expose the underlying muscle and bone. Sterile Hank's Balanced Solution (HBSS) (Sigma-Aldrich, St. Louis, MO) is used to rinse the exposed area. Using fresh instruments, the overlying and surrounding muscle is cut away from the femur. The femur is aseptically removed by cutting through the knee and cutting the ligaments securing the hip joint. Remaining muscle, tendon, and ligament

are removed using scissors and tweezers. HBSS is used to rinse the femur, then the epiphyses are cut off using scissors and tweezers, and the diaphysis is flushed using a syringe with 10 mL HBSS. The flushed solution is centrifuged at 1000 rpm for 5 minutes, the supernatant is removed, and the pellet is resuspended in growth medium, 12 mL for each set of two femurs, consisting of Dulbecco's Modified Eagles Medium (DMEM) (Sigma-Aldrich, St. Louis, MO), 10% fetal bovine serum (FBS) (BioWhittaker, Walkersville, MD), 100 U/mL antibiotic/antimycotic (Sigma-Aldrich, St. Louis, MO), and 10 nM dexamethasone (Sigma-Aldrich, St. Louis, MO). Cells are plated on 6-well tissue culture plates (Fisher Scientific, Hanover Park, IL) at 4 mL per well and grown to confluence, typically about 7 days. Media are changed every three days. Culture plates are kept in a 37 °C incubator at 5% CO_2 and 100% humidity. Once cells reach confluence, subculturing is completed to allow for further growth of the cell population. To complete subculturing, media solutions are removed and replaced with 0.25% trypsin-EDTA (Sigma-Aldrich, St. Louis, MO). The 0.25% trypsin-EDTA bathes the cells for approximately 1-5 minutes until the cells begin to detach from the plate. Gentle pipeting is used to detach any cells stuck on the plate. The cell suspension is placed in a centrifuge tube and centrifuged at 1000 rpm for 5 minutes. The supernatant is removed and the pellet is resuspended in growth media. Typically, a 1:2 or 1:3 dilution is used to replate the cells. Primary isolation and three subcultures, approximately every 3 days, are used to obtain the 17 6-well plates needed for the nonmineralizing cultures. Experiments are conducted using growth medium for evaluation of cell viability, collagen

production, and genetic expression. Primary isolation and three subcultures are used to obtain the 9 6-well plates needed for mineralizing cultures. Osteoinductive medium, consisting of the growth medium supplemented with 50 μg/mL ascorbic acid (Alfa Aesar, Ward Hill, MA) and 10 mM β-glycerophosphate (Sigma-Aldrich, St. Louis, MO), is used for experiments evaluating mineral crystal formation. Mineralizing cultures are grown in six-well culture dishes with a sterile glass cover slip placed in each well to allow for cell attachment and growth then subsequent removal after fixation. The culture medium is changed every three days.

2.1.2 Treatment

Cultures are treated with a daily dosage of polyelectrolyte (see Table 2.01). The polyelectrolyte solutions are made by dissolving the polyelectrolyte in DMEM to obtain the desired concentration. Control cultures are maintained using DMEM in place of the polyelectrolyte solution. For non-mineralizing cultures, 18 wells are in each treatment group, 9 of which are at a high dosage and 9 are at a low dosage, and 12 wells are kept for the control group. For mineralizing cultures, 9 wells of each treatment group are maintained using only the high dosage and 9 wells are kept for the control. Although the medium is changed every 3 days, polyelectrolyte solution is added every day in the amount specified in Table 2.01.

Table 2.01: Daily dosage of osteoblast-like cells using polyelectrolyte treatment.

Treatment	**Stock Solution (mM)**	**Low Dosage (µl/well/day)**	**High Dosage (µl/well/day)**	**Dosage Used in Previous Studies (molarity at the end of 3 days)**
DMEM (Control)		1	-	-
Poly Aspartic Acid	0.667	1 ($5x10^{-7}$)	2 ($1x10^{-6}$)	$0.9x10^{-6}$ [5]
Poly-L-Glutamic Acid	8.9	15 ($1x10^{-4}$)	75 ($5x10^{-4}$)	$1.5x10^{-6}$ [5] $5x10^{-6}$ [6] $1x10^{-4}$ [6,7] $4x10^{-4}$ [7] $5x10^{-4}$ [6,7] $7x10^{-4}$ [7]
Poly-L-Lysine	6.667	1 ($5x10^{-6}$)	2 ($1x10^{-5}$)	$5x10^{-6}$ [6] $0.1x10^{-3}$ [7] $7x10^{-3}$ [6] $12x10^{-3}$ [7] $1.5x10^{-2}$ [25-27,29]
Poly(sodium 4-styrene sulfonate)	6.667	1 ($5x10^{-6}$)	4 ($2x10^{-5}$)	$5x10^{-6}$ [6] $0.01x10^{-3}$ [7] $7x10^{-3}$ [6] $12x10^{-3}$ [7]
Sodium Citrate Tribasic Dihydrate	6.667	1 ($5x10^{-6}$)	4 ($2x10^{-5}$)	$2x10^{-4}$ [5]

Note: Values in parentheses denote the molarity of the media at the end of three days.

Both non-mineralizing and mineralizing cultures are maintained for three weeks. At the end of three weeks, remaining cells are immediately tested or fixed for testing at a later time.

2.2 Non-Mineralizing

2.2.1 Morphology

Morphological changes are evaluated in the non-mineralizing cultures at every medium change (day 3, 6, 9, 12, 15, 18, and 21). One representative well from each treatment group is photographed to monitor cellular morphology. Photographs are taken at 5 locations in each well (top, left side, middle, right side, and bottom). An inverted microscope with a long working distance 10x objective (Olympus, MPlan 10x/0.25, Japan) is used in conjunction with a digital photograph acquisition system. The appearance of the cell cultures is assessed qualitatively. All photographs are shown in Appendix C.

2.2.2 Viability

The purpose of evaluating viability was to determine whether the polyelectrolyte treatment influences the cell proliferation. Once a week (day 7, 14, and 21) in the non-mineralizing cultures, the number of living cells per well of each treatment group is evaluated. In each treatment group, cells from two wells are lifted and counted independently. Two counts from each well are completed for a total of 4 counts for each treatment group at each time point giving a total sample size of N=8 per time point. Specifically, the medium solution is removed from the cell cultures and replaced with 0.25% trypsin-EDTA for 1 to 5 minutes until the cells detach from the plate. The solution is gently pipeted to remove any cells stuck to the bottom. The solution is then placed in a centrifuge tube. The cell suspension is centrifuged at 1000 rpm for 5 minutes. The supernatant is

removed, and the cells are resuspended in 2 mL of DMEM. An aliquot of 50 µl of cell solution is added to 50 µl trypan blue stain (Sigma-Aldrich, St. Louis, MO). This solution is placed in the hemocytometer. The cells are counted using an inverted microscope with a 10x objective. The number of cells in each corner box and the center box are counted and averaged. This value is scaled up to determine the number of cells per well. The scale up is completed by multiplying the number of cells counted by the dilution factors. Appendix D lists for all raw data.

2.2.3 Collagen Production

Collagen production is evaluated in the non-mineralizing cultures using the Sircol Soluble Collagen Assay Kit (Biocolor Ltd, Newtonabbey, Northern Ireland) to determine if the polyelectrolyte treatment influences the expression of type I collagen. It is possible to measure the collagen in solution since ascorbic acid (vitamin C), which causes crosslinking of collagen, is not present in the solution. Media from 2 wells of each treatment group are independently saved at each medium change (days 3, 6, 9, 12, 15, 18, and 21). The medium is frozen in 15 mL centrifuge tubes at -20 °C until processed. A 100 µl aliquot of medium is added to 100 µl of fresh DMEM. To this 200 µl sample, 1 mL Sircol Dye Reagent is added. The tube is capped and gently mixed on a vertically rotating platform for 30 minutes. During this time, the Sircol Dye selectively binds to soluble collagen, causing precipitation of the collagen and dye. The tubes are centrifuged at 12000 rpm for 10 minutes. Unbound dye is removed by inverting

and draining the tubes. A delicate task wiper is used to remove remaining dye from the lip of the tube, and a cotton swab is used to carefully clean the inside of the tube for dye sticking to the walls. Next, 1 mL alkali reagent is added to each tube. The tube is recapped and vortexed to release the dye. The solution can remain in this state for 2 to 3 hours before measurement without degradation of the color. To complete the measurement of the solution, three 200 µl aliquots, which do not need to be further diluted, are transferred to a spectrophotometer plate. These 3 readings are averaged for each data point. The spectrophotometer (Spectomax Plus, Molecular Devices, Sunnyvale, CA) is set to read an endpoint assay at 540 nm with 5 seconds of pre-shaking. Reagent blanks and controls using a collagen standard are used to generate standard curves to which the unknowns are compared. The amounts of collagen used to generate the calibration curve include 50 µg, 25 µg, 12.5 µg and 0 (see Appendix E for calibration curves). Calibration curves were zoomed to show only data from 0 to 25 µg of collagen since this is the range of the experimental data. Two assays are completed for each well at each time point for a total of 4 counts for each treatment group at each time point giving a total sample size of N=8 per time point.

2.2.4 Genotypic Expression

Alkaline phosphatase, osteocalcin, osteopontin, osteonectin, collagen type I, and glyceraldehydes-3-phosphate-dehydrogenase (GAPDH) genetic expression are evaluated in the non-mineralizing cultures at the end of the study (day 21) using

reverse transcriptase-polymerase chain reaction (RT-PCR). GAPDH is used as a standard. Two wells from each code are lifted and the RNA is purified. The purified RNA is stored in microcentrifuge tubes at -80 °C until evaluation using RT-PCR. It has been shown that during fetal bone development osteonectin expression begins at day 17, collagen type I expression peaks at day 19 or 20, and osteopontin and alkaline phosphatase expression peaks on day 21. [21] This shows the expression during bone formation *in vivo*; however, genes may or may not peak at the same time periods *in vitro*.

Before RNA isolation is started, the work space is wiped with 70% ethanol and RNase Away (Invitrogen, Carlsbad, CA). The culture medium is then removed from the well of interest and replaced with 1 mL Trizol (Invitrogen, Carlsbad, CA). After 5 minutes, the Trizol suspension is transferred to a microcentrifuge tube. After waiting 5 additional minutes, 0.2 mL chloroform (Sigma-Aldrich, St. Louis, MO) is added. The tube is shaken manually, causing the solution to turn pink. After waiting 2-3 minutes at room temperature, the solution is centrifuged at 8000 rpm for 10 minutes. Three layers are visible. The bottom layer is pink, the thin middle layer is white, and the top layer is clear. The top layer is carefully removed using a micropipette and placed in a new centrifuge tube. The pink and white solutions are discarded. The next step is to add 0.5 mL isopropanol (Fisher, Hanover Park, IL) to the clear solution. The solution is shaken and allowed to sit for 10 minutes at room temperature. Then the solution is centrifuged at 10000 rpm for 10 minutes to obtain a small white pellet. The liquid

is removed and discarded. Next, 1 mL of 75% ethanol is added to the tube, but the pellet is not resuspended. The pellet and ethanol are centrifuged at 10000 rpm for 5 minutes. The ethanol is removed, and up to 250 µl RNase free water is added depending on the size of the white pellet. The larger the pellet, the more RNase free water is added up to 250 µl. The pellet is gently resuspended. To estimate the purity of the sample and the amount of RNA present, 5 µl RNA solution and 95 µl RNase free water are mixed in a UV-96 well spectrophotometer plate that is read at 260 nm and 280 nm using endpoint readings. Calculation of the A260/A280 ratio is used to estimate the purity of the RNA isolated (see Table 2.02).

Table 2.02: Rough estimate of isolated RNA purity.

A260/A280	%Protein/%RNA
0.57	100%/0%
1.87	50%/50%
2.00	0%/100%

The amount of RNA in the sample is also calculated.

$$\text{RNA } (\mu g) = \text{Dilution Factor} * A260 * 40\ \mu g/mL \quad \text{(Eq. 2.01)}$$

To prime the isolated RNA for reverse transcription, 1 µg of sample is added to 1 µl of random hexamer primer (Invitrogen, Carlsbad, CA) in a thin-walled PCR tube. The total volume is brought to 8 µl with RNase free water and held at 70 °C for 10 minutes in a thermocycler. Reverse transcription is completed by adding 4 µl 5X RT Buffer, 2 µl of 5mM dNTP mix, 2.5 µl RNase Inhibitor, 0.5 µl MMLV RT Enzyme, and 5 µl RNase free water to the thin-walled PCR tube (all reagents

from Fisher Scientific, Hanover Park, IL) then holding the solution at 42 °C for 1 hour. This results in a cDNA template being made from the isolated RNA.

PCR is completed in a thin-walled PCR tube by combining 1 µl of the cDNA template, 10 µl 2.5X PCR Master Mix (Eppendorf, Westbury, NY), 0.5 µl of each the sense and anti-sense primers (Invitrogen, Carlsbad, CA), and 13 µl RNase free water. Table 2.03 lists sense and anti-sense primers used for the genes of interest. The solution is held at 94 °C for 2 minutes, then the amplification cycle of 94 °C for 30 seconds, 53 °C for 30 seconds, and 72 °C for 1 minute is repeated for a set number of cycles (see Table 2.03). Finally, the solution is held at 72 °C for 10 minutes. Once PCR is completed, the solution is placed in a -20 °C freezer until analysis by gel electrophoresis.

Table 2.03: PCR sense and anti-sense primers used to determine the presence of given genes in cultured osteoblast-like cells.

Gene of Interest	Primers	Product Length	Amplification Cycles
Alkaline Phosphatase	ccttgaaaaatgccctgaaa (sense) cttggagagagccacaaagg (anti-sense)	191	35
Collagen Type Ia	tgctgccttttctgttcctt (sense) aaggtgctgggtagggaagt (anti-sense)	179	25
Osteocalcin	gagggcagtaaggtggtgaa (sense) cagtggcattaaccaacacg (anti-sense)	221	35
Osteonectin	ttcgactcttcctgccactt (sense) aggtgaccaggacgtttttg (anti-sense)	178	25
Osteopontin	gaggagaaggcgcattacag (sense) atggctttcattggagttgc (anti-sense)	165	25
GAPDH	ggcattgctctcaatgacaa (sense) tgtgagggagatgctcagtg (antisense)	223	25

Analysis of all PCR products is completed by running a 1.5% agarose gel electrophoresis. The gel is cast by using 100 mL of 0.5X TBE buffer mixed with

1.5 g agarose, microwaving to dissolve the agarose, adding 10 µl of 10mg/mL ethidium bromide solution, and casting into a mold. The gel sets within about 15 minutes. The gel is placed in an electrophoresis chamber and 0.5X TBE buffer is poured over the gel until it is covered at a depth of 1 cm of buffer. Samples of 5 µl PCR product mixed with 1 µl loading dye are loaded into the wells in the gel. An appropriate DNA marker ladder is also mixed with the loading dye and loaded into a well. The marker ladder is used to determine the approximate length of the PCR products. The gel is run at 10 V/cm for approximately 60-120 minutes until the bands have run about 2/3 of the way across the gel, or the PCR marker ladder spans the length of the gel. To view the bands, a UV light box is used. The UV causes the bands to fluoresce due to the presence of the ethidium bromide intercalating between the product strands. The product is qualitatively evaluated.

Alkaline phosphatase expression is also evaluated after 3 weeks in the non-mineralizing cultures using alkaline phosphatase kit (#85, Sigma-Aldrich, St. Louis, Missouri, USA). One well of each code is stained according to supplied instructions. Specifically, citrate working solution is made by diluting 2 mL citrate concentrate solution with 98 mL deionized water. The working solution is then brought to room temperature. While stirring, three volumes of acetone are added to two volumes of citrate working solution to make the fixative solution. The alkaline-dye mixture is made by dissolving a fast violet B capsule in 48 mL of room temperature distilled water. Once the dye is dissolved, 2 mL of Napthol

AS-MX phosphate alkaline solution are added to the dye solution. The procedure begins by fixing the tissue by immersion in the fixative solution for 30 seconds. Next, the tissue is gently rinsed in deionized water for 45 seconds. Without allowing the tissue to dry, the tissue is transferred to the room temperature alkaline-dye mixture for 30 minutes, rinsed in deionized water for 2 minutes, and placed in Mayer's Hematoxylin solution for 10 minutes. Finally, the tissue is rinsed in alkaline tap water for 2 minutes and evaluated microscopically. The stained wells are photographed using a Canon 7.1 MegaPixel camera (Canon Powershot SD550). The photographs are stored digitally. The appearance of the cell cultures are assessed qualitatively.

2.3 Mineralizing

2.3.1 Raman Spectroscopy

Raman spectroscopy was completed to determine if the chemical composition and structure of the bone nodules, specifically the crystals were altered. Nine wells of each mineralizing treatment group were evaluated using Raman spectroscopy (Horiba Inc., Edison, NJ) to analyze the chemical composition of the mineralized nodules. These nodules were grown on sterile glass cover slips due to the interference of plastic with Raman evaluation. The samples were fixed using an ethanol procedure consisting of submerging the sample attached to the glass cover slips in 70% ethanol for 15 minutes, followed by 85% ethanol for 10 minutes, and finally 100% ethanol for 10 minutes. Samples were allowed to air dry.

First, the Raman microscope is calibrated using established procedures. Silicon, which gives a single Raman peak at 520.7 cm^{-1}, is used as the calibration standard. An average of 3 readings are taken for 240 seconds (4 minutes) each using a long working distance 50x objective (Olympus, Japan). The hole is set at 1100 and the slit is 750. The spectrum is centered around 1280 cm^{-1}. Two or three nodules on each cover slip are evaluated until 20 spectra for each treatment group are collected.

Processing of the data is completed using custom MatLab software (see Appendix F, G, H, and I). The processing includes a 5-point moving average filtration, baseline correction, and normalization with respect to the intensity of the PO_4^{3-} peak located at a frequency of approximately 960 cm^{-1}. The software locates the exact frequencies of the peaks within the spectrum. It also calculates mineralization and crystallinity using ratios of $[PO_4^{3-}]/[CH_2wag]$ and $1/[PO_4^{3-}]$ full-width half-max bandwidth, respectively.

2.3.2 X-Ray Diffraction (XRD)

Mineral crystal morphology is evaluated using XRD. The nodules are fixed using the same procedure as above (see Raman Spectroscopy). Bone nodules that grew on the plastic culture plate surrounding the glass cover slip are scraped using a metal spatula. Three wells of scraped bone nodules are pooled to obtain enough material for evaluation. The nodules are placed along a line, which is

parallel to the incident beam, on the surface of a 1.8 cm x 1.8 cm square silicon wafer. The line of nodules is about 2 mm wide and about 10 mm in length. The silicon wafer is placed on an aluminum fixture that is clipped on the sample stage of the x-ray diffractometer (PANalytical X'Pert Pro Diffractometer, Natick, MA). Experiments are conducted in Bragg-Brantano geometry. The incident beam optics include a 0.04 radian soller slit, ¼° divergence slit, 10mm mask, and ½° antiscatter slit. The diffracted beam optics include a 5mm antiscatter slit, 0.04 radian soller slit, and nickel filter. The wavelength used was CuKα, and an X'Celerator detector was used. Evaluation was completed from 20° to 70° 2θ with a step size of 0.02° and a collection time of 180 seconds per step.

Processing of the data was completed using custom Matlab software (see Appendix J, K, L, and M). The processing includes a 5-point moving average filtration and baseline correction. The software locates the exact 2θ position of the peaks within the pattern. It also calculates the full-width at half-maximum (FWHM) of each peak. The program then uses the calibration pattern from lanthium boride (LaB_6) to correct the FWHM values for equipment related peak broadening. Using the corrected FWHM values, peak positions, and x-ray wavelength, the length of the crystal along given planes is calculated. Crystal length (D_{hkl}) along the 002, 004, and 130 directions were calculated using Debye-Scherrer's formula (see Eq. 2.02) using the Bragg angle (θ), bandwidth (β), and x-ray wavelength (λ). [22]

$$D_{hkl} = (0.9\lambda)/(\beta\cos\theta) \qquad \text{(Eq. 2.02)}$$

2.3.4 Vickers Microhardness

Evaluation of mineralizing cultures' hardness is completed using Vickers microhardness test. To prepare the specimen for testing, the fixed samples are embedded in a two-part epoxy (Buehler, Lake Bluff, IL). Specifically, the cover slips on which the bone nodules are located are placed on a base of the hardened epoxy. Liquid epoxy is poured over the base and cover slip. After approximately 24 hours, the epoxy has solidified. The samples are then sectioned to a thickness of 0.8 mm using a diamond blade low-speed saw. The cut is made at a speed of 350 rpm. The sections are polished (see Table 2.04).

Table 2.04: Polishing protocol

Polishing Paper	Time (min)
600 grit	3
800 grit	3
1200 grit	3
1 μm	5

The Vickers microhardness test (CM400AT, Clark, Dexter, MI) uses a diamond pyramid indentor at 50 grams-force (gf) for 15 seconds to indent the mineral crystal. The test is administered on all nodules obtained. Each indentation is measured three times. These readings are averaged to obtain the hardness for each indentation. Two readings are taken for each nodule as long as the size of the nodule is large enough. The indentations are spaced at a distance of 3 times

the indentation size to ensure previous indentations do not affect subsequent indentations.

2.4 Statistical Analysis

All statistical analysis was completed using statistical analysis software (Minitab 14, Minitab Inc., State Collage, PA). To test for significance of the non-mineralizing culture data, a general multivariate analysis of variance (MANOVA) was used. The three parameters tested include treatment (control, PLA, PLG, PLL, PSS, and PSS), dosage (high and low), and time (day 0, 3, 6, 9, 12, 15, 18, and 21 or day 0, 7, 14, and 21). Significance was set at $p<0.05$. Borderline significance was observed at $0.1<p<0.05$.

Both significant and borderline significant results were tested using a one-way analysis of variance (ANOVA). Significance using Tukey's test was set at $p<0.05$. Borderline significance was set at $0.05<p<0.1$. This test allows direct comparison between all combinations in a group.

To test for significance of the mineralizing culture data, a one-way ANOVA was used comparing investigated data to the treatment. Significance using Tukey's test was set at $p<0.05$. Borderline significance was set at $0.05<p<0.1$. This test allows direct comparison between all combinations in a group.

Chapter 3: Non-mineralizing Culture Results and Discussion

3.1 Morphology

Over the three week culture duration, cell morphology was observed by photographing one well from each treatment group using an inverted microscope equipped with a 10x objective. Photographs were taken every three days starting on day 0 and ending on day 21. Each well was photographed in five locations, top, left, center, right, and bottom.

On day 0, all cultures had a low density of cells with a spread, cuboidal morphology. Appendix C contains all cell culture photographs. The control cells maintained the typical spread morphology, as seen in osteoblasts, through the culture duration (see Figure 3.01). As time progressed, the density of the cells increased and confluence was maintained. On day 12, the cells began to form colonies where the cells became very concentrated. These colonies became more prominent as time passed through day 21.

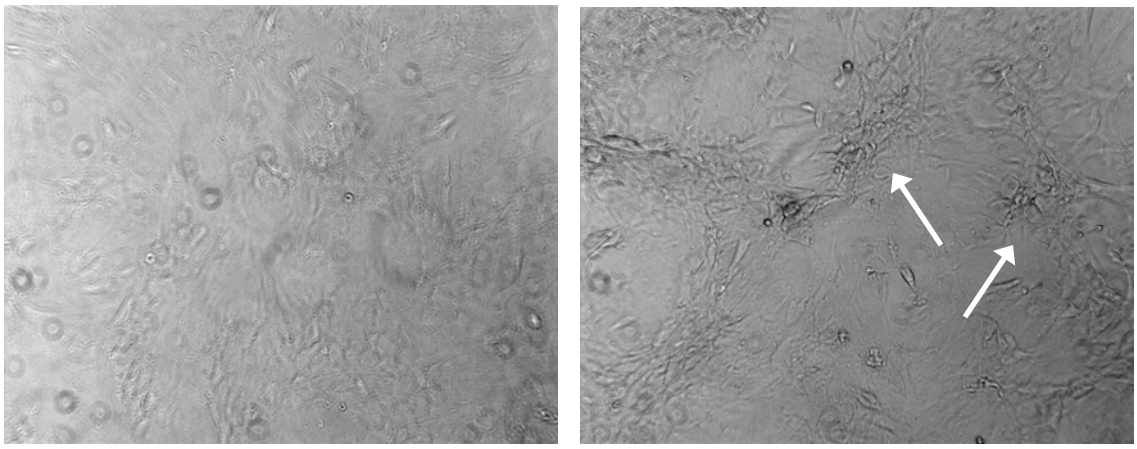

(a) (b)

Figure 3.01: Osteoblast-like cells with control treatment maintained a spread and cuboidal morphology throughout the culturing period. As time passed, colonies began to form and became more organized indicated by arrows. (a) Control cell culture on day 6 located in the center of the well. (b) Control cell culture on day 21 located at the bottom of the well.

Both PLA low and PLA high cultures maintained similar morphology to control cultures throughout the culture duration. The density of cells increased throughout the culture time. Colonies of cells became visible on day 12 in PLA low cultures and on day 9 in PLA high cultures. The colonies became more prominent as time passed (see Figure 3.02).

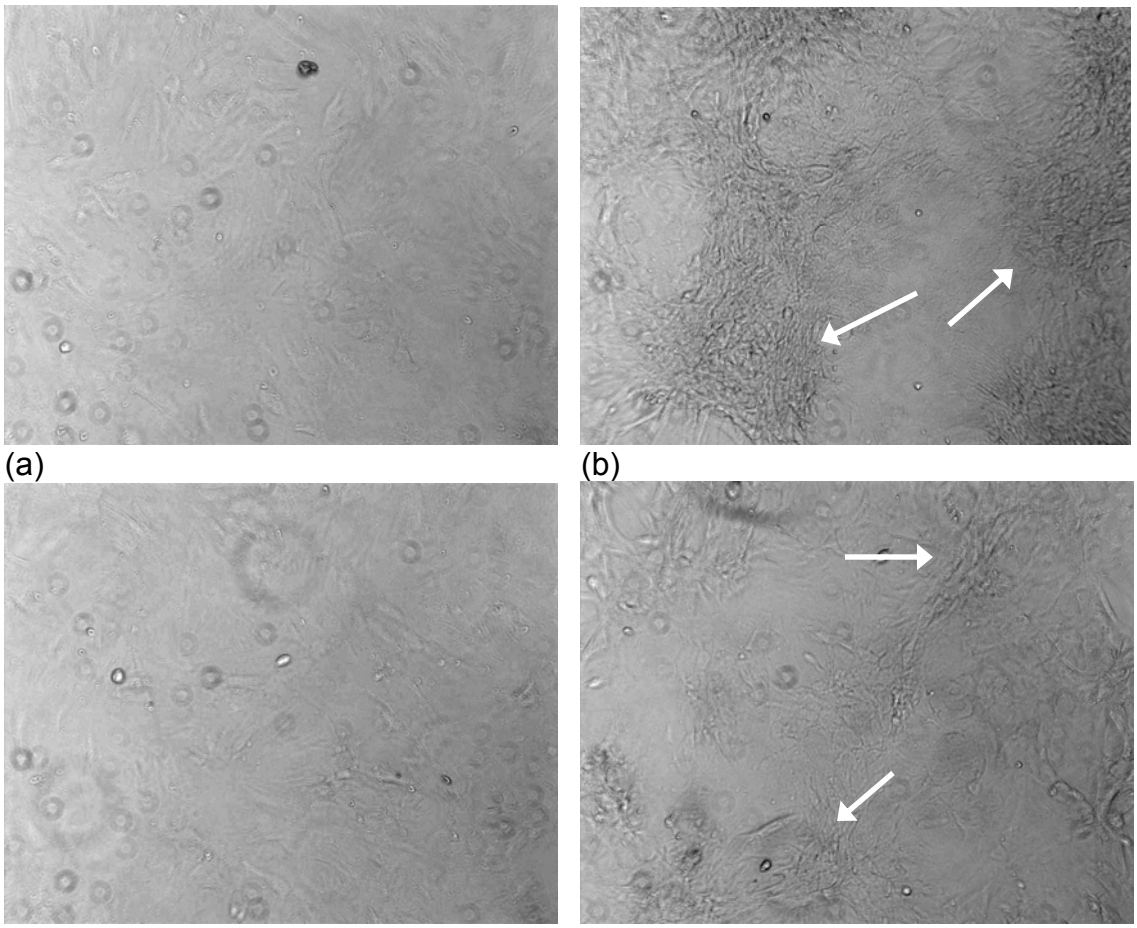

(a) (b)

(c) (d)

Figure 3.02: Osteoblast-like cells with PLA treatment maintained a spread and cuboidal morphology throughout the culturing period. As time passed, colonies began to form and became more organized. (a) PLA low cell culture on day 3 located in the center of the well. (b) PLA low cell culture on day 21 located at the right of the well. (c) PLA high cell culture on day 3 located at the center of the well. (d) PLA high cell culture on day 21 located at the center of the well.

Both PLG low and PLG high cultures maintained similar morphology to control cultures throughout the culture duration. The density of cells increased throughout the culture time. Colonies of cells became visible on day 6 in PLG low cultures and on day 3 in PLG high cultures. The colonies became more prominent as time passed (see Figure 3.03); furthermore, the colonies were

highly organized in the PLG high cultures. This is visible from the cells extending from the nodule to reach surrounding colonies (see Figure 3.03d).

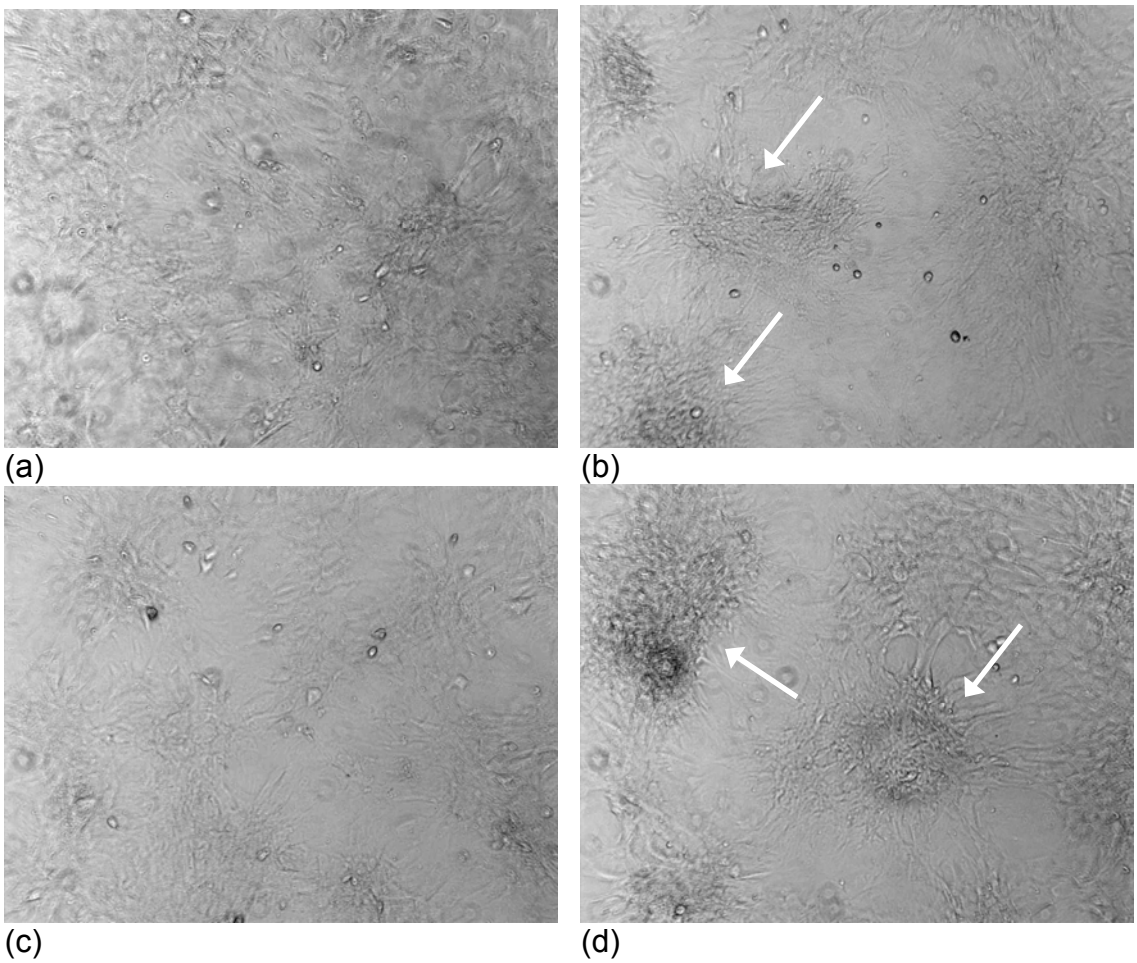

Figure 3.03: Osteoblast-like cells with PLG treatment maintained a spread and cuboidal morphology throughout the culturing period. As time passed, colonies began to form and became more organized. (a) PLG low cell culture on day 3 located in the top of the well. (b) PLG low cell culture on day 21 located at the bottom of the well. (c) PLG high cell culture on day 3 located at the top of the well. (d) PLG high cell culture on day 21 located at the center of the well.

Both PLL low and PLL high cultures maintained similar morphology to control cultures throughout the culture duration. The density of cells increased throughout the culture time. Colonies of cells became visible on day 12 in PLL

low cultures and on day 9 in PLL high cultures. The colonies became more prominent as time passed (see Figure 3.04).

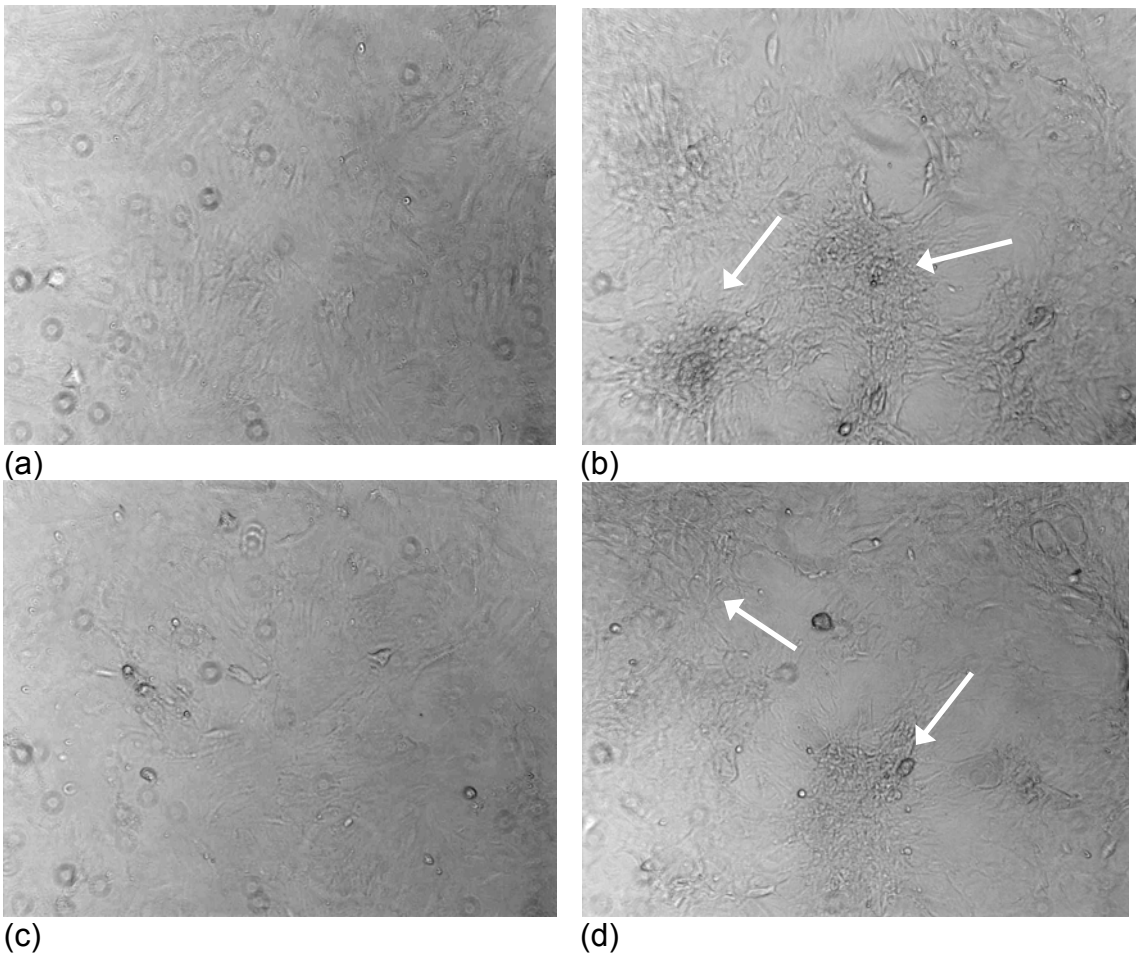

Figure 3.04: Osteoblast-like cells with PLL treatment maintained a spread and cuboidal morphology throughout the culturing period. As time passed, colonies began to form and became more organized. (a) PLL low cell culture on day 3 located in the center of the well. (b) PLL low cell culture on day 21 located at the bottom of the well. (c) PLL high cell culture on day 3 located at the top of the well. (d) PLL high cell culture on day 21 located at the center of the well.

Both PSS low and PSS high cultures started with the same morphology as control cultures; however, cells became more spindle-like within a few days. The density of cells increased slightly throughout the culture time. Colonies of cells became visible on day 12 in PSS low cultures and on day 3 in PSS high cultures.

The colonies became very dense and compact as time passed (see Figure 3.05). Colonies were not as wide-spread as in other treatments and control. In PSS high cultures, cells appeared to detach from the plate starting on day 15 and by day 21 cellular material was floating in the media.

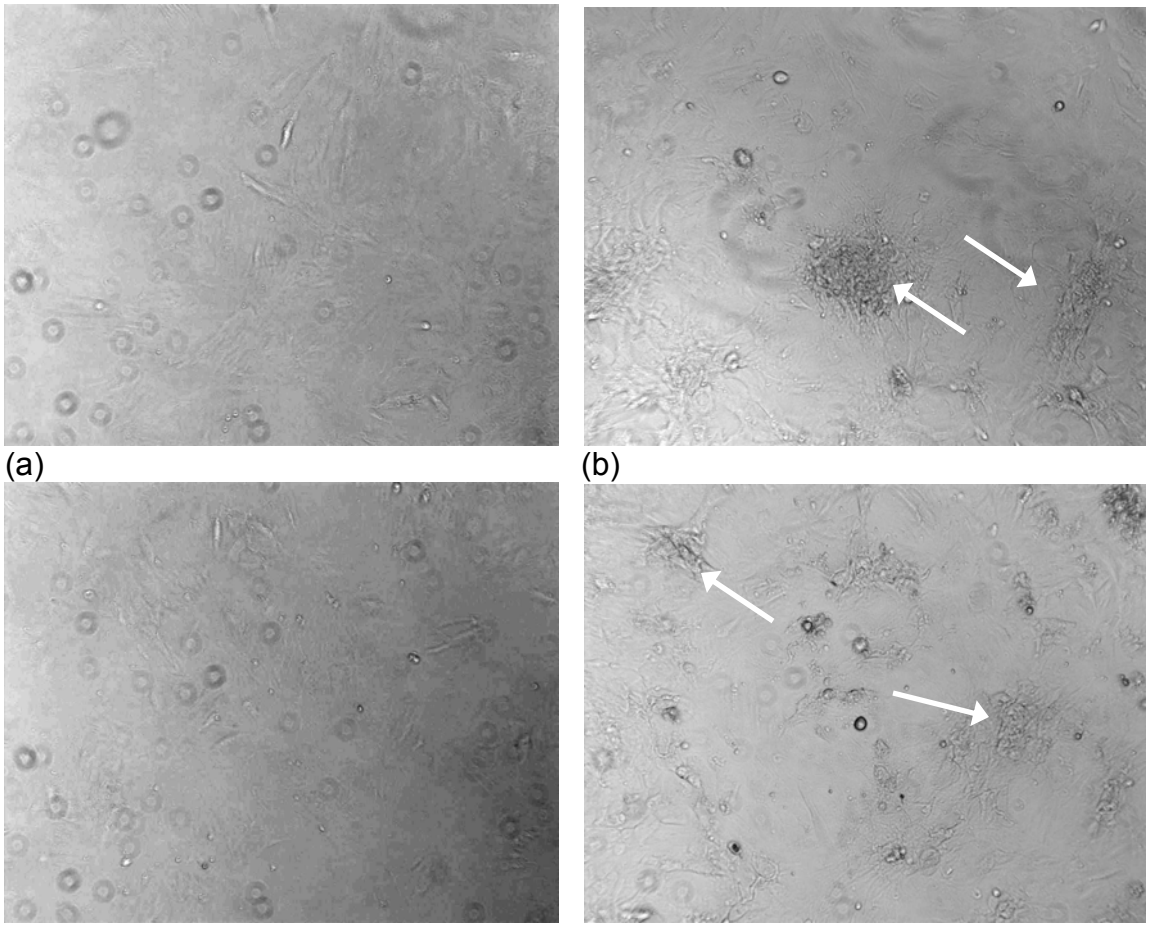

Figure 3.05: Osteoblast-like cells with PSS treatment had a more spindle-like morphology. As time passed, colonies began to form. By the end of the culture duration in PSS high treatment, cells were becoming detached from the culture plate. (a) PSS low cell culture on day 3 located in the center of the well. (b) PSS low cell culture on day 21 located at the left of the well. (c) PSS high cell culture on day 3 located at the right of the well. (d) PSS high cell culture on day 21 located at the top of the well.

Both SC low and SC high cultures maintained similar morphology to control cultures throughout the culture duration. The density of cells increased throughout the culture time. Colonies of cells became visible on day 9 in SC low cultures and on day 6 in SC high cultures. The colonies became very dense as time passed (see Figure 3.06), but overall the cells maintained a cuboidal, spread morphology.

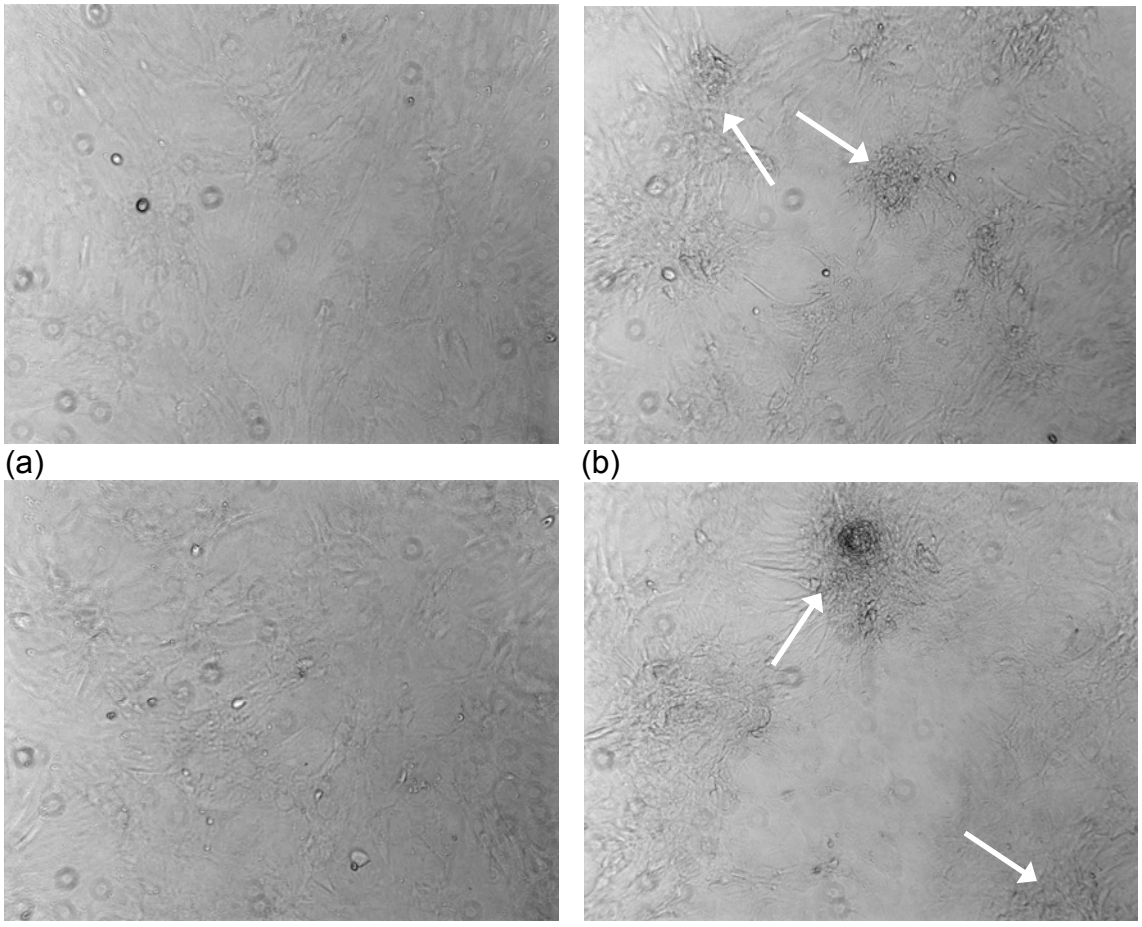

Figure 3.06: Osteoblast-like cells with SC treatment maintained a spread and cuboidal morphology throughout the culturing period. As time passed, colonies began to form and became more organized. (a) SC low cell culture on day 3 located in the center of the well. (b) SC low cell culture on day 21 located at the right of the well. (c) SC high cell culture on day 3 located at the top of the well. (d) SC high cell culture on day 21 located at the bottom of the well.

Overall, (1) cells treated with PLA, PLG, PLL, and SC maintained similar morphology and characteristics as control cells. Typically, (2) colonies formed a few days earlier for treated cells compared to control cells. The exceptions are (3) PLA low and PLL low dosage, which showed nodule formation on the same day as controls. (4) High dosage resulted in a quicker appearance of colonies. (5) PSS was the only polyelectrolyte investigated that noticeably caused a change in the morphology of the osteoblast-like cells.

3.2 Viability

Sixty-six wells were investigated over a 21 day period to determine the viability characteristics of untreated and treated osteoblast-like cells. All wells were originally plated on day 0 at a density of 77,000 cells +/- 11,000 cells per well. Two wells of each treatment at each dosage level were counted using trypan blue stain and a hemocytometer at 7, 14, and 21 days. Two aliquots were counted from each well. The sample number is 4 for each data point. The number of living cells per well for each treatment group at each dosage at each time point is shown in Table 3.01. Appendix D lists raw data and calculations.

Table 3.01: Osteoblast-like cell viability of the 6 treatment groups at high and low dosages at three time points, 7, 14, and 21 days. The value represents the total number of living cells per well +/- the standard deviation in thousands.

	Cells per Well ± Standard Deviation (x1000)		
Treatment Group	**Day 7**	**Day 14**	**Day 21**
Control	262 ± 12	854 ± 86	828 ± 93
PLA low	356 ± 49	616 ± 20	796 ± 107
PLA high	348 ± 37	562 ± 90	760 ± 68
PLG low	302 ± 31	614 ± 101	1136 ± 61
PLG high	250 ± 10	796 ± 107	1430 ± 204
PLL low	304 ± 35	440 ± 60	1084 ± 116
PLL high	202 ± 22	410 ± 51	782 ± 223
PSS low	202 ± 30	316 ± 38	514 ± 132
PSS high	154 ± 14	202 ± 26	418 ± 75
SC low	246 ± 25	556 ± 50	974 ± 82
SC high	262 ± 31	496 ± 84	1090 ± 248

Statistical analysis using general multi-variance analysis of variance (MANOVA) revealed time and treatment type were significant ($p<0.05$) (see Table 3.02); however, the dosage level was not significant. Therefore, the data from both high and low dosage levels was pooled for each treatment (see Table 3.03). All time points were significantly different ($p<0.05$) from each other using one-way analysis of variance (ANOVA) with all treatment groups pooled (see Table 3.04). Only PLG was significantly different from PSS ($p<0.05$) using one-way ANOVA with all time points pooled (see Table 3.05). When the final number of cells on day 21 was evaluated versus treatment using a one-way ANOVA, both PLG and PSS were significantly different ($p<0.05$) from the control (see Table 3.06).

Table 3.02: General MANOVA of cell number versus day, treatment, and dosage. + indicates $p<0.05$. - indicates $p>0.05$.

	Day	**Treatment**	**Dosage**
Cell Number	+	+	-

Table 3.03: Osteoblast-like cell viability of the 6 treatment groups (Control, PLA, PLG, PLL, PSS, and SC) at three time points (7, 14, and 21 days). Dosage levels are pooled since dosage was not statistically significant. The value represents the total number of living cells per well ± the standard deviation in thousands.

	Cells per Well ± Standard Deviation (x1000)		
Treatment Group	**Day 7**	**Day 14**	**Day 21**
Control	262 ± 12	854 ± 86	828 ± 93
PLA	352 ± 41	589 ± 67	778 ± 85
PLG	276 ± 35	705 ± 137	1283 ± 210
PLL	253 ± 61	425 ± 54	933 ± 230
PSS	178 ± 34	259 ± 68	446 ± 112
SC	254 ± 27	526 ± 72	1032 ± 182

Table 3.04: One-way ANOVA of cell number versus day.
+ indicates $p<0.05$. - indicates $p>0.05$.

	Day 7	**Day 14**	**Day 21**
Day 0	+	+	+
Day 7		+	+
Day 14			+

Table 3.05: One-way ANOVA of cell number versus treatment for all time points.
+ indicates $p<0.05$. - indicates $p>0.05$.

	PLA	**PLG**	**PLL**	**PSS**	**SC**
Control	-	-	-	-	-
PLA		-	-	-	-
PLG			-	+	-
PLL				-	-
PSS					-

Table 3.06: One-Way ANOVA of cell number versus treatment on day 21.
+ indicates $p<0.05$. - indicates $p>0.05$.

	PLA	**PLG**	**PLL**	**PSS**	**SC**
Control	-	+	-	+	-
PLA		+	-	+	+
PLG			+	+	-
PLL				+	-
PSS					+

Figure 3.07 shows the number of cells per well on days 0, 7, 14, and 21. The number of cells increases throughout the time course showing that the polyelectrolytes are not causing the cells to undergo apoptosis. PLG was shown to be significantly different from PSS when evaluated over all time points. Figure 3.08 shows the percent difference in cell number of the treatment groups compared to the control group on day 7. The data is generated by averaging the total number of cells in the control group, this value is considered 100%. Then the number of cells in each individual group is compared to the control group, or 100% value, to determine the percentage higher or lower than the control. These values are averaged and the standard deviation is taken. The data shows PLA enhances proliferation, whereas PSS decreases proliferation. Figure 3.09 shows the percent difference in cell number of the treatment groups compared to the control group on day 14. The data shows PLA, PLL, PSS, and SC have significantly less cells than controls. Figure 3.10 shows the percent difference in cell number of the treatment groups compared to the control group on day 21. The data shows PLG and PSS to be significantly different from control.

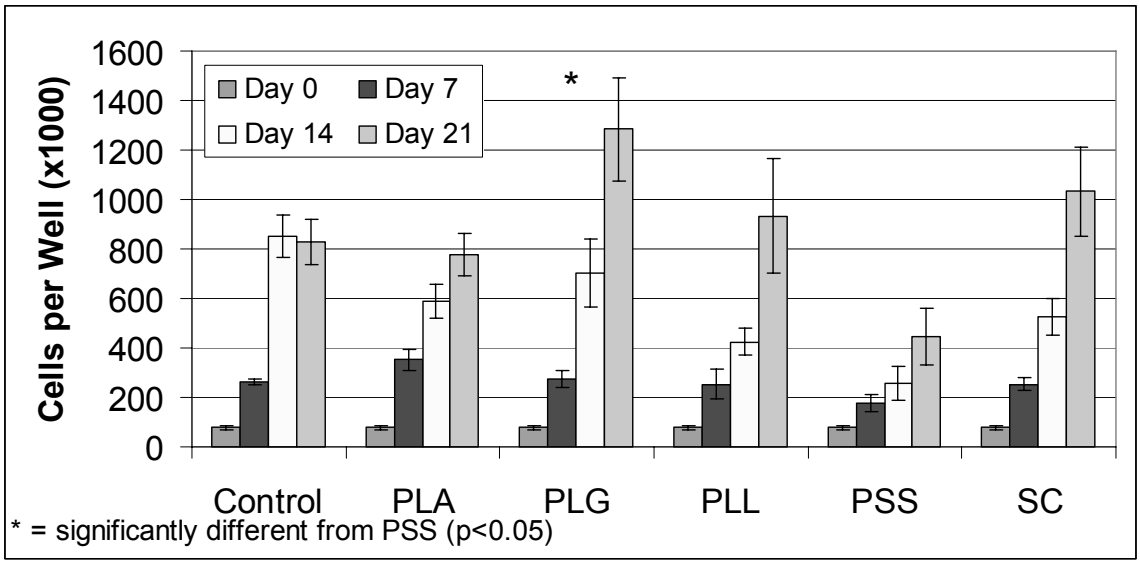

Figure 3.07: Osteoblast-like cell viability in different treatments over the course of 21 days. * denotes a significant difference ($p<0.05$) from PSS.

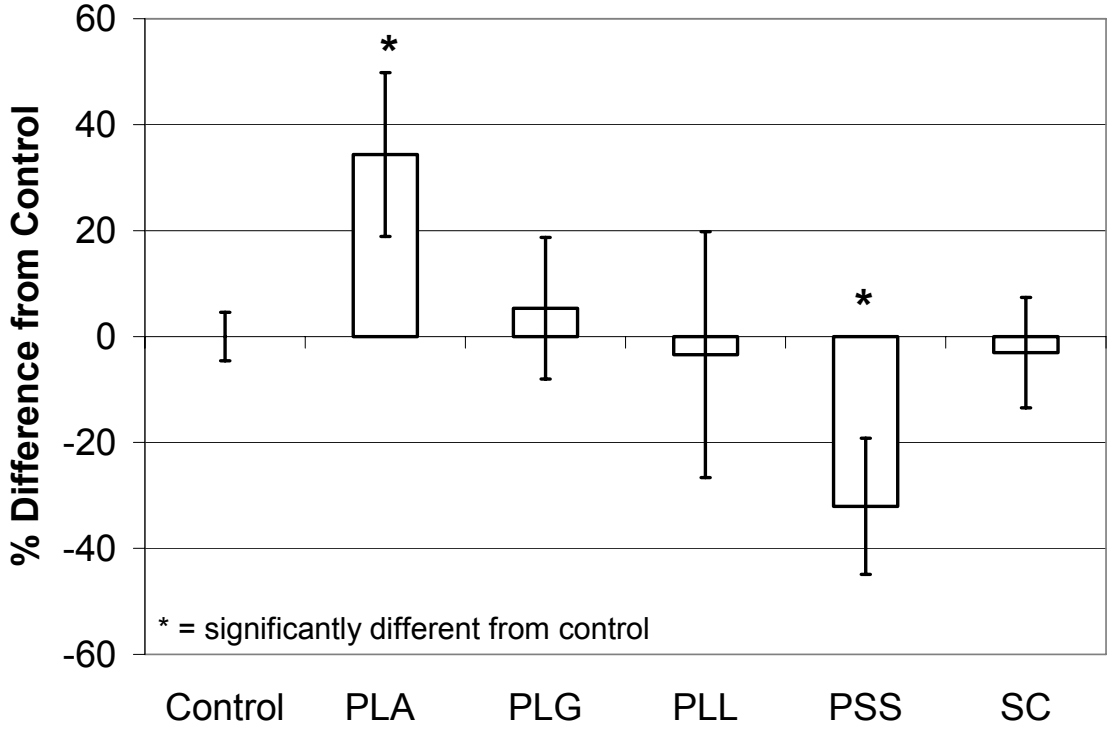

Figure 3.08: Total cell number of treatment group as percent difference from the control on day 7. Significance was determined using a one-way ANOVA ($p<0.05$).

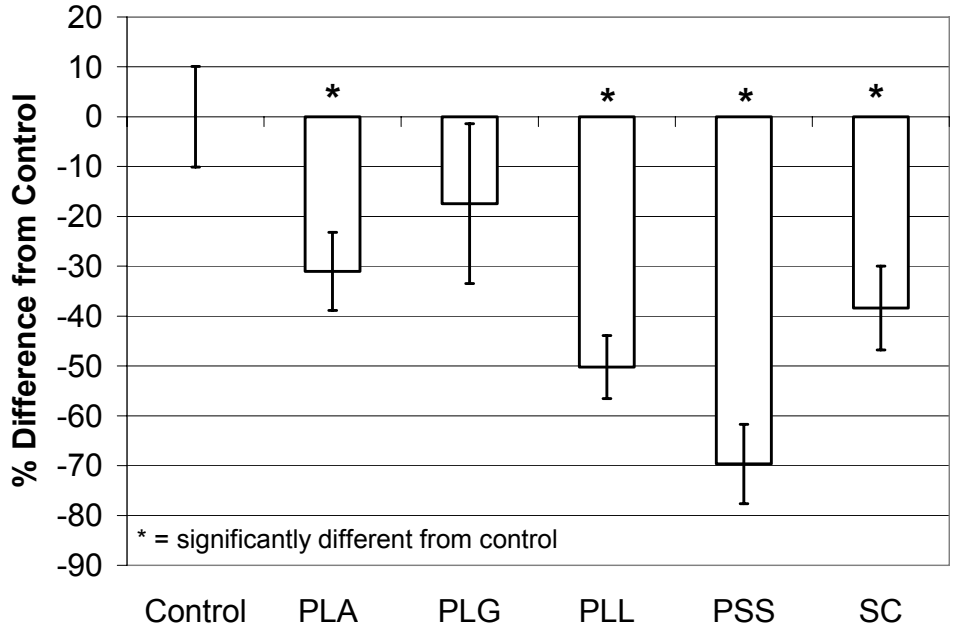

Figure 3.09: Total cell number of treatment group as percent difference from the control on day 14. Significance was determined using a one-way ANOVA ($p<0.05$).

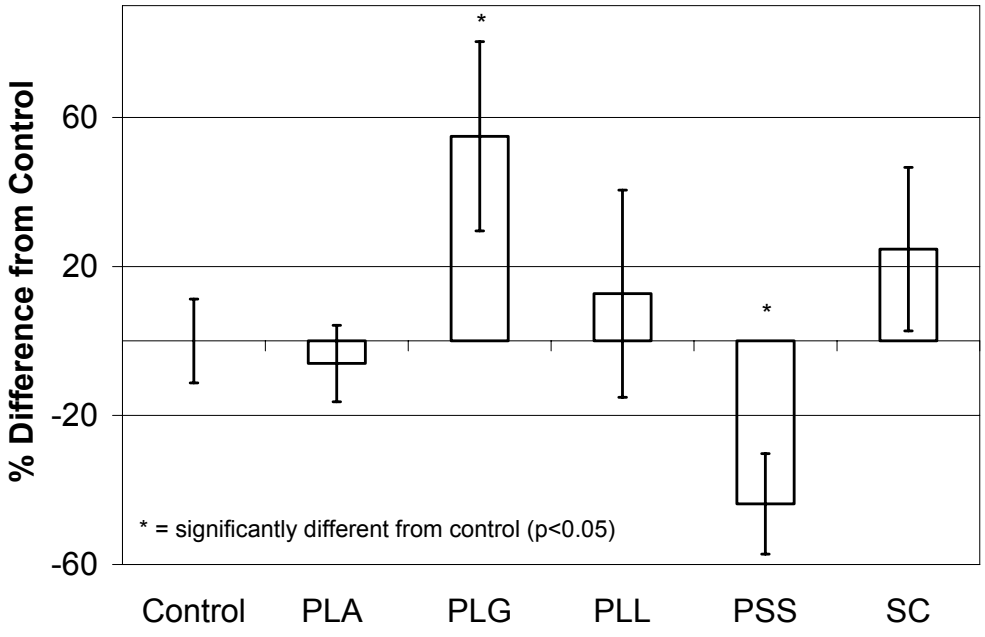

Figure 3.10: Total cell number of treatment group as percent difference from the control on day 21. Significance was determined using a one-way ANOVA ($p<0.05$).

The data indicates that (1) PLG is enhancing proliferation at the end of 21 days, whereas (2) PSS is inhibiting proliferation compared to the control over the entire time course. (3) While PLA, PLL, and SC show fluctuations in the cell number compared to the control, at the end of 21 days there is not a significant difference.

3.3 Collagen Production

3.3.1 Total Collagen

Twenty-two wells were investigated over a 21 day period to determine the collagen production characteristics of untreated and treated osteoblast-like cells. On day 0, medium was collected from the fresh growth media to determine if any collagen was already present. Medium was collected from two wells of each treatment at each dosage level on days 3, 6, 9, 12, 15, 18, and 21. All media were kept frozen until evaluation. Two aliquots were evaluated from each medium sample collected. The sample number is 4 for each data point. The amount of collagen for each treatment group at each dosage at each time point is shown in Table 3.07. Appendix E lists raw data and calculations. Two separate optical density standard curves were used because initially only one aliquot from each medium sample was evaluated. A new kit was used to evaluate the second aliquot; therefore, a new standard curve was generated using the new reagents.

Table 3.07: Soluble collagen production by untreated osteoblast-like cells and osteoblast-like cells treated with polyelectrolyte at low or high dosage. The value represents the soluble collagen produced in one well over a three day period ending on the specified day.

	Collagen +/- Stadard Deviation (µg)							
Treatment	**Day 3**	**Day 6**	**Day 9**	**Day 12**	**Day 15**	**Day 18**	**Day 21**	**Total**
Control	61.2 ± 33.4	65.8 ± 28.2	100.6 ± 49	86.5 ± 34.7	102.5 ± 26.2	125.9 ± 34.4	110.6 ± 45	653.1 ± 89.9
PLA low	40 ± 25.9	91.8 ± 23.9	126.6 ± 30.1	76.6 ± 31.5	104 ± 28.5	102.4 ± 23.4	107.3 ± 39.8	648.7 ± 69.2
PLA high	49.4 ± 47.7	55.4 ± 7.4	78.5 ± 28.8	91.5 ± 21.3	132.4 ± 57.4	107.4 ± 23.4	86.2 ± 23.5	600.8 ± 67.4
PLG low	35.5 ± 14.1	64.3 ± 36	68.5 ± 23.1	60.4 ± 18.7	74.2 ± 19.1	100 ± 9.3	97 ± 47.4	499.9 ± 31.8
PLG high	59.9 ± 16.5	68.6 ± 37.5	63.5 ± 17.7	49.1 ± 15.1	73.2 ± 19.6	58.8 ± 20.8	64.7 ± 65.7	437.7 ± 76.1
PLL low	43.4 ± 4.3	46.4 ± 8.7	68.4 ± 17.7	67.9 ± 13.2	60.1 ± 18.2	77.9 ± 34.1	77.6 ± 29.3	441.7 ± 45.9
PLL high	43.1 ± 15	38.1 ± 18.4	68.9 ± 12.4	70.8 ± 13.8	80.3 ± 15.5	111.8 ± 73.9	64.3 ± 17.4	477.4 ± 143.7
PSS low	41 ± 16	56.7 ± 23.2	83.1 ± 9.7	80.1 ± 22.6	66.3 ± 7.4	47 ± 7.8	45.2 ± 8.4	419.4 ± 30.2
PSS high	30.3 ± 13.8	46.2 ± 26.2	70.1 ± 11.1	40.3 ± 22.1	73.5 ± 31.6	87 ± 23.8	33.6 ± 19.6	381 ± 28.9
SC low	105.2 ± 31.6	75 ± 12.7	80.4 ± 20.1	92.9 ± 22.1	101.7 ± 8.4	64.5 ± 47.7	101.7 ± 20	621.3 ± 103.6
SC high	49.9 ± 5.3	51.6 ± 17.4	71.3 ± 31.2	85.5 ± 29.8	87.8 ± 31.2	112.6 ± 9.9	59.5 ± 13.9	518 ± 74.3

Statistical analysis using general MANOVA revealed that both time and treatment were significant ($p<0.05$) and dosage was borderline significant ($0.05<p<0.1$) (see Table 3.08). All data were then run using a one-way ANOVA to determine significance between days, time, and dosage in comparison to collagen production (see Tables 3.09, 3.10, and 3.11, respectively). Total collagen production was also evaluated in comparison to dosage and treatment using general MANOVA. Dosage was borderline significant ($p=0.08$), but when evaluated using a one-way ANOVA, it was not found to be significant. Therefore, the total collagen data was pooled over dosage levels. A one-way ANOVA comparing total collagen production and treatment was performed (see Table 3.12). Total collagen produced by PLG, PLL, and PSS were all significantly different from the control.

Table 3.08: General MANOVA of collagen production versus day, treatment, and dosage. * indicates significance p<0.05.
+ indicates borderline significance 0.05<p<0.1.

	Day	Treatment	Dosage
Collagen Production	*	*	+

Table 3.09: One-way ANOVA of collagen production versus day.
+ indicates p<0.05. - indicates p>0.05.

	6	9	12	15	18	21
3	-	+	+	+	+	+
6		+	-	+	+	-
9			-	-	-	-
12				-	-	-
15					-	-
18						-

Table 3.10: One-way ANOVA of collagen production versus treatment.
+ indicates p<0.05. - indicates p>0.05.

	PLA	PLG	PLL	PSS	SC
Control	-	+	+	+	-
PLA		+	+	+	-
PLG			-	-	-
PLL				-	-
PSS					-

Table 3.11: One-way ANOVA of collagen production versus dosage.
+ indicates p<0.05. - indicates p>0.05.

	high
low	-

Table 3.12: One-way ANOVA of total collagen production versus treatment.
+ indicates p<0.05. - indicates p>0.05.

	PLA	PLG	PLL	PSS	SC
Control	-	+	+	+	-
PLA		+	+	+	-
PLG			-	-	-
PLL				-	-
PSS					+
SC					

The total collagen production was investigated (see Figure 3.11). The number of cells for each time point was linearly interpolated from the viability data. This shows that the cells have an overall increasing trend in collagen production over the 21 day time period. However, there is not a significant difference comparing the control to treated samples for collagen production. Figure 3.12 is a representation of the total collagen produced over the 21 day period. Dosage level of the polyelectrolyte treatment was not significant. However, PLG, PLL, and PSS were all significantly different from the control ($p<0.05$). This indicates that PLG, PLL, and PSS all inhibited overall collagen production over the 21 day period.

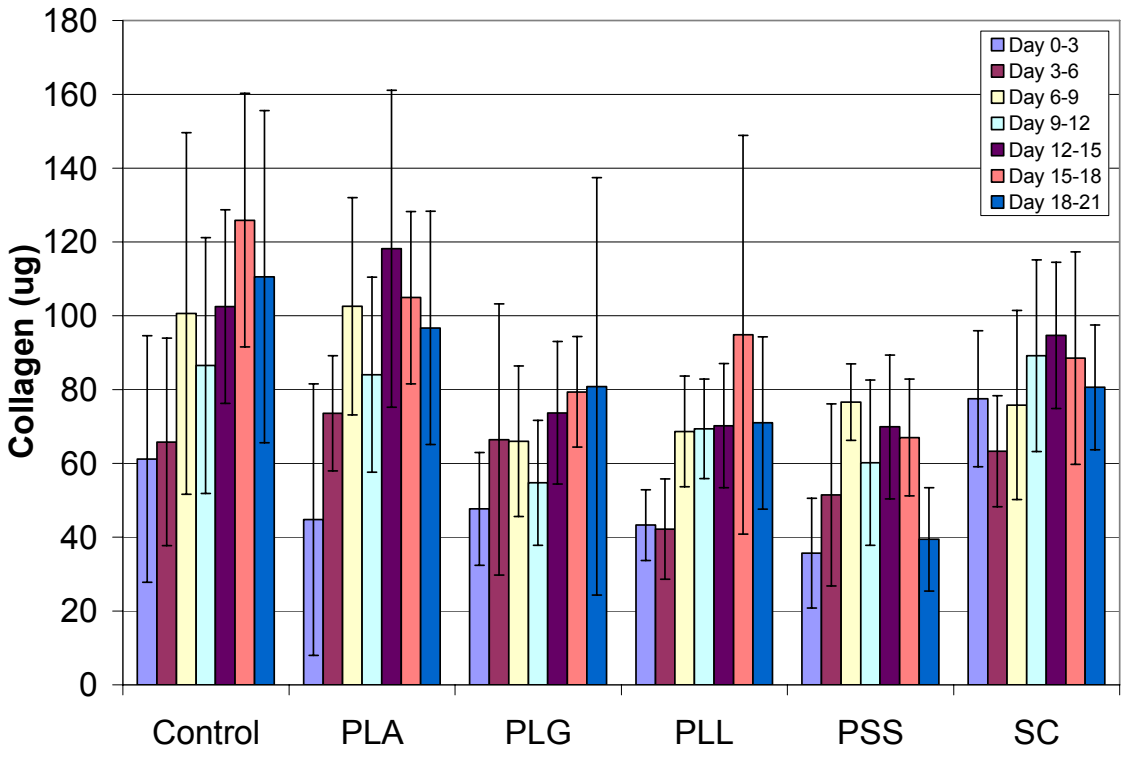

Figure 3.11: Collagen production at each 3 day time point. The number of cells was linearly interpolated from the viability data

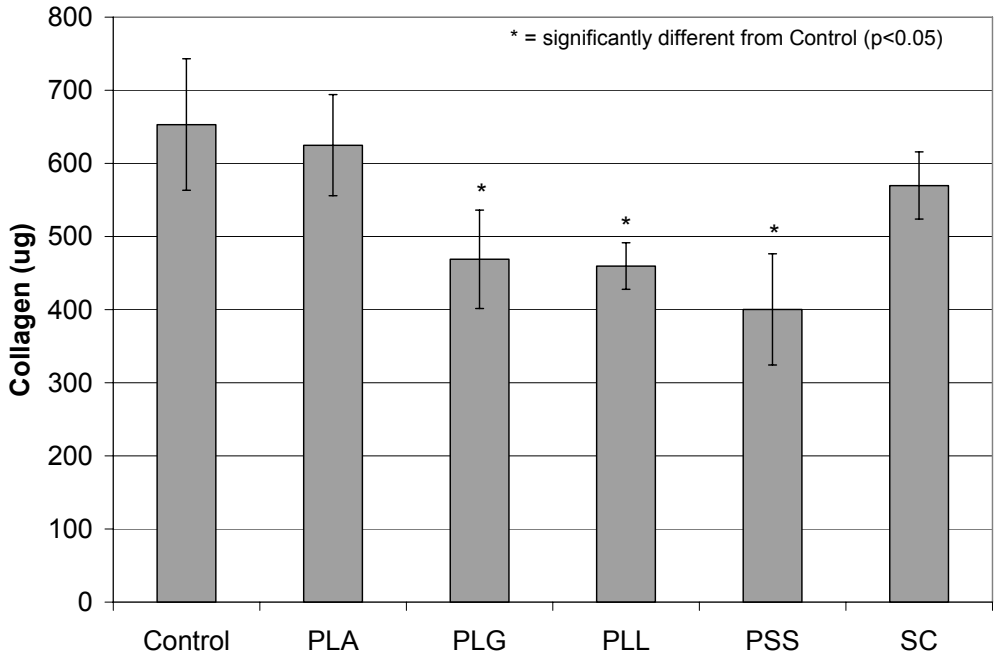

Figure 3.12: Total collagen produced over a 21 day period by osteoblast-like cells either untreated or treated with indicated polyelectrolytes.

3.3.2 Collagen Normalized to Cell Number

The effect on collagen production is also affected by the number of cells present in the well. Therefore, the total collagen production per cell was investigated (see Figure 3.13). The number of cells for each time point was linearly interpolated from the viability data. This shows that the cells have an overall decreasing trend in collagen production/cell over the 21 day time period; the decrease was significant. However, there is not a significant difference comparing control to treated collagen production/cell. But, for the total collagen produced per total cells at the end of the time period, it is seen that PLG, PLL, and SC are all significantly lower than the control (see Figures 3.14 and 3.15). Although PSS causes a decrease in viability of the cells, it does not cause cells

to produce less collagen per cell. Furthermore, PLG increases the number of viable cells at a cost to the collagen production.

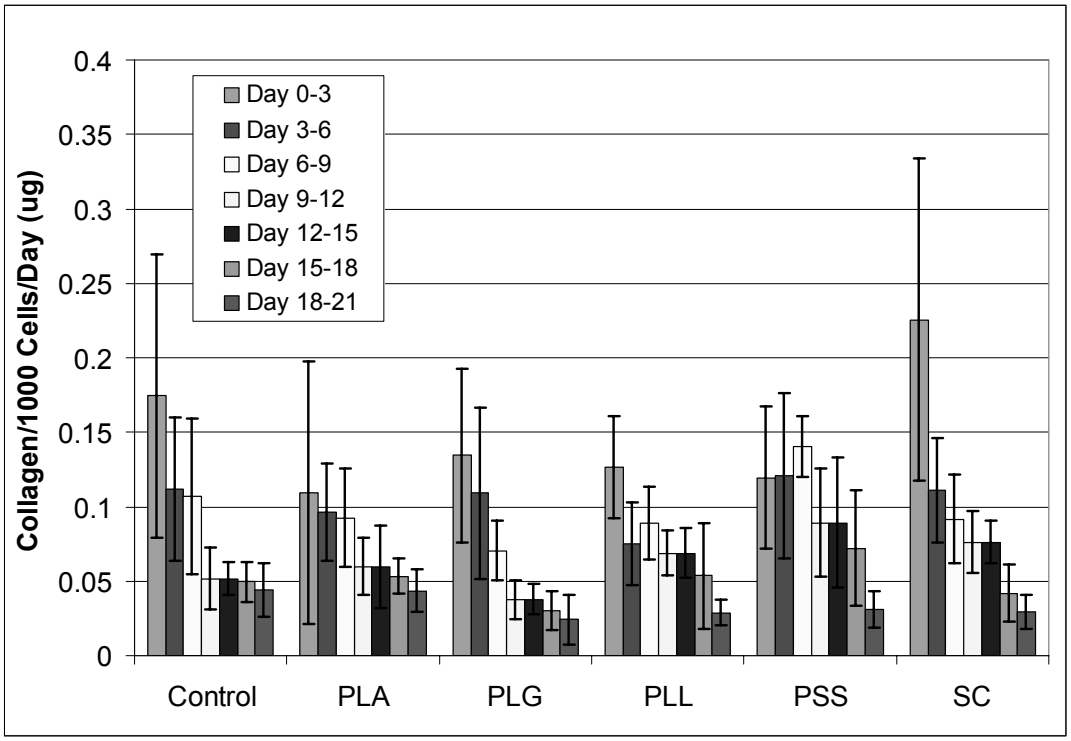

Figure 3.13: Collagen production per cell at each 3 day time point. The number of cells was linearly interpolated from the viability data.

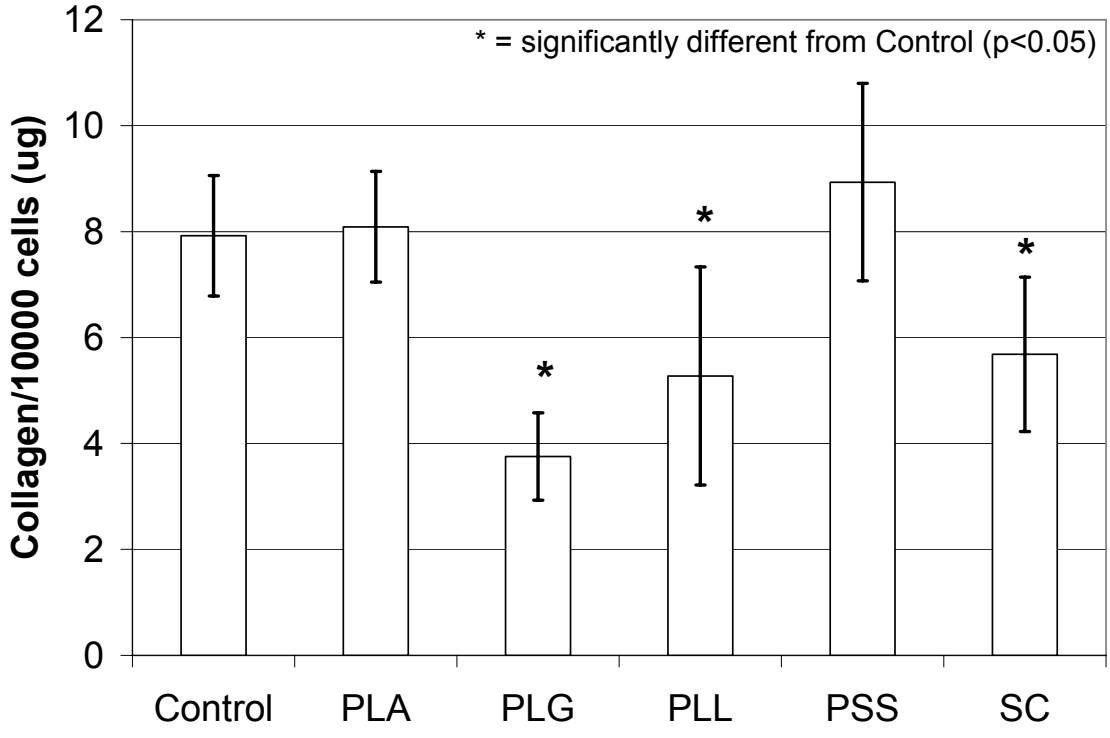

Figure 3.14: Total collagen production per 10,000 cells over a 21 day period by osteoblast-like cells either untreated or treated with indicated polyelectrolytes.

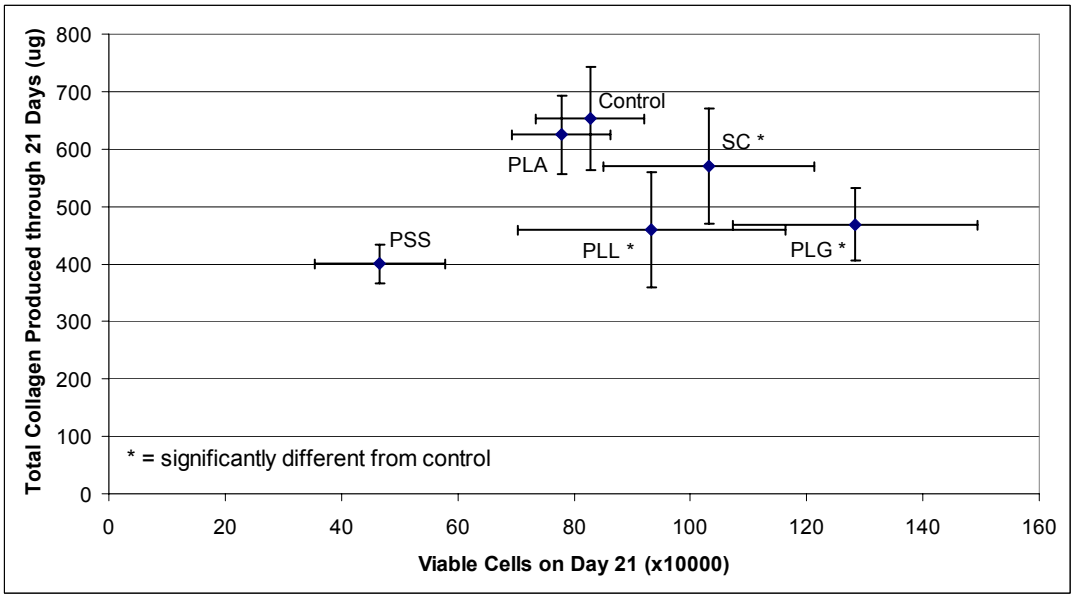

Figure 3.15: Total collagen produced per cell on day 21 compared to overall cell number on day 21. PSS and PLA have similar collagen production per cell; however, PLL, SC, and PLG all significantly inhibit the collagen production of the cells. PLG significantly increases the cell number at the expense of collagen production. PSS significantly decreases the cell number, but does not affect the collagen production on a per cell basis.

Overall, investigation of collagen production has shown that (1) PLG, PLL, and SC treated cells all inhibit type I collagen expression, and (2) although the total amount of collagen produced in PSS treated cells is significantly less than the control, it is because of the number of cells present, not the amount of type I collagen being produced per cell.

3.4 Genotypic Expression

Expression of alkaline phosphatase (ALP), collagen type I, osteonectin (ON), and osteopontin (OP) were investigated using semi-quantitative RT-PCR. The intensity of the band is a relative indicator of how much of the gene is present. Therefore, qualitative comparison can be completed between different treatment groups. Quantitative analysis using real-time RT-PCR was not completed because of the cost (anywhere from $65 to a couple of hundred dollars per primer depending on the real-time method used) and the technical issue regarding uncertainty of which primers would effectively work in PCR. Archived samples could be quantitatively evaluated using real-time RT-PCR. All gels were loaded from left to right in the following order: control, PLA low, PLA high, PLG low, PLG high, PLL low, PLL high, PSS low, PSS high, SC low, and SC high treated cultures.

GAPDH varies slightly between treatment groups (see Figure 3.16). The dosage does not appear to affect the expression. The expression of GAPDH is higher than in the control for PLA, PLG and PLL samples. PSS and SC samples both

have slightly lower expression than the control sample. SC high samples do not show any expression for GAPDH; however, this is due to the inability to obtain a clean RNA isolation. The reverse transcription of SC high RNA was not successful.

The intensity of the ALP expression is approximately the same for the control, PLA, PSS, and SC low samples. PLG high and PLL low samples have higher intensity bands. PLL high sample has no expression. However, the expression of ALP in the PLL high sample was shown at a similar level to all other samples using the staining kit (see Figure 3.16). Therefore, this result may not be accurate, and a problem may have occurred during the PCR or gel electrophoresis protocols. By qualitatively comparing the ALP expression to the GAPDH expression, it is shown that PLA may cause a slight drop in ALP expression, whereas PSS and SC may cause a slight increase in ALP expression. PLG and PLL do not appear to have an effect on ALP expression.

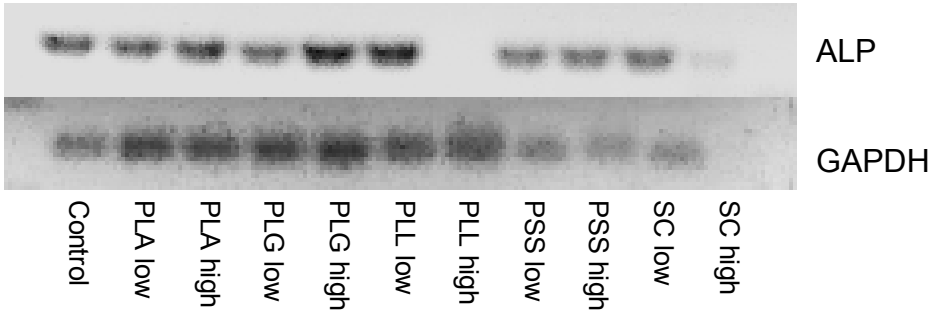

Figure 3.16: Expression of ALP in osteoblast-like cells that are not treated or treated with a specific polyelectrolyte. GAPDH is a gene present in all cells, which is used to qualitatively compare the results. ALP expression appears to be increased in PSS and SC treated samples and inhibited in PLA treated samples.

The intensity of the collagen type I expression is similar for control, PSS, and SC samples (see Figure 3.17). PLA, PLG, and PLL samples have slightly more intense bands. In PSS high samples, the band is nearly absent. By qualitative comparison of the collagen type I expression to the GAPDH expression, it is shown that the polyelectrolyte treatments did not have a large effect on the collagen expression. It may have been slightly inhibited in PLA, PLG, and PLL samples. The slight inhibition of collagen production in PLG and PLL samples is also shown above by the Sircol soluble collagen assay (see Figure 3.15).

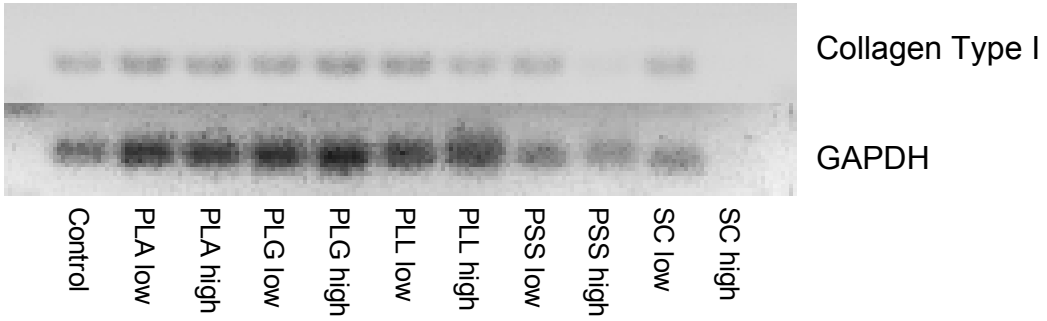

Figure 3.17: Expression of collagen type I in osteoblast-like cells that are not treated or treated with a specific polyelectrolyte. GAPDH is a gene present in all cells which is used to qualitatively compare the results. Collagen type I expression appears to be inhibited slightly in PLA, PLL, and PLG treated samples.

The intensity of osteonectin is higher than in the control for PLA, PLG, PLL, PSS, and SC samples (see Figure 3.18). When qualitatively compared to GAPDH, these results indicate that PSS and SC enhance osteonectin expression, whereas PLA, PLG, and PLL do not have an effect on osteonectin expression.

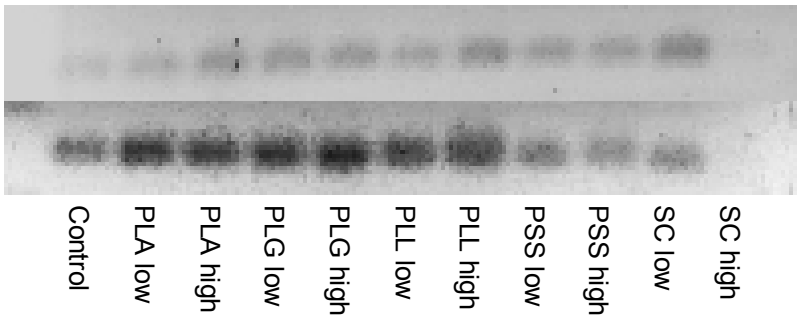

Figure 3.18: Expression of osteonectin in osteoblast-like cells that are not treated or treated with a specific polyelectrolyte. GAPDH is a gene present in all cells which is used to qualitatively compare the results. Osteonectin expression appears to be enhanced in PSS and SC treated cells and inhibited in PLA, PLG, and PLL treated cells.

The intensity of osteopontin tends to be higher in all polyelectrolyte treated samples tested (see Figure 3.19); however, when qualitatively compared to GAPDH, PSS and SC tend to enhance osteopontin expression while PLA, PLG, and PLL do not alter the expression of osteopontin compared to the controls.

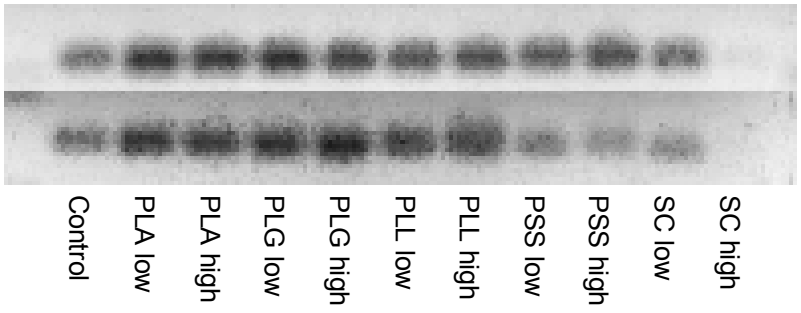

Figure 3.19: Expression of osteopontin in osteoblast-like cells that are not treated or treated with a specific polyelectrolyte. GAPDH is a gene present in all cells, which is used to qualitatively compare the results. Osteopontin expression appears to be enhanced in PSS and SC treated cells and unchanged in PLA, PLG, and PLL treated cells.

Expression of alkaline phosphatase (ALP) was also investigated using alkaline phosphatase kit (#85, Sigma-Aldrich, St. Louis, Missouri, USA). One well from

each treatment group was stained according to the manufacturer's instructions. Fast violet stain was used. The presence of a purple coloration of the cells indicates production of alkaline phosphatase. All cultures tested showed vivid purple coloration, indicating strong ALP expression (see Table 3.13). This agrees with the RT-PCR results, which also showed strong expression of ALP. Overall, (1) genetic expression was not inhibited by polyelectrolytes. (2) Mineralization should proceed as normal since required genes are not affected.

Table 3.13: Expression of alkaline phosphatase in osteoblast-like cells either not treated or treated with a specific polyelectrolyte. All cultures showed strong expression of ALP indicated by the purple coloration.

Treatment	Low Dosage	High Dosage
Control	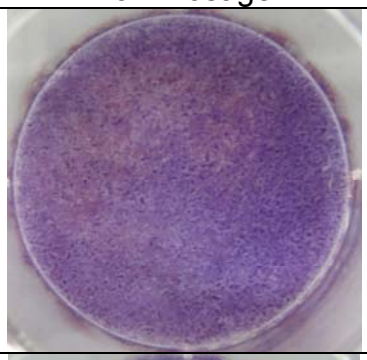	
PLA	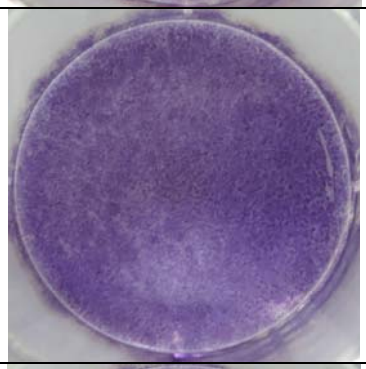	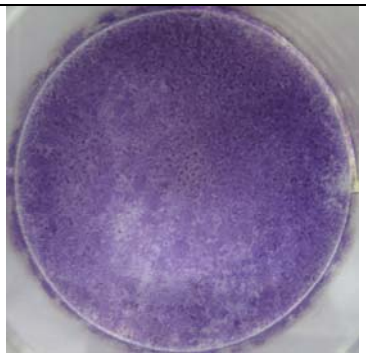
PLG	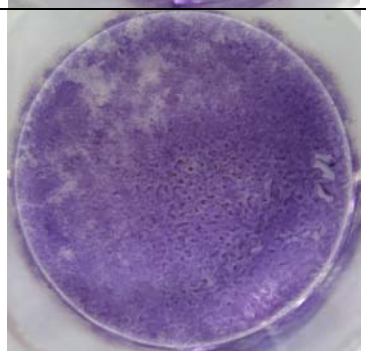	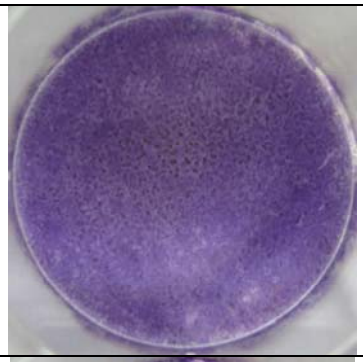
PLL	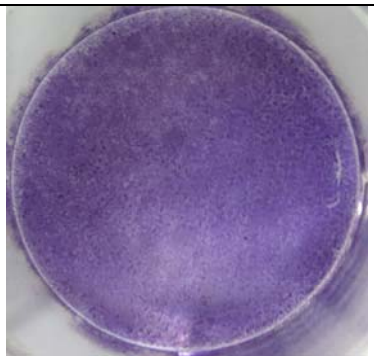	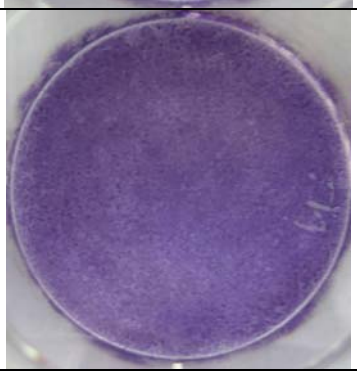

3.5 Interpretation of the Results of the Non-mineralizing Experiments

Cell morphology was maintained in all cultures compared to controls except in PSS treated cultures. Nagahata has also shown that normal human osteoblasts maintain morphology on cationic polyelectrolyte films made of chitosan. [23] In our study, both PLL and SC are cationic and showed no obvious change in morphology. Furthermore, Tryoen-Toth has shown that on PLG, PLL, and PSS polyelectrolyte films, osteoblast-like cells and human periodontal ligament cells maintained normal morphology. [24] Again, the results agree for PLG and PLL, which both maintained the morphology; however, over a period of 21 days, the cells treated with PSS changed their morphological characteristics in the current study. Tryoen-Toth may not have seen the change since cells were only studied for up to 48 hours, at which point the cells treated with PSS still looked similar to controls. Furthermore, the polyelectrolyte was in a thin-film, which may not have the same effect PSS would have in solution. Overall, the osteoblast-like cells maintain their characteristic morphology showing that PLA, PLG, PLL and SC are potentially biocompatible for extended periods of time. PLG and PLL are currently used in biological applications; therefore, they are considered biocompatible at certain concentrations. [24] However, prolonged exposure to PSS may have detrimental effects. This is seen by the change in morphology to a more spindle-like shape, and cell death as the cells begin to detach from the plate after approximately 2 weeks.

In the current study, it was shown that over the course of 21 days PLG caused an increase in cell number, whereas PSS caused a decrease in cell number. The decrease in cell number caused by PSS is also causing cells to detach from the plate. Therefore, the decreased viability may be a result of cell death and not lack of cell division. It is likely that the decrease in cell number is a combination of cell death and decreased cell growth since the morphology is changed and cells began lifting from the plate. It has been shown that PLL increases cell proliferation. [25,26] In the current study, the PLL cell number was slightly increased compared to the control, but not significantly. This may be a result of the small sample number (n=4) in the current study. Higher sample numbers would likely decrease the standard deviations, allowing trends to be observed more clearly. However, the proliferation of the PLL treated cells in studies by Torricelli was measured using the MTT proliferation assay, which is a spectrophotometric measure of the metabolic activity of the cells, which correlates to the number of cells present. [25,26] It assumes that all cells are metabolically similar. However, as seen in RT-PCR, GAPDH presence is actually higher in PLA, PLG, and PLL treated cells compared to the control, indicating higher metabolic activity. Therefore, the MTT proliferation assay results may be skewed due to differences in cellular metabolic activity.

PLG, PLL, and PSS had significantly lower total type I collagen production over the 21 day study. Since collagen is produced by the cells, the collagen production was then normalized to the total number of cells present on day 21.

This resulted in total collagen produced per cell. It was then seen that although PSS had significantly lower total collagen, the collagen on a per cell basis is similar to the control. PLG, PLL, and SC all had significantly lower collagen production per cell over the course of 21 days. PLG treated cells had significantly more proliferation compared to control cells according to the viability data, but this was at the expense of collagen production. Fini showed type I collagen production to be increased in normal osteoblasts and osteopenic osteoblasts when treated with both PLL and poly-L-arginine. [27] However, when lysine alone was investigated, there was no effect on type I collagen production. Fini stated that this may be due to the *in vivo* role of PLL to increase calcium uptake and retention. [27]

Expression of various genes was not significantly altered due to the polyelectrolyte treatments. ALP activity was not detrimentally affected, showing that osteoblast-like cells treated with polyelectrolytes should still be able to cleave the phosphate in order to make mineral crystals. The other genes investigated also have roles in mineralization. Since none of the genes were severely altered, the osteoblast-like cells should retain the ability to create mineral crystals given the appropriate environment. Other studies have shown varied results in ALP expression. Torricelli showed PLL to increase ALP expression; however, in another study by Torricelli, it was shown that the combination of PLL and poly-L-arginine decrease ALP expression in both treated and control cells. [25,26] Tryoen-Toth has shown ALP expression to be

maintained at control levels for 24 hours in PLG, PLL, and PSS treated cells. Therefore, it is not clear what role polyelectrolytes have in alkaline phosphatase expression.

The non-mineralizing results show that the polyelectrolytes are affecting the osteoblast-like cells in unique ways. PLA and SC do not seem to be altering cellular processes compared to control cells. PLG is causing an increase in proliferation but at a cost to collagen production compared to control cells. PLL is causing a decrease in collagen production capacity compared to control cells. PSS adversely affect cellular morphology and viability, but does not affect the amount of collagen being produced per cell compared to control cells. All treatments allow typical genetic expression to occur, indicating all treated cells have the capacity to produce mineralized nodules in an appropriate environment. Since all polyelectrolytes resulted in viable cells with the capacity for mineralization, all polyelectrolytes were used to study mineralization characteristics. Dosage did not seem to affect any of the investigated cellular responses; therefore, only the high dosage was investigated in mineralizing cultures.

Chapter 4: Mineralizing Culture Results and Discussion

4.1 Raman Spectroscopy

Cell cultures were allowed to mineralize for 21 days using growth media supplemented with β-glycerophosphate and ascorbic acid. In addition, high dosages of polyelectrolytes were added daily to selected cultures. At the end of 21 days, all cultures were fixed using an ethanol procedure to stop and preserve all cellular growth. Raman spectroscopy was completed on twenty bone nodules in each treatment group. Each spectrum in a given nodule was scanned using 3 averages at 4 minutes per scan to get one spectrum.

Average Raman peak positions, intensities, and other parameters are listed in Table 4.01 (see Appendix H for typical Raman spectra). Appendix I contains raw data regarding phosphate peak position, crystallinity, mineralization, and carbonation. Of most interest is the information about the mineral crystals that can be obtained from the Raman spectrum. Carbonated hydroxyapatite is the inorganic component typically found in bone. It shows several Raman peaks, with the strongest at approximately 960 cm^{-1} corresponding to PO_4. From the 960 cm^{-1} peak, the crystallinity defined as, $1/PO_4$ bandwidth, can be calculated. Also, the mineralization can be calculated by comparing the normalized peak

intensities of PO_4 to CH_2wag. Changes in these parameters compared to the controls indicate the mineral is altered in some fashion.

Table 4.01: Raman spectral data obtained from bone nodules grown *in vitro*. Cultures were treated with specified polyelectrolyte or left untreated to use as controls. Of primary interest is the mineral peak of PO_4 (v1PO4f) and the information obtained using that peak, specifically crystallinity (PO4BW) and mineralization (mn_CH2wg). Changes in these parameters indicate the mineral is somehow altered. (Continued on next page.)

Treatment	Control		PLA		PLG		PLL		PSS		SC	
	Average	Std Dev	Average	Std Dev	Average	Std Dev	Average	Std Dev	Average	Std Dev	Average	Std Dev
V1PO4f	959.562	1.565	958.649	0.431	959.610	1.354	959.923	1.347	958.254	1.867	961.238	0.387
V1PO4i	0.923	0.019	0.928	0.014	0.927	0.017	0.912	0.026	0.855	0.031	0.925	0.012
PO4BW	0.045	0.005	0.047	0.002	0.047	0.002	0.045	0.002	0.030	0.004	0.046	0.002
PO4hmg	0.250	0.000	0.250	0.000	0.250	0.000	0.250	0.000	0.250	0.000	0.250	0.000
PO4hml	0.461	0.009	0.464	0.007	0.464	0.009	0.456	0.013	0.427	0.015	0.462	0.006
V3HPO4f	1002.430	1.382	1001.414	0.514	1002.367	1.560	1002.524	1.472	1003.202	1.810	1003.599	2.193
V3HPO4i	0.151	0.057	0.154	0.043	0.158	0.070	0.214	0.100	0.375	0.100	0.160	0.051
V3POf	1031.055	5.181	1030.695	4.191	1031.940	5.340	1031.639	3.801	1033.551	3.640	1035.357	3.494
V3POi	0.105	0.050	0.104	0.021	0.122	0.035	0.135	0.053	0.173	0.033	0.108	0.031
V1CO3f	1072.420	2.496	1069.930	2.101	1071.358	4.383	1069.314	7.664	1077.271	5.486	1072.706	4.000
V1CO3i	0.106	0.026	0.106	0.010	0.136	0.024	0.134	0.033	0.157	0.041	0.110	0.016
amd3af	1246.753	5.398	1244.998	5.818	1246.998	3.359	1245.486	5.661	1253.243	4.139	1249.921	4.386
amd3ai	0.050	0.042	0.048	0.025	0.059	0.041	0.071	0.056	0.136	0.056	0.042	0.025
amd3bf	1262.149	10.498	1258.246	7.836	1259.104	8.881	1258.331	6.252	1257.155	6.448	1256.529	5.399
amd3bi	0.044	0.039	0.040	0.025	0.049	0.037	0.056	0.041	0.135	0.056	0.039	0.020
CH2wgf	1453.122	6.497	1451.551	4.102	1450.007	3.813	1450.283	5.805	1451.005	3.439	1452.994	3.973
CH2wgi	0.087	0.057	0.094	0.041	0.134	0.078	0.173	0.121	0.310	0.106	0.094	0.059
amd1f	1660.060	8.052	1660.837	7.797	1665.160	7.942	1664.309	7.269	1669.005	5.315	1659.451	6.472
amd1i	0.089	0.088	0.082	0.036	0.091	0.043	0.115	0.074	0.167	0.093	0.080	0.041
Av1PO4	58.328	6.157	55.916	2.141	56.700	3.236	59.190	4.250	76.768	5.865	56.266	2.625
Aamd3	2.864	2.144	3.009	1.591	3.126	1.668	3.199	2.677	7.101	3.375	2.179	1.413
ACH2wg	6.323	3.579	6.831	2.583	9.296	4.994	12.240	8.133	20.717	6.772	6.692	3.860
Aamd1	8.823	4.858	9.753	3.611	10.962	4.851	13.329	7.598	14.654	10.243	8.991	4.101
ACH2stG	1.503	1.017	1.596	0.760	1.981	1.532	2.207	1.739	5.343	2.131	1.559	0.885
RCO3	0.115	0.033	0.114	0.012	0.147	0.028	0.148	0.041	0.184	0.048	0.119	0.019
RHPO4	0.165	0.069	0.166	0.049	0.171	0.080	0.237	0.116	0.443	0.127	0.173	0.058
mn_amd1	14.658	5.997	12.963	4.388	12.541	5.602	11.787	6.965	9.198	10.367	13.864	5.409
mn_amd3a	27.654	14.674	24.714	13.980	22.036	11.372	22.209	14.634	7.707	4.061	35.284	44.463
mn_amd3b	35.731	24.950	30.852	18.209	29.934	20.759	30.477	22.954	7.865	4.429	35.478	38.139
mn_CH2wg	13.285	5.671	11.396	3.756	9.346	5.011	9.207	6.657	3.256	1.824	12.585	5.305
RAPO4_amd3	30.736	22.950	29.072	29.876	32.850	53.613	39.149	89.051	14.396	9.830	24.104	15.726
RAPO4_CH2wg	11.013	4.213	9.070	2.638	7.648	3.410	7.630	4.854	4.145	1.483	10.125	3.583
RAPO4_amd1	7.967	3.125	6.339	1.925	6.006	2.144	5.811	2.758	5.856	14.970	7.362	2.870
vCCaf	815.464	0.009	815.449	0.006	815.470	0.016	815.048	0.460	815.177	0.397	815.466	0.014

Table 4.01: Raman spectral data obtained from bone nodules grown *in vitro*. Cultures were treated with specified polyelectrolyte or left untreated to use as controls. Of primary interest is the mineral peak of PO_4 (v1PO4f) and the information obtained using that peak, specifically crystallinity (PO4BW) and mineralization (mn_CH2wg). Changes in these parameters indicate the mineral is somehow altered. (Continued from previous page.)

vCCai	0.006	0.015	0.002	0.016	-0.001	0.012	0.002	0.029	0.002	0.035	-0.002	0.018
dCCHf	855.344	0.008	855.330	0.006	855.351	0.016	855.427	0.051	855.355	0.117	855.345	0.015
dCCHi	0.043	0.031	0.040	0.014	0.034	0.024	0.050	0.030	0.087	0.048	0.039	0.020
labCO3f	1100.680	0.010	1100.665	0.005	1100.686	0.017	1100.760	0.051	1100.740	0.143	1100.683	0.014
labCO3i	0.033	0.018	0.032	0.013	0.038	0.014	0.039	0.019	0.070	0.015	0.033	0.014
vCCbf	1130.160	0.010	1130.145	0.005	1130.166	0.017	1130.240	0.051	1130.172	0.112	1130.163	0.014
vCCbi	0.017	0.011	0.013	0.007	0.025	0.019	0.030	0.026	0.139	0.056	0.023	0.013
dCOOf	1424.850	0.010	1424.835	0.005	1424.857	0.018	1424.930	0.041	1424.910	0.133	1424.854	0.011
dCOOi	0.024	0.011	0.029	0.013	0.052	0.029	0.036	0.027	0.073	0.037	0.022	0.011
vCCHf	1605.155	0.005	1605.145	0.005	1605.161	0.012	1605.220	0.041	1605.162	0.098	1605.156	0.011
vCCHi	0.021	0.019	0.019	0.011	0.019	0.014	0.030	0.019	0.030	0.028	0.017	0.011
vC_Cf	1637.185	0.005	1637.175	0.005	1637.191	0.012	1637.255	0.046	1637.195	0.102	1637.186	0.011
vC_Ci	0.034	0.016	0.037	0.014	0.039	0.016	0.051	0.031	0.032	0.050	0.034	0.014

The PO_4 peak location changes according to the maturity of the mineral crystal. As the mineral crystal matures, the peak shifts from about 954 cm^{-1} closer to 961 cm^{-1}. The control sample is at 959.5 cm^{-1} (see Figure 4.01). SC treated nodules have a peak location significantly higher than the control nodules, indicating the mineral crystals are more mature. PSS treated nodules have a peak location significantly lower than the control nodules, indicating the mineral crystals are less mature.

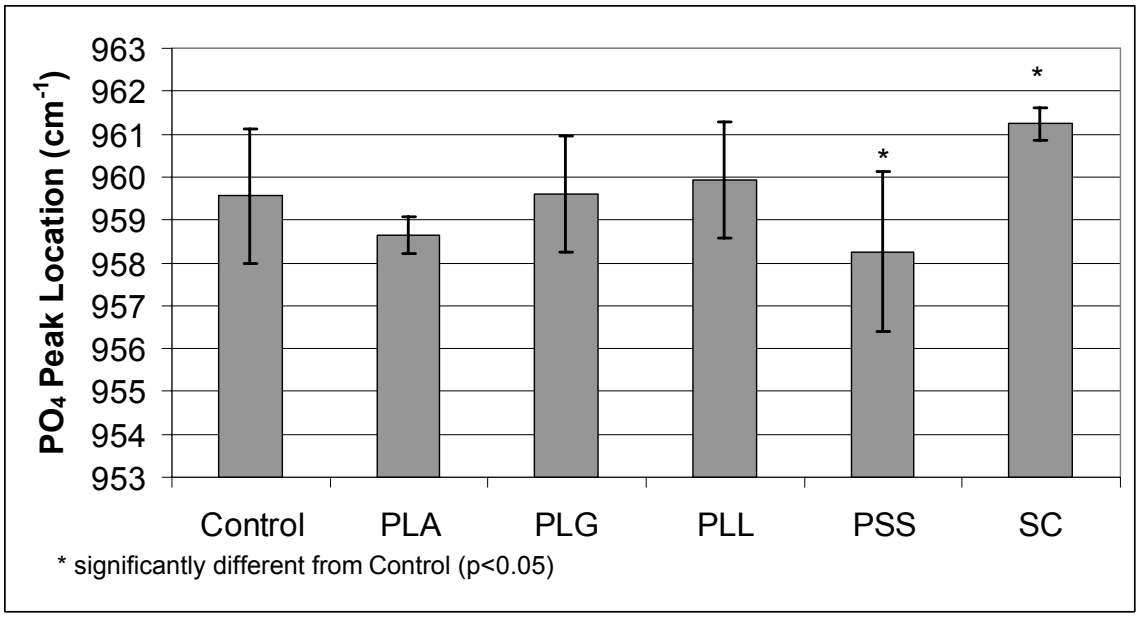

Figure 4.01: PO_4 peak locations for untreated and polyelectrolyte treated bone nodules grown *in vitro*. As the mineral matures, the peak location gets closer to 961 cm^{-1}. PSS treated nodules are significantly lower than control nodules, whereas SC treated nodules are significantly higher than control nodules.

Crystallinity is defined as the inverse of the full-width at half maximum of the PO_4 bandwidth. It is an indication of the perfection of the crystal structure. The higher the number, the more perfect the crystal structure. PSS treated nodules have significantly lower crystallinity than the control nodules (see Figure 4.02). This indicates that the crystal structure is less perfect, less ordered, than the control cultures and other polyelectrolyte treated cultures.

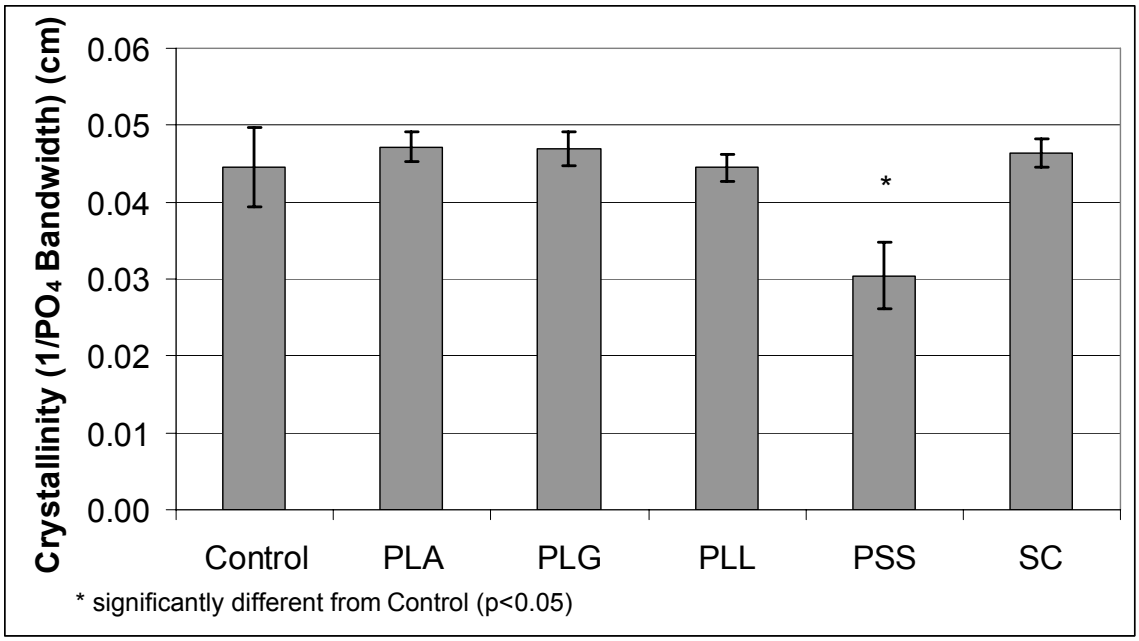

Figure 4.02: Crystallinity for untreated and polyelectrolyte treated bone nodules grown *in vitro*. As the mineral becomes more perfect, the crystallinity increases. PSS treated nodules show significantly lower numbers than control nodules, indicating a more disordered crystal structure.

Mineralization is defined as the ratio of the PO_4 intensity over the CH_2wag intensity. CH_2wag is a peak caused by the organic portion of bone; therefore, mineralization compares the inorganic to the organic portion of bone. The higher the number, the more mineralized the nodule. PSS treated nodules have significantly lower mineralization than the control nodules (see Figure 4.03). This indicates that there is less mineral crystal in the organic matrix compared to the control cultures and other polyelectrolyte treated cultures. Therefore, PSS treated nodules are less mature, more amorphous, and less mineralized than control cultures and other polyelectrolyte treated cultures.

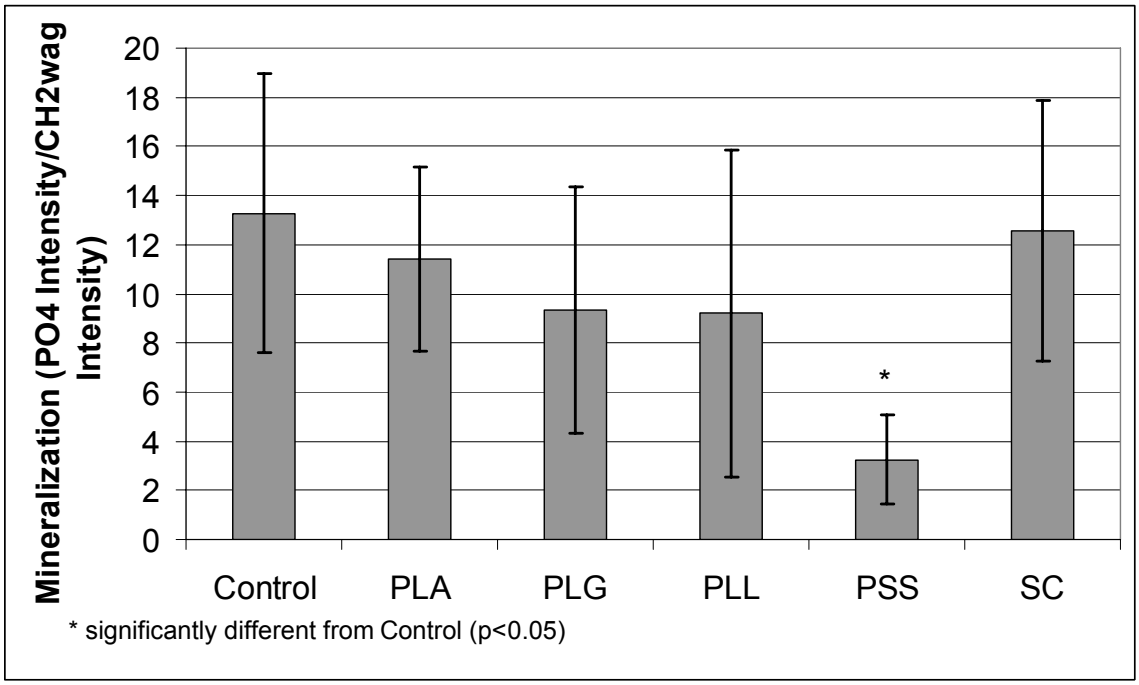

Figure 4.03: Mineralization for untreated and polyelectrolyte treated bone nodules grown *in vitro*. As the mineral/collagen ratio increases, the mineralization increases. Numbers for PSS treated nodules are significantly lower than control nodules, indicating a smaller amount of mineral crystal in the organic matrix.

Carbonation is the ratio of the intensity of the CO_3 peak to the PO_4 peak. The higher the number, the more carbonate is substituted for phosphate in the mineral crystal. PLG, PLL, and PSS treated nodules have significantly more carbonation than the control nodules (see Figure 4.04). This indicates that PLG, PLL, and PSS are facilitating substitution of the carbonate in place of the phosphate.

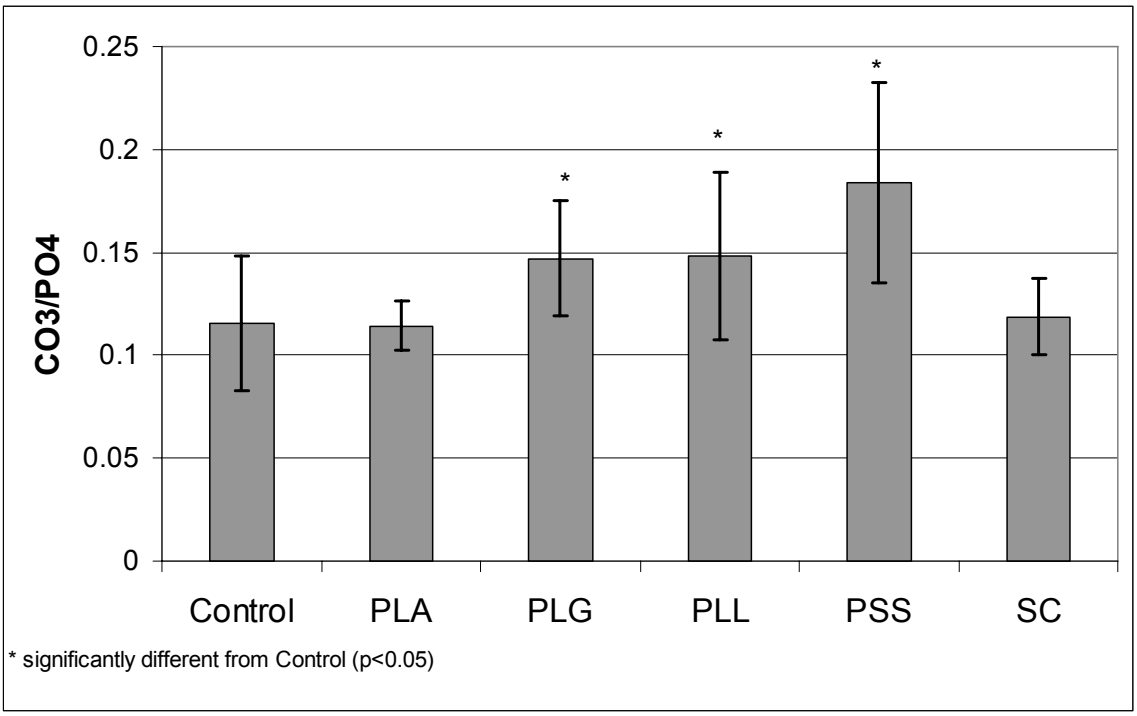

Figure 4.04: Carbonation for untreated and polyelectrolyte treated bone nodules grown *in vitro*. Higher carbonation indicates a higher number of carbonate substitutions for phosphates in the mineral crystal. PLG, PLL, and PSS treated nodules have significantly higher carbonation than control nodules, indicating an increased amount of carbonate substitution for phosphate in the mineral crystal.

4.2 X-Ray Diffraction

X-ray diffraction was carried out on bone nodules scraped from the plastic cell culture well. Specifically, three wells of a common treatment group were scraped and pooled to obtain enough material to acquire results. Four samples from each treatment group (control, PLA, PLG, PLL, and SC) were tested. PSS had only one sample tested because the nodules obtained did not result in an x-ray diffraction pattern. Since there was a similar amount of nodules scraped; this may be due to a lack of defined crystalline structure and the relative lack of mineralization. The Raman spectroscopy results support the lack of crystalline

structure; it was found that PSS was much less crystalline and more amorphous than the other samples.

Individual peaks corresponding to the 002 plane (~26.1°), 130 plane (~39.8°), and the 004 plane (~53.6°) were investigated. The 002 and 004 planes are planes along the same crystal direction; therefore, the crystal lengths obtained from these two directions should be very similar. The measurement for the length along the 002 and 004 planes was averaged for each sample to determine the average length along that plane. Average peak locations, intensities, and FWHM values were determined (see Table 4.02). Appendix L lists raw data. Appendix M shows typical XRD patterns. From this information, crystal lengths in the specified directions were calculated (see Figure 4.05). It was found that none of the crystals were significantly different from crystals in other treatment groups. This may be due to the very small sample number. Furthermore, it is expected that if data could have been obtained for PSS treated crystals, the crystal lengths would have been different. The ratio of crystal lengths in the 002 direction to the 130 direction were calculated (see Figure 4.06). Data analysis confirmed that there was not a significant difference in the aspect ratio of the mineral crystals for any of the treatment groups.

Table 4.02: X-ray diffraction data obtained from bone nodules grown *in vitro*. Cultures were treated with specified polyelectrolytes or left untreated to use as controls. Of primary interest are the 002, 004, and 130 planes. From these peaks, crystal length along these directions can be calculated.

Treatment	Control		PLA		PLG		PLL		SC	
Pattern_ID	Avg	STD	Avg	STD	Avg	STD	Avg	STD	Avg	STD
002p_d	26.15	0.05	26.16	0.06	26.24	0.01	26.21	0.05	26.22	0.05
002p_r	0.46	0.00	0.46	0.00	0.46	0.00	0.46	0.00	0.46	0.00
002i	623.71	230.01	753.09	131.12	1083.09	301.98	774.10	282.87	900.07	274.47
002FWHM_d	0.55	0.06	0.57	0.01	0.60	0.03	0.58	0.01	0.58	0.05
002FWHM_r	0.01	0.00	0.01	0.00	0.01	0.00	0.01	0.00	0.01	0.00
130p_d	39.81	0.05	39.90	0.15	39.87	0.12	39.91	0.10	39.83	0.10
130p_r	0.69	0.00	0.70	0.00	0.70	0.00	0.70	0.00	0.70	0.00
130i	159.18	73.40	202.87	61.91	262.82	74.61	198.52	106.64	244.68	59.30
130FWHM_d	1.60	0.10	1.68	0.10	1.87	0.17	1.91	0.51	1.78	0.12
130FWHM_r	0.03	0.00	0.03	0.00	0.03	0.00	0.03	0.01	0.03	0.00
004p_d	53.58	0.09	53.58	0.08	53.67	0.04	53.59	0.10	53.68	0.07
004p_r	0.94	0.00	0.94	0.00	0.94	0.00	0.94	0.00	0.94	0.00
004i	197.73	101.17	270.97	73.75	414.64	78.38	259.25	119.16	322.77	80.43
004FWHM_d	0.86	0.02	0.76	0.03	0.74	0.04	0.86	0.10	0.81	0.03
004FWHM_r	0.01	0.00	0.01	0.00	0.01	0.00	0.02	0.00	0.01	0.00
L002 (nm)	17.81	0.78	19.36	0.76	19.03	1.70	17.86	1.50	18.66	1.37
L130 (nm)	6.88	0.45	6.54	0.40	5.87	0.55	6.11	1.99	6.16	0.45
L002/L130	2.58	0.23	2.97	0.18	3.27	0.40	3.16	1.01	3.04	0.25

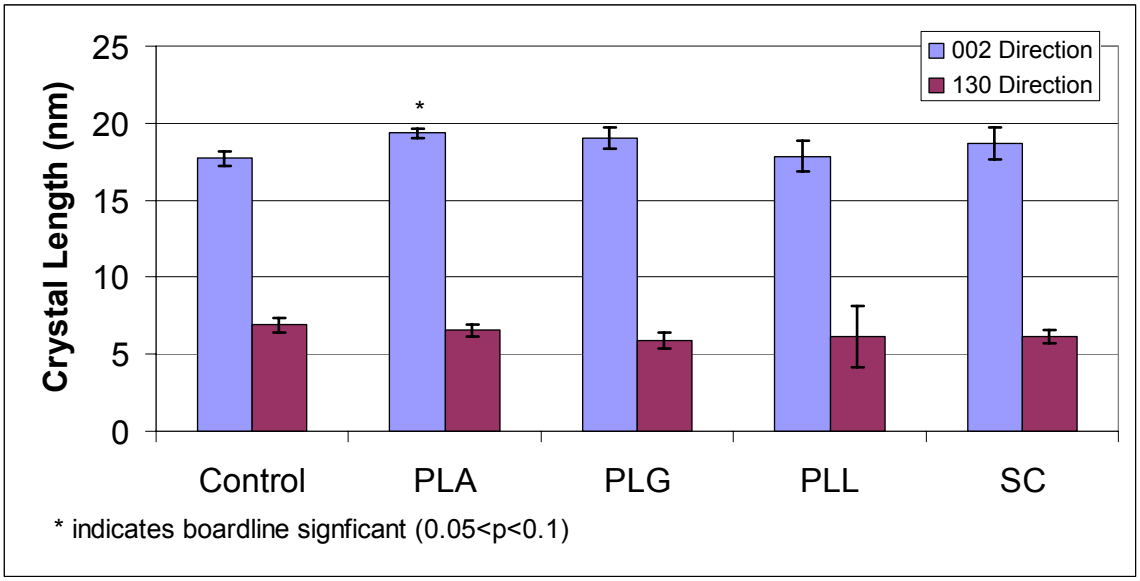

Figure 4.05: Crystal lengths along given directions for untreated and polyelectrolyte treated bone nodules grown *in vitro* as determined by x-ray diffraction. PSS data is not included because the nodules were too amorphous to obtain an x-ray diffraction pattern.

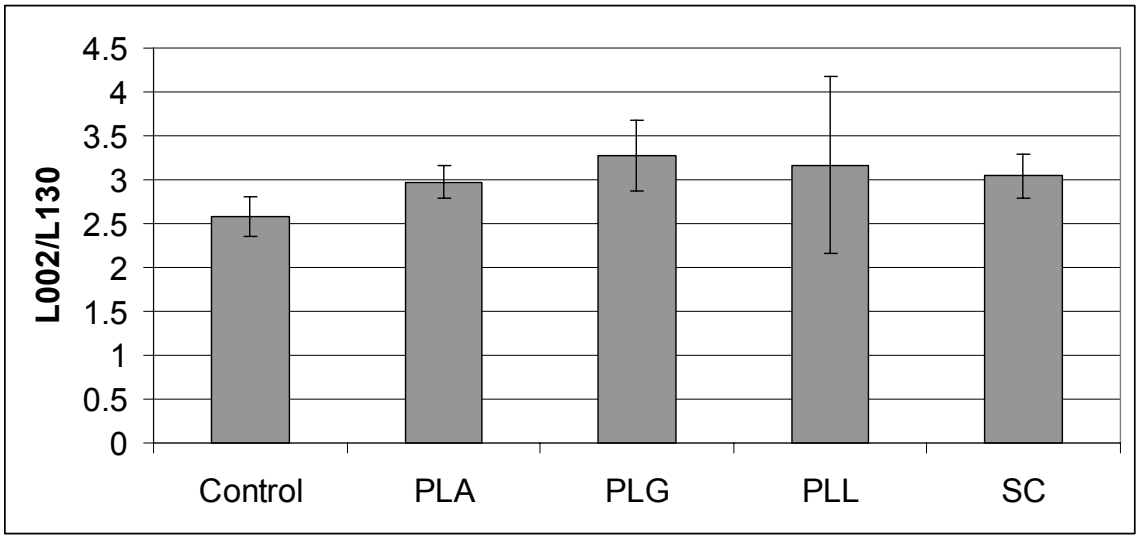

Figure 4.06: Aspect ratio of 002 direction crystal length to the 130 direction crystal length for untreated and polyelectrolyte treated bone nodules grown *in vitro* as determined by x-ray diffraction. PSS data is not included because the nodules were too amorphous to obtain an x-ray diffraction pattern.

4.3 Vickers Microhardness

Vickers microhardness testing was completed on bone nodules which were embedded, sectioned, and polished from three wells of each treatment group. All samples obtained from each treatment group (control: n=27, PLA: n=29, PLG: n=9, PLL: n=36, PSS: n=7, and SC: n=48) were tested.

Average Vickers microhardness values are shown in Figure 4.07 below. Appendix N lists raw data. No statistical significance was found between the treatment groups using ANOVA. The Vickers microhardness value of plastic, approximately 10, was much different than that of bone nodules; this shows that the nodules were truly on the surface of the section and hardness of the plastic was not being measured.

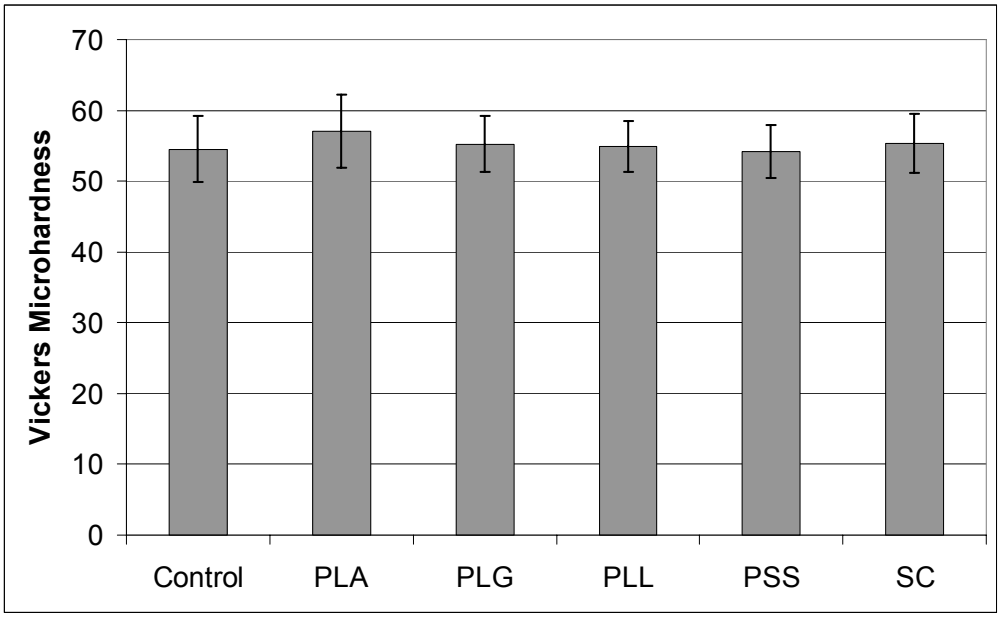

Figure 4.07: Vickers microhardness of bone nodules grown *in vitro* treated with polyelectrolyte. No statistical difference was seen between different treatment groups.

4.4 Interpretation of the Results of the Mineralizing Experiments

Raman spectroscopy revealed that treatment with PSS resulted in much different mineral characteristics compared to control treatment. Osteoblast-like cells treated with PSS grew bone nodules that were much less mature, less crystalline, and less mineralized than either the control cells or the cells treated with any of the other polyelectrolytes (PLA, PLG, PLL, or SC). Overall, PSS treatment resulted in amorphous bone nodules. This lack of order to the bone nodule resulted in no detectable peaks in the XRD pattern. These results are supported by benchtop studies that indicated that specific concentrations of PSS in solution can result in changes in nucleation and crystal growth. [5-8]

Analysis of XRD patterns showed that PLA modulated the length of the crystal in the 002 direction, resulting in approximately a 10% increase in length. Eanes

found in benchtop studies that PLA resulted in 20% thicker crystals. [5] In the same study, it was found that PLG also resulted in 20% thicker crystals; this result was not confirmed by this study. [5] Bigi also found that PLA and PLG modify the structure of the crystals, the specific changes were not reported. [28] This implies that thickness may be a function of the concentration of the polyelectrolyte present in the solution.

Vickers microhardness did not show any difference between any of the treatment groups. Torricelli also found that bone nodules which were grown during treatment with poly-L-arginine and PLL were not significantly different from bone nodules grown under control conditions; both had microhardness values of about 60 which is similar to the values found in this study. [29] However, all of these studies were completed *in vitro*; thus, the results may be different using *in vivo* studies. One of the components missing when using *in vitro* studies is the cyclic loading of the bone. The loading and unloading cycle may result in the alignment of collagen fibers, whereas the bone nodules grown *in vitro* do not have any alignment to their collagen fibers. This alignment may result in an overall stronger nodule. Depending on how the mineral crystals interact in the aligned collagen, the overall hardness of the bone nodules may change with the changing alignment of collagen. Furthermore, the crystals themselves are not measured, the combination of the collagen, mineral crystal, and other organics and inorganics in the bone nodule are measured. It was shown that PSS treated nodules resulted in similar hardness to other treated and untreated nodules,

whereas the mineralization of these nodules was significantly lower than for the control or other treated nodules. This is because the hardness is not just a measure of the mineral crystal, but the overall bone nodule as stated earlier.

The current study has demonstrated that polyelectrolyte administration can affect the geometry and stoichiometry of mineral crystals grown under *in vitro* conditions. The effect varied between polyelectrolytes, with PSS treatment yielding the most amorphous crystal structure with higher carbonate substitution. PLL and PLG treatment caused higher carbonate substitutions within the mineral crystals, probably by facilitating the diffusion of carbonate ions in the vicinity of growing mineral crystals. Polyelectrolytes may also affect the crystal growth directly by binding on crystal surfaces or indirectly by affecting cellular activity.

The results of this preliminary study indicate that polyelectrolytes can selectively alter carbonated hydroxyapatite crystal size, morphology, and stoichiometry *in vitro*. The effects of these changes in crystal structure on the hardness may be investigated as the next step using nanoindentation tests. The size of the mineral crystals is on the order of nanometers; therefore, nanoindentation would need to be completed to determine the hardness values for the mineral crystals. Further investigation of other polyelectrolytes as well as a broader study of current polyelectrolytes needs to be conducted to identify those that can positively influence bone strength via tailoring carbonated hydroxyapatite crystal

quality. In the long term, such a modality could be utilized to improve bone quality and help alleviate fracture risk.

Appendix A: Sample Assignments

Non-mineralizing Cultures	Control	PLA		PLG		PLL		PSS		SC	
Evaluation Procedure (Day of Study Completed)	Low	Low	High	Low	High	Low	High	Low	High	Low	High
Photograph (Days 0, 3, 6, 9, 12, 15, 18, 21)	151	451	454	751	754	1051	1054	1351	1354	1651	1654
ALP Assay (Day 21)	151	451	454	751	754	1051	1054	1351	1354	1651	1654
Purify RNA (Day 21)	152	452	455	752	755	1052	1055	1352	1355	1652	1655
	153	453	456	753	756	1053	1056	1353	1356	1653	1656
Count (Day 7)	251	351	551	651	851	951	1151	1251	1451	1551	1751
	254	354	554	654	854	954	1154	1254	1454	1554	1754
Count (Day 14)	252	352	552	652	852	952	1152	1252	1452	1552	1752
	255	355	555	655	855	955	1155	1255	1455	1555	1755
Count (Day 21)	253	353	553	653	853	953	1153	1253	1453	1553	1753
	256	356	556	656	856	956	1156	1256	1456	1556	1756
Collagen (Days 3, 6, 9, 12, 15, 18, 21)	253	353	553	653	853	953	1153	1253	1453	1553	1753
	256	356	556	656	856	956	1156	1256	1456	1556	1756

Note: The numbers within the table are the code numbers used to identify the individual wells throughout the culture duration and experimental evaluation.

Mineralizing Cultures	Control	PLA	PLG	PLL	PSS	SC
Evaluation Procedure (Day of Study Completed)	**Low**	**High**	**High**	**High**	**High**	**High**
Raman Microspectroscopy (21)	311	324	341	354	371	384
	312	325	342	355	372	385
	313	326	343	356	373	385
	314	331	344	361	374	391
	315	332	345	362	375	392
	316	333	346	363	376	393
	321	334	351	364	381	394
	322	335	352	365	382	395
	323	336	353	366	383	396
Microhardness (21)	311	324	341	354	371	384
	312	325	342	355	372	385
	313	326	343	356	373	385
X-ray Diffraction (21)	311-313	324-326	341-343	354-356	371-373	384-386
	314-316	331-333	344-346	361-363	374-376	391-393
	321-323	334-336	351-353	364-366	381-383	394-396

Appendix B: Experimental Protocols

Protocol for Osteoblast-like Cell Culture from Neonatal Rat Femur

A. Materials

Chemicals

1. Dulbecco's Modified Eagles Medium (DMEM) (Sigma, D5796, St. Louis, MO)
2. Fetal Bovine Serum (FBS) (Fisher Scientific, 14-502E, Biowhittaker, Walkersville, Maryland)
3. Antibiotic/Antimycotic (Sigma, A7292, St. Louis, MO)
4. Dexamethasone (Sigma, D4902, St. Louis, MO)
5. Hanks Balanced Solution (HBSS) (Sigma, H9269, St. Louis, MO)
    a. pH near 7.4
6. 70% Ethanol (Fisher Scientific, A405, Hanover Park, IL)

Supplies

1. 50 mL centrifuge tubes (Fisher Scientific, 05-539-7, Hanover Park, IL)
2. Pipettes
    a. 1 mL (Fisher Scientific, 13-675-15C, Hanover Park, IL)
    b. 5 mL (Fisher Scientific, 13-678-11D, Hanover Park, IL)
    c. 10 mL (Fisher Scientific, 13-678-11E, Hanover Park, IL)
    d. 25 mL (Fisher Scientific, 13-678-11, Hanover Park, IL)
3. Scissors (Fisher Scientific, 08-951-5, Hanover Park, IL)
4. Tweezers (Fisher Scientific, 13-812-41, Hanover Park, IL)
5. Petri dishes (Fisher Scientific, 08-757-12, Hanover Park, IL)
6. 6-well treated culture plates (Fisher Scientific, 07-200-83, Hanover Park, IL)
7. Syringes with 20 or 21-gauge needles
8. Small glass beakers (50 mL) (Fisher Scientific, 02-539G, Hanover Park, IL)
9. Medium bottles
    a. 250 mL (Fisher Scientific, 06-404B, Hanover Park, IL)
    b. 500 mL (Fisher Scientific, 06-404D, Hanover Park, IL)
    c. 1 L (Fisher Scientific, 06-404E, Hanover Park, IL)
10. Wash bottle, autoclavable

Equipment

1. Incubator (Napco CO_2 6000, 51201071, Precision, Winchester, Virginia)

2. Laminar flow hood (Nuaire Biological Safety Cabinets, NU-425-600 Series 22, Plymouth, MN)
3. Bunsen burner
    a. Striker
4. Centrifuge (IEC Centra GP8R)
5. Water bath (Polyscience, 10L-M, Niles, IL)
    a. 37 °C
6. Autoclave
7. Electric shaver
8. Pipette aid (Fisher Scientific, 13-681-15D, Hanover Park, IL)

B. Things to do before extraction and isolation

1. Autoclave all glassware, instruments, and wash bottles
2. Prepare the rinsing media (20 mL/femur)
    a. 90% DMEM
    b. 10% FBS
    c. Warm to 37 °C in a water bath
3. Prepare plating media (12 mL/femur)
    a. DMEM
    b. 10% FBS
    c. 100 units/mL antibiotic/antimycotic
    d. 10 nM dexamethasone
    e. Warm to 37 °C in a water bath

C. Procedures

Extraction

1. Sacrifice the neonatal rat.
2. Shave the specimen's back and lower limbs (if needed).
3. Place the specimen on its stomach or side in a Petri dish.
4. Clean the body parts of the specimen that were shaved in step 2 with 70% ethanol.
5. Using tweezers, lift the skin above the femur on the hind leg.
6. Cut lifted skin using scissors to expose the underlying muscles and bones.
7. Rinse the exposed area with Hank's Balanced Solution.
8. Using fresh instruments cut the overlying muscle to expose the femur.
9. Remove muscles surrounding the femur using scissors and tweezers.
10. Using fresh instruments hold the femur with tweezers.
    a. Cut through the distal end of the knee without cutting through the femur.
    b. Cut the ligaments at the hip to release the femur.
    c. Clean off any remaining muscle, tendon, ligament, etc using tweezers.
    d. Rinse extracted femur using Hank's Balanced Solution.
11. Place the femur in Hank's Balanced Solution.
12. Repeat steps 3-10 for second femur.

13. Repeat all steps for additional neonatal rats.

Notes:
1. Place instrument tips in 70% ethanol while not in use.
2. Flame instrument tips before using after soaking in ethanol.
    a. Allow instruments to cool before using.

Isolation

1. Wash the femurs in Hank's Balanced Solution.
2. Cut off both epiphyses in a sterile Petri dish to expose the bone marrow cavity.
3. Flush the marrow from the midshaft with 7-10 mL rinsing solution.
    a. Collect in a sterile 50 mL centrifuge tube.
    b. Pipette solution to break up the clumps.
4. Centrifuge at 1000 rpm for 5 minutes.
5. Resuspend the pellet in rinsing solution, 8 mL/femur.
6. Centrifuge at 1000 rpm for 5 minutes.
7. Resuspend the pellet in plating solution, 12 mL/femur.
8. Plate in a 6-well treated culture plate.
    a. 2 femurs/plate
    b. 4 mL plating solution/well
9. Incubate for 3-4 days.
    a. 5% CO_2
    b. 37 °C
    c. 100% humidity

Osteogenic Differentiation

1. Remove plating media.
2. Remove hematopoietic cells and other unattached cells by repeatedly washing wells with rinsing solution.
3. Add fresh plating media, 4 mL/well.
    a. DMEM
    b. FBS
    c. 100 units/mL antibiotic/antimycotic
    d. 10 nM dexamethasone
4. Change media every 3 days until layers reach confluence.

Protocol for Osteoblast-like Cell Sub-Culture

A. Materials

Chemicals

1. 0.25% Trypsin-EDTA Solution (Sigma, T4049, St. Louis, MO)
2. Dulbecco's Modified Eagles Medium (DMEM) (Sigma, D5796, St. Louis, MO)
3. Fetal Bovine Serum (FBS) (Fisher Scientific, 14-502E, Biowhittaker, Walkersville, Maryland)
4. Antibiotic/Antimycotic (Sigma, A7292, St. Louis, MO)
5. 10^-5 M dexamethasone (Sigma, D 4902, St. Louis, MO)

Supplies

1. 50 mL centrifuge tubes (Fisher Scientific, 05-539-7, Hanover Park, IL)
2. Pipettes
    a. 1 mL (Fisher Scientific, 13-675-15C, Hanover Park, IL)
    b. 5 mL (Fisher Scientific, 13-678-11D, Hanover Park, IL)
    c. 10 mL (Fisher Scientific, 13-678-11E, Hanover Park, IL)
    d. 25 mL (Fisher Scientific, 13-678-11, Hanover Park, IL)
3. T-75 cell-culture flasks (Fisher Scientific, 10-126-37, Hanover Park, IL) or 6-well culture plates (Fisher Scientific, 07-200-83, Hanover Park, IL)
4. Medium bottles
    a. 250 mL (Fisher Scientific, 06-404B, Hanover Park, IL)
    b. 500 mL (Fisher Scientific, 06-404D, Hanover Park, IL)
    c. 1 L (Fisher Scientific, 06-404E, Hanover Park, IL)

Equipment

1. Incubator (Napco CO_2 6000, 51201071, Precision, Winchester, Virginia)
2. Laminar flow hood (Nuaire Biological Safety Cabinets, NU-425-600 Series 22, Plymouth, MN)
3. Centrifuge (IEC Centra GP8R)
4. Water bath (Polyscience, 10L-M, Niles, IL)
    a. 37 °C
5. Autoclave
6. Pipette aide (Fisher Scientific, 13-681-15D, Hanover Park, IL)

B. Things to do ahead of time

1. Autoclave all glassware and water
2. Prepare plating media
    a. DMEM
    b. 10% FBS
    c. 100 units/mL antibiotic/antimycotic

    d. 10 nM dexamethosone
    e. Warm to 37 °C in a water bath
3. Prepare the rinsing media
    a. 90% DMEM
    b. 10% FBS
    c. Warm to 37 °C in a water bath
4. Warm Trypsin-EDTA to 37 °C in a water bath

C. Procedure

1. Remove medium solution.
2. Add 0.25% Trypsin-EDTA solution.
    a. Use same amount as culture media
3. Set for 1-5 minutes in incubator until cells detach from well-plate.
4. Gently pipette solution to remove any cells stuck on the bottom.
5. Place solution in a 50 mL centrifuge tube.
6. Centrifuge at 1000 rpm for 5 minutes.
7. Remove supernatant.
8. Resuspend cells in rinsing solution.
9. Centrifuge at 1000 rpm for 5 minutes.
10. Remove supernatant.
11. Resuspend cells in plating media.
12. Replate cells at desired density.
    a. 4 mL plating media/well in 6-well plate
    b. 15 mL plating media/T-75 flask
13. Change media every 2-3 days.

Protocol for Osteoblast-like Cell Counting

A. Materials

Chemicals

1. 0.25% Trypsin-EDTA Solution (Sigma, T4049, St. Louis, MO)
2. Dulbecco's Modified Eagles Medium (DMEM) (Sigma, D5796, St. Louis, MO)
3. Fetal Bovine Serum (FBS) (Fisher Scientific, 14-502E, Biowhittaker, Walkersville, Maryland)
4. Trypan Blue (Sigma, T8154, St. Louis MO)

Supplies

1. 50 mL centrifuge tubes (Fisher Scientific, 05-539-7, Hanover Park, IL)
2. Pipettes
    a. 1 mL (Fisher Scientific, 13-675-15C, Hanover Park, IL)
    b. 5 mL (Fisher Scientific, 13-678-11D, Hanover Park, IL)
    c. 10 mL (Fisher Scientific, 13-678-11E, Hanover Park, IL)
    d. 25 mL (Fisher Scientific, 13-678-11, Hanover Park, IL)
3. 2.0 mL microcentrifuge tubes (Fisher Scientific, 05-408-138, Hanover Park, IL)
4. Medium bottles
    a. 250 mL (Fisher Scientific, 06-404B, Hanover Park, IL)
    b. 500 mL (Fisher Scientific, 06-404D, Hanover Park, IL)
    c. 1 L (Fisher Scientific, 06-404E, Hanover Park, IL)
5. Micropipette tips

Equipment

1. Hemocytometer (Fisher Scientific, 02-671-5, Hanover Park, IL)
2. Laminar flow hood (Nuaire Biological Safety Cabinets, NU-425-600 Series 22, Plymouth, MN)
3. Centrifuge (IEC Centra GP8R)
4. Water bath (Polyscience, 10L-M, Niles, IL)
    a. 37 °C
5. Autoclave
6. Pipette aide (Fisher Scientific, 13-681-15D, Hanover Park, IL)
7. Inverted Microscope (Olympus Optical Co. Ltd., CK30-F100, Japan)
8. 10X Objective (Olympus Optical Co., A10PL, Japan)
9. Micropipettes

B. Things to do ahead of time

1. Autoclave all glassware
2. Prepare the rinsing media
    a. 90% DMEM

b. 10% FBS
c. Warm to 37 °C in a water bath
3. Warm Trypsin-EDTA to 37 °C in a water bath

C. Procedure

1. Remove media solution.
2. Add 0.25% Trypsin-EDTA solution.
    a. Use same amount as culture media.
3. Set for 1-5 minutes in incubator until cells detach from well-plate.
4. Gently pipette solution to remove any cells stuck on the bottom.
5. Place solution in a 50 mL centrifuge tube.
6. Centrifuge at 1000 rpm for 5 minutes.
7. Remove supernatant.
8. Resuspend cells in rinsing solution.
9. Centrifuge at 1000 rpm for 5 minutes.
10. Remove supernatant.
11. Resuspend cells in rinsing solution.
    a. Use approximately 1 mL per lifted well.
12. Add 50 µl trypan blue to a microcentrifuge tube.
13. Add 50 µl cell solution to microcentrifuge tube.
14. Mix.
15. Take trypan blue+cell solution and place on hemocytometer.
    a. Place glass slide on top of hemocytometer.
    b. At the v-notch on the side, carefully pipette a small amount of solution.
    c. Solution will automatically wick into the hemocytometer.
    d. Add solution until hemocytometer plate is covered.
16. Count cells.
    a. Place hemocytometer on inverted microscope with 10X objective.
    b. Count cells in each corner box and center box.
    c. Average the 5 readings to obtain one reading.
    d. Scale up according to dilution and concentration.
17. Replate cell solution at desired density or discard.

Sicrol Collagen Assay Protocol

Notes: Sample can be tested in culture medium that does not contain more than 5% fetal bovine serum. If the medium has more than 5%, reduce the FBS concentration to 5%, use affinity chromatography to remove the FBS, or precipitate the collagen from the culture media.

A. Materials

Chemicals

1. SIRCOL Soluble Collagen Assay Kit (Biocolor Ltd., S1000, Newtonabbey, Northern Ireland)
    a. Collagen Standards
    b. Sircol Dye Reagent
    c. Alkaline Reagent
4. Dulbecco's Modified Eagles Medium (DMEM) (Sigma, D5796, St. Louis, MO)
5. Fetal Bovine Serum (FBS) (Fisher Scientific, 14-502E, Biowhittaker, Walkersville, Maryland)

Supplies

1. Micropipette tips
2. Microcentrifuge tubes (2.0 mL) (Fisher Scientific, 05-408-138, Hanover Park, IL)
3. Kimwipes (Fisher Scientific, 06-666A, Hanover Park, IL)
4. Q-Tip
5. Spectrophotometer Plate (96 well)

Equipment

1. Micropipettes
2. Rotator/Shaker
3. Microcentrifuge (Marsh 1816, National Labnet Co., Woodbridge, NJ)
4. Vortex (Fisher Scientific, 12-812, Scientific Industries, Inc., Bohemia, NY)
5. Spectrophotometer

B. Preparation

1. Reagent Blank
    a. 100 µl fresh unused tissue culture media
    b. 100 µl fresh DMEM
2. Collagen Standards
    a. 5, 10, 15, 20, 50 µg in 100 µl fresh unused tissue culture media + QA to 200 µl with fresh DMEM
    b. Initial run: duplication of at least 0, 12.5, 25, and 50 µg in 200 µl

c. Subsequent batches: duplication at mid-range and blank within 5%

3. Test Samples
    a. 100 µl used culture media
    b. 100 µl fresh DMEM

C. Procedure

1. Add 1mL Sircol Dye reagent to each tube and cap.
2. Mix tube by inverting.
3. Place tubes in mechanical shaker for 30 minutes.
    a. During this time the Sircol dye will bind to soluble collagen.
    b. The dye is designed so that the collagen-dye complex will precipitate out of solution.
4. Centrifuge tubes in a microcentrifuge at >10000 x g for 10 minutes.
5. Remove the unbound dye solution by carefully inverting and draining the tubes on a kim wipe.
6. Remove any remaining droplets by gently tapping the tube or carefully cleaning inside with a q-tip.
7. Add 1 mL alkali reagent to each tube.
8. Recap tubes.
9. Release dye with the vortex mixer.
    a. Dye should be dissolved within a minute.
    b. Solutions can remain in this state for 2-3 hours before measurement.
10. Transfer 200 µl into the spectrophotometer plate.
11. Set spectrophotometer to 540 nm wavelength.
    a. Endpoint reading
12. Read wells.
13. Subtract the reagent blank reading from standards and test samples.
14. Plot standards on graph and use the graph to calculate the collagen content of the test sample.

Protocol for Alkaline Phosphatase Assay

A. Materials

Chemicals

1. Alkaline Phosphatase Kit No. 85L3R (Sigma, 85L3R, St. Louis, MO)
    a. Fast Violet B Salt
    b. Mayer's Hematoxylin Solution
    c. Napthol AS-MX Phosphate Alkaline Solution
    d. Citrate Concentrated Solution
2. Deionized Water
3. Acetone (Fisher Scientific, A18, Hanover Park, IL)
4. Tap Water

Supplies

1. Pipettes
    a. 5 mL (Fisher Scientific, 13-678-11D, Hanover Park, IL)
    b. 10 mL (Fisher Scientific, 13-678-11E, Hanover Park, IL)
2. Beakers (50 mL) (Fisher Scientific, 02-539G, Hanover Park, IL)
3. Stir bar

Equipment

1. Pipette Aide (Fisher Scientific, 13-681-15D, Hanover Park, IL)
2. Magnetic Stir Plate
3. Timer

B. Preparation

Citrate Working Solution

1. Dilute 2 mL Citrate Concentrate Solution to 100 mL with deionized water.

Fixative Solution

1. Warm Citrate Working Solution to room temperature.
2. With constant stirring, add 2 volumes of Citrate Working Solution to 3 volumes of acetone.
3. Bring to room temperature (18-26 °C).

Alkaline-Dye Mixture

1. Measure 48 mL distilled water into a beaker and adjust temperature to 18-26 °C.
2. Dissolve a Fast Violet B capsule in the distilled water using a magnetic stir bar.
3. Add 2 mL Napthol AS-MX Phosphate Alkaline Solution.
4. Mix.

C. Procedure

1. Fix slides by immersing in citrate buffered acetone for 30 seconds.
2. Rinse gently in deionized water for 45 seconds.
    a. Do NOT allow slides to dry.
3. Add slides to alkaline-dye mixture.
4. Incubate at 18-26 °C for 30 minutes.
    a. Protect immersed slides from direct light.
5. After 30 minutes, remove slides and rinse thoroughly in deionized water for 2 minutes.
    a. Do NOT allow slides to dry.
6. Place slides in Mayer's Hematoxylin Solution for 10 minutes.
7. Rinse slides in tap water (if alkaline) or immerse in Scott's Tap water Substitute for 2 minutes.
8. Evaluate microscopically.

Protocol for RNA Isolation from Osteoblast-like Cells

A. Materials

Chemicals

1. RNAse free sterile water (Fisher Scientific, BP561-1, Hanover Park, IL)
2. RNAse Away (Invitrogen, 10328-011, Carlsbad, CA)
3. Trizol (Invitrogen, 15596-026, Carlsbad, CA)
4. 75% Ethanol (Fisher Scientific, A18, Hanover Park, IL)
5. Chloroform (Sigma, 366919, St. Louis, MO)
6. Isopropanol (Fisher Scientific, A416, Hanover Park, IL)

Supplies

1. RNAse free pipette tips (1-200 µl and 200-1000 µl)
    a. 0.1-10 µl (Fisher Scientific, 02-707-301, Hanover Park, IL)
    b. 1-200 µl (Fisher Scientific, 02-707-309, Hanover Park, IL)
    c. 200-1000 µl (Fisher Scientific, 02-707-324, Hanover Park, IL)
2. 2.0 mL RNAse free microcentrifuge tubes (Fisher Scientific, 02-681-321, Hanover Park, IL)
3. UV spectrophotometer plate (96 well)
4. Kimwipes (Fisher Scientific, 06-666A, Hanover Park, IL)

Equipment

1. Microcentrifuge (Marsh 1816, National Labnet Co., Woodbridge, NJ)
2. Micropipettes
3. Spectrophotometer

B. Things to do Ahead of Time

1. Make 75% Ethanol

C. Procedure

1. Wipe work space with ethanol.
2. Wipe work space with RNAse Away.
3. Remove culture media from well.
4. Add 1 mL Trizol to well in culture plate.
    a. After 5 minutes, move Trizol and cells from well to microcentrifuge tube.
    b. Wait 5 more minutes.
6. Add 0.2 mL chloroform.
7. Shake tube.
    a. Color will become pink.
8. Wait 2 to 3 minutes at room temperature.

9. Centrifuge at 8,000 rpm for 10 minutes.
    a. Layers will form: clear on top, thin white layer in middle, pink layer on bottom.
10. Carefully remove clear layer with a pipette and place in new tube.
    a. Discard tube with pink and white solution.
11. Add 0.5 mL isopropanol.
12. Shake.
13. Wait for 10 minutes at room temperature.
14. Centrifuge at 10,000 rpm for 10 minutes.
    a. Obtain a small white pellet.
15. Remove and discard all liquid by pipette.
16. Add 1 mL 75% ethanol.
    a. Do NOT resuspend the pellet.
17. Centrifuge at 10,000 rpm for 5 minutes.
18. Remove the ethanol.
19. Add up to 250 µl RNAse free water.
    a. Amount added depends on size of RNA pellet.
20. Mix 5 µl RNA+RNAse free water and 95 µl RNAse free water in UV 96-well plate.
21. Read on a spectrophotometer.
    a. 260 nm endpoint reading
    b. 280 nm endpoint reading
    c. Blank - 100 µl RNAse free water
22. Calculate the A260/A280 ratio (rough estimate of RNA purity).
    a. A260/A280 = 0.57 = 100% protein/0%RNA
    b. A260/A280 = 1.87 = 50% protein/50% RNA
    c. A260/A280 = 2.00 = 0% protein/100% RNA
23. Calculate the amount of RNA in your sample.
    a. Dilution x A260 x Conversion Factor
    b. Conversion Factor for RNA = 40 µg/mL per A260 unit

Protocol for RT-PCR

A. Materials

Chemicals

1. RNAse free sterile water (Fisher Scientific, BP561-1, Hanover Park, IL)
2. MMLV Reverse Transcriptase Enzyme (Fisher Scientific, PR-M1701, Hanover Park, IL)
3. 5x MMLV RT Buffer (Fisher Scientific, M531A, Hanover Park, IL)
4. RNAse Inhibitor (Fisher Scientific, BP3222-1, Hanover Park, IL)
5. dNTP Set (100mM) (Fisher Scientific, BP25641, Hanover Park, IL)
6. Eppendorf Master Mix 2.5X (Fisher Scientific, E0032002501, Hanover Park, IL)
7. Random Hexamer Primer (Invitrogen, Carlsbad, CA)
8. Primers (Invitrogen, Carlsbad, CA)
9. Tris-Base
10. Boric Acid
11. EDTA·$2H_2O$
12. Agarose
13. Ethidium Bromide
14. Loading Dye
15. DNA Marker Ladder

Supplies

1. RNAse free pipette tips (1-200 µl and 200-1000 µl)
    a. 0.1-10 µl (Fisher Scientific, 02-707-301, Hanover Park, IL)
    b. 1-200 µl (Fisher Scientific, 02-707-309, Hanover Park, IL)
    c. 200-1000 µl (Fisher Scientific, 02-707-324, Hanover Park, IL)
2. 2.0 mL RNAse free microcentrifuge tubes (Fisher Scientific, 02-681-321, Hanover Park, IL)
3. 0.5 mL Thin-wall PCR Tubes (Fisher Scientific, 07-200-252, Hanover Park, IL)
4. Media bottles
    a. 250 mL (Fisher Scientific, 06-404B, Hanover Park, IL)
    b. 500 mL (Fisher Scientific, 06-404D, Hanover Park, IL)
    c. 1 L (Fisher Scientific, 06-404E, Hanover Park, IL)

Equipment

1. Microcentrifuge (Marsh 1816, National Labnet Co., Woodbridge, NJ)
2. Micropipettes
3. Thermocycle
4. Gel Electrophoresis Equipment
5. Light Box

B. Things to do Ahead of Time

1. Isolate RNA
2. Prepare 5mM dNTP mix
    a. 2.5µl dATP (100mM)
    b. 2.5µl dTTP (100mM)
    c. 2.5µl dGTP (100mM)
    d. 2.5µl dCTP (100mM)
    e. 190µl RNase-Free H_2O

C. Procedure

1. Add 1 µg sample and 1 µl random hexamer primer to a thermocycle tube.
    a. 40 ug RNA/OD260
2. QA with RNAse free water to 8 µl.
3. Place in thermocycler at 70 °C for 10 minutes.
4. In thermocycle tube add.
    a. 4.0 µl 5X RT Buffer
    b. 2.0 µl dNTP mix (5mM)
    c. 2.5 µl RNAse Inhibitor
    d. 0.5 µl MMLV RT Enzyme
    e. 5.0 µl RNAse free water
    f. Total = 20 µl
5. Place in thermocycler at 42 °C for 1 hour.
    a. Results in a cDNA template
6. In new thermocycle tube add.
    a. 10.0 µl 2.5X PCR master mix
    b. 0.5 µl sense primer
    c. 0.5 µl antisense primer
    d. 13.0 µl RNAse free water
    e. 1.0 µl cDNA template
    f. Total = 25 µl
7. Place in thermocycler.
8. Hold at 94 °C for 2 minutes.
9. Repeat following for 24 cycles.
    a. 94 °C for 30 seconds
    b. 53 °C for 30 seconds
    c. 72 °C for 1 minutes
10. Hold at 72 °C for 10 minutes.
11. Hold at 4 °C for 24 hours (or until removed from thermocycler).
12. Place in freezer.
13. Prepare 0.5X TBE Buffer.
    a. 100 mL 5X TBE Buffer
        i. 27 g Tris-Base
        ii. 13.75 g Boric Acid
        iii. 1.86 g $EDTA \cdot 2H_20$

iv. QA to 1 L using ultrapure H_20
v. pH to 7.4 +/- 0.4 (before final 1L QA)

b. 900 mL ultrapure H_20

14. Prepare 1.5% agarose gel.
    a. 100 mL 0.5X TBE buffer
    b. 1.5 g agarose
15. Microwave agarose solution until all agarose is dissolved.
16. Cool agarose solution enough to hold bottle.
17. Add 10 µL ethidium bromide.
18. Prepare agarose gel mold.
    a. Place comb.
    b. Place mold in clamps.
19. Pour agarose solution slowly into mold.
    a. Be sure to not induce bubble formation.
20. Allow gel to set, approximately 20 minutes.
21. Remove comb by pulling slowly vertically.
22. Remove gel and platform from clamp.
23. Place gel and platform in electrophoresis chamber.
    a. Wells away from yellow tape.
    b. Samples run toward yellow tape.
24. Gently add 0.5X TBE buffer.
    a. Fill one basin.
    b. Fill opposite basin.
    c. Gently pour directly on top of agarose gel.
    d. Cover gel completely to a depth of approximately 1 cm.
25. Prepare samples for electrophoresis gel.
    a. 5 µL PCR product
    b. 1 µL loading dye
26. Load samples using standard micropipettes.
27. Load appropriate DNA marker ladder.
28. Run at 50 V for 60 min.
29. Check progress of samples.
    a. Run longer if desired.
30. View bands by placing on the light box in darkened room.

Protocol for Osteoblast-like Cell and/or Bone Nodule Fixing

A. Materials

Chemicals

1. Ethanol (Fisher Scientific, A18, Hanover Park, IL)
2. Distilled Water

Supplies

1. 50 mL beakers (Fisher Scientific, 02-539G, Hanover Park, IL)
2. Pipettes
    a. 1 mL (Fisher Scientific, 13-675-15C, Hanover Park, IL)
    b. 5 mL (Fisher Scientific, 13-678-11D, Hanover Park, IL)
    c. 10 mL (Fisher Scientific, 13-678-11E, Hanover Park, IL)
    d. 25 mL (Fisher Scientific, 13-678-11, Hanover Park, IL)
3. Tweezers (Fisher Scientific, 13-812-41, Hanover Park, IL)

Equipment

1. Pipette aide (Fisher Scientific, 13-681-15D, Hanover Park, IL)
2. Fume Hood

B. Things to do ahead of time

1. Prepare 70% ethanol
2. Prepare 85% ethanol

C. Procedure

1. Remove glass cover slip with nodules from medium solution.
2. Using tweezers place in 70% ethanol for 30 minutes.
3. Using tweezers, take glass cover slip from 70% ethanol and place in 85% ethanol for 15 minutes.
4. Using tweezers, take glass cover slip from 85% ethanol and place in 100% ethanol for 15 minutes.

Appendix C: Morphology

Control – Well 151 – 10x objective – inverted microscope

Day	Top	Left	Center	Right	Bottom
Day 0	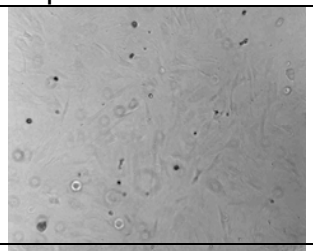	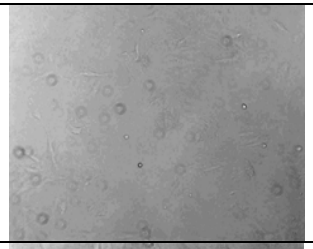	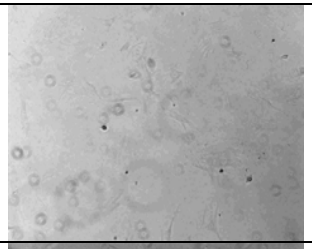	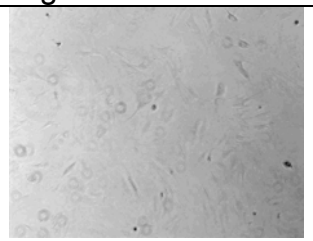	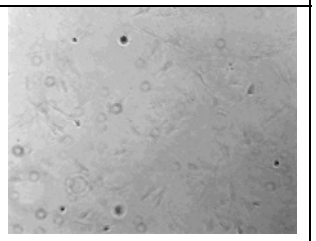
Day 3	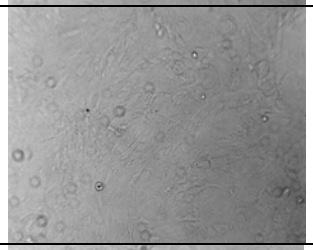	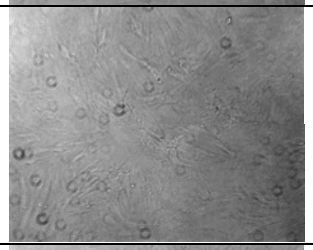	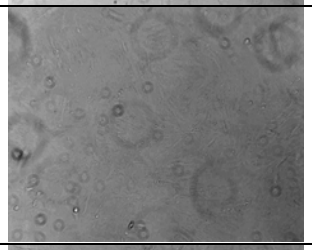	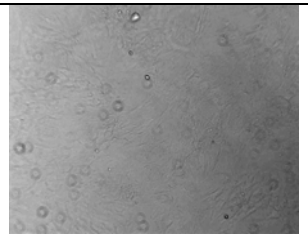	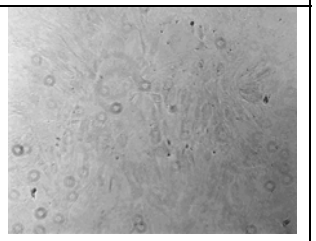
Day 6	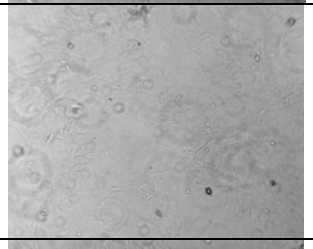	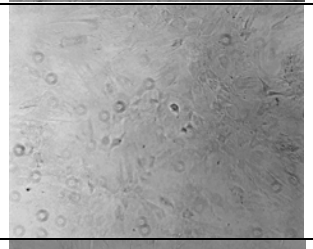	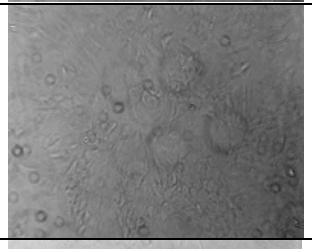	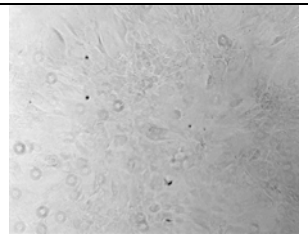	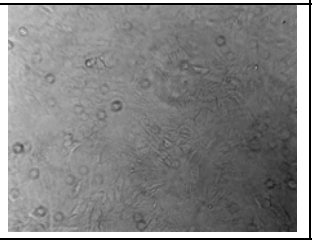
Day 9	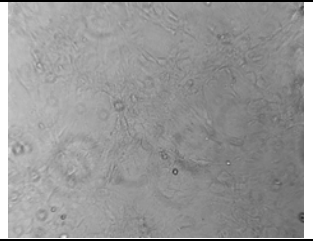	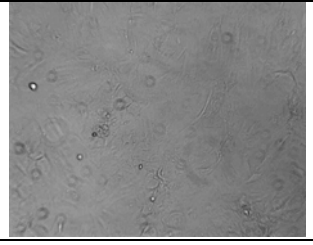	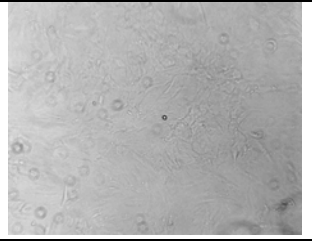	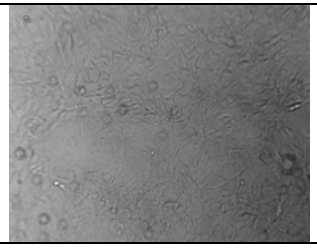	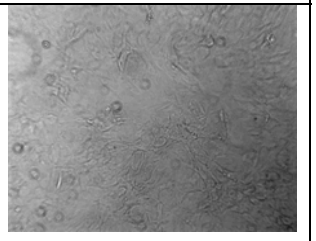

Day	Top	Left	Center	Right	Bottom
Day 12	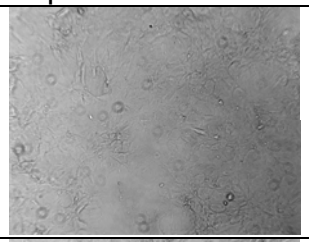	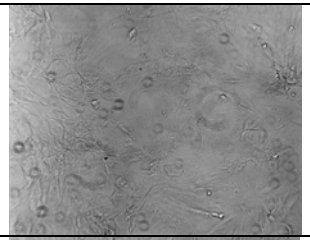	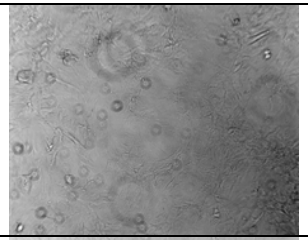	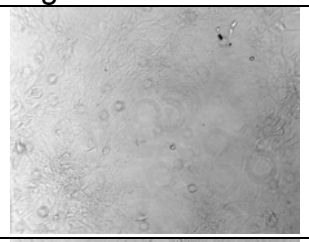	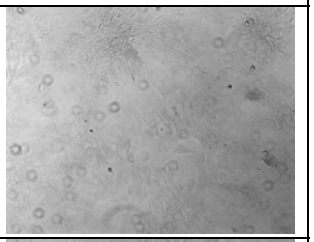
Day 15	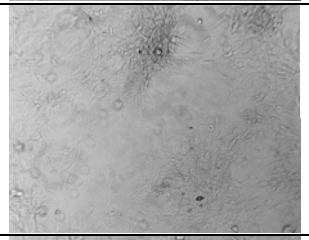	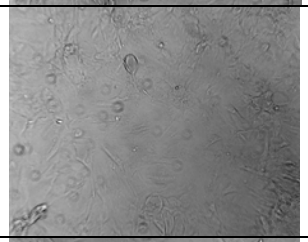	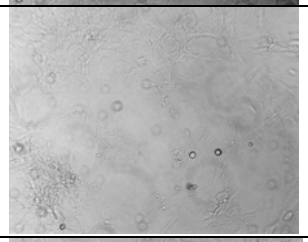	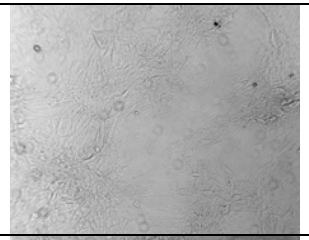	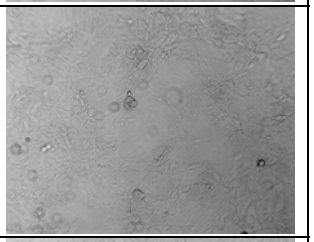
Day 18	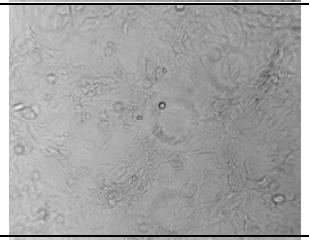	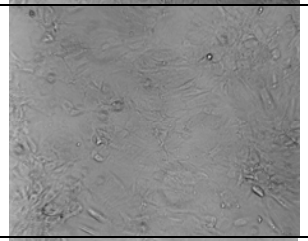	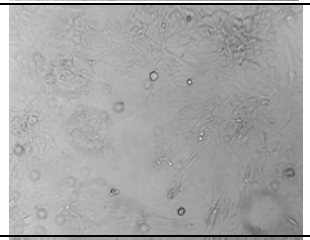	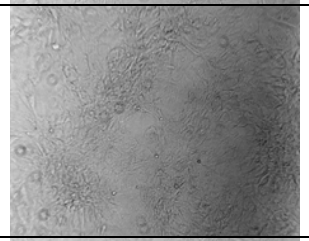	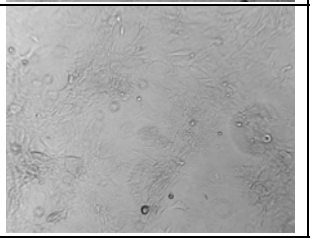
Day 21	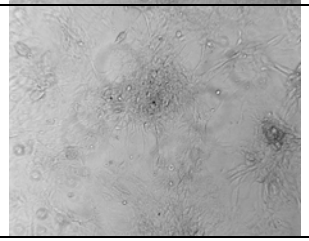	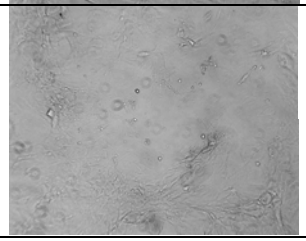	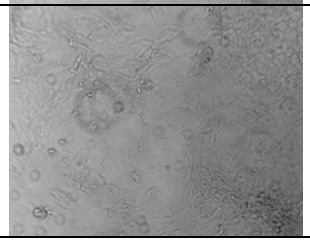	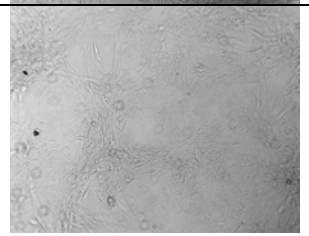	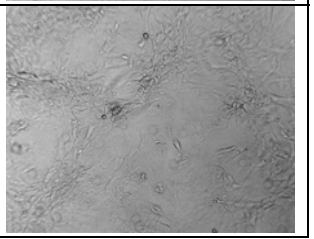

PLA low – Well 451 - 10x objective – inverted microscope

Day	Top	Left	Center	Right	Bottom
Day 0	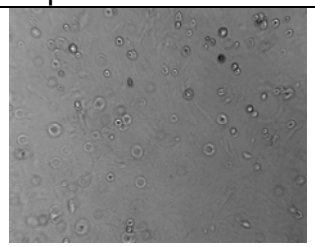	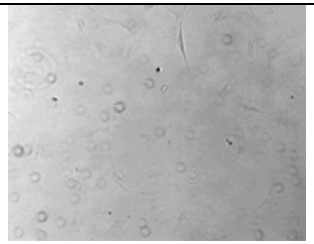	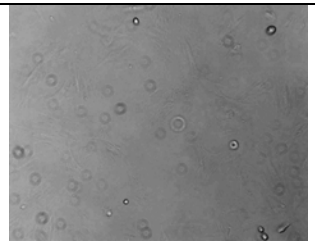	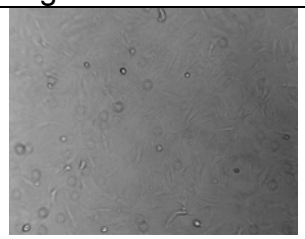	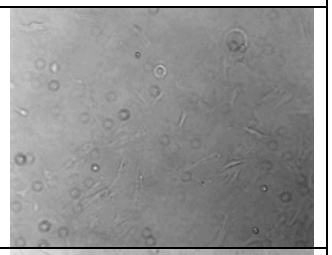
Day 3	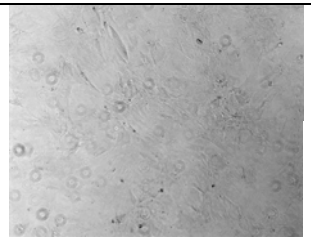	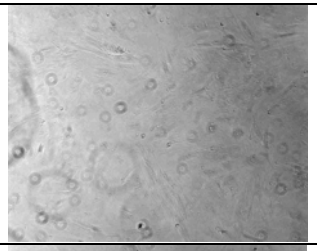	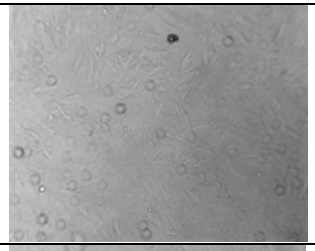	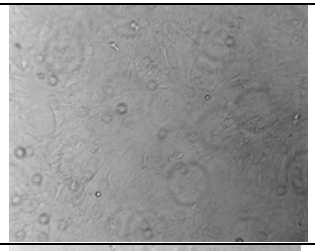	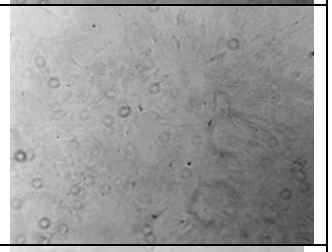
Day 6	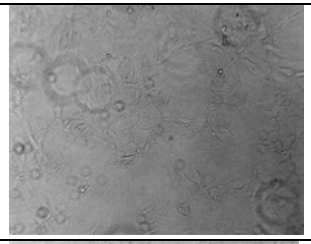	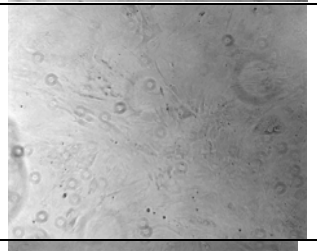	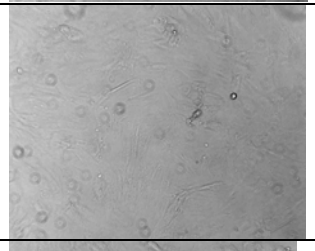	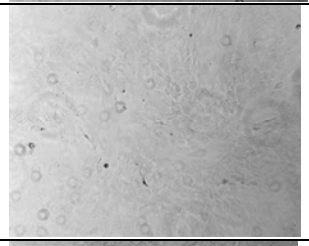	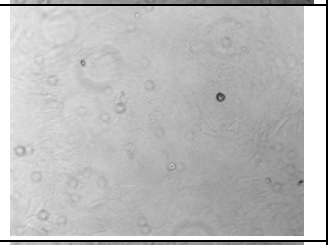
Day 9	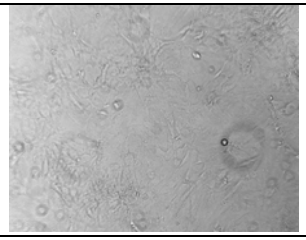	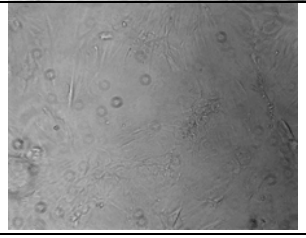	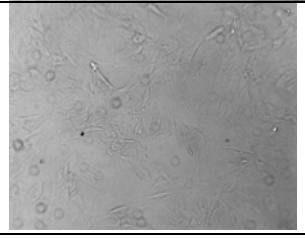	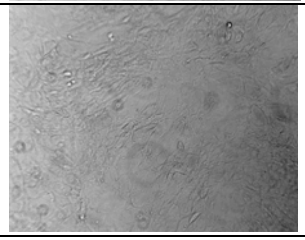	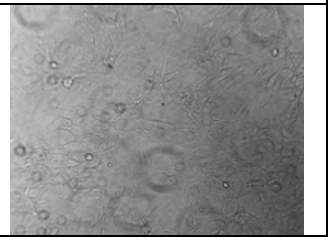

Day	Top	Left	Center	Right	Bottom
Day 12	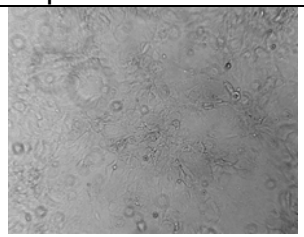	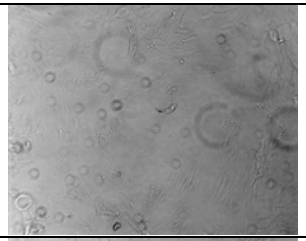	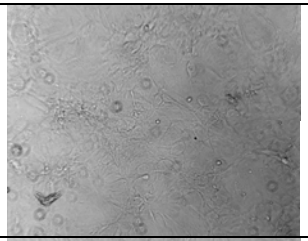	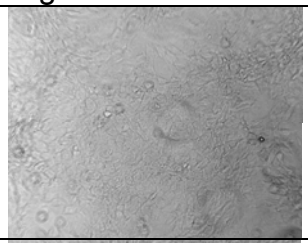	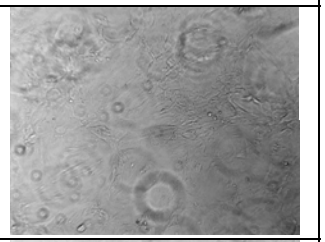
Day 15	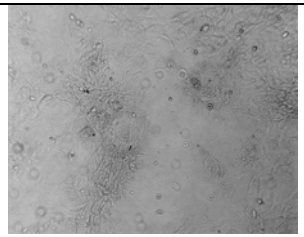	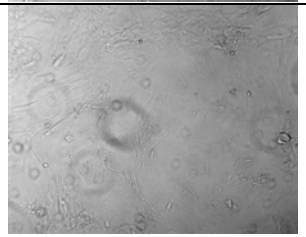	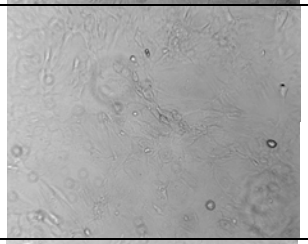	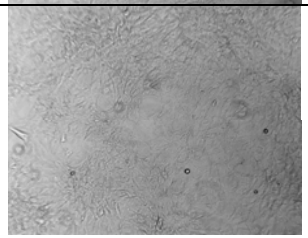	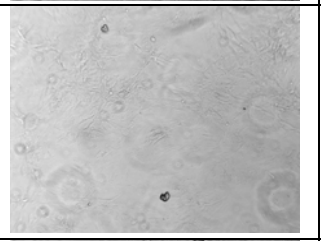
Day 18	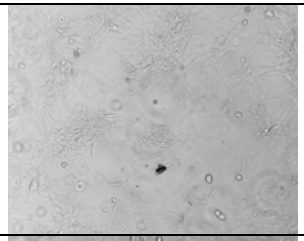	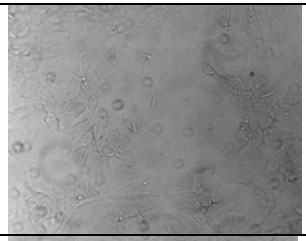	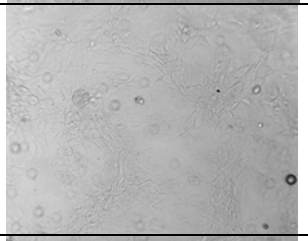	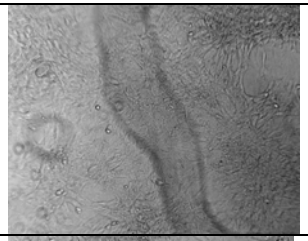	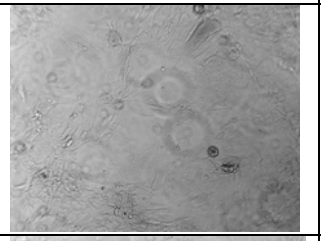
Day 21	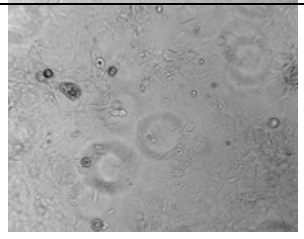	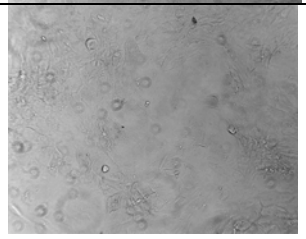	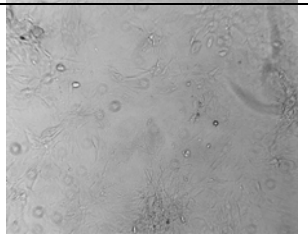	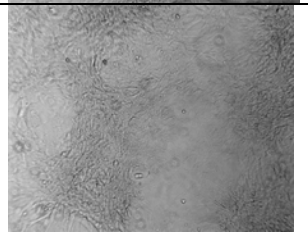	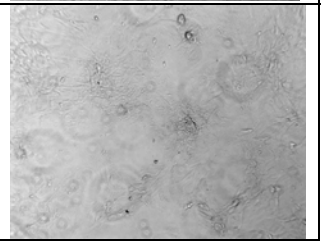

PLA high – Well 454 – 10x objective – inverted microscope

Day	Top	Left	Center	Right	Bottom
Day 0	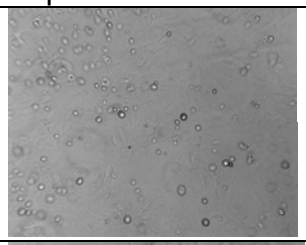	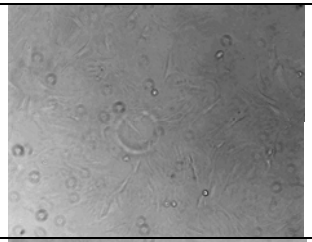	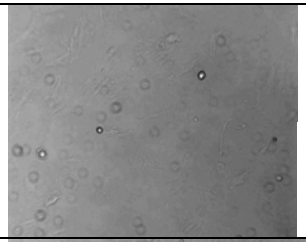	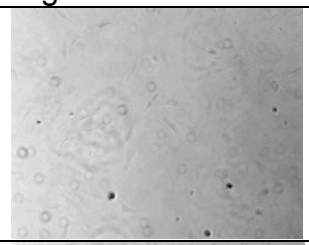	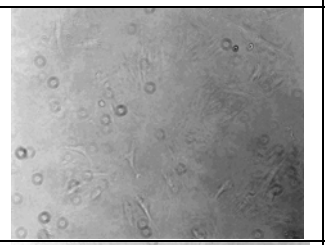
Day 3	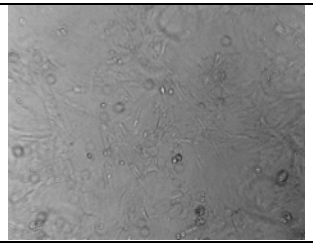	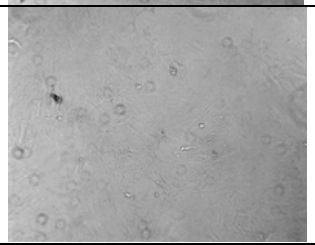	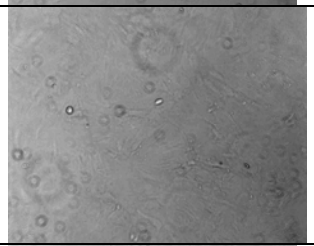	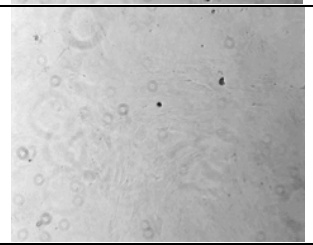	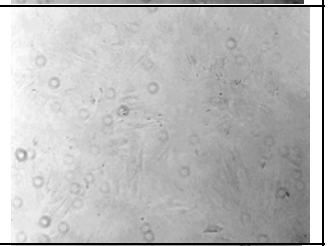
Day 6	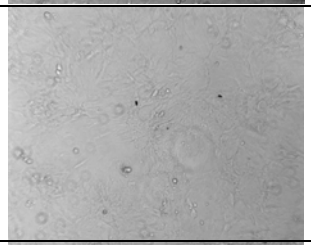	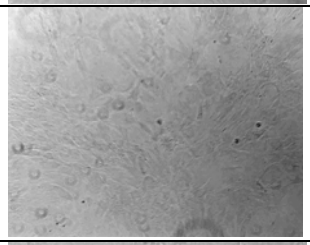	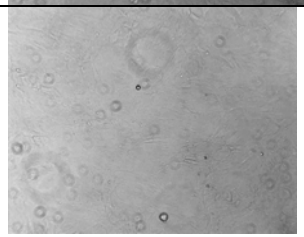	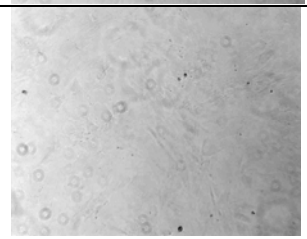	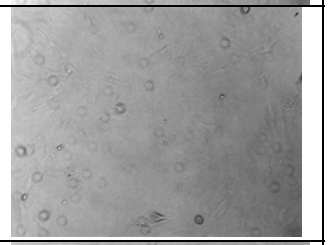
Day 9	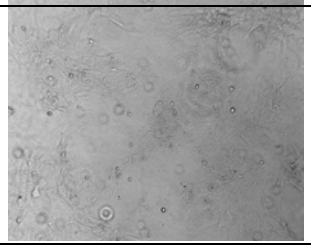	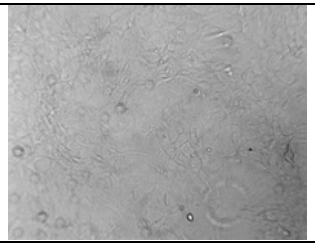	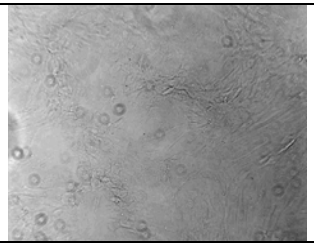	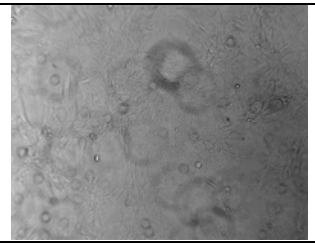	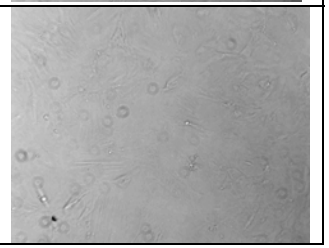

Day	Top	Left	Center	Right	Bottom
Day 12	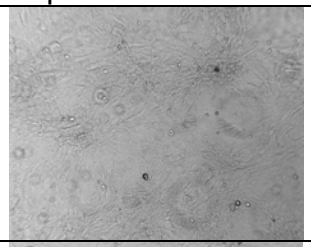	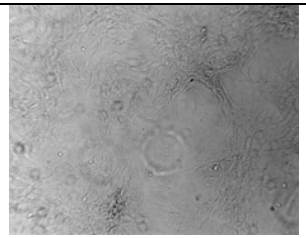	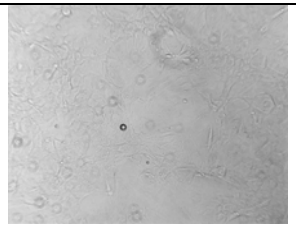	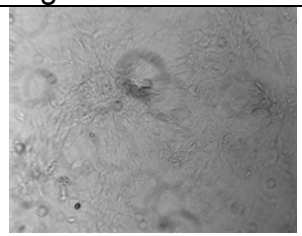	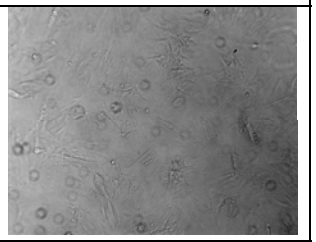
Day 15	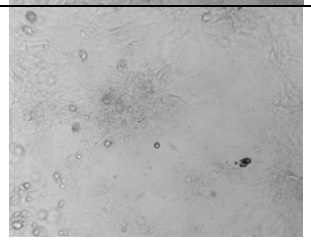	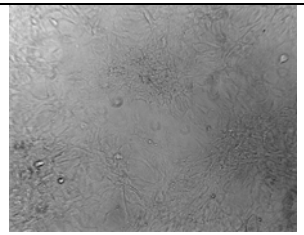	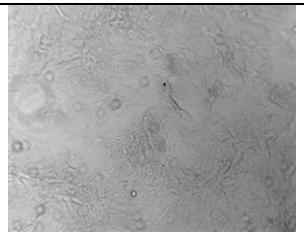	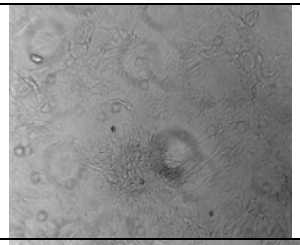	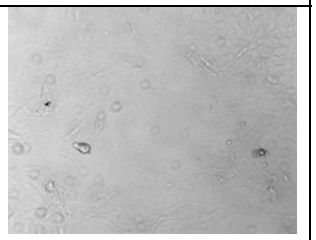
Day 18	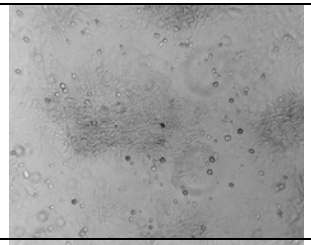	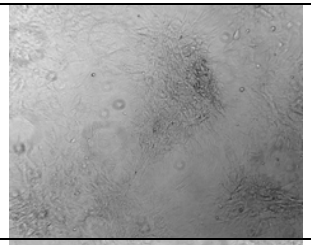	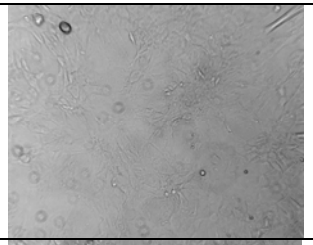	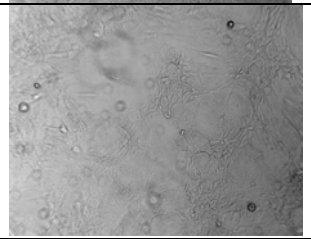	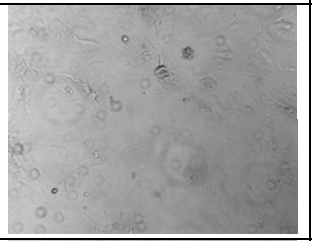
Day 21	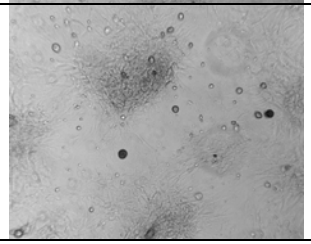	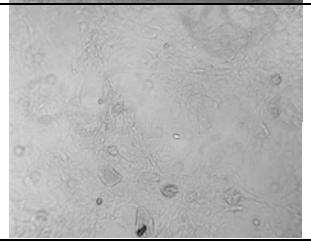	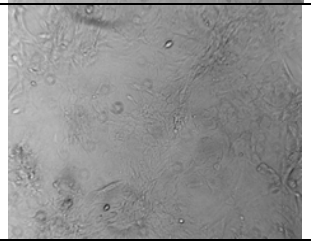	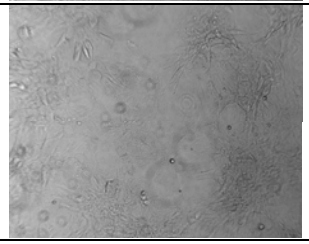	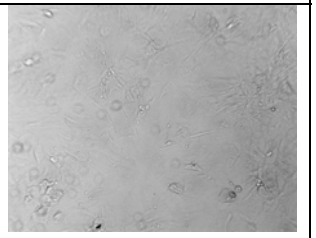

PLG low – Well 751 – 10x objective – inverted microscope

Day	Top	Left	Center	Right	Bottom
Day 0	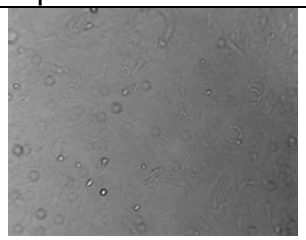	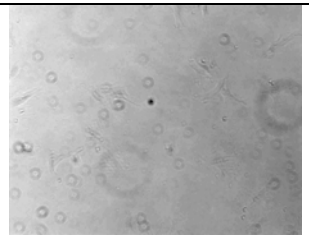	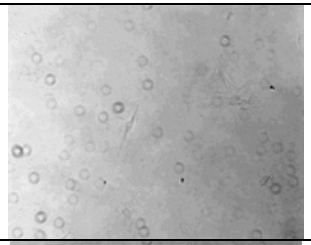	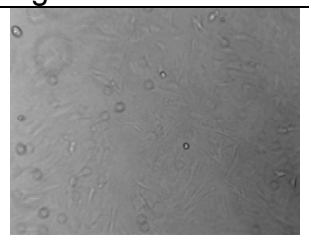	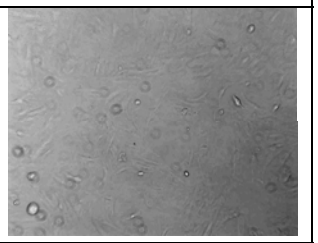
Day 3	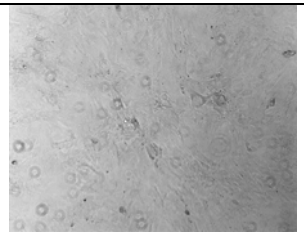	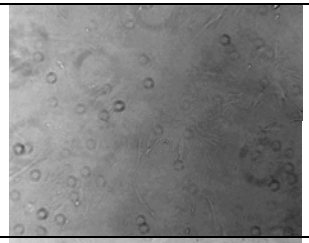	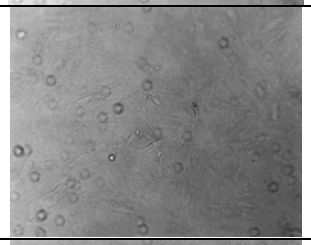	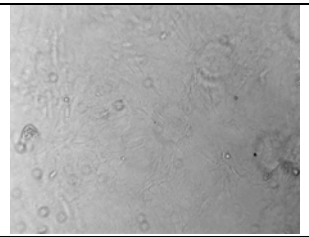	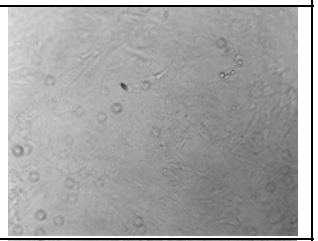
Day 6	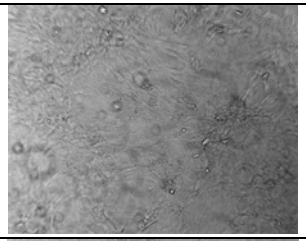	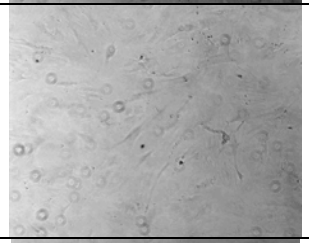	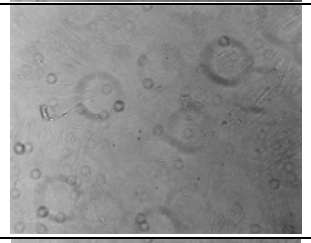	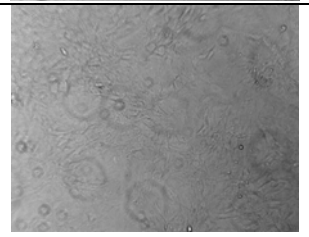	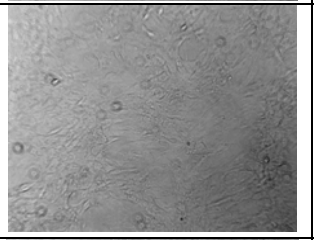
Day 9	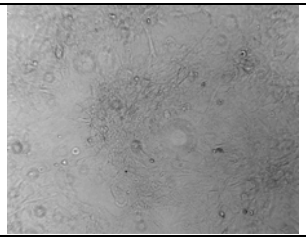	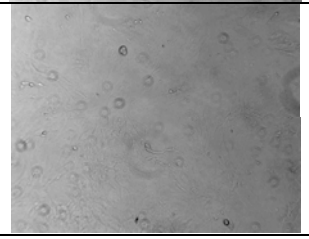	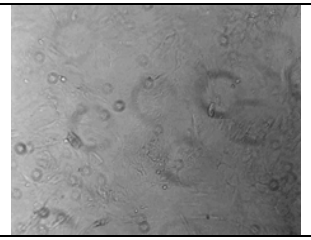	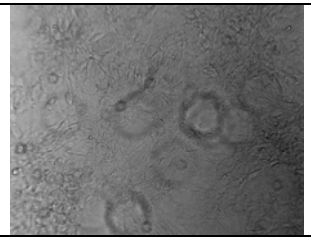	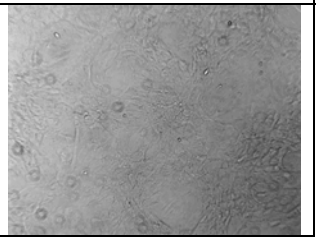

Day	Top	Left	Center	Right	Bottom
Day 12	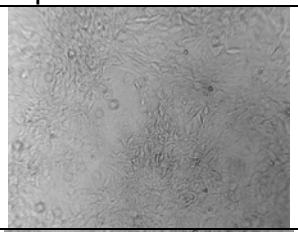	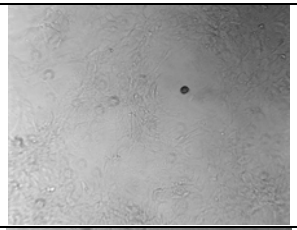	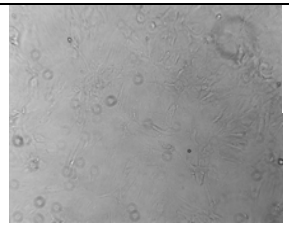	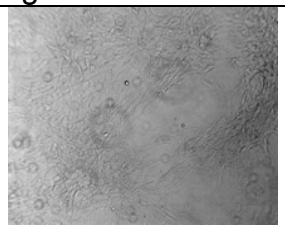	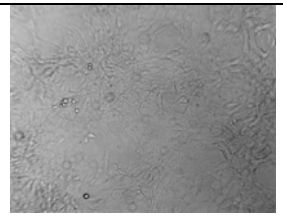
Day 15	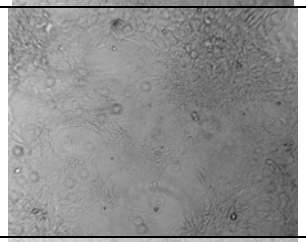	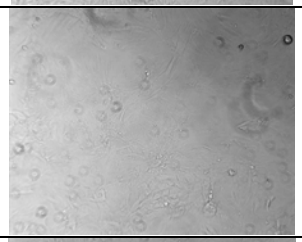	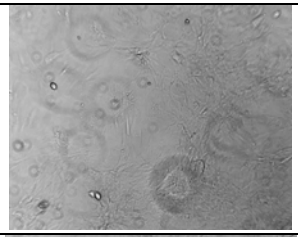	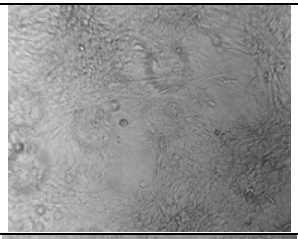	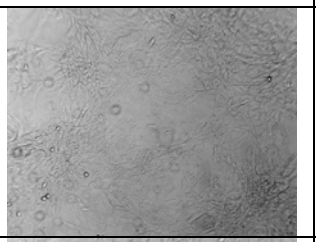
Day 18	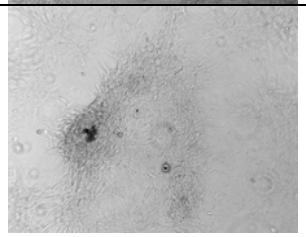	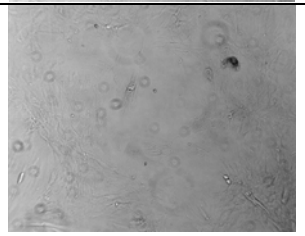	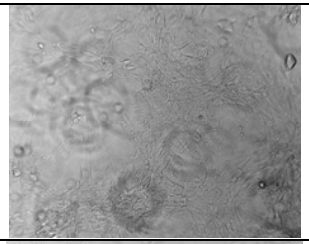	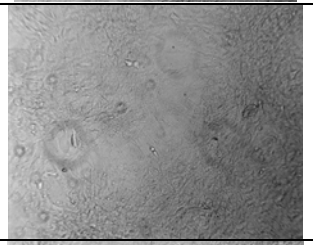	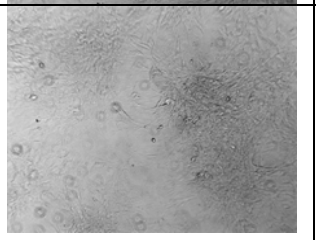
Day 21	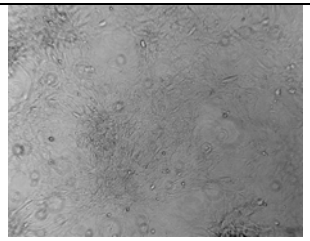	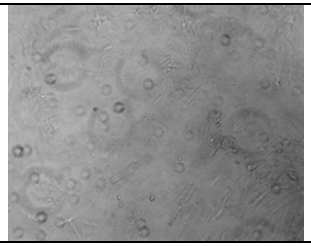	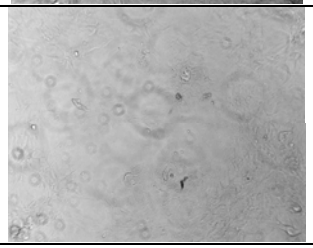	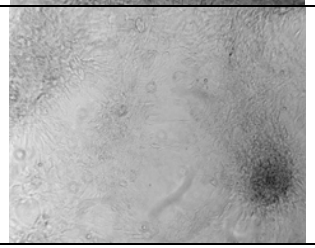	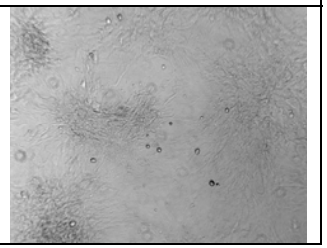

PLG high – Well 754 – 10x objective – inverted microscope

Day	Top	Left	Center	Right	Bottom
Day 0	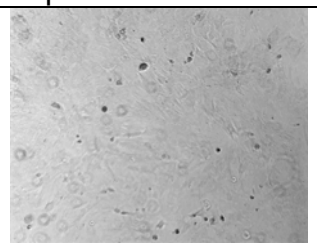	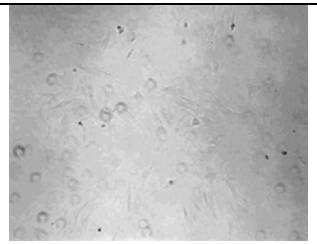	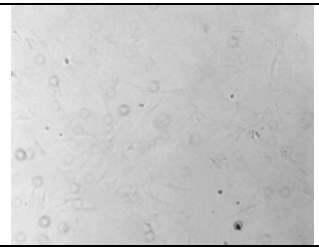	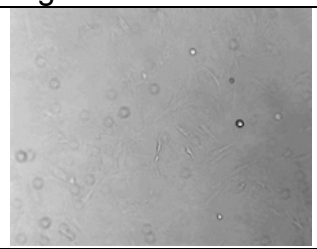	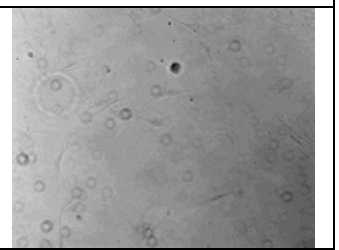
Day 3	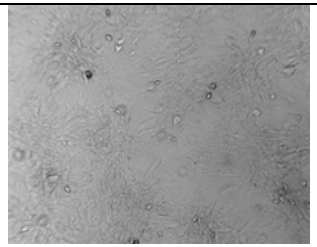	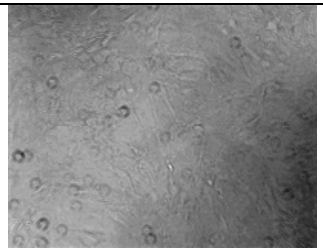	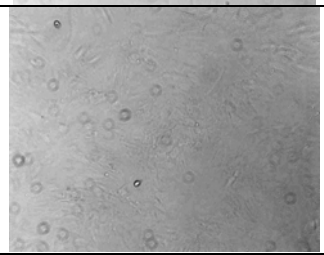	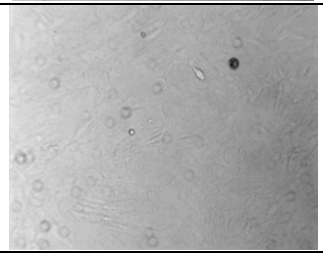	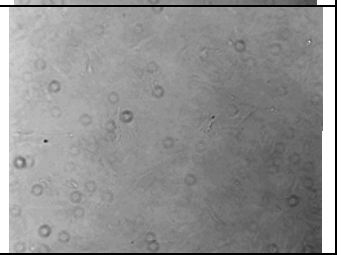
Day 6	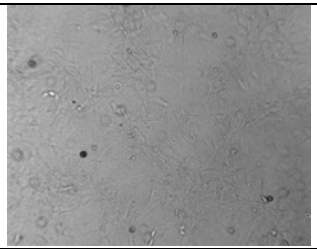	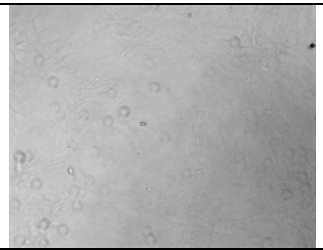	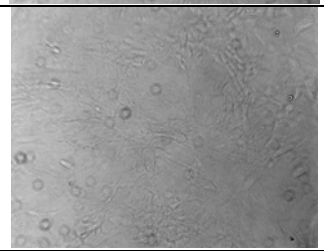	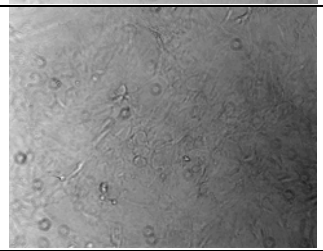	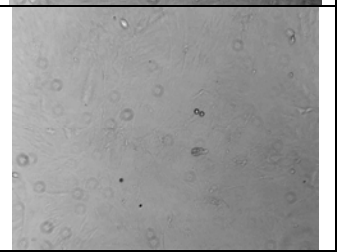
Day 9	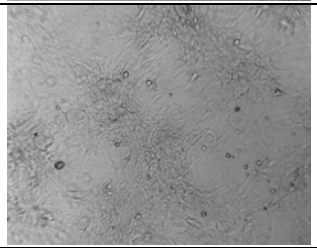	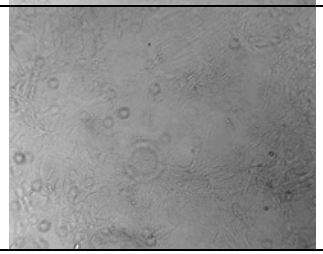	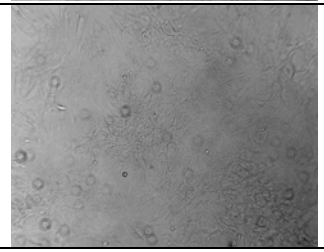	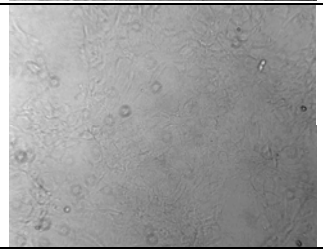	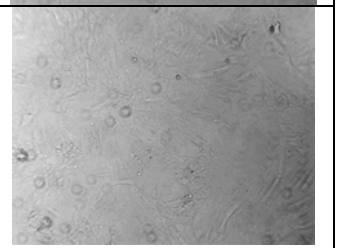

Day	Top	Left	Center	Right	Bottom
Day 12	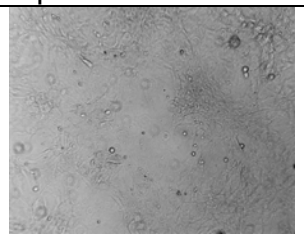	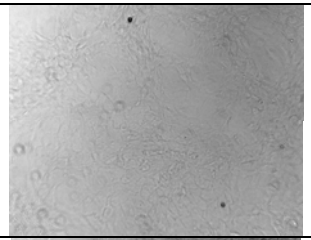	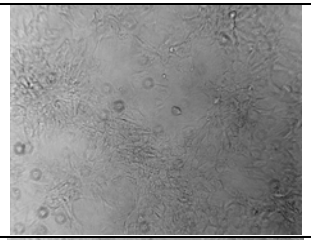	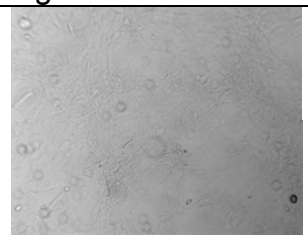	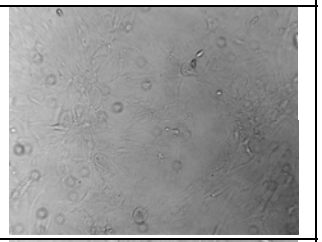
Day 15	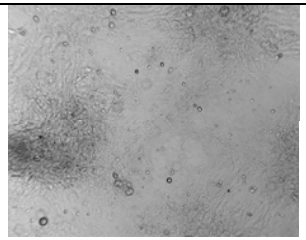	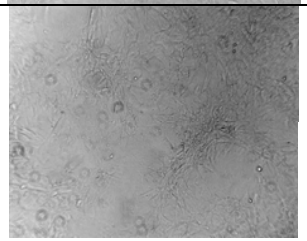	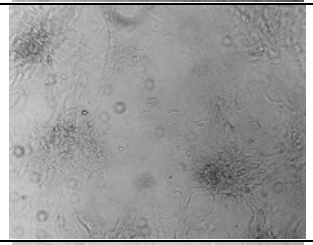	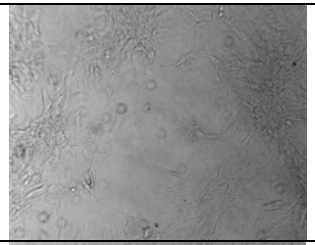	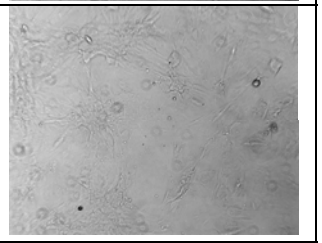
Day 18	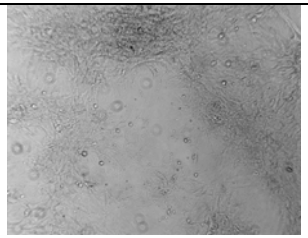	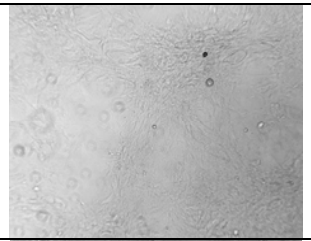	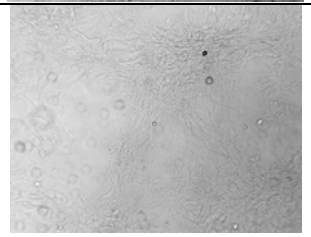	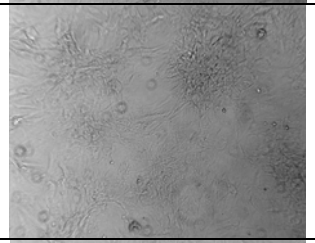	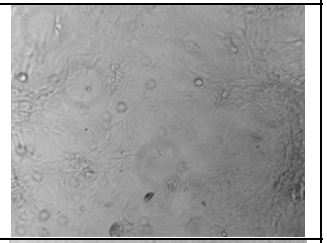
Day 21	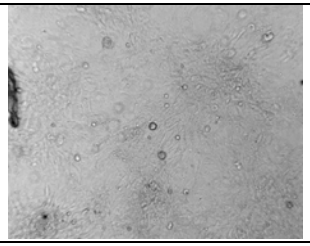	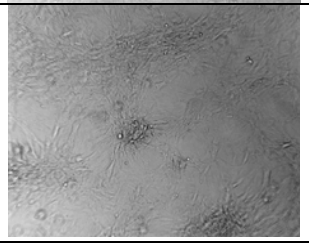	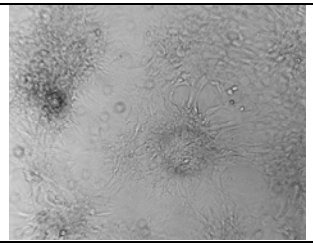	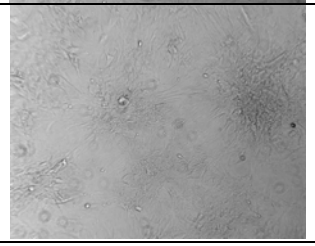	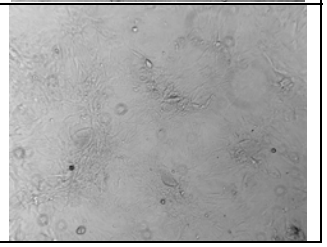

PLL low – Well 1051 – 10x objective – inverted microscope

Day	Top	Left	Center	Right	Bottom
Day 0	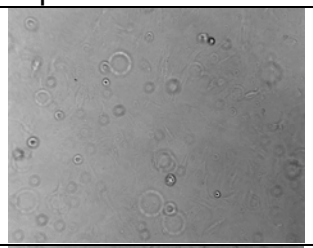	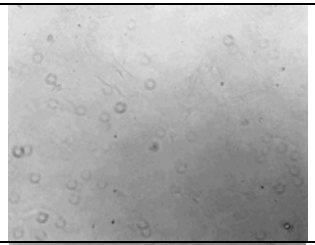	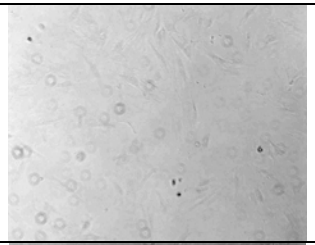	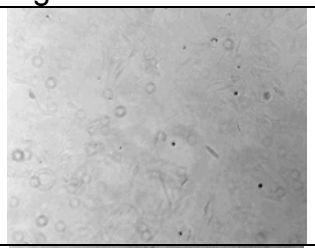	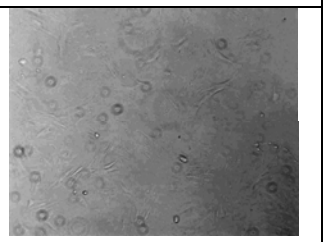
Day 3	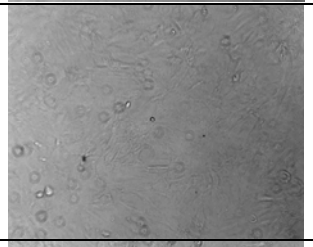	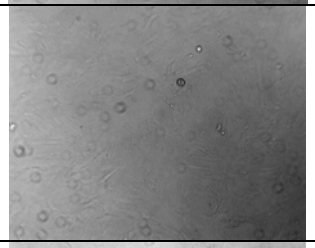	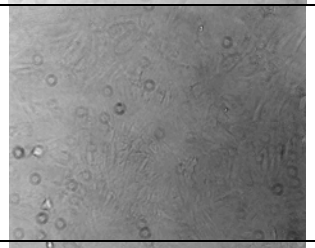	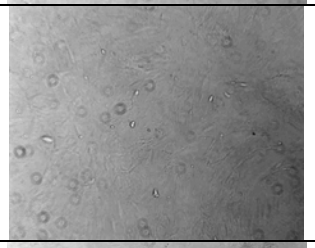	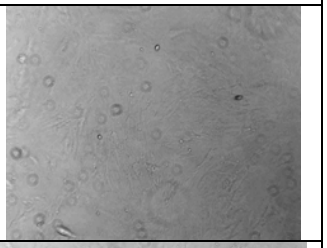
Day 6	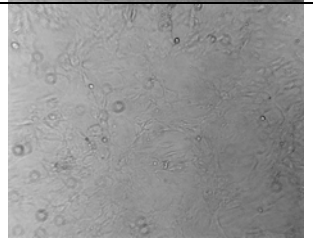	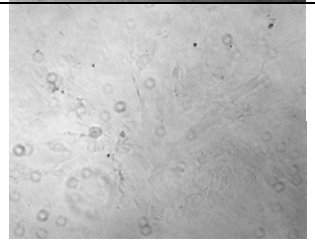	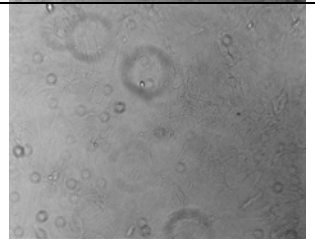	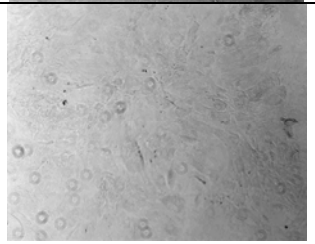	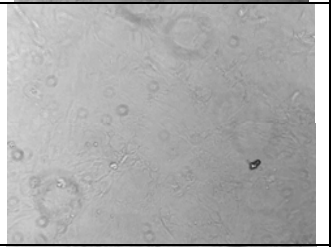
Day 9	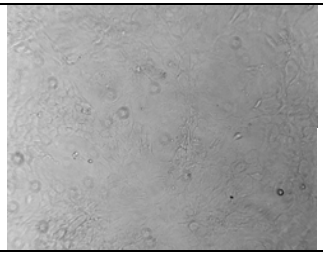	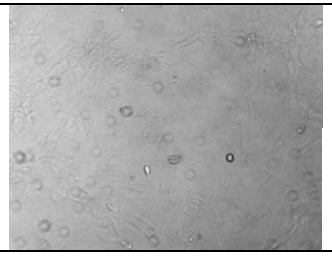	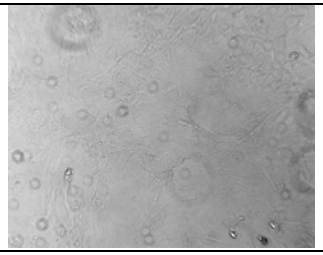	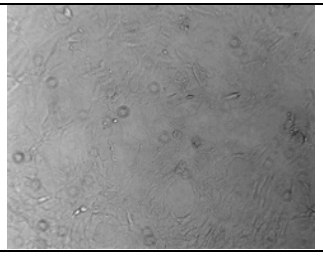	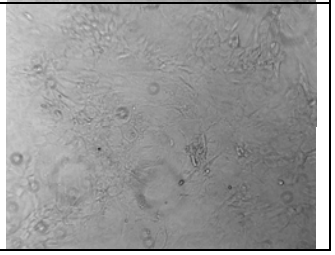

Day	Top	Left	Center	Right	Bottom
Day 12	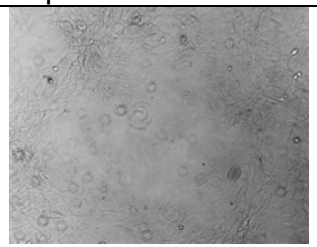	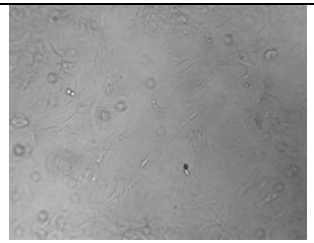	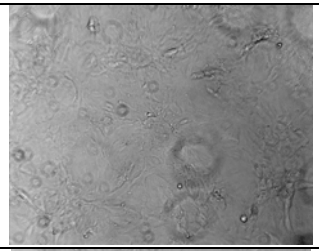	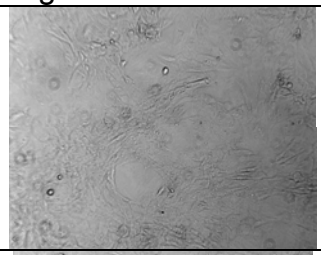	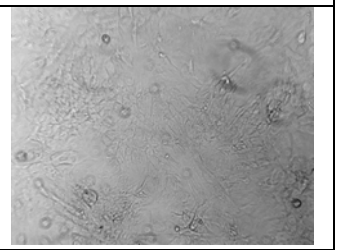
Day 15	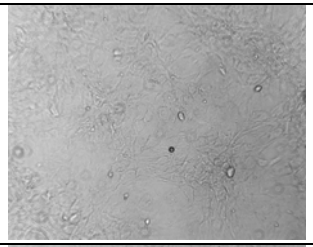	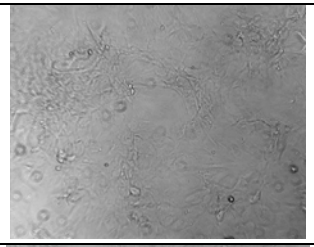	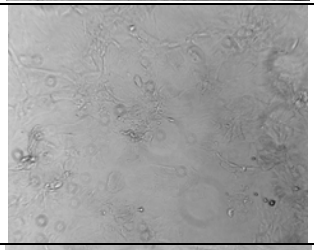	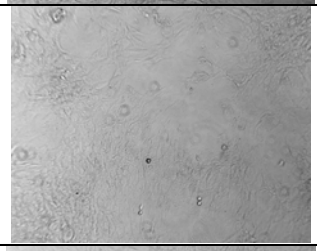	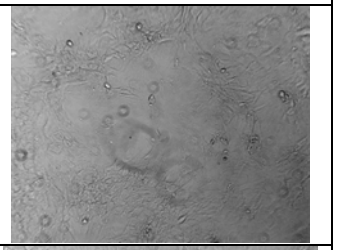
Day 18	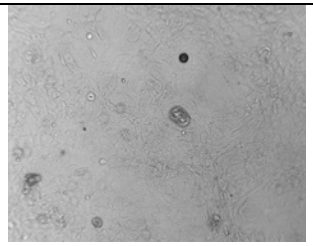	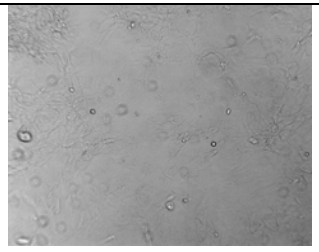	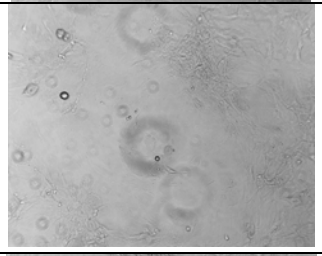	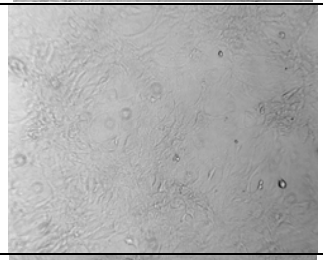	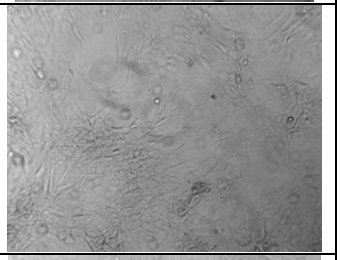
Day 21	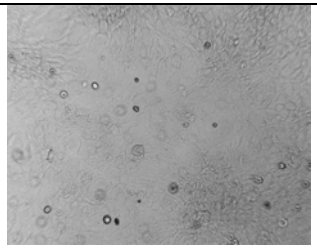	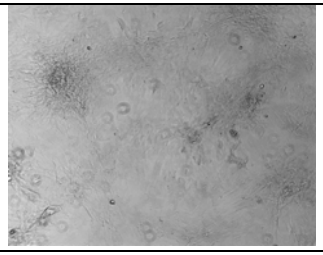	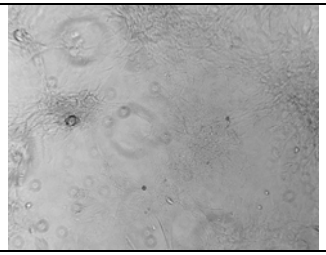	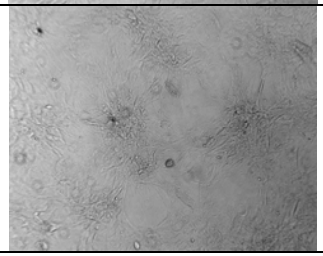	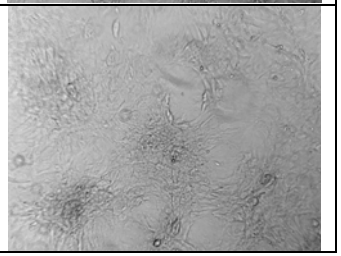

PLL high – Well 1054 – 10x objective – inverted microscope

Day	Top	Left	Center	Right	Bottom
Day 0	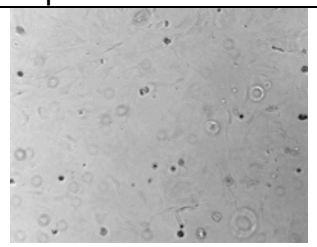	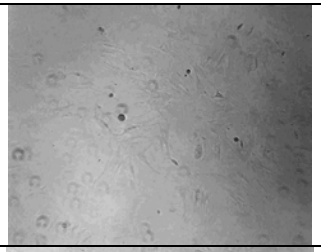	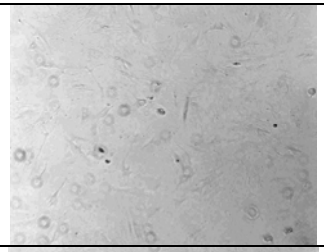	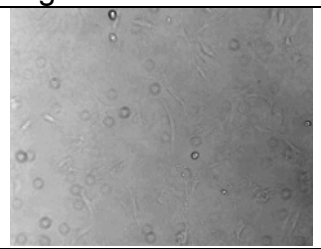	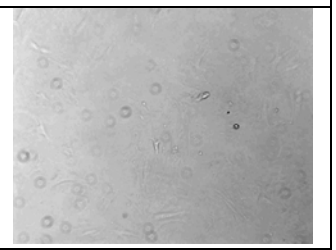
Day 3	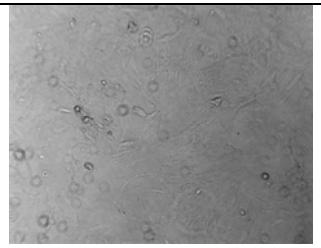	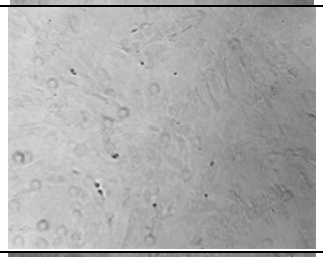	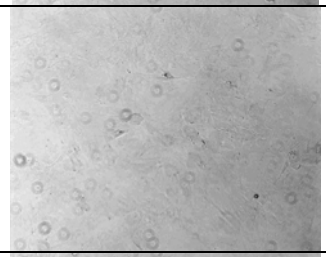	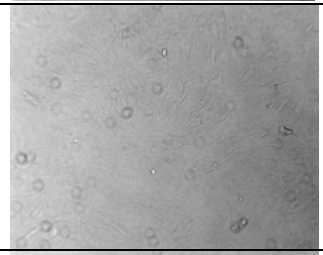	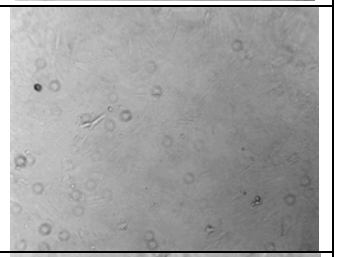
Day 6	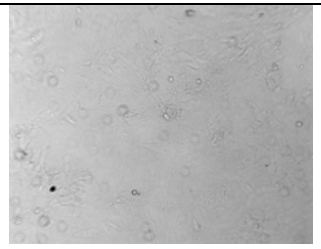	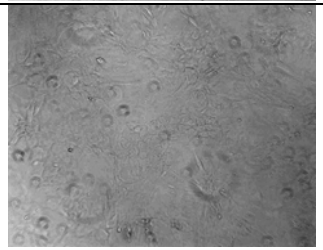	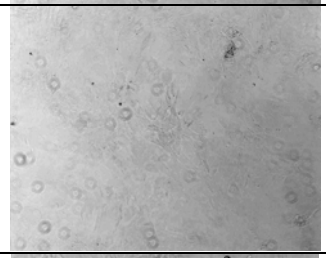	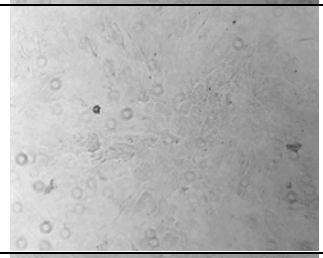	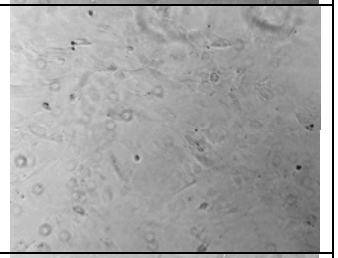
Day 9	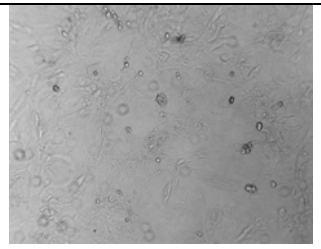	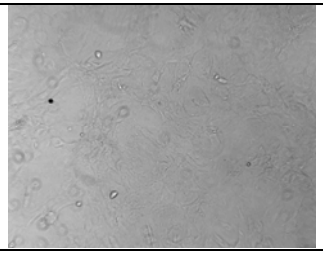	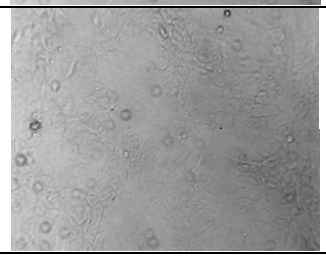	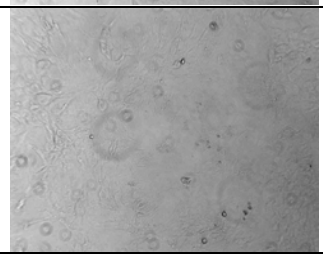	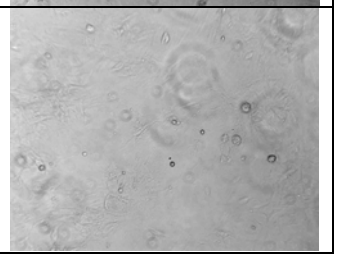

Day	Top	Left	Center	Right	Bottom
Day 12	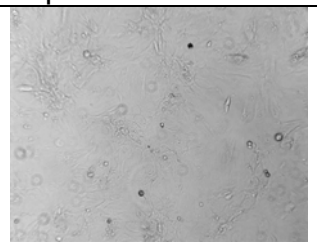	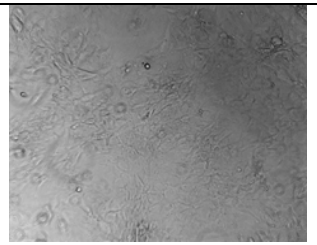	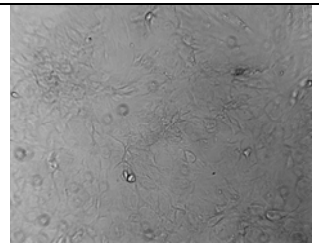	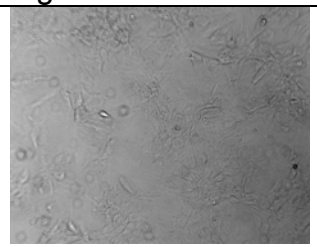	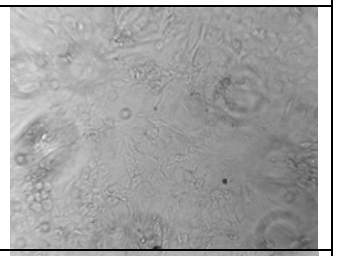
Day 15	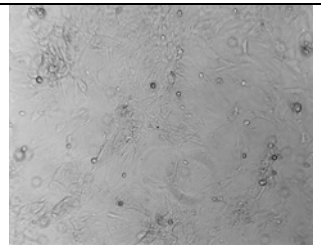	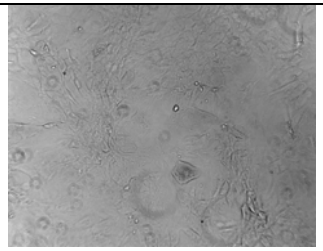	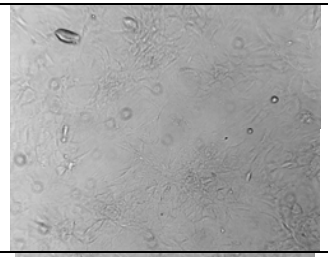	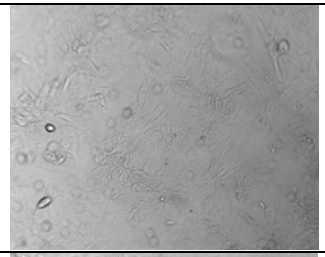	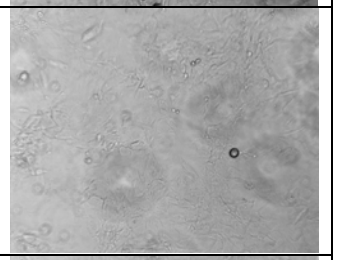
Day 18	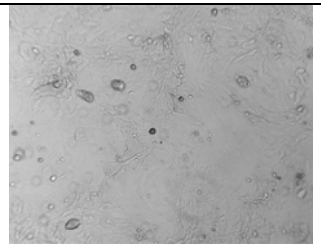	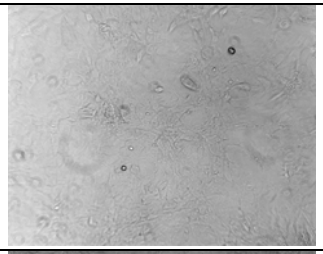	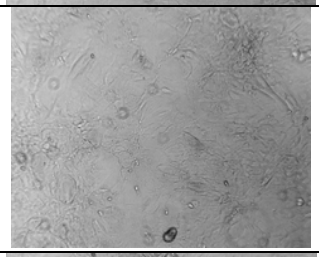	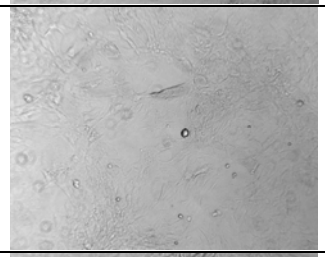	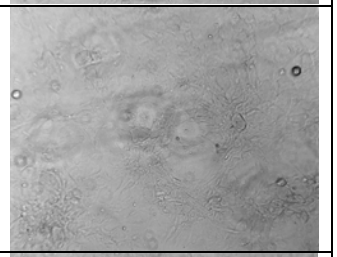
Day 21	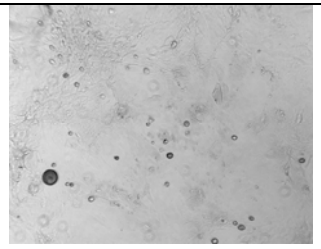	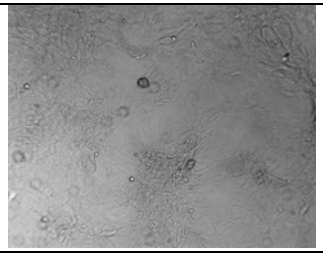	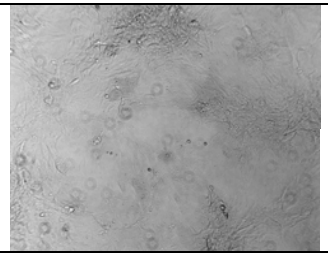	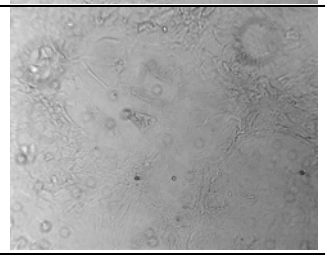	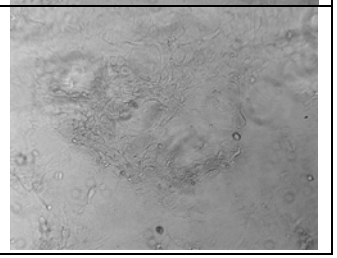

PSS low – Well 1351 – 10x objective – inverted microscope

Day	Top	Left	Center	Right	Bottom
Day 0	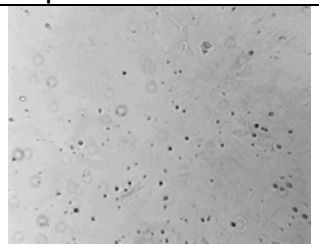	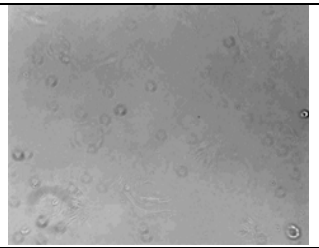	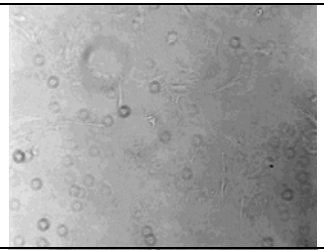	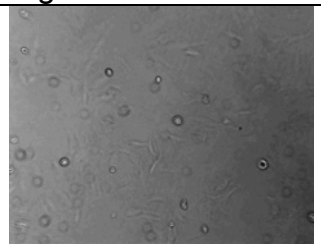	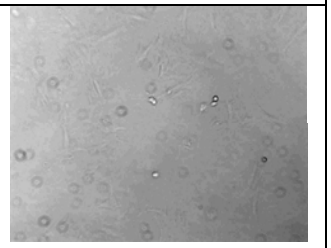
Day 3	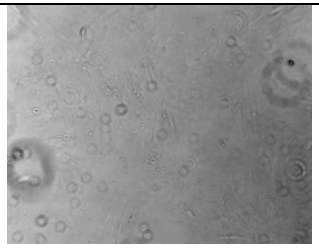	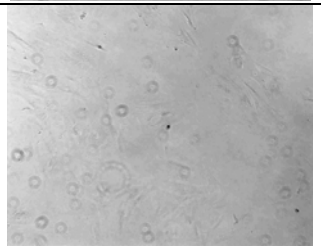	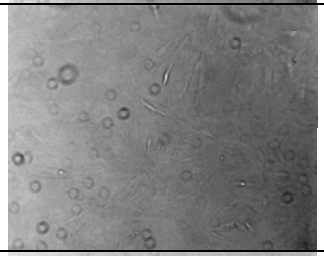	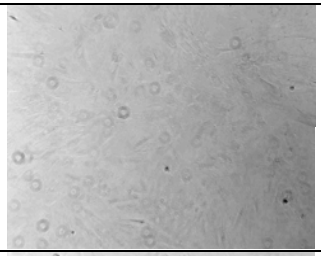	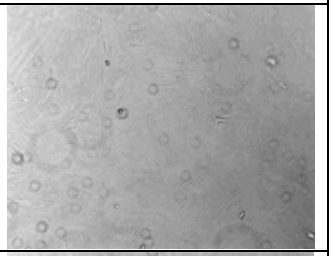
Day 6	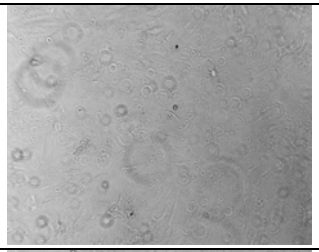	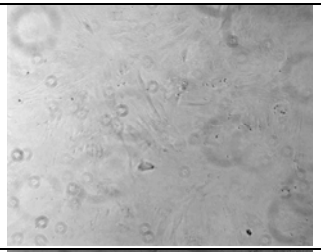	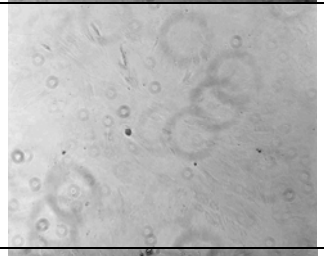	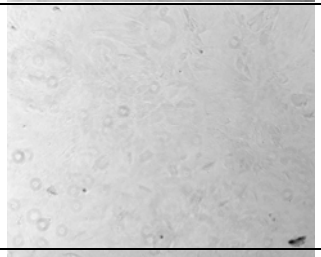	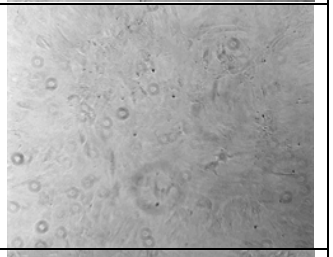
Day 9	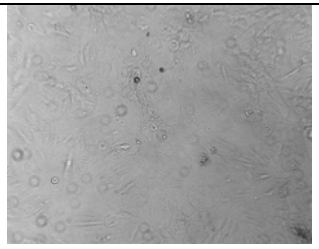	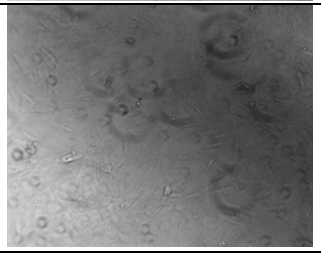	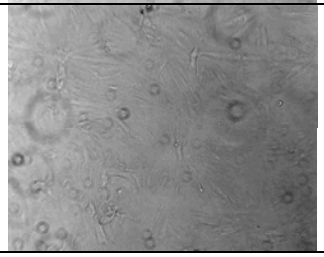	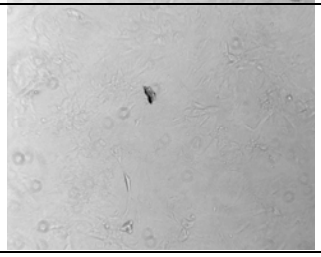	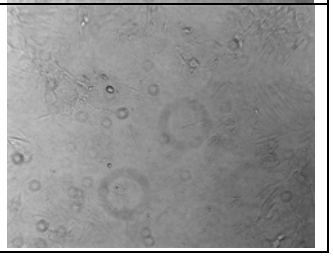

Day	Top	Left	Center	Right	Bottom
Day 12	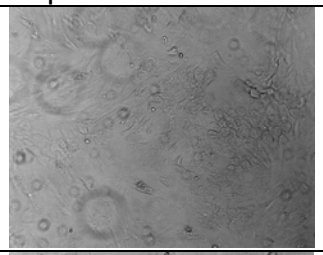	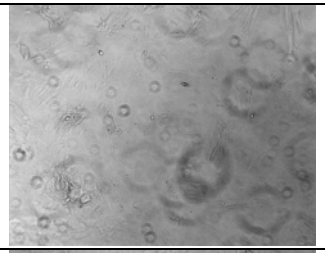	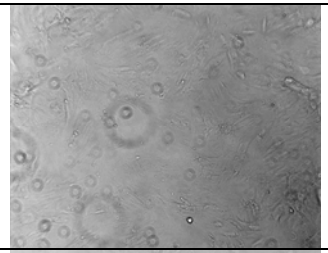	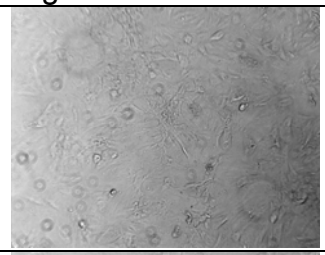	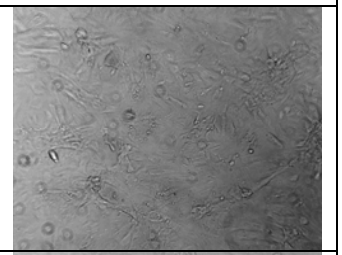
Day 15	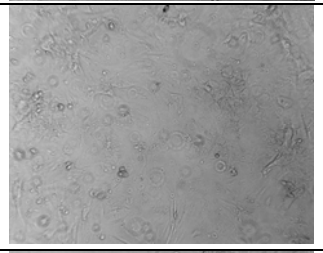	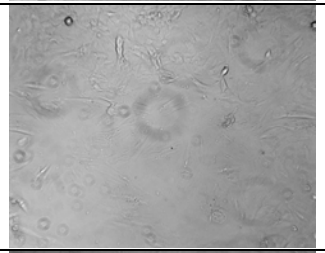	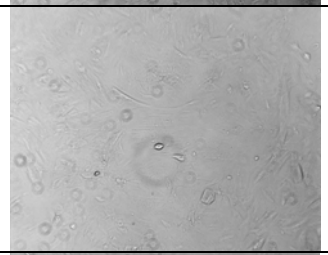	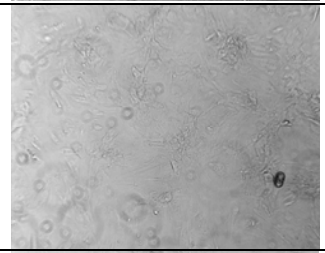	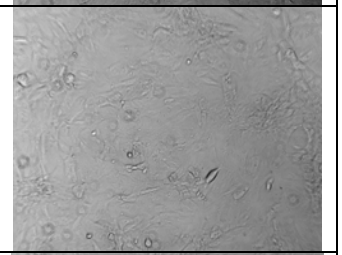
Day 18	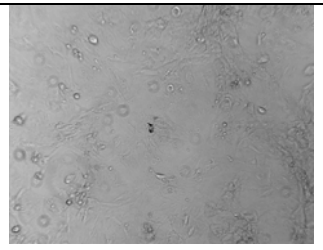	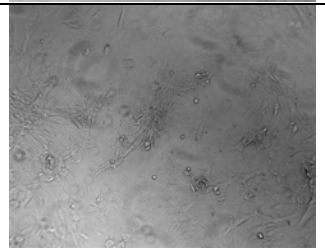	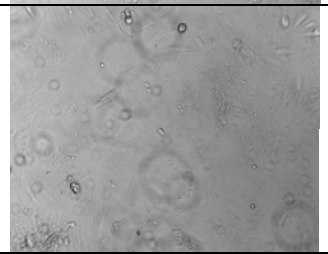	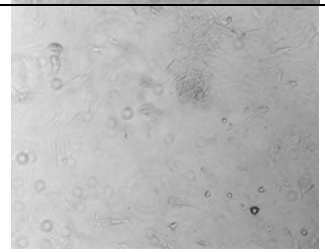	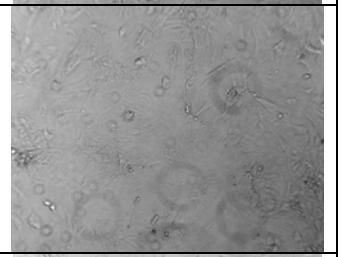
Day 21	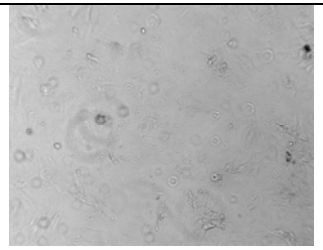	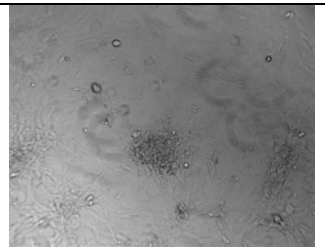	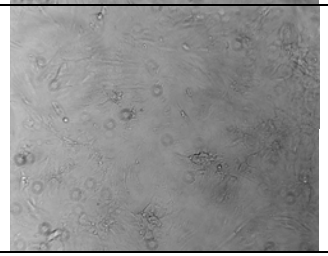	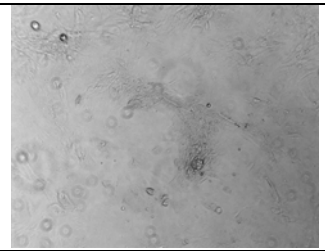	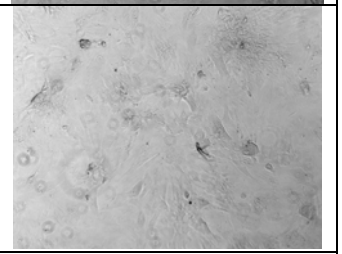

PSS high – Well 1354 – 10x objective – inverted microscope

Day	Top	Left	Center	Right	Bottom
Day 0	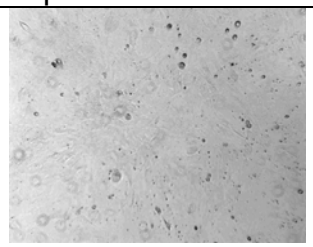	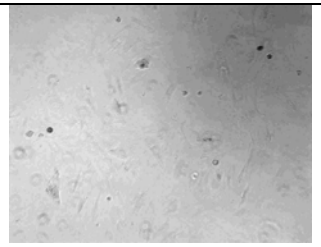	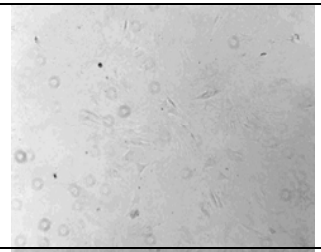	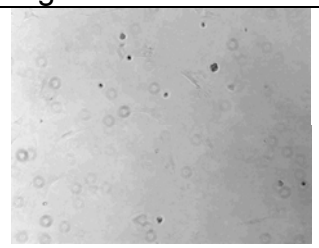	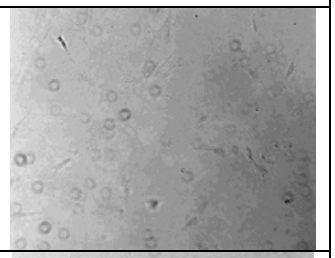
Day 3	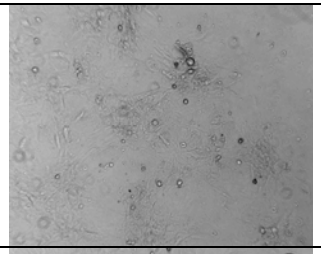	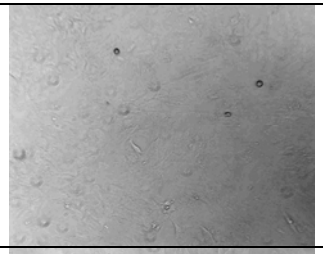	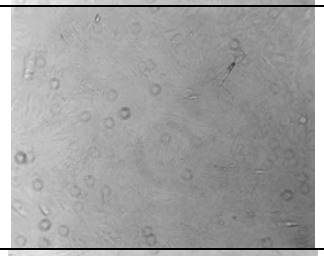	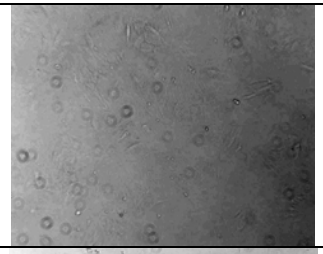	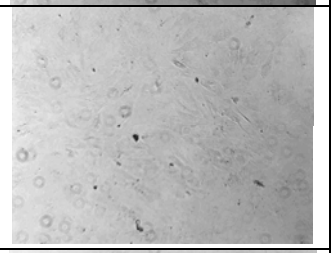
Day 6	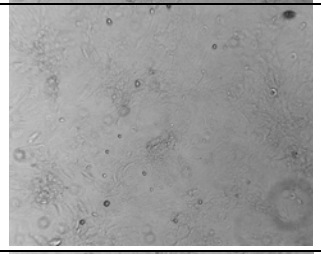	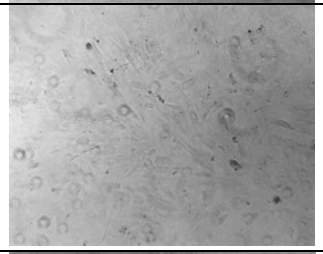	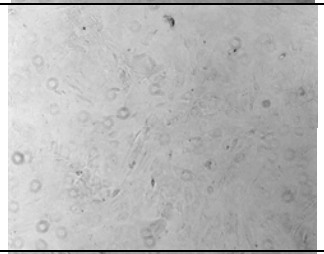	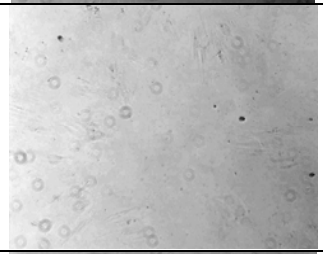	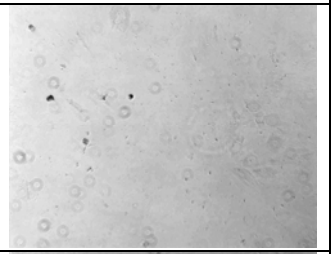
Day 9	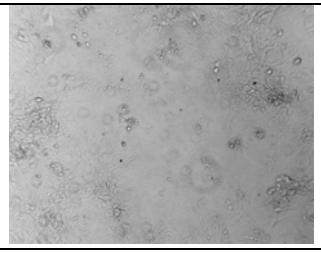	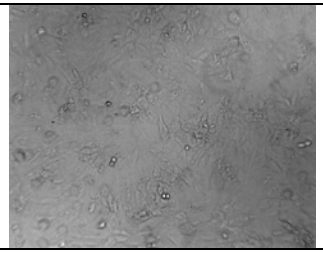	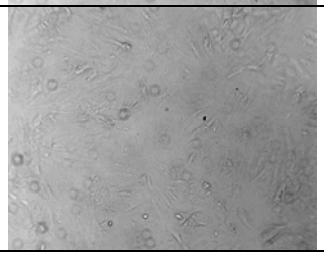	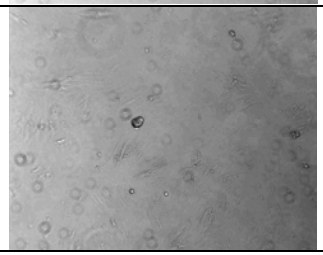	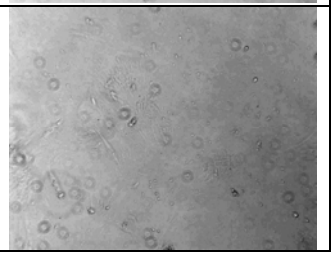

Day	Top	Left	Center	Right	Bottom
Day 12	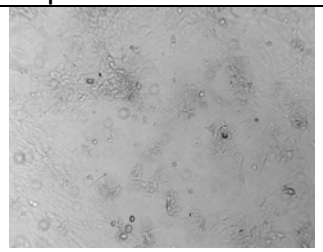	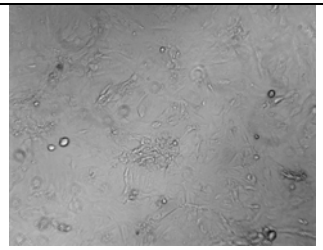	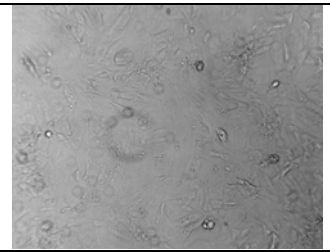	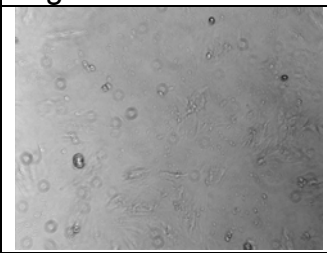	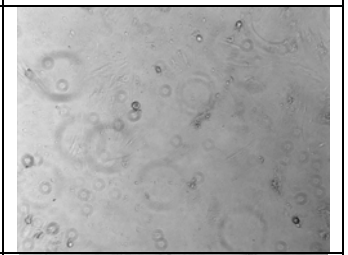
Day 15	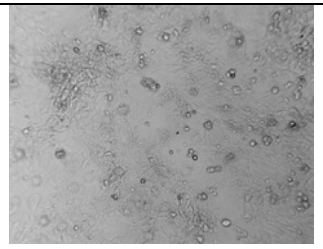	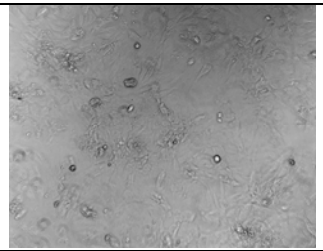	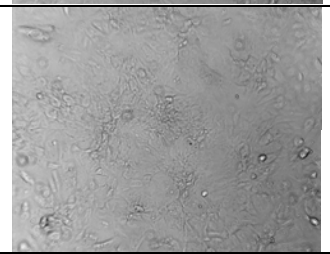	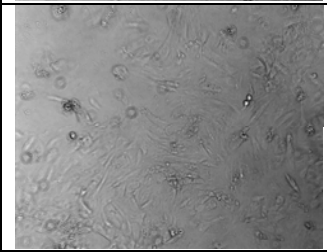	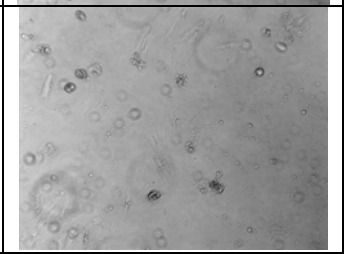
Day 18	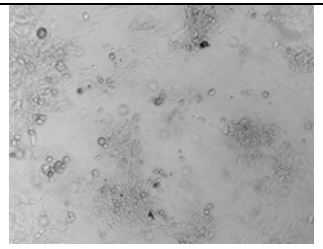	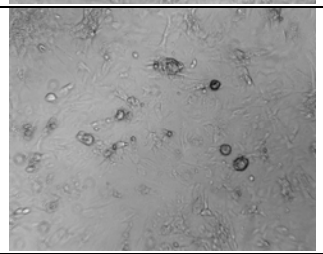	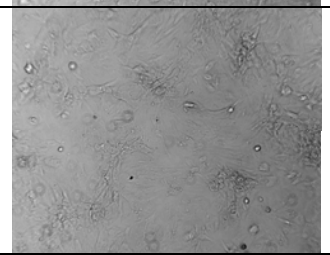	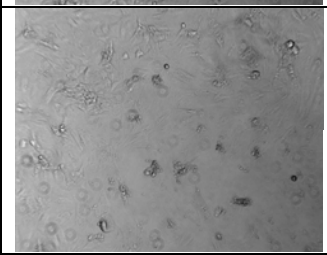	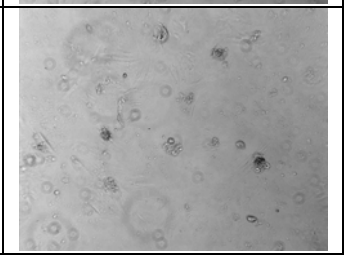
Day 21	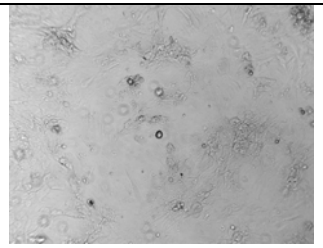	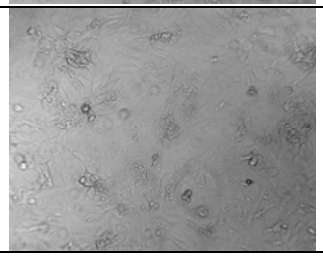	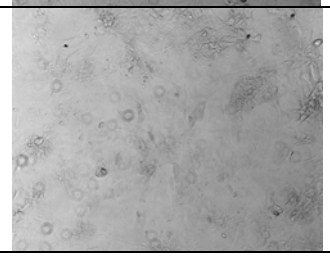	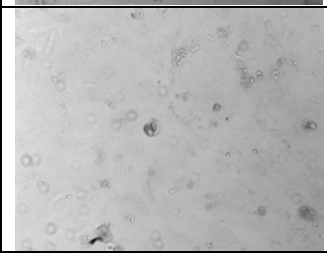	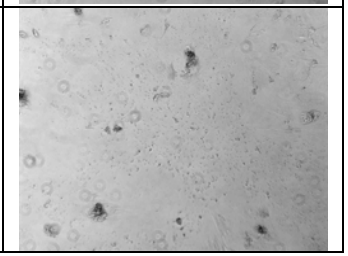

SC low – Well 1651 – 10x objective – inverted microscope

Day	Top	Left	Center	Right	Bottom
Day 0	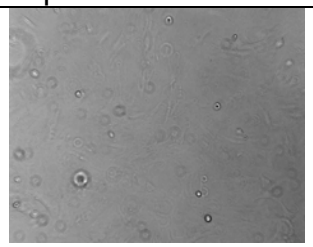	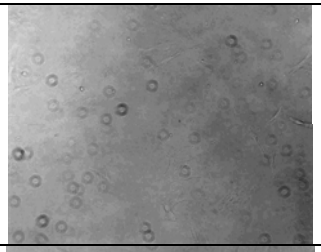	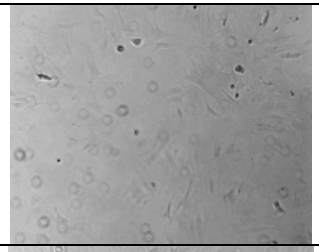	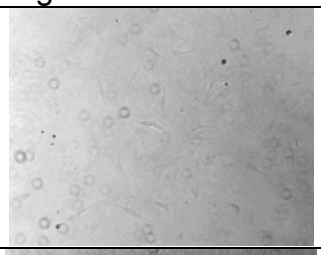	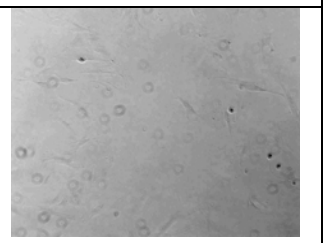
Day 3	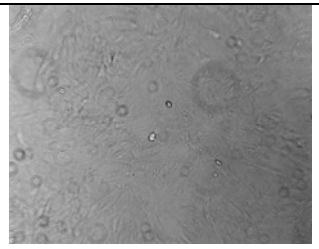	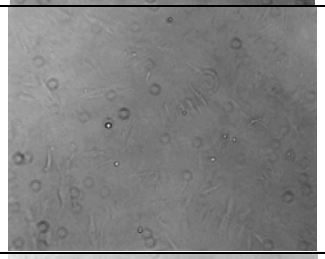	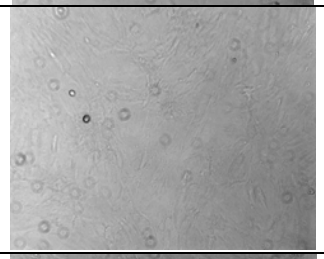	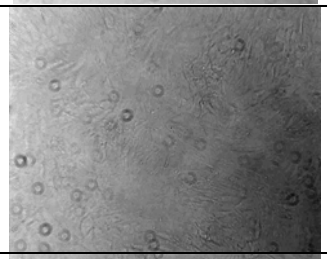	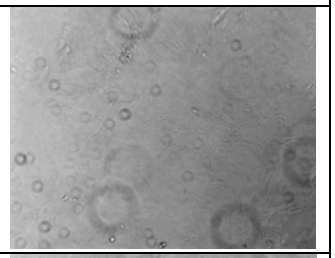
Day 6	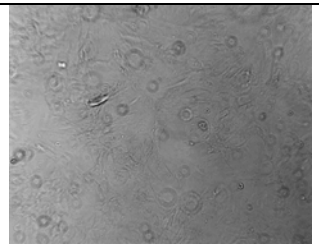	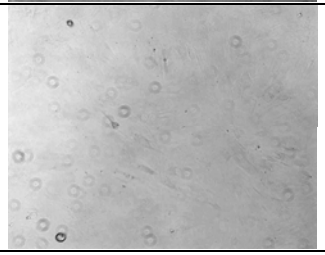	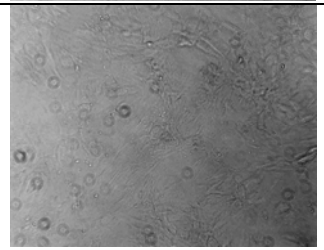	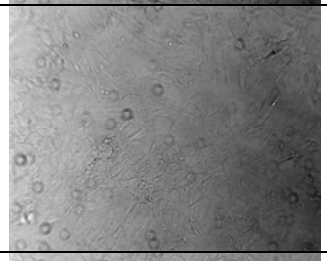	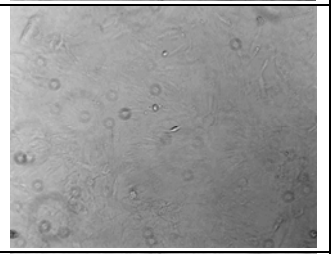
Day 9	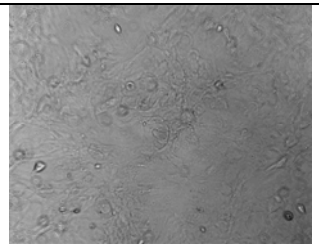		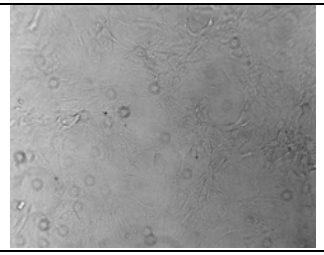	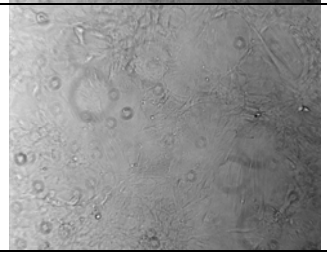	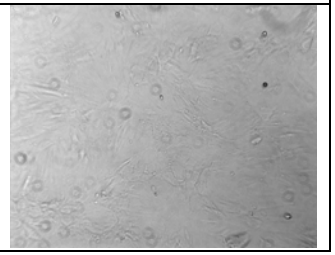

Day	Top	Left	Center	Right	Bottom
Day 12	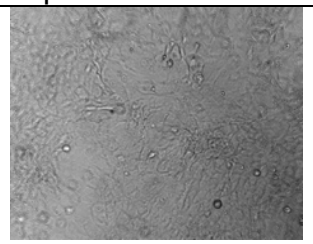	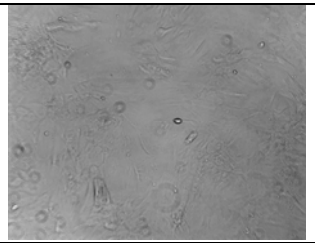	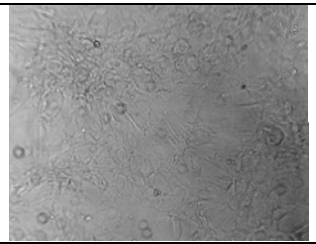	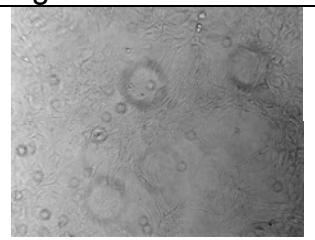	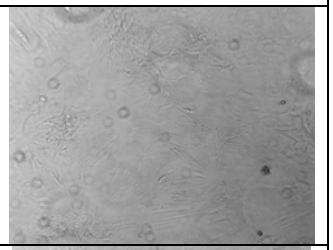
Day 15	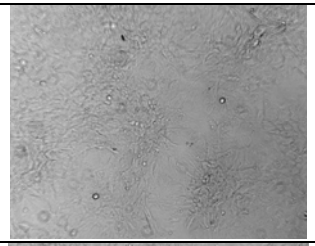	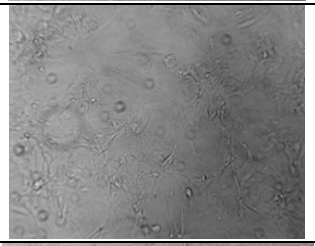	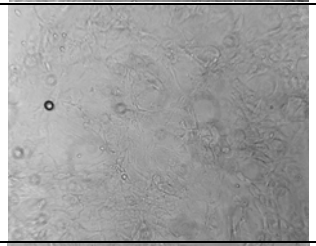	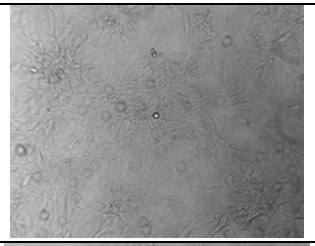	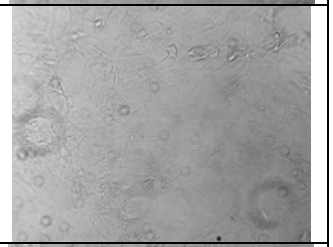
Day 18	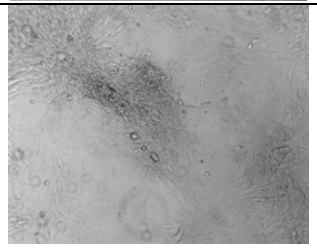	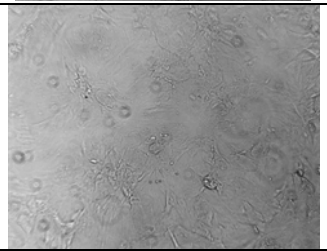	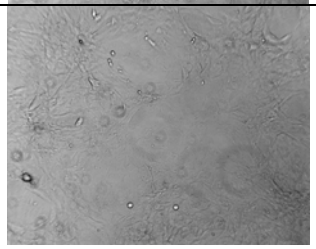	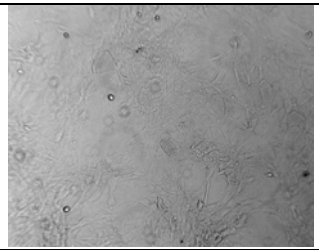	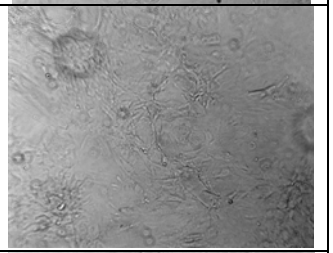
Day 21	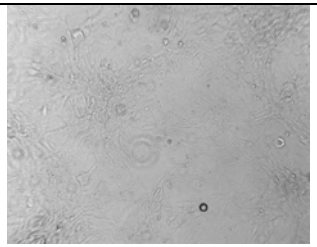	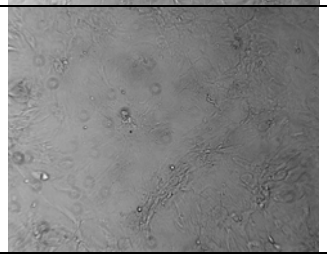	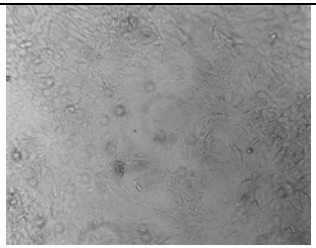	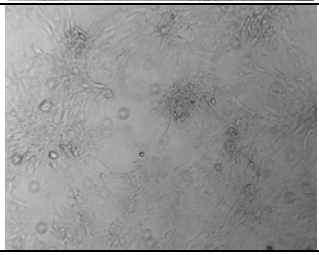	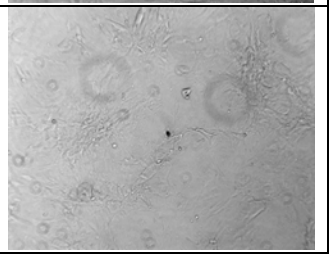

SC high – Well 1654 – 10x objective – inverted microscope

Day	Top	Left	Center	Right	Bottom
Day 0	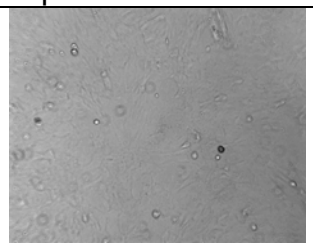	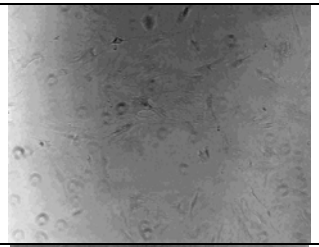	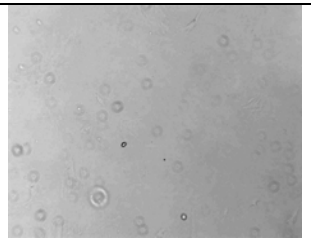		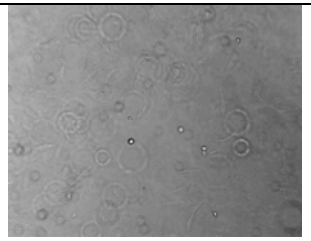
Day 3	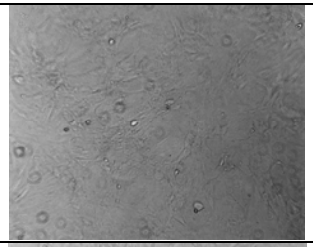	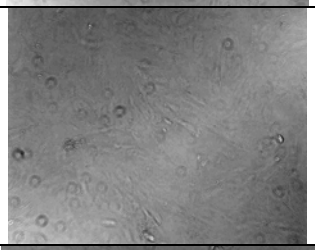	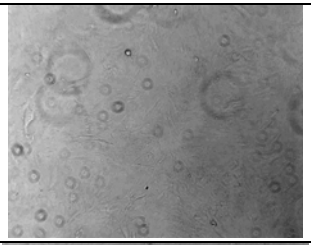	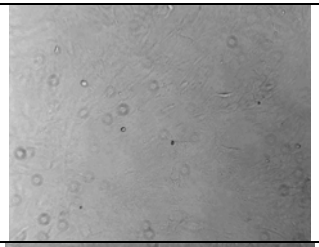	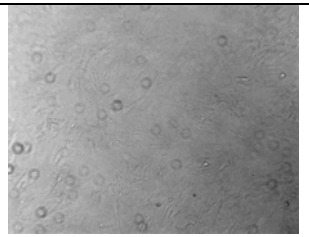
Day 6	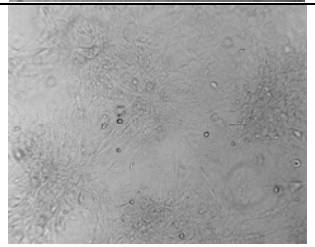	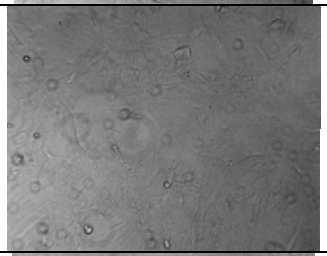	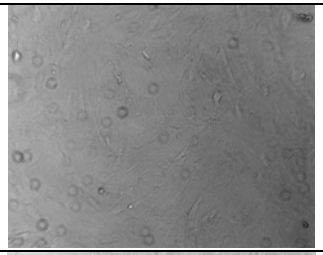	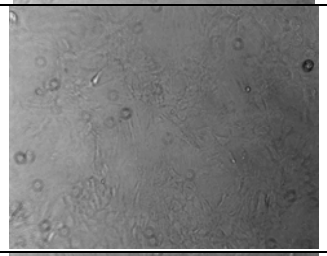	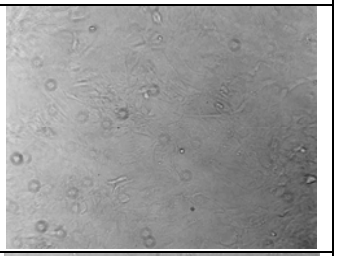
Day 9	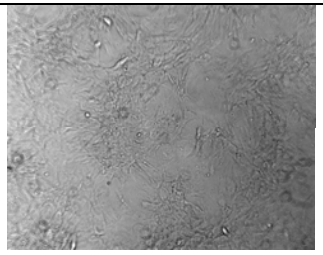	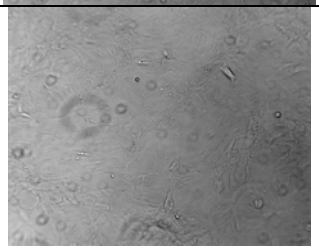	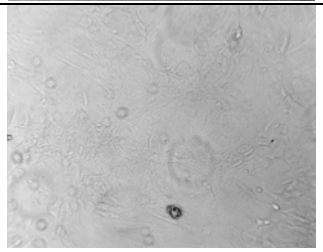	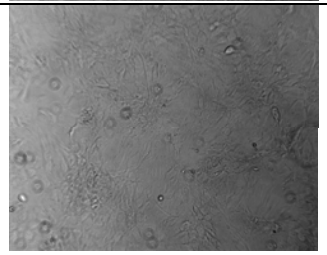	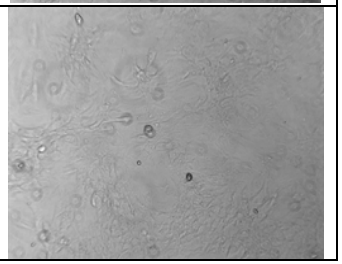

Day	Top	Left	Center	Right	Bottom
Day 12	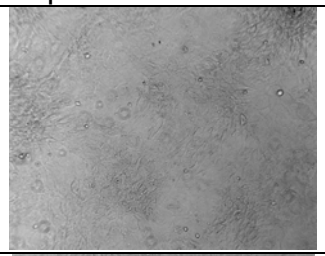	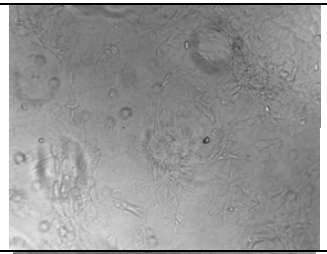	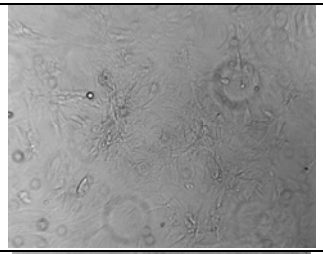	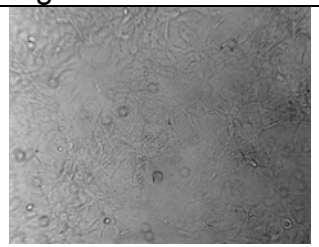	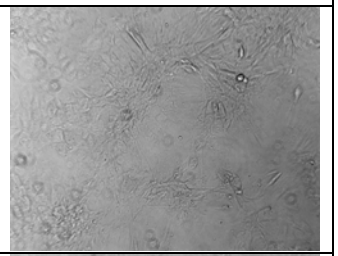
Day 15	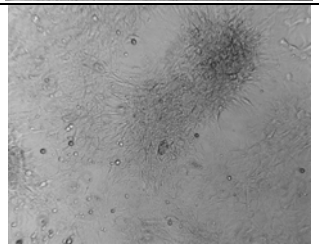	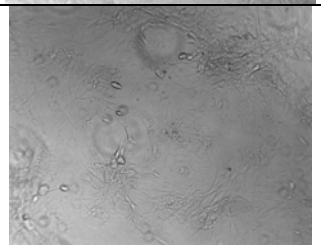	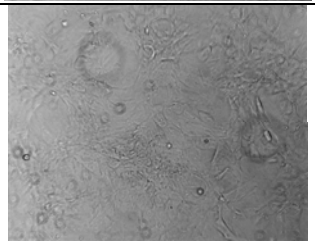	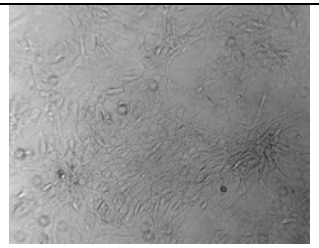	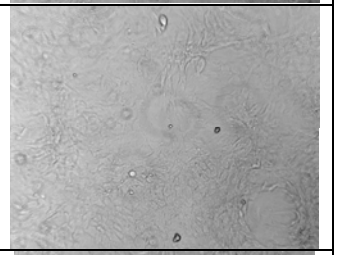
Day 18	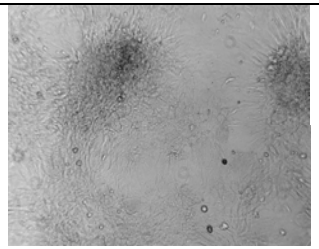	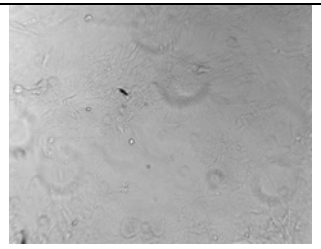	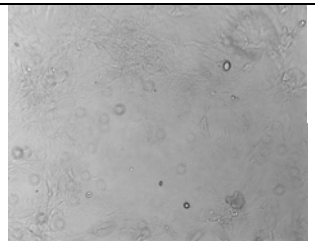	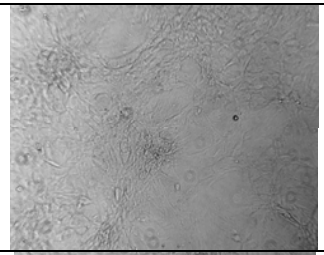	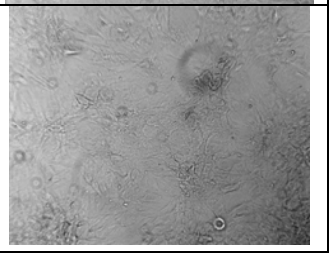
Day 21	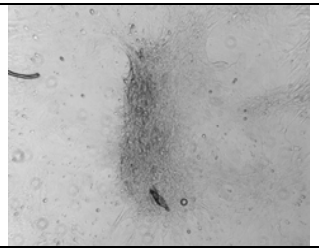	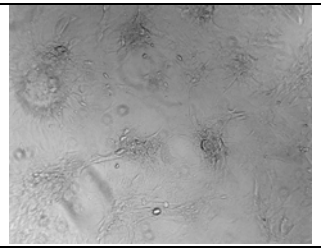	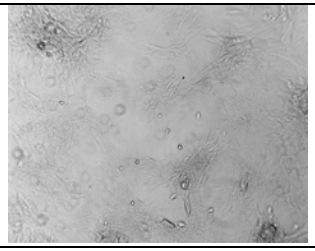	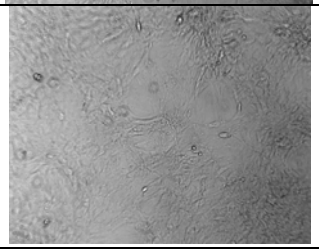	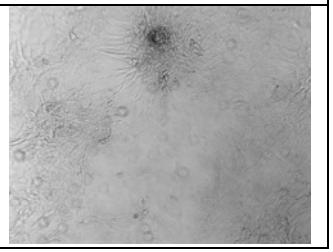

Appendix D: Viability Data

Day 0

	Count					Average Count	Total Number of Cells	Cells Per Well
Sample	**1**	**2**	**3**	**4**	**5**			
1	16	16	12	11	9	12.8	7680000	67400
1	19	18	17	15	23	18.4	11040000	96800
2	12	18	11	13	11	13	7800000	68400
2	13	17	21	9	16	15.2	9120000	80000
3	13	17	16	15	16	15.4	9240000	81100
3	14	14	15	11	13	13.4	8040000	70500
Average						14.7	8820000	77400
Std Dev						2.12697	1276182	11200

Note: The number of cells is calculated from the average count by multiplying by the dilution factors (see Materials and Methods). The total number of cells was divided by the total number of wells to get the cells per well.

Day 7

			Count								
Treament	**Dosage**	**Well**	**1**	**2**	**3**	**4**	**5**	**Average**	**Number of Cells/Well**	**Average Number of Cells/Well**	**Std Dev**
Control	**Low**	251	6	11	6	4	5	6.4	256000	262000	12000
		251	10	4	4	6	8	6.4	256000		
		254	7	6	7	5	7	6.4	256000		
		254	8	7	10	4	6	7	280000		
PLA	**Low**	351	9	11	5	5	10	8	320000	356000	49099
		351	13	4	7	10	11	9	360000		
		354	9	13	5	12	14	10.6	424000		
		354	7	7	6	11	9	8	320000		
	High	551	4	12	8	9	11	8.8	352000	348000	37238
		551	11	5	9	7	5	7.4	296000		
		554	8	10	7	11	12	9.6	384000		
		554	8	7	11	9	10	9	360000		
PLG	**Low**	651	7	11	10	8	7	8.6	344000	302000	30898
		651	6	8	8	7	7	7.2	288000		
		654	8	8	8	6	8	7.6	304000		
		654	5	6	7	6	10	6.8	272000		
	High	851	8	9	4	4	6	6.2	248000	250000	10066
		851	9	8	3	6	5	6.2	248000		
		854	6	8	3	7	6	6	240000		
		854	8	4	3	12	6	6.6	264000		
PLL	**Low**	951	5	10	4	7	12	7.6	304000	304000	34564
		951	4	4	6	10	10	6.8	272000		
		954	11	7	8	11	7	8.8	352000		
		954	10	5	10	6	5	7.2	288000		
	High	1151	5	4	4	6	5	4.8	192000	202000	22030
		1151	4	4	4	5	5	4.4	176000		
		1154	6	7	5	6	3	5.4	216000		
		1154	4	6	6	4	8	5.6	224000		
PSS	**Low**	1251	4	7	3	4	3	4.2	168000	202000	30199
		1251	8	4	12	5	1	6	240000		
		1254	4	3	8	5	6	5.2	208000		
		1254	4	5	4	4	7	4.8	192000		
	High	1451	4	4	5	5	3	4.2	168000	154000	13663
		1451	3	4	5	4	3	3.8	152000		
		1454	4	3	3	4	3	3.4	136000		
		1454	6	6	2	1	5	4	160000		
SC	**Low**	1551	6	8	6	7	8	7	280000	246000	24766
		1551	7	6	5	5	5	5.6	224000		
		1554	9	3	5	4	8	5.8	232000		
		1554	8	7	4	6	6	6.2	248000		
	High	1751	7	8	7	7	8	7.4	296000	262000	30898
		1751	4	7	6	6	6	5.8	232000		
		1754	7	6	5	4	8	6	240000		
		1754	9	6	4	8	8	7	280000		

Day 14

			Count								
Treament	**Dosage**	**Well**	**1**	**2**	**3**	**4**	**5**	**Average**	**Number of Cells/Well**	**Average Number of Cells/Well**	**Std Dev**
Control	**Low**	252	23	28	25	14	21	22.2	888000	854000	86255
		252	34	24	20	17	25	24	960000		
		255	21	22	18	14	24	19.8	792000		
		255	12	24	22	18	21	19.4	776000		
PLA	**Low**	352	17	16	13	16	16	15.6	624000	616000	19596
		352	21	13	12	13	16	15	600000		
		355	11	17	16	20	16	16	640000		
		355	12	11	13	17	22	15	600000		
	High	552	13	16	14	18	11	14.4	576000	562000	89651
		552	11	17	7	11	9	11	440000		
		555	16	20	16	8	12	14.4	576000		
		555	14	14	17	13	24	16.4	656000		
PLG	**Low**	652	24	13	17	16	20	18	720000	614000	100850
		652	6	18	17	10	16	13.4	536000		
		655	20	19	17	16	13	17	680000		
		655	13	13	16	10	13	13	520000		
	High	852	21	28	20	26	22	23.4	936000	796000	107232
		852	15	24	23	20	21	20.6	824000		
		855	16	20	21	17	15	17.8	712000		
		855	15	17	20	18	19	17.8	712000		
PLL	**Low**	952	6	8	9	11	11	9	360000	440000	59867
		952	13	13	9	10	12	11.4	456000		
		955	7	16	12	12	16	12.6	504000		
		955	13	7	10	16	9	11	440000		
	High	1152	11	12	14	16	5	11.6	464000	410000	51173
		1152	8	9	5	9	12	8.6	344000		
		1155	10	7	7	10	16	10	400000		
		1155	9	14	15	9	7	10.8	432000		
PSS	**Low**	1252	10	10	8	6	9	8.6	344000	316000	38367
		1252	5	11	8	4	9	7.4	296000		
		1255	17	3	4	6	4	6.8	272000		
		1255	11	9	3	11	10	8.8	352000		
	High	1452	7	7	3	8	4	5.8	232000	202000	26432
		1452	4	5	6	5	5	5	200000		
		1455	1	4	7	4	5	4.2	168000		
		1455	3	4	7	6	6	5.2	208000		
SC	**Low**	1552	10	11	17	12	17	13.4	536000	556000	49960
		1552	14	17	17	11	17	15.2	608000		
		1555	10	11	10	18	24	14.6	584000		
		1555	16	13	10	10	13	12.4	496000		
	High	1752	13	11	11	19	15	13.8	552000	496000	84412
		1752	12	21	12	11	17	14.6	584000		
		1755	10	11	3	18	10	10.4	416000		
		1755	12	11	9	12	10	10.8	432000		

Day 21

			Count								
Treament	**Dosage**	**Well**	**1**	**2**	**3**	**4**	**5**	**Average**	**Number of Cells/Well**	**Average Number of Cells/Well**	**Std Dev**
Control	**Low**	253	18	21	18	18	20	19	760000	828000	93409
		253	20	28	16	24	18	21.2	848000		
		256	21	14	17	24	18	18.8	752000		
		256	23	24	26	26	20	23.8	952000		
PLA	**Low**	353	25	22	28	23	21	23.8	952000	796000	106633
		353	20	16	19	16	18	17.8	712000		
		356	22	29	11	17	15	18.8	752000		
		356	11	22	16	24	23	19.2	768000		
	High	553	20	21	18	23	25	21.4	856000	760000	67882
		553	16	14	18	24	21	18.6	744000		
		556	25	11	18	18	15	17.4	696000		
		556	21	18	18	20	16	18.6	744000		
PLG	**Low**	653	30	33	30	32	27	30.4	1216000	1136000	61275
		653	35	20	27	19	35	27.2	1088000		
		656	29	41	23	22	29	28.8	1152000		
		656	27	29	25	23	32	27.2	1088000		
	High	853	39	34	46	25	29	34.6	1384000	1430000	204105
		853	33	40	32	35	35	35	1400000		
		856	42	45	43	40	44	42.8	1712000		
		856	29	38	32	25	29	30.6	1224000		
PLL	**Low**	953	29	33	23	21	17	24.6	984000	1084000	116207
		953	36	33	29	26	26	30	1200000		
		956	29	21	26	26	21	24.6	984000		
		956	25	38	22	32	29	29.2	1168000		
	High	1153	17	15	15	10	15	14.4	576000	782000	222699
		1153	13	13	15	12	23	15.2	608000		
		1156	15	25	31	20	25	23.2	928000		
		1156	27	32	24	20	24	25.4	1016000		
PSS	**Low**	1253	17	21	9	8	4	11.8	472000	514000	131676
		1253	18	16	25	14	15	17.6	704000		
		1256	11	11	7	11	10	10	400000		
		1256	10	18	10	11	11	12	480000		
	High	1453	5	16	8	11	9	9.8	392000	418000	74869
		1453	16	11	11	14	14	13.2	528000		
		1456	14	7	12	9	7	9.8	392000		
		1456	9	5	11	9	11	9	360000		
SC	**Low**	1553	16	24	22	28	28	23.6	944000	974000	81682
		1553	29	26	38	24	19	27.2	1088000		
		1556	15	28	17	27	25	22.4	896000		
		1556	25	27	28	21	20	24.2	968000		
	High	1753	32	27	32	29	37	31.4	1256000	1090000	247989
		1753	39	47	25	27	29	33.4	1336000		
		1756	26	17	21	28	28	24	960000		
		1756	22	26	12	19	22	20.2	808000		

Appendix E: Collagen Data

Standard Curve – Assay Set 1

		Spec Reading								
Treatment	Collagen (ug)	1	2	3	Average	Std Dev	Average	Std Dev	Baseline	Baseline Corrected
Blank	0	0.1158	0.1191	0.1199	0.118267	0.00217	0.09274	0.02337	0.092744	0
PLA		0.089	0.09	0.091	0.09	0.001				
PLG		0.0804	0.0866	0.0811	0.0827	0.0034				
PLL		0.0885	0.088	0.0903	0.088933	0.00121				
PSS		0.0572	0.0571	0.0577	0.057333	0.00032				
SC		0.1173	0.1184	0.122	0.119233	0.00246				
Blank	12.5	0.583	0.5729	0.5709	0.5756	0.00649	0.51391	0.17055	0.092744	0.4211611
PLA		0.553	0.558	0.564	0.558333	0.00551				
PLG		0.477	0.4867	0.4834	0.482367	0.00493				
PLL		0.6706	0.7048	0.6992	0.691533	0.01834				
PSS		0.1887	0.196	0.1966	0.193767	0.0044				
SC		0.5614	0.5909	0.5932	0.581833	0.01773				
Blank	25	0.9141	0.9266	0.9312	0.923967	0.00885	0.86981	0.15276	0.092744	0.7770667
PLA		0.827	0.835	0.861	0.841	0.01778				
PLG		0.5878	0.6088	0.6044	0.600333	0.01107				
PLL		1.0664	1.0737	1.0402	1.0601	0.01762				
PSS		0.8358	0.8785	0.8671	0.860467	0.02211				
SC		0.9293	0.9245	0.9452	0.933	0.01083				
Blank	50	1.2235	1.2231	1.2378	1.228133	0.00837	1.32354	0.42695	0.092744	1.2307944
PLA		1.211	1.217	1.217	1.215	0.00346				
PLG		1.3769	1.3989	1.3984	1.3914	0.01256				
PLL		2.005	2.0776	2.0819	2.054833	0.04321				
PSS		0.69	0.7745	0.7284	0.730967	0.04231				
SC		1.3096	1.3136	1.3395	1.3209	0.01623				

Note: This table shows the spectrophotometric readings of the calibration data. There are 3 readings for each treatment at each known collagen level. The baseline is the average spectrophotometric reading when no collagen is present. This is subtracted from the measured spectrophotometric readings to create a new baseline where zero collagen has zero

spectrophotometric reading. Each collagen level was measured in the presence of the different polyelectrolytes to be sure that the polyelectrolyte did not interfere with the dye binding to the collagen. Two different calibration assays were completed since two kits with different lots of solutions were used to evaluate the amount of collagen present.

Standard Curve for Soluble Collagen Content – Assay Set 1

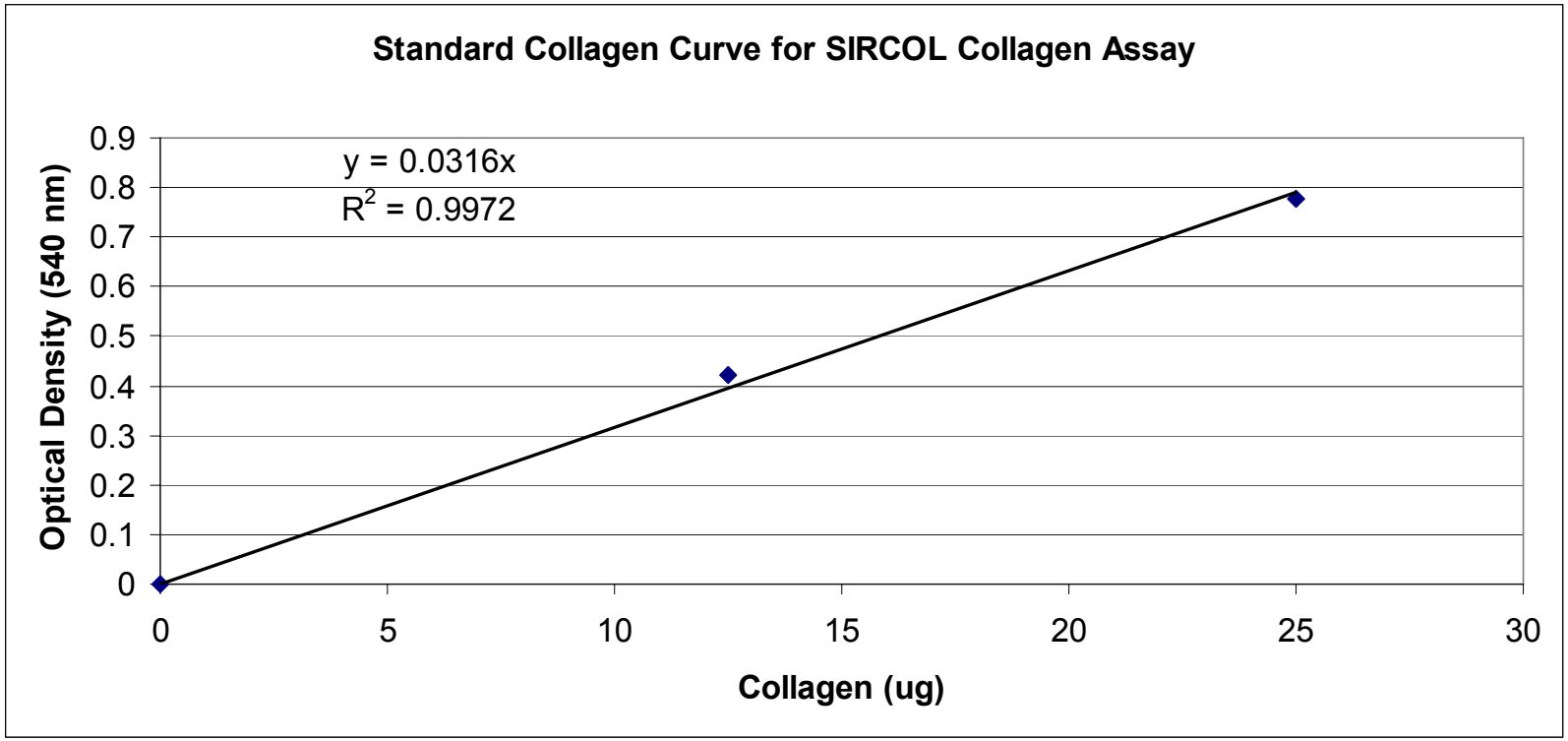

Note: 50 µg data was removed because actual testing showed collagen to be in the range of less than 10 µg. The line of best fit is generated using all data points, but the graph portion of the graph used for determining the amount of collagen present was enlarged for better visibility.

Standard Curve – Assay Set 2

		Spec Reading								
	Collagen (ug)	**1**	**2**	**3**	**Average**	**Std Dev**	**Average**	**Std Dev**	**Baseline**	**Baseline Corrected**
Blank		0.1356	0.1374	0.1375	0.13683	0.00107				
Blank		0.1497	0.1501	0.1523	0.1507	0.0014				
PLA	**0**	0.1357	0.1414	0.1441	0.1404	0.00429	0.14302	0.01083	0.14302	0
PLG		0.1266	0.1297	0.1294	0.12857	0.00171				
PSS		0.1583	0.1574	0.1629	0.15953	0.00295				
SC		0.1404	0.1431	0.1428	0.1421	0.00148				
Blank		0.4639	0.466	0.4592	0.46303	0.00348				
Blank		0.5264	0.5269	0.5376	0.5303	0.00633				
PLA	**12.5**	0.4648	0.4786	0.4602	0.46787	0.00958	0.49258	0.04089	0.14302	0.3495611
PLG		0.4405	0.4466	0.4316	0.43957	0.00754				
PSS		0.5254	0.5196	0.5055	0.51683	0.01023				
SC		0.5399	0.5429	0.5309	0.5379	0.00624				
Blank		0.6617	0.6721	0.6359	0.65657	0.01864				
Blank		0.6581	0.6789	0.6704	0.66913	0.01046				
PLA	**25**	0.6581	0.6615	0.6337	0.6511	0.01516	0.66357	0.02923	0.14302	0.52055
PLG		0.6521	0.6217	0.5775	0.6171	0.03751				
PSS		0.6993	0.6983	0.6682	0.6886	0.01767				
SC		0.6721	0.7208	0.7039	0.69893	0.02473				
Blank		0.8811	0.8952	0.899	0.89177	0.00943				
Blank		0.9055	0.9461	0.917	0.92287	0.02093				
PLA	**50**	0.902	0.9178	0.9036	0.9078	0.0087	0.89867	0.01434	0.14302	0.7556444
PLG		0.8699	0.863	0.9162	0.88303	0.02893				
PSS		0.8663	0.9138	0.8936	0.89123	0.02384				
SC		0.8833	0.9057	0.8969	0.8953	0.01129				

Standard Curve for Soluble Collagen Content – Assay Set 2

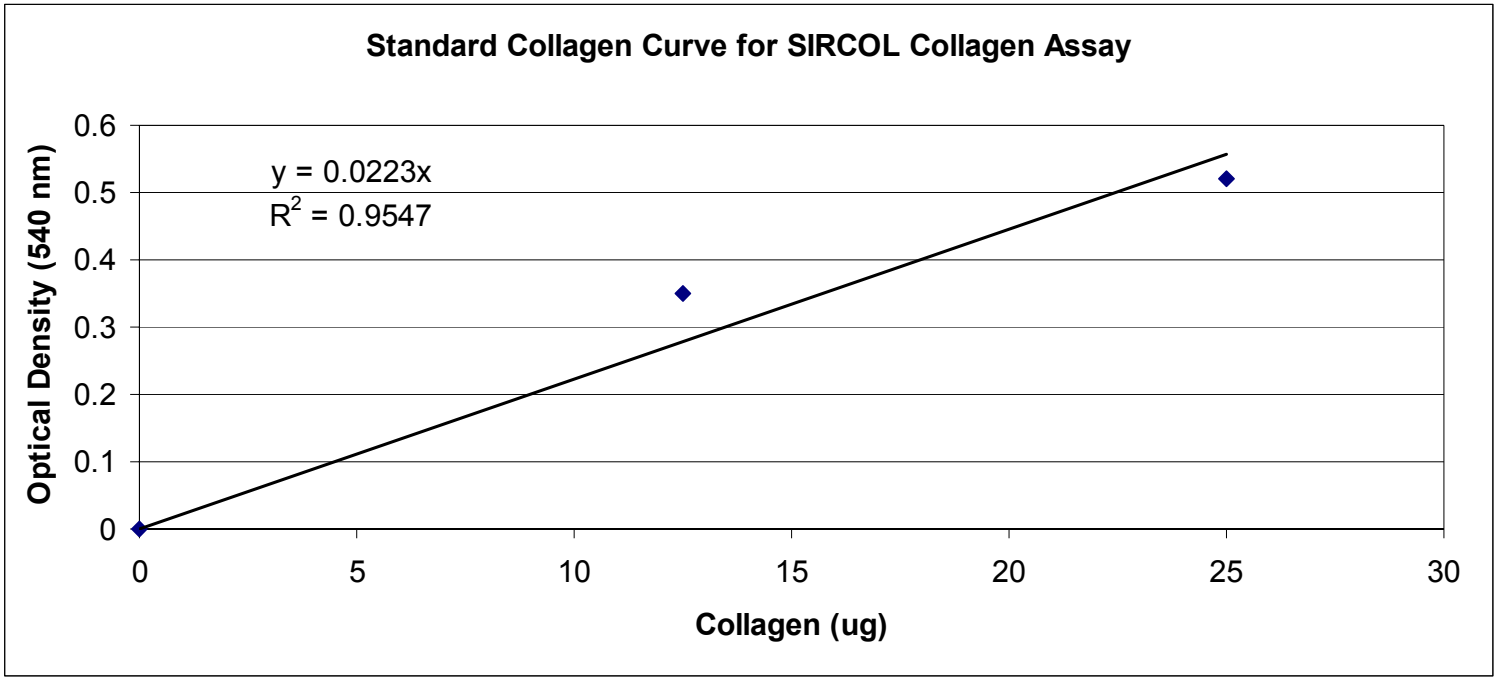

Day 0

Sample	Assay Set	Spec Reading 1	2	3	Average	Standard Deviation	Baseline	Baseline Corrected	Collagen (ug)	Total Collagen in Well (ug)
1	1	0.1136	0.1163	0.1188	0.1162333	0.0026006	0.0927444	0.0234889	0.7433193	29.732771
2	1	0.1161	0.1169	0.1186	0.1172	0.0012767	0.0927444	0.0244556	0.77391	30.956399
3	2	0.1377	0.1437	0.1423	0.1412333	0.003139	0.1430222	-0.001789	-0.080219	-3.208769
4	2	0.158	0.1625	0.1606	0.1603667	0.0022591	0.1430222	0.0173444	0.7777778	31.111111
									Average	22.147878
									Std Dev	16.915671

Control

			Spec Reading										
Day	Well	Assay Set	1	2	3	Average	Std Dev	Baseline	Baseline Corrected	Collagen (ug)	Total Collagen in Well (ug)	Average (ug)	Std Dev
3	253	1	0.1198	0.1233	0.1241	0.1224	0.0023	0.092744	0.0296556	0.938467	37.53868	61.1803	33.3803
	253	2	0.1955	0.1983	0.197	0.19693	0.0014	0.143022	0.0539111	2.417539	96.70154		
	256	1	0.1522	0.1624	0.1584	0.15767	0.0051	0.092744	0.0649222	2.054501	82.18003		
	256	2	0.1522	0.158	0.1662	0.1588	0.007	0.143022	0.0157778	0.707524	28.30095		
6	253	1	0.1346	0.1384	0.1388	0.13727	0.0023	0.092744	0.0445222	1.408931	56.35724	65.8225	28.1526
	253	2	0.1592	0.1641	0.1649	0.16273	0.0031	0.143022	0.0197111	0.883906	35.35625		
	256	1	0.1449	0.1486	0.1483	0.14727	0.0021	0.092744	0.0545222	1.725387	69.01547		
	256	2	0.2042	0.197	0.1994	0.2002	0.0037	0.143022	0.0571778	2.564026	102.561		
9	253	1	0.1373	0.1394	0.1403	0.139	0.0015	0.092744	0.0462556	1.463783	58.55134	100.601	48.9937
	253	2	0.187	0.1925	0.193	0.19083	0.0033	0.143022	0.0478111	2.143996	85.75984		
	256	1	0.1575	0.1631	0.163	0.1612	0.0032	0.092744	0.0684556	2.166315	86.6526		
	256	2	0.2325	0.246	0.2373	0.2386	0.0068	0.143022	0.0955778	4.285999	171.44		
12	253	1	0.1337	0.1358	0.1354	0.13497	0.0011	0.092744	0.0422222	1.336146	53.44585	86.4996	34.6608
	253	2	0.1736	0.1864	0.1777	0.17923	0.0065	0.143022	0.0362111	1.623817	64.95267		
	256	1	0.1657	0.1714	0.1713	0.16947	0.0033	0.092744	0.0767222	2.427918	97.11674		
	256	2	0.2105	0.2209	0.2159	0.21577	0.0052	0.143022	0.0727444	3.262083	130.4833		
15	253	1	0.148	0.1541	0.1519	0.15133	0.0031	0.092744	0.0585889	1.854079	74.16315	102.468	26.2179
	253	2	0.1926	0.1991	0.2161	0.2026	0.0121	0.143022	0.0595778	2.671649	106.866		
	256	1	0.1735	0.1607	0.1634	0.16587	0.0067	0.092744	0.0731222	2.313994	92.55977		
	256	2	0.217	0.2209	0.2191	0.219	0.002	0.143022	0.0759778	3.407075	136.283		
18	253	1	0.1917	0.1974	0.1991	0.19607	0.0039	0.092744	0.1033222	3.269691	130.7876	125.9	34.3654
	253	2	0.2318	0.2423	0.2347	0.23627	0.0054	0.143022	0.0932444	4.181365	167.2546		
	256	1	0.1858	0.1901	0.1915	0.18913	0.003	0.092744	0.0963889	3.050281	122.0113		
	256	2	0.1879	0.1924	0.1885	0.1896	0.0024	0.143022	0.0465778	2.08869	83.54758		
21	253	1	0.1781	0.1841	0.1828	0.18167	0.0032	0.092744	0.0889222	2.813994	112.5598	110.588	45.0154
	253	2	0.1992	0.2025	0.2022	0.2013	0.0018	0.143022	0.0582778	2.613353	104.5341		
	256	1	0.2025	0.2622	0.2106	0.2251	0.0324	0.092744	0.1323556	4.188467	167.5387		
	256	2	0.1692	0.1821	0.1743	0.1752	0.0065	0.143022	0.0321778	1.44295	57.71799		
											Total	653.059	

PLA Low

			Spec Reading										
Day	Well	Assay Set	1	2	3	Average	Std Dev	Baseline	Baseline Corrected	Collagen (ug)	Total Collagen in Well (ug)	Average (ug)	Std Dev
3	353	1	0.1396	0.1442	0.1441	0.14263	0.0026	0.092744	0.0498889	1.578762	63.15049	40.0451	25.8969
	353	2	0.1467	0.1734	0.1635	0.1612	0.0135	0.143022	0.0181778	0.815147	32.60588		
	356	1	0.1359	0.1397	0.1394	0.13833	0.0021	0.092744	0.0455889	1.442686	57.70745		
	356	2	0.1447	0.1486	0.147	0.14677	0.002	0.143022	0.0037444	0.167912	6.716492		
6	353	1	0.1476	0.1571	0.1869	0.16387	0.0205	0.092744	0.0711222	2.250703	90.02813	91.7534	23.8692
	353	2	0.201	0.2033	0.2009	0.20173	0.0014	0.143022	0.0587111	2.632785	105.3114		
	356	1	0.1359	0.1401	0.1418	0.13927	0.003	0.092744	0.0465222	1.472222	58.88889		
	356	2	0.2038	0.2067	0.2072	0.2059	0.0018	0.143022	0.0628778	2.819631	112.7853		
9	353	1	0.164	0.1699	0.1699	0.16793	0.0034	0.092744	0.0751889	2.379395	95.17581	126.599	30.1419
	353	2	0.224	0.2232	0.2197	0.2223	0.0023	0.143022	0.0792778	3.555057	142.2023		
	356	1	0.1732	0.1787	0.1831	0.17833	0.005	0.092744	0.0855889	2.708509	108.3404		
	356	2	0.2249	0.2356	0.2373	0.2326	0.0067	0.143022	0.0895778	4.016941	160.6776		
12	353	1	0.1456	0.1494	0.1517	0.1489	0.0031	0.092744	0.0561556	1.777075	71.08298	76.6358	31.4992
	353	2	0.1585	0.1676	0.1676	0.16457	0.0053	0.143022	0.0215444	0.966119	38.64474		
	356	1	0.154	0.1576	0.1604	0.15733	0.0032	0.092744	0.0645889	2.043952	81.75809		
	356	2	0.2035	0.2101	0.2079	0.20717	0.0034	0.143022	0.0641444	2.876432	115.0573		
15	353	1	0.1531	0.1575	0.16	0.15687	0.0035	0.092744	0.0641222	2.029184	81.16737	104.014	28.4735
	353	2	0.2086	0.2177	0.2162	0.21417	0.0049	0.143022	0.0711444	3.190334	127.6134		
	356	1	0.2516	0.1617	0.1722	0.19517	0.0492	0.092744	0.1024222	3.24121	129.6484		
	356	2	0.1843	0.1879	0.1867	0.1863	0.0018	0.143022	0.0432778	1.940708	77.6283		
18	353	1	0.1758	0.1805	0.1811	0.17913	0.0029	0.092744	0.0863889	2.733826	109.353	102.428	23.3623
	353	2	0.1838	0.1826	0.1794	0.18193	0.0023	0.143022	0.0389111	1.744893	69.79571		
	356	1	0.1887	0.1917	0.1944	0.1916	0.0029	0.092744	0.0988556	3.12834	125.1336		
	356	2	0.1992	0.2026	0.2036	0.2018	0.0023	0.143022	0.0587778	2.635775	105.431		
21	353	1	0.15	0.1543	0.1877	0.164	0.0206	0.092744	0.0712556	2.254923	90.19691	107.262	39.7672
	353	2	0.1815	0.1913	0.1901	0.18763	0.0053	0.143022	0.0446111	2.000498	80.01993		
	356	1	0.1614	0.166	0.17	0.1658	0.0043	0.092744	0.0730556	2.311885	92.47539		
	356	2	0.2335	0.2368	0.237	0.23577	0.002	0.143022	0.0927444	4.158944	166.3577		
											Total	648.738	

PLA High

			Spec Reading											
Day	Well	Assay Set	1	2	3	Average	Std Dev	Baseline	Baseline Corrected	Collagen (ug)	Total Collagen in Well (ug)	Average (ug)	Std Dev
3	553	1	0.1911	0.1786	0.1878	0.18583	0.0065	0.092744	0.0930889	2.945851	117.834	49.4356	47.6766
	553	2	0.1456	0.1517	0.1499	0.14907	0.0031	0.143022	0.0060444	0.271051	10.84205		
	556	1	0.1233	0.1351	0.1258	0.12807	0.0062	0.092744	0.0353222	1.117792	44.71167		
	556	2	0.1537	0.1578	0.1583	0.1566	0.0025	0.143022	0.0135778	0.608869	24.35476		
6	553	1	0.1336	0.1376	0.1378	0.13633	0.0024	0.092744	0.0435889	1.379395	55.17581	55.4082	7.36313
	553	2	0.1782	0.1763	0.1707	0.17507	0.0039	0.143022	0.0320444	1.436971	57.47882		
	556	1	0.1285	0.1293	0.1286	0.1288	0.0004	0.092744	0.0360556	1.140999	45.63994		
	556	2	0.1761	0.1802	0.1787	0.17833	0.0021	0.143022	0.0353111	1.583458	63.33832		
9	553	1	0.1758	0.1816	0.184	0.18047	0.0042	0.092744	0.0877222	2.77602	111.0408	78.5068	28.7799
	553	2	0.1878	0.193	0.199	0.19327	0.0056	0.143022	0.0502444	2.253114	90.12456		
	556	1	0.1456	0.1453	0.1509	0.14727	0.0032	0.092744	0.0545222	1.725387	69.01547		
	556	2	0.164	0.169	0.1694	0.16747	0.003	0.143022	0.0244444	1.096163	43.84654		
12	553	1	0.1413	0.155	0.1459	0.1474	0.007	0.092744	0.0546556	1.729606	69.18425	91.473	21.3483
	553	2	0.1961	0.1805	0.1823	0.1863	0.0085	0.143022	0.0432778	1.940708	77.6283		
	556	1	0.1704	0.1828	0.1761	0.17643	0.0062	0.092744	0.0836889	2.648383	105.9353		
	556	2	0.198	0.2051	0.2152	0.2061	0.0086	0.143022	0.0630778	2.8286	113.144		
15	553	1	0.172	0.1625	0.1709	0.16847	0.0052	0.092744	0.0757222	2.396273	95.85091	132.367	57.4258
	553	2	0.221	0.225	0.2247	0.22357	0.0022	0.143022	0.0805444	3.611858	144.4743		
	556	1	0.1536	0.1583	0.158	0.15663	0.0026	0.092744	0.0638889	2.0218	80.87201		
	556	2	0.2469	0.2596	0.2709	0.25913	0.012	0.143022	0.1161111	5.206776	208.2711		
18	553	1	0.1958	0.1948	0.1952	0.19527	0.0005	0.092744	0.1025222	3.244374	129.775	107.425	23.3513
	553	2	0.1924	0.195	0.1927	0.19337	0.0014	0.143022	0.0503444	2.257598	90.30394		
	556	1	0.1848	0.1993	0.1908	0.19163	0.0073	0.092744	0.0988889	3.129395	125.1758		
	556	2	0.185	0.1962	0.1891	0.1901	0.0057	0.143022	0.0470778	2.111111	84.44444		
21	553	1	0.1568	0.1569	0.1574	0.15703	0.0003	0.092744	0.0642889	2.034459	81.37834	86.2171	23.5243
	553	2	0.1769	0.1851	0.1839	0.18197	0.0044	0.143022	0.0389444	1.746388	69.85551		
	556	1	0.1422	0.1516	0.1572	0.15033	0.0076	0.092744	0.0575889	1.822433	72.89733		
	556	2	0.2017	0.2205	0.2088	0.21033	0.0095	0.143022	0.0673111	3.018435	120.7374		
											Total	600.833	

PLG Low

			Spec Reading										
Day	Well	Assay Set	1	2	3	Average	Std Dev	Baseline	Baseline Corrected	Collagen (ug)	Total Collagen in Well (ug)	Average (ug)	Std Dev
3	653	1	0.1311	0.1351	0.1373	0.1345	0.0031	0.092744	0.0417556	1.321378	52.85513	35.4764	14.0826
	653	2	0.1506	0.1584	0.1597	0.15623	0.0049	0.143022	0.0132111	0.592427	23.69706		
	656	1	0.1224	0.1268	0.1262	0.12513	0.0024	0.092744	0.0323889	1.024965	40.99859		
	656	2	0.1532	0.1582	0.1584	0.1566	0.0029	0.143022	0.0135778	0.608869	24.35476		
6	653	1	0.1558	0.1472	0.1496	0.15087	0.0044	0.092744	0.0581222	1.839311	73.57243	64.3244	36.0063
	653	2	0.1997	0.208	0.2077	0.20513	0.0047	0.143022	0.0621111	2.785252	111.4101		
	656	1	0.1196	0.1222	0.1219	0.12123	0.0014	0.092744	0.0284889	0.901547	36.06188		
	656	2	0.1593	0.1648	0.1656	0.16323	0.0034	0.143022	0.0202111	0.906328	36.25311		
9	653	1	0.1295	0.1328	0.1369	0.13307	0.0037	0.092744	0.0403222	1.27602	51.04079	68.5112	23.134
	653	2	0.1929	0.2026	0.1977	0.19773	0.0049	0.143022	0.0547111	2.453413	98.13652		
	656	1	0.1499	0.1537	0.1539	0.1525	0.0023	0.092744	0.0597556	1.890999	75.63994		
	656	2	0.1676	0.1719	0.1719	0.17047	0.0025	0.143022	0.0274444	1.230693	49.2277		
12	653	1	0.1239	0.1378	0.1266	0.12943	0.0074	0.092744	0.0366889	1.161041	46.44163	60.4012	18.6662
	653	2	0.1721	0.1702	0.1751	0.17247	0.0025	0.143022	0.0294444	1.320379	52.81515		
	656	1	0.1577	0.1632	0.1657	0.1622	0.0041	0.092744	0.0694556	2.197961	87.91842		
	656	2	0.1764	0.1725	0.1712	0.17337	0.0027	0.143022	0.0303444	1.360737	54.4295		
15	653	1	0.155	0.1606	0.1626	0.1594	0.0039	0.092744	0.0666556	2.109353	84.37412	74.1881	19.0793
	653	2	0.1796	0.1851	0.1854	0.18337	0.0033	0.143022	0.0403444	1.809168	72.36672		
	656	1	0.1634	0.1679	0.1645	0.16527	0.0023	0.092744	0.0725222	2.295007	91.80028		
	656	2	0.1662	0.1714	0.1721	0.1699	0.0032	0.143022	0.0268778	1.205282	48.21126		
18	653	1	0.1693	0.1761	0.1764	0.17393	0.004	0.092744	0.0811889	2.569269	102.7707	100.021	9.27793
	653	2	0.1937	0.1914	0.1944	0.19317	0.0016	0.143022	0.0501444	2.24863	89.94519		
	656	1	0.1767	0.1828	0.183	0.18083	0.0036	0.092744	0.0880889	2.787623	111.5049		
	656	2	0.1901	0.1962	0.2031	0.19647	0.0065	0.143022	0.0534444	2.396612	95.86447		
21	653	1	0.1645	0.1725	0.1717	0.16957	0.0044	0.092744	0.0768222	2.431083	97.24332	97.006	47.4166
	653	2	0.1618	0.1665	0.1671	0.16513	0.0029	0.143022	0.0221111	0.99153	39.66119		
	656	1	0.163	0.1697	0.1715	0.16807	0.0045	0.092744	0.0753222	2.383615	95.34459		
	656	2	0.2211	0.235	0.2335	0.22987	0.0076	0.143022	0.0868444	3.89437	155.7748		
											Total	499.929	

PLG High

			Spec Reading										
Day	Well	Assay Set	1	2	3	Average	Std Dev	Baseline	Baseline Corrected	Collagen (ug)	Total Collagen in Well (ug)	Average (ug)	Std Dev
3	853	1	0.1284	0.1327	0.1319	0.131	0.0023	0.092744	0.0382556	1.210619	48.42475	59.864	16.5129
	853	2	0.1726	0.1827	0.1806	0.17863	0.0053	0.143022	0.0356111	1.596911	63.87643		
	856	1	0.1266	0.1299	0.1299	0.1288	0.0019	0.092744	0.0360556	1.140999	45.63994		
	856	2	0.1808	0.1944	0.1902	0.18847	0.007	0.143022	0.0454444	2.037867	81.5147		
6	853	1	0.1463	0.1531	0.1601	0.15317	0.0069	0.092744	0.0604222	1.912096	76.48383	68.5723	37.4817
	853	2	0.1809	0.1854	0.1843	0.18353	0.0023	0.143022	0.0405111	1.816642	72.66567		
	856	1	0.106	0.1063	0.1074	0.10657	0.0007	0.092744	0.0138222	0.437412	17.49648		
	856	2	0.2006	0.2048	0.2037	0.20303	0.0022	0.143022	0.0600111	2.691081	107.6432		
9	853	1	0.1204	0.1238	0.1231	0.12243	0.0018	0.092744	0.0296889	0.939522	37.58087	63.4563	17.6707
	853	2	0.1771	0.1843	0.1792	0.1802	0.0037	0.143022	0.0371778	1.667165	66.6866		
	856	1	0.1481	0.1537	0.1547	0.15217	0.0036	0.092744	0.0594222	1.88045	75.218		
	856	2	0.1806	0.1875	0.1853	0.18447	0.0035	0.143022	0.0414444	1.858495	74.33981		
12	853	1	0.1387	0.1486	0.1422	0.14317	0.005	0.092744	0.0504222	1.59564	63.8256	49.0666	15.1446
	853	2	0.1673	0.1688	0.1766	0.1709	0.005	0.143022	0.0278778	1.250125	50.00498		
	856	1	0.1347	0.1355	0.1369	0.1357	0.0011	0.092744	0.0429556	1.359353	54.37412		
	856	2	0.1552	0.1601	0.1607	0.15867	0.003	0.143022	0.0156444	0.701545	28.06178		
15	853	1	0.1417	0.1464	0.153	0.14703	0.0057	0.092744	0.0542889	1.718003	68.72011	73.2183	19.5703
	853	2	0.1897	0.2053	0.2018	0.19893	0.0082	0.143022	0.0559111	2.507225	100.289		
	856	1	0.1318	0.1361	0.1372	0.13503	0.0029	0.092744	0.0422889	1.338256	53.53024		
	856	2	0.1806	0.1846	0.1815	0.18223	0.0021	0.143022	0.0392111	1.758346	70.33383		
18	853	1	0.1367	0.1408	0.1452	0.1409	0.0043	0.092744	0.0481556	1.52391	60.9564	58.7799	20.785
	853	2	0.1696	0.1758	0.1727	0.1727	0.0031	0.143022	0.0296778	1.330842	53.23368		
	856	1	0.1562	0.1617	0.163	0.1603	0.0036	0.092744	0.0675556	2.137834	85.51336		
	856	2	0.1592	0.1637	0.1654	0.16277	0.0032	0.143022	0.0197444	0.885401	35.41604		
21	853	1	0.1333	0.139	0.1401	0.13747	0.0037	0.092744	0.0447222	1.41526	56.61041	64.737	65.7269
	853	2	0.213	0.2296	0.2257	0.22277	0.0087	0.143022	0.0797444	3.575984	143.0394		
	856	1	0.1504	0.1544	0.1536	0.1528	0.0021	0.092744	0.0600556	1.900492	76.01969		
	856	2	0.1312	0.1347	0.1352	0.1337	0.0022	0.143022	-0.009322	-0.41804	-16.7215		
											Total	437.694	

PLL Low

			Spec Reading											
Day	Well	Assay Set	1	2	3	Average	Std Dev	Baseline	Baseline Corrected	Collagen (ug)	Total Collagen in Well (ug)	Average (ug)	Std Dev
3	953	1	0.1188	0.124	0.1243	0.12237	0.0031	0.092744	0.0296222	0.937412	37.49648	43.3907	4.26711
	953	2	0.162	0.1752	0.1714	0.16953	0.0068	0.143022	0.0265111	1.188839	47.55356		
	956	1	0.1249	0.126	0.1305	0.12713	0.003	0.092744	0.0343889	1.088256	43.53024		
	956	2	0.1646	0.1708	0.1689	0.1681	0.0032	0.143022	0.0250778	1.124564	44.98256		
6	953	1	0.1195	0.1188	0.1224	0.12023	0.0019	0.092744	0.0274889	0.869902	34.79606	46.3526	8.70617
	953	2	0.1668	0.1773	0.1746	0.1729	0.0055	0.143022	0.0298778	1.339811	53.59243		
	956	1	0.1334	0.1344	0.1349	0.13423	0.0008	0.092744	0.0414889	1.31294	52.51758		
	956	2	0.1642	0.1709	0.1684	0.16783	0.0034	0.143022	0.0248111	1.112606	44.50424		
9	953	1	0.1334	0.1353	0.1433	0.13733	0.0053	0.092744	0.0445889	1.411041	56.44163	68.4331	17.6569
	953	2	0.1714	0.179	0.1771	0.17583	0.004	0.143022	0.0328111	1.47135	58.85401		
	956	1	0.1621	0.1704	0.1697	0.1674	0.0046	0.092744	0.0746556	2.362518	94.5007		
	956	2	0.1748	0.181	0.1802	0.17867	0.0034	0.143022	0.0356444	1.598406	63.93622		
12	953	1	0.1525	0.1569	0.1502	0.1532	0.0034	0.092744	0.0604556	1.91315	76.52602	67.9038	13.1557
	953	2	0.1801	0.1861	0.184	0.1834	0.003	0.143022	0.0403778	1.810663	72.42651		
	956	1	0.1491	0.1546	0.1507	0.15147	0.0028	0.092744	0.0587222	1.858298	74.33193		
	956	2	0.1675	0.1714	0.171	0.16997	0.0021	0.143022	0.0269444	1.208271	48.33084		
15	953	1	0.1486	0.1557	0.1548	0.15303	0.0039	0.092744	0.0602889	1.907876	76.31505	60.1005	18.2441
	953	2	0.1717	0.1776	0.1756	0.17497	0.003	0.143022	0.0319444	1.432486	57.29945		
	956	1	0.1469	0.1499	0.1503	0.14903	0.0019	0.092744	0.0562889	1.781294	71.25176		
	956	2	0.1625	0.1618	0.1642	0.16283	0.0012	0.143022	0.0198111	0.888391	35.53563		
18	953	1	0.134	0.14	0.1412	0.1384	0.0039	0.092744	0.0456556	1.444796	57.79184	77.9042	34.111
	953	2	0.2081	0.2163	0.2202	0.21487	0.0062	0.143022	0.0718444	3.221724	128.869		
	956	1	0.1371	0.1409	0.1423	0.1401	0.0027	0.092744	0.0473556	1.498594	59.94374		
	956	2	0.1784	0.1804	0.179	0.17927	0.001	0.143022	0.0362444	1.625311	65.01246		
21	953	1	0.1436	0.1484	0.1491	0.14703	0.003	0.092744	0.0542889	1.718003	68.72011	77.5956	29.3078
	953	2	0.1629	0.1666	0.1665	0.16533	0.0021	0.143022	0.0223111	1.000498	40.01993		
	956	1	0.169	0.1741	0.1786	0.1739	0.0048	0.092744	0.0811556	2.568214	102.7286		
	956	2	0.1902	0.1972	0.2071	0.19817	0.0085	0.143022	0.0551444	2.472845	98.9138		
											Total	441.681	

PLL High

			Spec Reading										
Day	Well	Assay Set	1	2	3	Average	Std Dev	Baseline	Baseline Corrected	Collagen (ug)	Total Collagen in Well (ug)	Average (ug)	Std Dev
3	1153	1	0.1361	0.1397	0.1441	0.13997	0.004	0.092744	0.0472222	1.494374	59.77496	43.1463	14.9583
	1153	2	0.1527	0.155	0.1609	0.1562	0.0042	0.143022	0.0131778	0.590932	23.63727		
	1156	1	0.126	0.1313	0.1319	0.12973	0.0032	0.092744	0.0369889	1.170534	46.82138		
	1156	2	0.1624	0.1694	0.1681	0.16663	0.0037	0.143022	0.0236111	1.058794	42.35177		
6	1153	1	0.1286	0.1305	0.1435	0.1342	0.0081	0.092744	0.0414556	1.311885	52.47539	38.109	18.4279
	1153	2	0.1496	0.1524	0.1539	0.15197	0.0022	0.143022	0.0089444	0.401096	16.04385		
	1156	1	0.1318	0.1358	0.1389	0.1355	0.0036	0.092744	0.0427556	1.353024	54.12096		
	1156	2	0.1568	0.1601	0.162	0.15963	0.0026	0.143022	0.0166111	0.744893	29.79571		
9	1153	1	0.1361	0.1398	0.1481	0.14133	0.0061	0.092744	0.0485889	1.537623	61.50492	68.8738	12.3654
	1153	2	0.1769	0.1819	0.1809	0.1799	0.0026	0.143022	0.0368778	1.653712	66.14848		
	1156	1	0.1563	0.1643	0.164	0.16153	0.0045	0.092744	0.0687889	2.176864	87.07454		
	1156	2	0.1727	0.1776	0.1804	0.1769	0.0039	0.143022	0.0338778	1.519183	60.76731		
12	1153	1	0.1568	0.1629	0.1621	0.1606	0.0033	0.092744	0.0678556	2.147328	85.89311	70.7582	13.8126
	1153	2	0.169	0.1739	0.1741	0.17233	0.0029	0.143022	0.0293111	1.3144	52.57598		
	1156	1	0.1476	0.1538	0.1529	0.15143	0.0034	0.092744	0.0586889	1.857243	74.28973		
	1156	2	0.1809	0.1807	0.185	0.1822	0.0024	0.143022	0.0391778	1.756851	70.27404		
15	1153	1	0.1479	0.1533	0.1535	0.15157	0.0032	0.092744	0.0588222	1.861463	74.45851	80.337	15.4772
	1153	2	0.1621	0.1677	0.2052	0.17833	0.0234	0.143022	0.0353111	1.583458	63.33832		
	1156	1	0.1661	0.176	0.173	0.1717	0.0051	0.092744	0.0789556	2.498594	99.94374		
	1156	2	0.1847	0.1904	0.1938	0.18963	0.0046	0.143022	0.0466111	2.090184	83.60737		
18	1153	1	0.2101	0.2117	0.2176	0.21313	0.004	0.092744	0.1203889	3.809775	152.391	111.816	73.8939
	1153	2	0.1761	0.1801	0.1803	0.17883	0.0024	0.143022	0.0358111	1.605879	64.23518		
	1156	1	0.2418	0.2469	0.2498	0.24617	0.0041	0.092744	0.1534222	4.855134	194.2053		
	1156	2	0.1614	0.1663	0.1623	0.16333	0.0026	0.143022	0.0203111	0.910812	36.43249		
21	1153	1	0.1373	0.1386	0.1402	0.1387	0.0015	0.092744	0.0459556	1.45429	58.17159	64.3341	17.4466
	1153	2	0.1707	0.1742	0.1747	0.1732	0.0022	0.143022	0.0301778	1.353264	54.13054		
	1156	1	0.1499	0.1821	0.1604	0.16413	0.0164	0.092744	0.0713889	2.259142	90.36568		
	1156	2	0.1696	0.175	0.1759	0.1735	0.0034	0.143022	0.0304778	1.366716	54.66866		
											Total	477.374	

PSS Low

			Spec Reading										
Day	Well	Assay Set	1	2	3	Average	Std Dev	Baseline	Baseline Corrected	Collagen (ug)	Total Collagen in Well (ug)	Average (ug)	Std Dev
3	1253	1	0.1114	0.1137	0.1197	0.11493	0.0043	0.092744	0.0221889	0.70218	28.0872	41.0131	15.9632
	1253	2	0.1719	0.1779	0.1752	0.175	0.003	0.143022	0.0319778	1.433981	57.35924		
	1256	1	0.112	0.1128	0.1164	0.11373	0.0023	0.092744	0.0209889	0.664205	26.56821		
	1256	2	0.1671	0.1788	0.1702	0.17203	0.0061	0.143022	0.0290111	1.300947	52.03787		
6	1253	1	0.1296	0.1336	0.1396	0.13427	0.005	0.092744	0.0415222	1.313994	52.55977	56.7364	23.239
	1253	2	0.1647	0.1681	0.1684	0.16707	0.0021	0.143022	0.0240444	1.078226	43.12905		
	1256	1	0.117	0.1209	0.1364	0.12477	0.0103	0.092744	0.0320222	1.013361	40.53446		
	1256	2	0.1929	0.1946	0.1933	0.1936	0.0009	0.143022	0.0505778	2.268062	90.72247		
9	1253	1	0.1481	0.1526	0.161	0.1539	0.0065	0.092744	0.0611556	1.935302	77.4121	83.0721	9.6867
	1253	2	0.1798	0.1898	0.1813	0.18363	0.0054	0.143022	0.0406111	1.821126	72.84504		
	1256	1	0.1581	0.1636	0.165	0.16223	0.0036	0.092744	0.0694889	2.199015	87.96062		
	1256	2	0.198	0.1943	0.1941	0.19547	0.0022	0.143022	0.0524444	2.351769	94.07075		
12	1253	1	0.1416	0.145	0.1556	0.1474	0.0073	0.092744	0.0546556	1.729606	69.18425	80.0656	22.6431
	1253	2	0.1922	0.1997	0.1986	0.19683	0.0041	0.143022	0.0538111	2.413054	96.52217		
	1256	1	0.1677	0.1734	0.1767	0.1726	0.0046	0.092744	0.0798556	2.527075	101.083		
	1256	2	0.1574	0.1958	0.1653	0.17283	0.0203	0.143022	0.0298111	1.336821	53.47285		
15	1253	1	0.1364	0.1394	0.1419	0.13923	0.0028	0.092744	0.0464889	1.471167	58.84669	66.3152	7.36992
	1253	2	0.1767	0.1863	0.18	0.181	0.0049	0.143022	0.0379778	1.703039	68.12157		
	1256	1	0.1344	0.1531	0.1389	0.14213	0.0098	0.092744	0.0493889	1.56294	62.51758		
	1256	2	0.1824	0.1871	0.1863	0.18527	0.0025	0.143022	0.0422444	1.89437	75.77479		
18	1253	1	0.1323	0.1347	0.1375	0.13483	0.0026	0.092744	0.0420889	1.331927	53.27707	47.03	7.79955
	1253	2	0.1648	0.165	0.1657	0.16517	0.0005	0.143022	0.0221444	0.993024	39.72098		
	1256	1	0.1217	0.1251	0.1283	0.12503	0.0033	0.092744	0.0322889	1.0218	40.87201		
	1256	2	0.1701	0.1759	0.1738	0.17327	0.0029	0.143022	0.0302444	1.356253	54.25012		
21	1253	1	0.1239	0.1279	0.129	0.12693	0.0027	0.092744	0.0341889	1.081927	43.27707	45.1885	8.38065
	1253	2	0.1637	0.1688	0.1729	0.16847	0.0046	0.143022	0.0254444	1.141006	45.64026		
	1256	1	0.1347	0.1377	0.1387	0.13703	0.0021	0.092744	0.0442889	1.401547	56.06188		
	1256	2	0.1599	0.1636	0.1654	0.16297	0.0028	0.143022	0.0199444	0.89437	35.77479		
											Total	419.421	

PSS High

			Spec Reading										
Day	Well	Assay Set	1	2	3	Average	Std Dev	Baseline	Baseline Corrected	Collagen (ug)	Total Collagen in Well (ug)	Average (ug)	Std Dev
3	1453	1	0.1289	0.1308	0.1319	0.13053	0.0015	0.092744	0.0377889	1.195851	47.83404	30.3167	13.7603
	1453	2	0.1528	0.1589	0.1546	0.15543	0.0031	0.143022	0.0124111	0.556552	22.26208		
	1456	1	0.1166	0.1206	0.1223	0.11983	0.0029	0.092744	0.0270889	0.857243	34.28973		
	1456	2	0.1507	0.1532	0.1534	0.15243	0.0015	0.143022	0.0094111	0.422023	16.88092		
6	1453	1	0.1182	0.1159	0.1193	0.1178	0.0017	0.092744	0.0250556	0.792897	31.71589	46.1914	26.1896
	1453	2	0.1541	0.1571	0.1572	0.15613	0.0018	0.143022	0.0131111	0.587942	23.51769		
	1456	1	0.1264	0.1315	0.1313	0.12973	0.0029	0.092744	0.0369889	1.170534	46.82138		
	1456	2	0.1849	0.1918	0.1907	0.18913	0.0037	0.143022	0.0461111	2.067763	82.71051		
9	1453	1	0.1546	0.1608	0.1595	0.1583	0.0033	0.092744	0.0655556	2.074543	82.98172	70.1254	11.0515
	1453	2	0.1761	0.1797	0.1784	0.17807	0.0018	0.143022	0.0350444	1.5715	62.85999		
	1456	1	0.1343	0.1399	0.1443	0.1395	0.005	0.092744	0.0467556	1.479606	59.18425		
	1456	2	0.1796	0.1841	0.1916	0.1851	0.0061	0.143022	0.0420778	1.886896	75.47583		
12	1453	1	0.1344	0.1371	0.1372	0.13623	0.0016	0.092744	0.0434889	1.376231	55.04923	40.3157	22.1369
	1453	2	0.1648	0.1673	0.1678	0.16663	0.0016	0.143022	0.0236111	1.058794	42.35177		
	1456	1	0.1349	0.1364	0.1384	0.13657	0.0018	0.092744	0.0438222	1.386779	55.47117		
	1456	2	0.145	0.1491	0.149	0.1477	0.0023	0.143022	0.0046778	0.209766	8.390633		
15	1453	1	0.1263	0.1295	0.1319	0.12923	0.0028	0.092744	0.0364889	1.154712	46.18847	73.4573	31.6217
	1453	2	0.2018	0.2091	0.2113	0.2074	0.005	0.143022	0.0643778	2.886896	115.4758		
	1456	1	0.131	0.1334	0.1377	0.13403	0.0034	0.092744	0.0412889	1.30661	52.26442		
	1456	2	0.18	0.2031	0.1796	0.18757	0.0135	0.143022	0.0445444	1.997509	79.90035		
18	1453	1	0.1506	0.155	0.1611	0.15557	0.0053	0.092744	0.0628222	1.988045	79.5218	86.9777	23.8378
	1453	2	0.1897	0.1924	0.1931	0.19173	0.0018	0.143022	0.0487111	2.184355	87.37419		
	1456	1	0.139	0.1426	0.1436	0.14173	0.0024	0.092744	0.0489889	1.550281	62.01125		
	1456	2	0.2063	0.2118	0.21	0.20937	0.0028	0.143022	0.0663444	2.975087	119.0035		
21	1453	1	0.1116	0.1136	0.115	0.1134	0.0017	0.092744	0.0206556	0.653657	26.14627	33.6289	19.6095
	1453	2	0.1467	0.1498	0.1502	0.1489	0.0019	0.143022	0.0058778	0.263577	10.5431		
	1456	1	0.1347	0.1378	0.1382	0.1369	0.0019	0.092744	0.0441556	1.397328	55.89311		
	1456	2	0.1623	0.1671	0.1698	0.1664	0.0038	0.143022	0.0233778	1.048331	41.93323		
											Total	381.013	

SC Low

			Spec Reading										
Day	Well	Assay Set	1	2	3	Average	Std Dev	Baseline	Baseline Corrected	Collagen (ug)	Total Collagen in Well (ug)	Average (ug)	Std Dev
3	1553	1	0.2044	0.212	0.2186	0.21167	0.0071	0.092744	0.1189222	3.763361	150.5345	105.204	31.6124
	1553	2	0.1918	0.207	0.189	0.19593	0.0097	0.143022	0.0529111	2.372696	94.90782		
	1556	1	0.146	0.1595	0.1555	0.15367	0.0069	0.092744	0.0609222	1.927918	77.11674		
	1556	2	0.194	0.2012	0.1982	0.1978	0.0036	0.143022	0.0547778	2.456403	98.2561		
6	1553	1	0.1436	0.1466	0.1515	0.14723	0.004	0.092744	0.0544889	1.724332	68.97328	74.9678	12.7375
	1553	2	0.1731	0.1778	0.1786	0.1765	0.003	0.143022	0.0334778	1.501246	60.04983		
	1556	1	0.1567	0.1595	0.1593	0.1585	0.0016	0.092744	0.0657556	2.080872	83.23488		
	1556	2	0.1894	0.1937	0.1925	0.19187	0.0022	0.143022	0.0488444	2.190334	87.61335		
9	1553	1	0.15	0.1701	0.1647	0.1616	0.0104	0.092744	0.0688556	2.178973	87.15893	80.3572	20.1496
	1553	2	0.17	0.1736	0.1733	0.1723	0.002	0.143022	0.0292778	1.312905	52.51619		
	1556	1	0.1677	0.1727	0.1754	0.17193	0.0039	0.092744	0.0791889	2.505977	100.2391		
	1556	2	0.1847	0.191	0.1897	0.18847	0.0033	0.143022	0.0454444	2.037867	81.5147		
12	1553	1	0.1731	0.1841	0.1933	0.1835	0.0101	0.092744	0.0907556	2.872011	114.8805	92.881	22.1062
	1553	2	0.1818	0.1897	0.1889	0.1868	0.0043	0.143022	0.0437778	1.963129	78.52516		
	1556	1	0.1748	0.1784	0.1819	0.17837	0.0036	0.092744	0.0856222	2.709564	108.3826		
	1556	2	0.1762	0.183	0.1865	0.1819	0.0052	0.143022	0.0388778	1.743398	69.73592		
15	1553	1	0.1647	0.171	0.1728	0.1695	0.0043	0.092744	0.0767556	2.428973	97.15893	101.659	8.43362
	1553	2	0.1944	0.1992	0.2014	0.19833	0.0036	0.143022	0.0553111	2.480319	99.21276		
	1556	1	0.1714	0.1734	0.1612	0.16867	0.0065	0.092744	0.0759222	2.402602	96.10408		
	1556	2	0.2015	0.21	0.2085	0.20667	0.0045	0.143022	0.0636444	2.854011	114.1604		
18	1553	1	0.1641	0.1694	0.1739	0.16913	0.0049	0.092744	0.0763889	2.41737	96.6948	64.514	47.7084
	1553	2	0.1613	0.1691	0.1664	0.1656	0.004	0.143022	0.0225778	1.012456	40.49826		
	1556	1	0.1765	0.1839	0.1817	0.1807	0.0038	0.092744	0.0879556	2.783404	111.3361		
	1556	2	0.1546	0.1458	0.1446	0.14833	0.0055	0.143022	0.0053111	0.238166	9.526657		
21	1553	1	0.1728	0.1812	0.1772	0.17707	0.0042	0.092744	0.0843222	2.668425	106.737	101.69	19.9505
	1553	2	0.1939	0.1948	0.2121	0.20027	0.0103	0.143022	0.0572444	2.567015	102.6806		
	1556	1	0.1825	0.1949	0.1915	0.18963	0.0064	0.092744	0.0968889	3.066104	122.6442		
	1556	2	0.1792	0.1872	0.1876	0.18467	0.0047	0.143022	0.0416444	1.867464	74.69856		
											Total	621.273	

SC High

			Spec Reading										
Day	Well	Assay Set	1	2	3	Average	Std Dev	Baseline	Baseline Corrected	Collagen (ug)	Total Collagen in Well (ug)	Average (ug)	Std Dev
3	1753	1	0.1365	0.1335	0.1346	0.13487	0.0015	0.092744	0.0421222	1.332982	53.31927	49.8848	5.26978
	1753	2	0.1683	0.1753	0.1782	0.17393	0.0051	0.143022	0.0309111	1.386148	55.44594		
	1756	1	0.1274	0.1278	0.13	0.1284	0.0014	0.092744	0.0356556	1.12834	45.13361		
	1756	2	0.1701	0.1688	0.1665	0.16847	0.0018	0.143022	0.0254444	1.141006	45.64026		
6	1753	1	0.1272	0.1356	0.1409	0.13457	0.0069	0.092744	0.0418222	1.323488	52.93952	51.6273	17.3617
	1753	2	0.1649	0.1692	0.1694	0.16783	0.0025	0.143022	0.0248111	1.112606	44.50424		
	1756	1	0.1509	0.1499	0.1551	0.15197	0.0028	0.092744	0.0592222	1.874121	74.96484		
	1756	2	0.1601	0.1635	0.1625	0.16203	0.0017	0.143022	0.0190111	0.852516	34.10065		
9	1753	1	0.1746	0.185	0.1861	0.1819	0.0063	0.092744	0.0891556	2.821378	112.8551	71.2795	31.1752
	1753	2	0.1651	0.1662	0.1669	0.16607	0.0009	0.143022	0.0230444	1.033383	41.33533		
	1756	1	0.1468	0.1561	0.1555	0.1528	0.0052	0.092744	0.0600556	1.900492	76.01969		
	1756	2	0.1669	0.1822	0.1718	0.17363	0.0078	0.143022	0.0306111	1.372696	54.90782		
12	1753	1	0.1424	0.1493	0.1457	0.1458	0.0035	0.092744	0.0530556	1.678973	67.15893	85.4566	29.8376
	1753	2	0.174	0.1792	0.1779	0.17703	0.0027	0.143022	0.0340111	1.525162	61.00648		
	1756	1	0.1464	0.1611	0.1758	0.1611	0.0147	0.092744	0.0683556	2.16315	86.52602		
	1756	2	0.207	0.2184	0.2163	0.2139	0.0061	0.143022	0.0708778	3.178376	127.135		
15	1753	1	0.1817	0.1877	0.1908	0.18673	0.0046	0.092744	0.0939889	2.974332	118.9733	87.704	31.1908
	1753	2	0.1869	0.1913	0.1913	0.18983	0.0025	0.143022	0.0468111	2.099153	83.96612		
	1756	1	0.1681	0.176	0.1753	0.17313	0.0044	0.092744	0.0803889	2.543952	101.7581		
	1756	2	0.1612	0.1679	0.1771	0.16873	0.008	0.143022	0.0257111	1.152965	46.11858		
18	1753	1	0.189	0.1942	0.1953	0.19283	0.0034	0.092744	0.1000889	3.16737	126.6948	112.559	9.88977
	1753	2	0.1988	0.2075	0.2059	0.20407	0.0046	0.143022	0.0610444	2.737419	109.4968		
	1756	1	0.1761	0.1805	0.1833	0.17997	0.0036	0.092744	0.0872222	2.760197	110.4079		
	1756	2	0.1964	0.2019	0.2041	0.2008	0.004	0.143022	0.0577778	2.590932	103.6373		
21	1753	1	0.1452	0.1501	0.1496	0.1483	0.0027	0.092744	0.0555556	1.758087	70.32349	59.5246	13.9012
	1753	2	0.1734	0.1812	0.1831	0.17923	0.0051	0.143022	0.0362111	1.623817	64.95267		
	1756	1	0.1404	0.1411	0.1477	0.14307	0.004	0.092744	0.0503222	1.592475	63.69902		
	1756	2	0.1568	0.1762	0.1615	0.16483	0.0101	0.143022	0.0218111	0.978077	39.12307		
											Total	518.036	

Appendix F: Raman Spectral Analysis Software:

This is a transcript of the Matlab M-file used for the analysis of Raman Spectral Scan data of bone from fixed bone nodules grown *in vitro*.

```
%   A single spectra's file name is entered here
clear;clc;
load c:\temp\N10562.txt;       %my text file of the spectrum
o_spec = N10562;               %file name
sfilename = 'N10562';          %file name

tag = [795 1145 1215 1315 1360 1500 1550 1575 1600 1720 1730]; %see
instructions (2) for what these
peaks_pp = [815 855 1101 1130 1425 1605 1637];                 %parameters
represent
peaks_cf = [960 1001 1030 1068 1245 1270 1451 1667];

ana_spec = fopen('nodule_analysisN10562.txt','A');  % creates output file
%bc_spec = fopen('blc_spec.txt','A');
fprintf(ana_spec,'Spec_ID v1PO4f v1PO4i PO4BW PO4hmg PO4hml v3HPO4f
v3HPO4i v3POf v3POi v1CO3f v1CO3i amd3af amd3ai amd3bf amd3bi CH2wgf
CH2wgi amd1f amd1i Av1PO4 Aamd3 ACH2wg Aamd1 ACH2stG RCO3 RHPO4
mn_amd1 mn_amd3a mn_amd3b mn_CH2wg RAPO4_amd3 RAPO4_CH2wg
RAPO4_amd1 vCCaf vCCai dCCHf dCCHi labCO3f labCO3i vCCbf vCCbi
dCOOf dCOOi vCCHf vCCHi vC_Cf vC_Ci \n');     %the header in the output file

o_freq = o_spec(:,1);       %original frequencies from the spectrum
o_inten = o_spec(:,2);      %original intesities from the spectrum

%       The following section filters the intensity data from the original data to
remove
%   noise.  This is done through a 5-pt moving average filter.

n_pts = max(size(o_freq));

   for I = 1:n_pts;

       if I == 1
          f_inten(I,1) = o_inten(I);         %keep original values for first two and last
two
       else if I == 2                        %points since can't average them
```

```
        f_inten(I,1) = o_inten(I);
    else if I == n_pts-1
        f_inten(I,1) = o_inten(I);
    else if I == n_pts
        f_inten(I,1) = o_inten(I);
    else
        f_inten(I,1) = (o_inten(I-2)+o_inten(I-
1)+o_inten(I)+o_inten(I+1)+o_inten(I+2))/5;  %5 point average of the remaining
points
        % end
    end
    end
    end
    end

  f_spec(I,1) = o_freq(I);    %creates an array that holds the frequencies with the
averaged intensities
  f_spec(I,2) = f_inten(I);

  end

%+++++++++++++++++++++++++++++++++++++++++++++++++++++++++++++++++++++++++++++++
++++++++++++++++++++++++++++++++
%   This section will search through the filtered intensity data and generate data
points
%   corresponding to selected frequencies.

n_t_pts = max(size(tag));       %the number of points in baseline correction p-w
line

for J = 1:n_t_pts;

  diff = abs(o_freq - tag(J) * ones(size(o_freq)));   %this loop finds the index in
the
  min_diff = min(diff);                          %array where the specific frequency
  index(J,1) = find(diff == min_diff);              %is occuring so it can be
                                          %baseline corrected
  t_freq = o_freq(index);
  t_inten = f_inten(index);

  bc(J,1) = t_freq(J);
  bc(J,2) = t_inten(J);

end

for K = 1:(n_t_pts-1);
```

```
   dy = bc((K+1),2) - bc(K,2);          %this loop finds the slope of the
   dx = bc((K+1),1) - bc(K,1);          %baseline correction lines
   m(K,1) = dy/dx;

end

%   These points will be connected in a linear-piecewise fashion to create
%   the background correction curve.

n_i_pts = max(size(index));
t_bc_inten = [];

for I2 = 1:(n_i_pts - 1);

   bc_inten = [];
   seg_freq = o_freq(index(I2) : index(I2+1));     %isolate the frequencies for each
segment
   y_int = bc(I2,2) - m(I2) * (bc(I2,1));          %find the y-intercept for each
segment

   n_pts2 = (index(I2+1) - index(I2) + 1);     %finds the number of frequency
points in the segment

   for J2 = 1:(n_pts2-1);

      bc_inten(J2,1) = m(I2)*(seg_freq(J2)) + y_int;  %finds the intensity of the
baseline correction line

   end

   t_bc_inten = [t_bc_inten ; bc_inten];   %includes all baseline correction line
intensities into one array

end

%   Now the last intensity data point is added to the basline intensity matrix.

t_bc_inten = [t_bc_inten ; bc(n_i_pts,2)];

%   The next section creates the baseline curve and removes it from the spectra.

co_inten = f_inten - t_bc_inten;
co_inten = co_inten/max(co_inten);  % Normalization of the intensity signal.
co_spec(:,1) = o_freq;              %places baseline corrected, filtered,
co_spec(:,2) = co_inten;            %normalized data into one array
```

```
plot(o_freq,co_inten,'b')          %plots correccted spectrum
title('Spectrum Analysis')
xlabel('Wavenumber (cm^-1)')
ylabel('Normalized Intensity')
title('Spectum Analysis:N10562')

%fprintf(spec2,'%g \n',o_freq,co_inten); % Outputs the normalized, baseline
corrected data.
%fclose(spec2);

%++++++++++++++++++++++++++++++++++++++++++++++++++++++++++++++++++++++++
++++++++++++++++++++++++++++++++
%   At this point, the baseline curve has been created and subtracted from the
%   spectra to correct for the background fluorescence.  Next, the peak intensity
%   values and their corresponding frequencies are found.

%   For these points, the peak intensity is found through a 3-point average of the
%   points at the maximum intensity value for the frequencies selected below.

n_ppp = max(size(peaks_pp));

for I3 = 1:n_ppp;

   ppdiff = abs(o_freq - peaks_pp(I3)*ones(size(o_freq)));
   mppdiff = min(ppdiff);                    %this loop finds the indexs where
   ppf_index = find(ppdiff == mppdiff);       %peaks_pp occur

   pp_peaks(I3,2) = co_inten(ppf_index);      %pulls out the intensity and
   pp_peaks(I3,1) = o_freq(ppf_index);       %frequency at the indexes

end

n_cfp = max(size(peaks_cf));

for I4 = 1:n_cfp;

   if I4 == 1
         tol = 7e-6;
         np = 15;
    else if I4 == 2
         tol = 2e-5;
         np = 9;
    else if I4 == 3
         tol = 5e-6;
         np = 9;
```

```
    else if l4 == 4
        tol = 2e-4;
        np = 15;
    else if l4 == 5
        tol = 2e-4;
        np = 15;
    else if l4 == 6
        tol = 2e-5;
        np = 13;
     else if l4 == 7
        tol = 1e-3;
        np = 15;
     else if l4 == 8
        tol = 8e-4;
        np = 15;

    else

    end
    end
    end
    end
    end
    end
    end
  end

  diff3 = abs(o_freq - peaks_cf(l4) * ones(size(o_freq)));
  min_diff3 = min(diff3);                    %finds the index where specific
  index3(l4,1) = find(diff3 == min_diff3);    %peak occurs

  range2_f = o_freq((index3(l4)-5):(index3(l4)+5));   %isolates the part of the
data
  range2_i = co_inten((index3(l4)-5):(index3(l4)+5)); %for the specific peak

  %   The maximum intensity value over this range of intensities is not always at
  %   the frequency stated, so a new range of values is found that is centered on
  %   the maximum intensity.

  mrange_i = max(range2_i);
  ipeak(l4,1) = find(co_inten == mrange_i);

  range3_f = o_freq((ipeak(l4)-np):(ipeak(l4)+np));
  range3_i = co_inten((ipeak(l4)-np):(ipeak(l4)+np));

  xdata = range3_f;
```

```
    ydata = range3_i;

    %   Now a spline curve will be fitted around the peaks of interest.
    %   The splines have different stiffness'  and numbers of points used
    %   to adjust for the best-fit curve.

    cs=csapi(xdata,ydata);
    splinevalues = fnval(cs,xdata);
    scs = spaps(xdata,splinevalues,tol);
    xdata2 = xdata(1):0.1:xdata(np*2+1);
    splinevalues = fnval(scs,xdata2);
    %plot(xdata,ydata,'r.');
    %plot(xdata2,splinevalues,'k:');

    mx_i = max(splinevalues);
    pk_idx = find(splinevalues == mx_i);
    pi = mx_i;                  %peak intensity
    pf = xdata2(pk_idx);        %peak frequency
    peaks(I4,1) = pf;
    peaks(I4,2) = pi;

end

%
++++++++++++++++++++++++++++++++++++++++++++++++++++++++++++++++++++++++++++++++
%   This section will determine the half-max bandwidth of the primary PO4 peak.
PO4_ends = [900 990];
nPO4_pts = max(size(PO4_ends));

for J4 = 1:nPO4_pts;

    diff4 = abs(o_freq - PO4_ends(J4) * ones(size(o_freq)));
    min_diff4 = min(diff4);                   %locates the index of 900
    index4(J4,1) = find(diff4 == min_diff4);    %and 990 frequencies

    range4_f = o_freq((index4(J4)-15):(index4(J4)+15));     %isolates the data
containing
    range4_i = co_inten((index4(J4)-15):(index4(J4)+15));   %frequencies between
900 and 900

    min_r4i = min(range4_i);                %finds the minimum intensity
    index5 = find(range4_i == min_r4i);     %indexes the minimum intensity

    PO4LinePts(J4,1) = range4_f(index5);    %places frequency and intensities
    PO4LinePts(J4,2) = range4_i(index5);    %at 900 and 990 into an array
```

```
end

%   Now a line will be constructed between these sets two points.
PO4m = (PO4LinePts(2,2)-PO4LinePts(1,2))/(PO4LinePts(2,1)-
PO4LinePts(1,1));     %slope of the line
PO4y_int = PO4LinePts(2,2)-PO4m*(PO4LinePts(2,1));      %y-intercept of the
line

PO4LineX = min(PO4_ends):0.01:max(PO4_ends);    %array of values between
900 and 990 with a step size of 0.01
PO4LineY = PO4m*(PO4LineX) + PO4y_int;          %y-values associated with the
frequency values

PO4Line(1,:) = PO4LineX;        %array of the line data
PO4Line(2,:) = PO4LineY;

%plot(PO4LineX, PO4LineY, 'c')

%   The peak intensity and corresponding frequency from the spline-fit.
PO4Pk_i = peaks(1,2);
PO4Pk_f = peaks(1,1);

%   The intensity on the local baseline at the peak frequency.
PO4BL_i = PO4m*(PO4Pk_f) + PO4y_int;

%   The half-max intensities.
PO4_mxL = PO4Pk_i - PO4BL_i;    %  The intensity from the local baseline
                        %  Used for mineralization calculations
hmi(1) = PO4Pk_i/2;             %  The half-max from the global baseline

%   The bandwidth at the half-max intensity is determined below.
BWPks = [peaks(1,1)];
n_BWPks = max(size(BWPks));

for J5 = 1:n_BWPks;

   diff6 = abs(o_freq - BWPks(J5) * ones(size(o_freq)));   %finds the index of the
max
   min_diff6 = min(diff6);                          %at the PO4 peak
   index8(J5,1) = find(diff6 == min_diff6);

   LSrange_f = o_freq((index8(J5)):(index8(J5)+20));       %range of frequencies
and intensities to
   LSrange_i = co_inten((index8(J5)):(index8(J5)+20));     %the right side of the
peak
```

```
   LSdiff = abs(LSrange_i - hmi(J5));
   LSmindiff = min(LSdiff);                  %finds and indexes the 1/2 max intensity
   LSPtId(J5) = find(LSdiff == LSmindiff);

   LSPtA_i = LSrange_i(LSPtId-1);          %indexes and pulls out the 2 points
surrounding
   LSPtB_i = LSrange_i(LSPtId+1);          %the half max intensity point
   LSPtA_f = LSrange_f(LSPtId-1);
   LSPtB_f = LSrange_f(LSPtId+1);
   LSPtA =[LSPtA_f LSPtA_i];
   LSPtB = [LSPtB_f LSPtB_i];

   RSrange_f = o_freq((index8(J5)-20):(index8(J5)));       %range of frequencies
and intensities to
   RSrange_i = co_inten((index8(J5)-20):(index8(J5)));     %the left side of the
peak
   RSdiff = abs(RSrange_i - hmi(J5));
   RSmindiff = min(RSdiff);               %finds and indexes the 1/2 max intensity
   RSPtId(J5) = find(RSdiff == RSmindiff);

   RSPtA_i = RSrange_i(RSPtId-1);          %indexes and pulls out the 2 points
surrounding
   RSPtB_i = RSrange_i(RSPtId+1);          %the half max intensity point
   RSPtA_f = RSrange_f(RSPtId-1);
   RSPtB_f = RSrange_f(RSPtId+1);
   RSPtA = [RSPtA_f RSPtA_i];
   RSPtB = [RSPtB_f RSPtB_i];

   LSm = (LSPtA(1,2)-LSPtB(1,2))/(LSPtA(1,1)-LSPtB(1,1));  %slope of the right
side line
   RSm = (RSPtA(1,2)-RSPtB(1,2))/(RSPtA(1,1)-RSPtB(1,1));  %slope of the left
side line
   LSy_int = LSPtA(1,2) - LSm*LSPtA(1,1);      %y-intercept of the right side line
   RSy_int = RSPtA(1,2) - RSm*RSPtA(1,1);      %y-intercept of the left side line

   LSfreq(J5,1) = (hmi(J5)-LSy_int)/LSm;       %finds the exact frequency of the
half max
   RSfreq(J5,1) = (hmi(J5)-RSy_int)/RSm;       %intensitites on either side of the
peak

   BW(J5,1) = LSfreq(J5,1) - RSfreq(J5,1);     %bandwidth at the 1/2 max
intensity

end
```

```
%++++++++++++++++++++++++++++++++++++++++++++++++++++++++++++++++++++++++
++++++++++++++++++++++++++
%   This section will determine the band area beneath the desired curves
%   Currently, only the CC and OH bands at ~2935 & 3320 are examined.
diff6 = abs(o_freq - peaks(6,1) * ones(size(o_freq)));
min_diff6 = min(diff6);
index8 = find(diff6 == min_diff6);
CH2peakf = o_freq(index8);

CH2Avar = 0.01;     % This is the percentage on either side of the peak for area
calculations
CH2R = CH2peakf + CH2Avar*CH2peakf;
CH2L = CH2peakf - CH2Avar*CH2peakf;

Apts = [900 990 1215 1310 1430 1500 1600 1715 CH2L CH2R];
nApts = max(size(Apts));

for I5 = 1:nApts;

    diff5 = abs(o_freq - Apts(I5) * ones(size(o_freq)));
    min_diff5 = min(diff5);
   index6 = find(diff5 == min_diff5);

    Apts2(I5,1) = o_freq(index6(1));
    Apts2(I5,2) = co_inten(index6(1));

    diff7 = abs(o_freq - Apts2(I5) * ones(size(o_freq)));
    mdiff7 = min(diff7);
    index7(I5,1) = find(diff7 == mdiff7);

end

A_v1PO4x = o_freq(index7(1):index7(2));
A_v1PO4y = co_inten(index7(1):index7(2));
A_amd3x = o_freq(index7(3):index7(4));
A_amd3y = co_inten(index7(3):index7(4));
A_CH2wgx = o_freq(index7(5):index7(6));
A_CH2wgy = co_inten(index7(5):index7(6));
A_amd1x = o_freq(index7(7):index7(8));
A_amd1y = co_inten(index7(7):index7(8));
CH2stGx = o_freq(index7(9):index7(10));         %   Gniadecka parameters
CH2stGy = co_inten(index7(9):index7(10));       %   Gniadecka parameters

%plot(A_v1PO4x,A_v1PO4y,'g.',A_amd3x,A_amd3y,'g.',A_CH2wgx,A_CH2wgy,'
g.',A_amd1x,A_amd1y,'g.',CH2stGx,CH2stGy,'g.')
```

```
A_v1PO4n = max(size(A_v1PO4x));
A_amd3n = max(size(A_amd3x));
A_CH2wgn = max(size(A_CH2wgx));
A_amd1n = max(size(A_amd1x));
%CH2stn = max(size(CH2stx));     %   Whole band
%OHn = max(size(OHx));           %   Whole band
CH2stGn = max(size(CH2stGx));   %   Gniadecka parameters
%OHGn = max(size(OHGx));         %   Gniadecka parameters

A_v1PO4 = dot(A_v1PO4x(2:A_v1PO4n),A_v1PO4y(1:(A_v1PO4n-1)))-
dot(A_v1PO4x(1:(A_v1PO4n-1)),A_v1PO4y(2:A_v1PO4n))-
(A_v1PO4x(1)*A_v1PO4y(1))+(A_v1PO4x(A_v1PO4n)*A_v1PO4y(A_v1PO4n));
A_amd3 = dot(A_amd3x(2:A_amd3n),A_amd3y(1:(A_amd3n-1)))-
dot(A_amd3x(1:(A_amd3n-1)),A_amd3y(2:A_amd3n))-
(A_amd3x(1)*A_amd3y(1))+(A_amd3x(A_amd3n)*A_amd3y(A_amd3n));
A_CH2wg = dot(A_CH2wgx(2:A_CH2wgn),A_CH2wgy(1:(A_CH2wgn-1)))-
dot(A_CH2wgx(1:(A_CH2wgn-1)),A_CH2wgy(2:A_CH2wgn))-
(A_CH2wgx(1)*A_CH2wgy(1))+(A_CH2wgx(A_CH2wgn)*A_CH2wgy(A_CH2wgn
));
A_amd1 = dot(A_amd1x(2:A_amd1n),A_amd1y(1:(A_amd1n-1)))-
dot(A_amd1x(1:(A_amd1n-1)),A_amd1y(2:A_amd1n))-
(A_amd1x(1)*A_amd1y(1))+(A_amd1x(A_amd1n)*A_amd1y(A_amd1n));
A_CH2stG = dot(CH2stGx(2:CH2stGn),CH2stGy(1:(CH2stGn-1)))-
dot(CH2stGx(1:(CH2stGn-1)),CH2stGy(2:CH2stGn))-
(CH2stGx(1)*CH2stGy(1))+(CH2stGx(CH2stGn)*CH2stGy(CH2stGn));

%++++++++++++++++++++++++++++++++++++++++++++++++++++++++++++++++
++++++++++++++++++++++++++
%   Below the intensity and frequency data obtained is formatted for the output
file.

%   The spline fit peak intensities and corresponding frequencies

v1PO4f = peaks(1,1);v1PO4i = PO4_mxL;          %   Intenstiy from local baseline
v3HPO4f = peaks(2,1);v3HPO4i = peaks(2,2);
v3POf = peaks(3,1);v3POi = peaks(3,2);
v1CO3f = peaks(4,1);v1CO3i = peaks(4,2);
amd3af = peaks(5,1);amd3ai = peaks(5,2);
amd3bf = peaks(6,1);amd3bi = peaks(6,2);
CH2wgf = peaks(7,1);CH2wgi = peaks(7,2);
amd1f = peaks(8,1);amd1i = peaks(8,2);

%   The 'pick-a-frequency' points
vCCaf = pp_peaks(1,1);vCCai = pp_peaks(1,2);
dCCHf = pp_peaks(2,1);dCCHi = pp_peaks(2,2);
labCO3f = pp_peaks(3,1);labCO3i = pp_peaks(3,2);
```

```
vCCbf = pp_peaks(4,1);vCCbi = pp_peaks(4,2);
dCOOf = pp_peaks(5,1);dCOOi = pp_peaks(5,2);
vCCHf = pp_peaks(6,1);vCCHi = pp_peaks(6,2);
vC_Cf = pp_peaks(7,1);vC_Ci = pp_peaks(7,2);

%   The half-max and full-width @ half max values
PO4BW = 1/BW(1,1);
PO4hmg = hmi(1)/2;
PO4hml = PO4_mxL/2;

%   The area under the CH2-stretch and OH-stretch bands
Av1PO4 = A_v1PO4;
Aamd3 = A_amd3;
ACH2wg = A_CH2wg;
Aamd1 = A_amd1;
ACH2stG = A_CH2stG;     %   Gniadecka parameters

%   The ratio calculations for crystallinity, mineralization, and hydration
RCO3 = v1CO3i/v1PO4i;           %   Crystallinity
RHPO4 = v3HPO4i/v1PO4i;         %   Crystallinity
mn_amd1 = v1PO4i/amd1i;         %   Intensity - Mineralization
mn_amd3a = v1PO4i/amd3ai;       %   Intensity - Mineralization
mn_amd3b = v1PO4i/amd3bi;       %   Intensity - Mineralization
mn_CH2wg = v1PO4i/CH2wgi;       %   Intensity - Mineralization
RAPO4_amd3 = Av1PO4/Aamd3;      %   Area - Mineralization
RAPO4_CH2wg = Av1PO4/ACH2wg;    %   Area - Mineralization
RAPO4_amd1 = Av1PO4/Aamd1;      %   Area - Mineralization

fprintf(ana_spec,'%s %g %g %g %g %g %g %g %g %g %g %g %g %g %g %g %g
%g %g %g %g %g %g %g %g %g %g %g %g %g %g %g %g %g %g %g %g %g %g %g
%g %g %g %g %g %g %g %g %g %g %g %g %g %g %g %g %g %g %g %g %g %g %g
%g %g %g %g %g %g %g %g %g %g %g %g %g %g %g %g %g %g %g %g %g %g %g
\n',sfilename,v1PO4f,v1PO4i,PO4BW,PO4hmg,PO4hml,v3HPO4f,v3HPO4i,v3P
Of,v3POi,v1CO3f,v1CO3i,amd3af,amd3ai,amd3bf,amd3bi,CH2wgf,CH2wgi,amd
1f,amd1i,Av1PO4,Aamd3,ACH2wg,Aamd1,ACH2stG,RCO3,RHPO4,mn_amd1,
mn_amd3a,mn_amd3b,mn_CH2wg,RAPO4_amd3,RAPO4_CH2wg,RAPO4_am
d1,vCCaf,vCCai,dCCHf,dCCHi,labCO3f,labCO3i,vCCbf,vCCbi,dCOOf,dCOOi,vC
CHf,vCCHi,vC_Cf,vC_Ci);

fclose(ana_spec);
```

Appendix G: Spectrum Analysis Software Output Variables

variables ending in 'f' are frequencies; variables ending in 'i' are intensities

Variable	Definition
Curve-fit Peaks ('peaks_cf')	
v1PO4f, v1PO4i	~ 960 cm^{-1} v_1 (PO_4) symmetric stretch
PO4BW	v_1 (PO4) full-width at half-max (local baseline correction)
PO4hmg	v_1 (PO4) half-max intensity (global baseline correction)
PO4hml	v_1 (PO4) half-max intensity (local baseline correction)
v3HPO4f, v3HPO4i	~ 1001 cm^{-1} v_3 (HPO_4)
v3POf, v3POi	~ 1030 cm^{-1} v_3 (PO_4) anti-symmetric stetch
v1CO3f, v1CO3i	~ 1068 cm^{-1} v_1 (CO_3)
amd3af, amd3ai	~ 1245 cm^{-1} δ (NH) Amide III
amd3bf, amd3bi	~ 1270 cm^{-1} δ (NH) Amide III
CH2wgf, CH2wgi	~ 1451 cm^{-1} δ (CH_2) wagging, scissors
amd1f, amd1i	~ 1667 cm^{-1} v (C=O) Amide I
Areas	
Av1PO4	area under the v_1 (PO_4) [900-990 cm^{-1}]
Aamd3	area under the δ (NH) Amide III [1215-1310 cm^{-1}]
ACH2wg	area under the δ (CH_2) wagging [1430-1500 cm^{-1}]
Aamd1	area under the v (C=O) Amide I [1600-1715 cm^{-1}]
Ratios	
RAPO4_amd3	area(v_1 PO_4) / area(amide III)
RAPO4_CH2wg	area(v_1 PO_4) / area(CH_2 wag)
RAPO4_amd1	area(v_1 PO_4) / area(amide I)
RCO3	intensity(v_1 (CO_3)) / intensity(v_1 (PO_4))
RHPO4	intensity(v_3 (HPO_4)) / intensity(v_1 (PO_4))
mn_amd1	intensity(Amide I) / intensity(v_1 (PO_4))
mn_amd3a	intensity(Amide III 'a') / intensity(v_1 (PO_4))
mn_amd3b	intensity(Amide III 'b') / intensity(v_1 (PO_4))
mn_CH2wg	intensity(CH_2 wagging) / intensity(v_1 (PO_4))
'Peak-a-frequency' Points ('peaks_pp')	
vCCaf, vCCai	815 cm^{-1} v (CC) stretching, skeletal backbone
dCCHf, dCCHi	855 cm^{-1} δ (CCH) aromatic, v (CC) proline

labCO3	1101 cm^{-1}	labile CO_3
vCCbf, vCCbi	1130 cm^{-1}	v (CC)
dCOOf, dCOOi	1425 cm^{-1}	δ (COO)
vCCHf, vCCHi	1605 cm^{-1}	v (CCH) aromatic
vC_Cf, vC_Ci	1637 cm^{-1}	v (C=C)

Appendix H: Typical Raman Spectra

Control

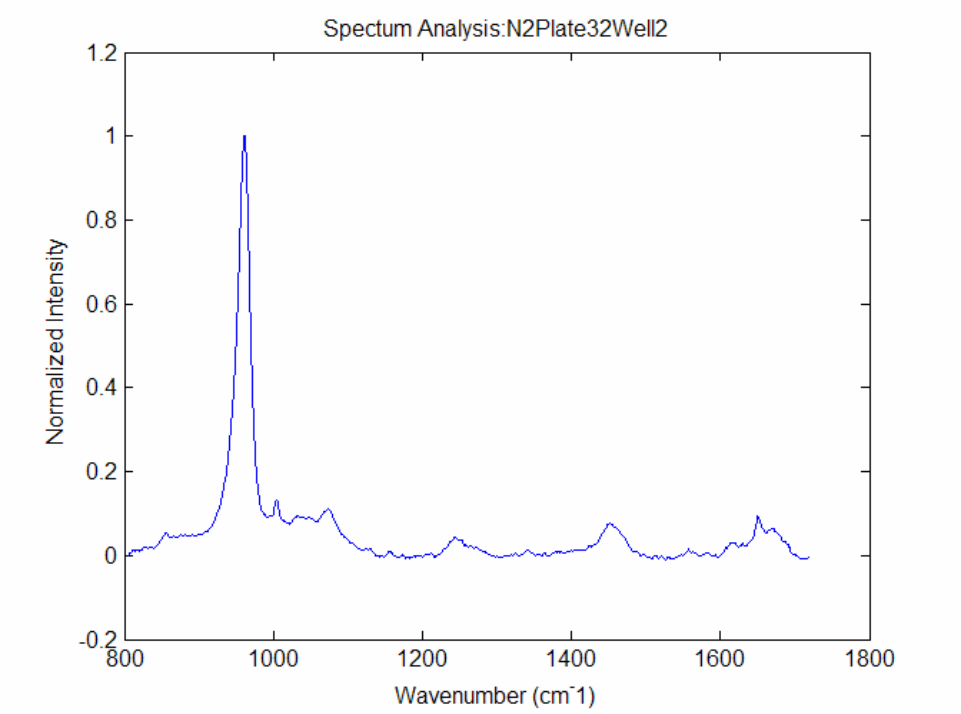

PLA

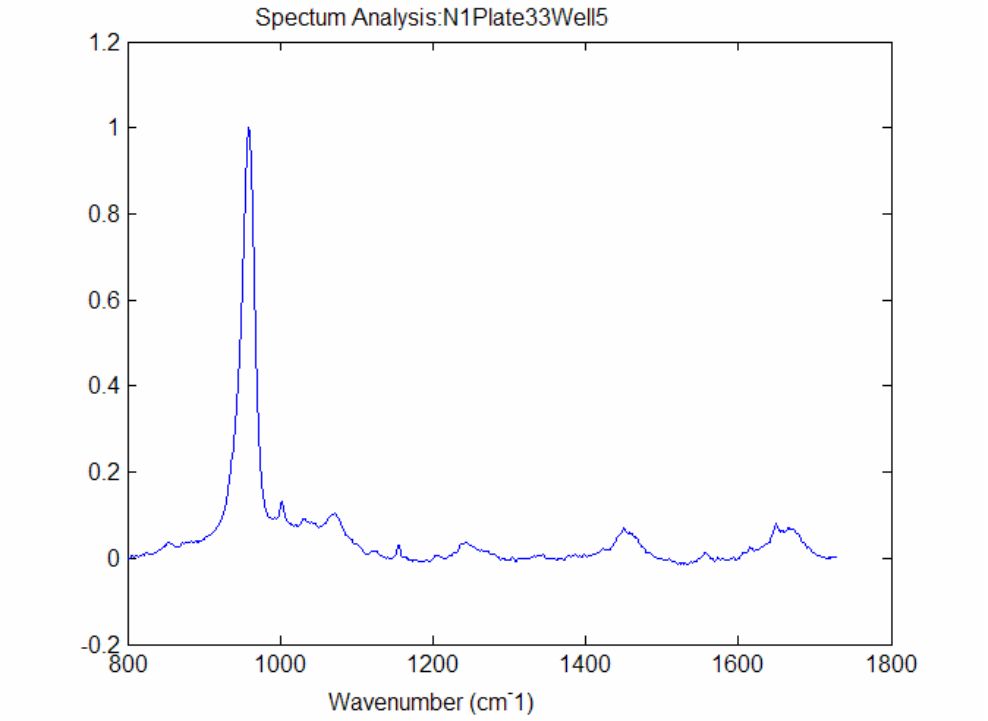

PLG

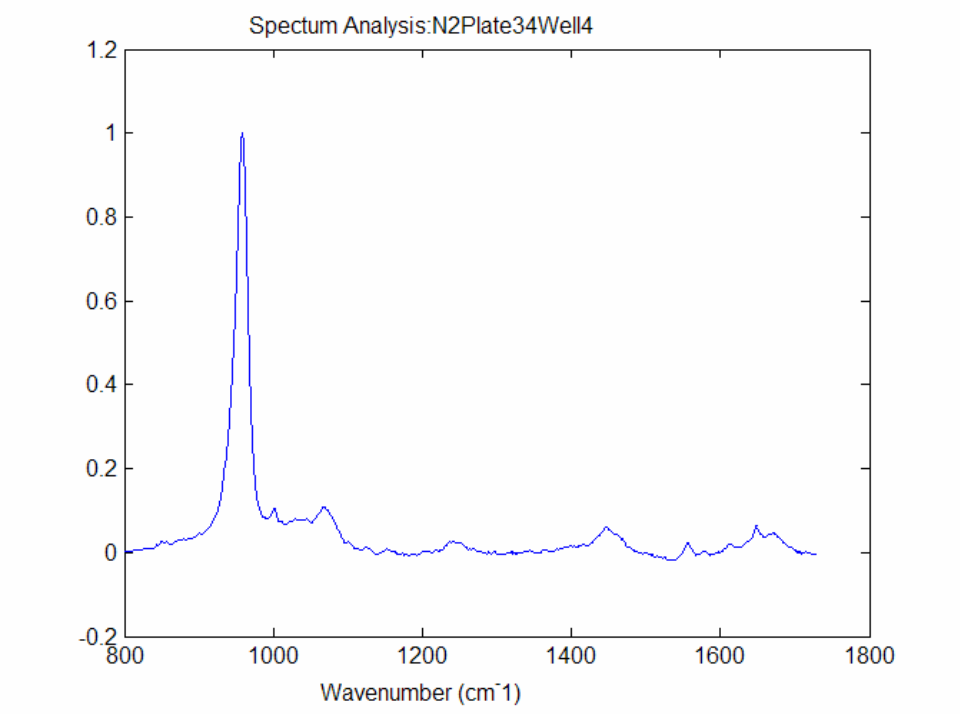
Spectum Analysis:N2Plate34Well4
1.2
1
0.8
0.6
0.4
0.2
0
-0.2
800
1000
1200
1400
1600
1800
Wavenumber (cm-1)

PLL

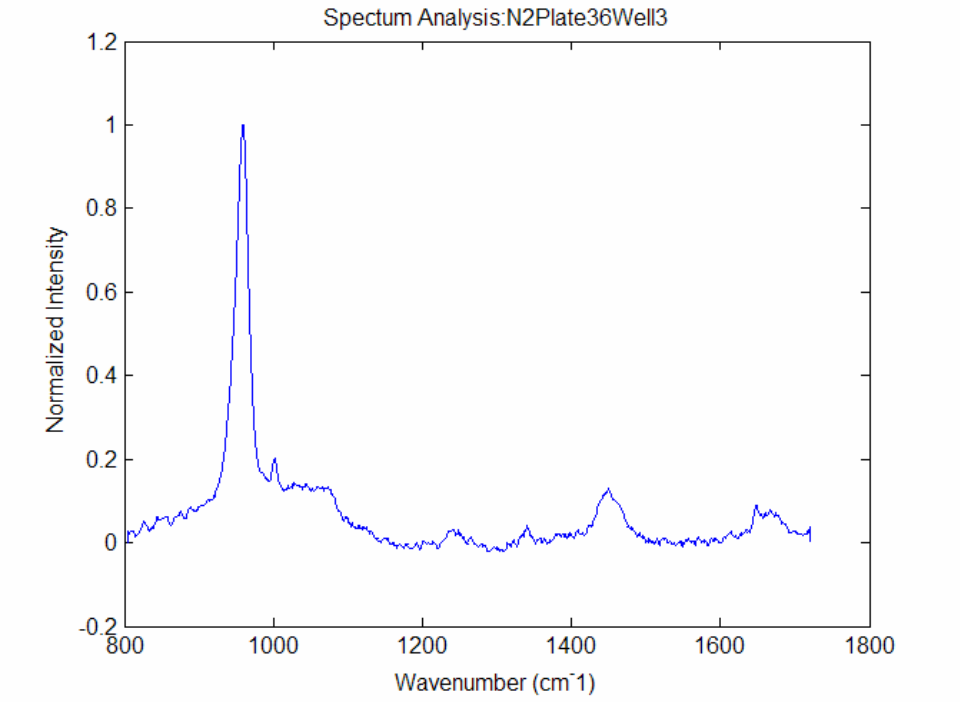
Spectum Analysis:N2Plate36Well3
Normalized Intensity
1.2
1
0.8
0.6
0.4
0.2
0
-0.2
800
1000
1200
1400
1600
1800
Wavenumber (cm-1)

PSS

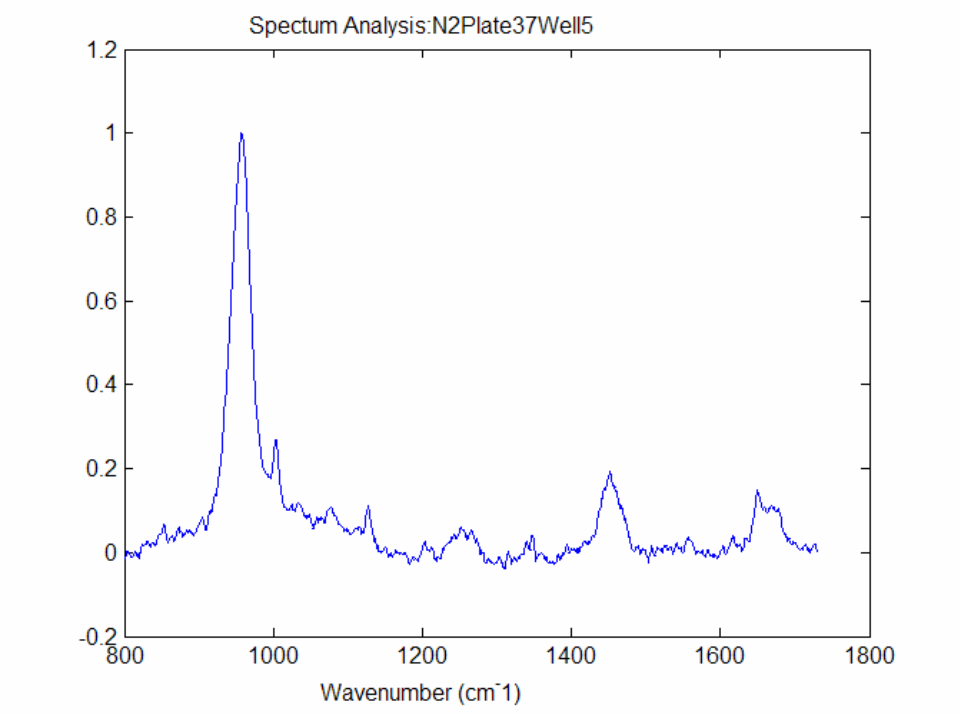
Spectum Analysis:N2Plate37Well5
1.2
1
0.8
0.6
0.4
0.2
0
-0.2
800
1000
1200
1400
1600
1800
Wavenumber (cm-1)

SC

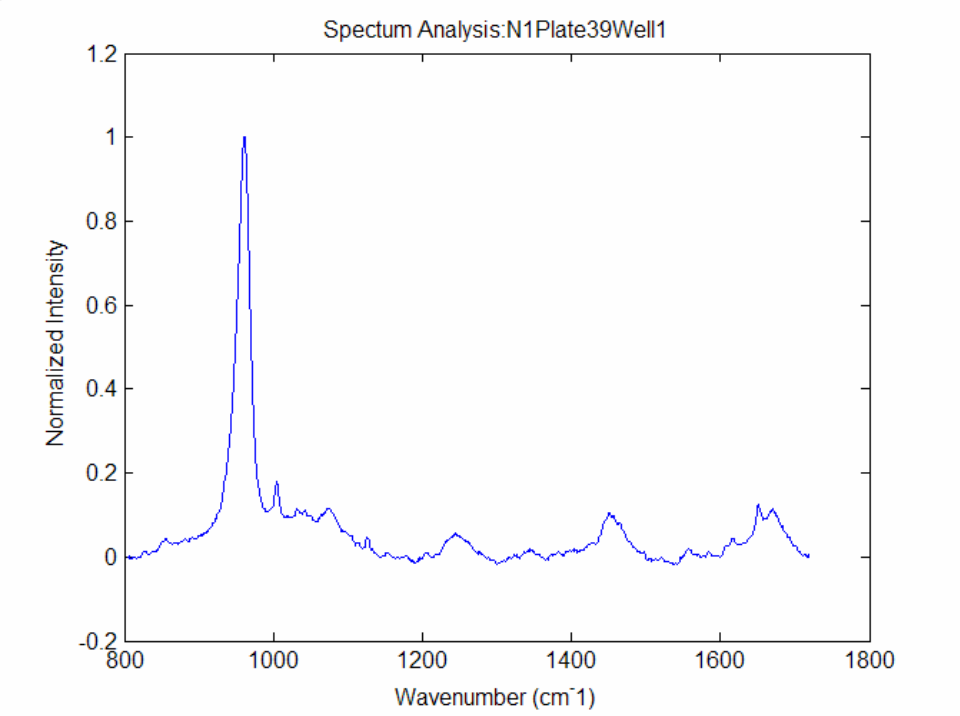
Spectum Analysis:N1Plate39Well1
Normalized Intensity
1.2
1
0.8
0.6
0.4
0.2
0
-0.2
800
1000
1200
1400
1600
1800
Wavenumber (cm-1)

Appendix I: Raman Spectroscopy Data

Control				
Spec_ID	**PO4 Peak Frequency**	**Crystallinity**	**Mineralization**	**Carbonation**
N1Plate31Well1	955.2	0.0299794	7.11385	0.0893059
N2Plate31Well1	958.416	0.0421146	13.7965	0.0927839
N3Plate31Well1	958.241	0.041423	10.3622	0.116853
N1Plate31Well2	959.116	0.0482539	21.5679	0.109606
N2Plate31Well2	958.516	0.0430455	8.80515	0.118782
N3Plate31Well2	958.916	0.0458477	13.1931	0.106755
N1Plate31Well3	958.616	0.0476082	12.7337	0.124161
N2Plate31Well3	958.816	0.0487916	13.8616	0.0994831
N1Plate31Well4	958.041	0.0468104	15.4896	0.107788
N2Plate31Well4	958.516	0.0471729	16.7541	0.101305
N1Plate31Well5	961.196	0.04653	29.065	0.102024
N2Plate31Well5	960.896	0.0453299	15.7966	0.107254
N1Plate31Well6	960.996	0.0418486	6.0006	0.128205
N2Plate31Well6	960.796	0.0435449	13.4821	0.103676
N1Plate32Well1	960.696	0.0464225	16.8985	0.0923059
N2Plate32Well1	960.896	0.03269	2.89486	0.246286
N1Plate32Well2	960.796	0.0484302	10.075	0.113178
N2Plate32Well2	961.275	0.0483951	13.4168	0.115555
N1Plate32Well3	960.596	0.0491781	15.0123	0.111362
N2Plate32Well3	960.696	0.0482134	9.37369	0.122807
Average	959.56165	0.044581495	13.2846575	0.11547379
Standard Deviation	1.565434336	0.005164015	5.67142594	0.032596544

PLA				
Spec_ID	PO4 Peak Frequency	Crystallinity	Mineralization	Carbonation
N1Plate32Well4	958.241	0.045826	9.96008	0.113078
N2Plate32Well4	958.616	0.0481731	14.1199	0.109084
N3Plate32Well4	958.416	0.0448898	10.5781	0.121075
N1Plate32Well5	958.416	0.0453943	5.50706	0.126662
N2Plate32Well5	958.416	0.0512363	12.4885	0.115113
N3Plate32Well5	957.941	0.0490577	8.45868	0.0846381
N1Plate32Well6	958.316	0.0460547	17.8713	0.116442
N2Plate32Well6	958.716	0.0488589	5.46644	0.111948
N1Plate33Well1	958.241	0.0461651	13.5258	0.109825
N2Plate33Well1	957.941	0.0471046	10.2202	0.117238
N1Plate33Well2	959.204	0.0491361	12.8352	0.109018
N2Plate33Well2	959.204	0.0493677	7.09633	0.125726
N1Plate33Well3	959.004	0.0471937	11.3034	0.110572
N2Plate33Well3	958.704	0.0475349	13.3558	0.106406
N1Plate33Well4	958.904	0.0435024	4.51301	0.147624
N2Plate33Well4	959.584	0.0483998	11.3473	0.115551
N1Plate33Well5	958.804	0.0477872	15.064	0.10889
N2Plate33Well5	958.604	0.0468785	16.0572	0.103567
N1Plate33Well6	958.604	0.0460634	16.2089	0.121667
N2Plate33Well6	959.104	0.0446398	11.9506	0.113925
Average	958.649	0.0471632	11.39639	0.114402455
Standard Deviation	0.431291817	0.001895394	3.756381163	0.011903284

PLG				
Spec_ID	PO4 Peak Frequency	Crystallinity	Mineralization	Carbonation
N1Plate34Well1	958.241	0.046126	5.87881	0.159413
N2Plate34Well1	958.416	0.0460297	7.00325	0.186224
N3Plate34Well1	957.841	0.0462743	6.59506	0.17028
N1Plate34Well2	958.716	0.0476596	3.04916	0.148719
N2Plate34Well2	958.241	0.0455555	4.89518	0.168637
N3Plate34Well2	958.516	0.0405862	3.55655	0.189443
N1Plate34Well3	958.141	0.048519	16.6322	0.117263
N2Plate34Well3	958.616	0.0485141	14.8461	0.114441
N1Plate34Well4	958.141	0.0485406	14.5835	0.128602
N2Plate34Well4	958.316	0.0481746	18.5095	0.111076
N1Plate34Well5	960.803	0.0512914	9.7964	0.111999
N2Plate34Well5	961.284	0.0484212	16.0682	0.109692
N1Plate34Well6	961.003	0.0452567	2.92308	0.198507
N2Plate34Well6	961.384	0.0464574	6.59239	0.151011
N1Plate35Well1	961.017	0.0494902	15.279	0.122535
N2Plate35Well1	960.517	0.0476954	12.0517	0.154055
N3Plate35Well1	960.803	0.0453202	5.8047	0.154832
N1Plate35Well2	960.603	0.0462467	6.0997	0.165577
N2Plate35Well2	961.103	0.0463117	9.5128	0.143609
N1Plate35Well3	960.503	0.0465335	7.23785	0.136419
Average	959.61025	0.0469502	9.3457565	0.1471167
Standard Deviation	1.353920773	0.002161001	5.011019534	0.027667612

PLL				
Spec_ID	**PO4 Peak Frequency**	**Crystallinity**	**Mineralization**	**Carbonation**
N1Plate35Well4	961.797	0.0433222	3.42262	0.133115
N2Plate35Well4	961.797	0.0433581	4.82925	0.15054
N3Plate35Well4	960.817	0.045791	3.15326	0.145295
N1Plate35Well5	961.017	0.045572	9.50523	0.137763
N2Plate35Well5	961.017	0.0456615	11.6253	0.128274
N3Plate35Well5	960.137	0.0425118	3.0596	0.157256
N1Plate35Well6	961.697	0.0463601	10.4551	0.136457
N2Plate35Well6	961.117	0.0456966	20.0406	0.117479
N1Plate36Well1	960.617	0.0420978	2.36766	0.214447
N2Plate36Well1	961.297	0.0439433	18.7592	0.111543
N1Plate36Well2	959.838	0.0422096	2.64677	0.252766
N2Plate36Well2	958.379	0.0416538	2.76152	0.180253
N1Plate36Well3	958.658	0.0464746	19.1854	0.106845
N2Plate36Well3	959.358	0.0429465	7.66435	0.152768
N1Plate36Well4	958.558	0.0446515	2.64039	0.210921
N2Plate36Well4	959.058	0.0444684	3.41024	0.174724
N1Plate36Well5	958.179	0.0461936	11.7527	0.13484
N2Plate36Well5	958.179	0.0439856	11.9222	0.10353
N1Plate36Well6	958.379	0.0480552	21.843	0.10059
N2Plate36Well6	958.558	0.0452983	13.1011	0.114863
Average	959.9227	0.044512575	9.2072745	0.14821345
Standard Deviation	1.346671769	0.001745233	6.656544721	0.040733726

PSS				
Spec_ID	PO4 Peak Frequency	Crystallinity	Mineralization	Carbonation
N1Plate37Well1	957.301	0.0279147	4.35605	0.306679
N2Plate37Well1	962.312	0.0463784	9.93128	0.205517
N3Plate37Well1	959.376	0.0271616	3.73943	0.257159
N1Plate37Well2	958.996	0.02809	2.60641	0.16639
N2Plate37Well2	960.456	0.0281486	1.78371	0.209312
N3Plate37Well2	960.456	0.0314114	2.18415	0.191821
N1Plate37Well3	959.476	0.0274571	1.82981	0.17169
N2Plate37Well3	958.496	0.028972	3.09875	0.118905
N1Plate37Well4	959.676	0.0301366	2.45692	0.179307
N2Plate37Well4	958.496	0.0298429	4.47718	0.126672
N1Plate37Well5	959.623	0.0270277	2.30335	0.141628
N2Plate37Well5	957.088	0.0303961	4.92564	0.122158
N1Plate37Well6	956.388	0.0291419	1.62171	0.169176
N2Plate37Well6	955.518	0.0293808	2.99235	0.254893
N2Plate38Well1	958.279	0.0298137	2.49503	0.160642
N3Plate38Well1	956.7	0.0310295	3.18864	0.145285
N1Plate38Well2	957.4	0.0364711	2.36375	0.176048
N2Plate38Well2	957.3	0.0323934	2.26689	0.21887
N1Plate38Well3	957.3	0.0289418	2.74917	0.160061
N2Plate38Well3	954.442	0.0279867	3.74548	0.19529
Average	958.25395	0.0304048	3.255785	0.18387515
Standard Deviation	1.866786247	0.004340728	1.824113089	0.048375705

SC				
Spec_ID	PO4 Peak Frequency	Crystallinity	Mineralization	Carbonation
N1Plate38Well4	961.736	0.0424483	7.10819	0.169401
N2Plate38Well4	962.136	0.0437291	19.334	0.0990141
N3Plate38Well4	961.836	0.0457101	14.4809	0.0910307
N1Plate38Well5	961.467	0.0466625	5.37357	0.130249
N2Plate38Well5	961.467	0.0460613	4.43536	0.125481
N3Plate38Well5	961.467	0.0466811	9.39163	0.127625
N1Plate38Well6	961.375	0.0475205	20.084	0.101999
N2Plate38Well6	961.096	0.0448391	12.2654	0.110888
N1Plate39Well1	961.196	0.0459039	9.59561	0.122726
N2Plate39Well1	961.275	0.0484433	16.1529	0.10918
N1Plate39Well2	961.196	0.0482569	15.3216	0.109827
N2Plate39Well2	961.275	0.0469487	13.4838	0.11639
N1Plate39Well3	960.596	0.0474633	21.8552	0.108849
N1Plate39Well4	960.696	0.0471682	12.6032	0.130026
N2Plate39Well4	960.996	0.0465251	17.6583	0.101963
N3Plate39Well4	961.275	0.0489848	17.6438	0.114882
N1Plate39Well5	960.996	0.0487692	12.3791	0.115076
N2Plate39Well5	961.096	0.0466325	10.2035	0.102285
N1Plate39Well6	960.796	0.044935	3.40671	0.139946
N2Plate39Well6	960.796	0.0435686	8.92051	0.146779
Average	961.23845	0.046362575	12.584864	0.11868084
Standard Deviation	0.387287936	0.001770672	5.304954894	0.018575614

Appendix J: XRD Pattern Analysis Software:

This is a transcript of the Matlab M-file used for the analysis of x-ray diffraction patterns of bone from fixed bone nodules grown *in vitro*.

```
%   A single pattern's file name is entered here

clear;clc;
load c:\temp\Plate38Wells456.xy;       %my text file of the pattern
o_pattern = Plate38Wells456;             %file name
sfilename = 'Plate38Wells456';          %file name

tag = [20 22.5 25 27 37 43 52.5 55 57.5 60 68 70];          %see instructions (2) for
what these
peaks_cd = [26.1 40 53.5];                      %parameters represent

ana_pattern = fopen('pattern_analysisPlate38Wells456.txt','A');  % creates output
file

fprintf(ana_pattern,'Pattern_ID 002p_d 002p_r 002i 002FWHM_d 002FWHM_r
130p_d 130p_r 130i 130FWHM_d 130FWHM_r 004p_d 004p_r 004i
004FWHM_d 004FWHM_r L002 L130 L004 \n');     %the header in the output file

o_deg = o_pattern(:,1);       %original 2 Theta position from the pattern
o_inten = o_pattern(:,2);      %original intesities from the pattern

%       The following section filters the intensity data from the original data to
remove
%   noise.  This is done through a 5-pt moving average filter.

n_pts = max(size(o_deg));

   for I = 1:n_pts;

       if I == 1
          d_inten(I,1) = o_inten(I);         %keep original values for first two and last
two
       else if I == 2                       %points since can't average them
          d_inten(I,1) = o_inten(I);
       else if I == n_pts-1
          d_inten(I,1) = o_inten(I);
```

```
        else if I == n_pts
           d_inten(I,1) = o_inten(I);
        else
           d_inten(I,1) = (o_inten(I-2)+o_inten(I-
1)+o_inten(I)+o_inten(I+1)+o_inten(I+2))/5;  %5 point average of the remaining
points
           % end
        end
        end
        end
        end

    d_pattern(I,1) = o_deg(I);    %creates an array that holds the 2 Theta values
with the averaged intensities
    d_pattern(I,2) = d_inten(I);

    end

%+++++++++++++++++++++++++++++++++++++++++++++++++++++++++++++++++++++++++
++++++++++++++++++++++++++++++++
%   This section will search through the filtered intensity data and generate data
points
%   corresponding to selected 2 Theta positions.

n_t_pts = max(size(tag));       %the number of points in baseline correction p-w
line

for J = 1:n_t_pts;

    diff = abs(o_deg - tag(J) * ones(size(o_deg)));   %this loop finds the index in
the
    min_diff = min(diff);                          %array where the specific 2 Theta
    index(J,1) = find(diff == min_diff);               %position is occuring so it can
                                          %be baseline corrected
    t_deg = o_deg(index);
    t_inten = d_inten(index);

    bc(J,1) = t_deg(J);
    bc(J,2) = t_inten(J);

end

for K = 1:(n_t_pts-1);

    dy = bc((K+1),2) - bc(K,2);           %this loop finds the slope of the
    dx = bc((K+1),1) - bc(K,1);           %baseline correction lines
```

```
   m(K,1) = dy/dx;

end

%   These points will be connected in a linear-piecewise fashion to create
%   the background correction curve.

n_i_pts = max(size(index));
t_bc_inten = [];

for I2 = 1:(n_i_pts - 1);

   bc_inten = [];
   seg_deg = o_deg(index(I2) : index(I2+1));     %isolate the 2 Theta position for
each segment
   y_int = bc(I2,2) - m(I2) * (bc(I2,1));          %find the y-intercept for each
segment

   n_pts2 = (index(I2+1) - index(I2) + 1);     %finds the number of 2 Theta points
in the segment

   for J2 = 1:(n_pts2-1);

      bc_inten(J2,1) = m(I2)*(seg_deg(J2)) + y_int;  %finds the intensity of the
baseline correction line

   end

   t_bc_inten = [t_bc_inten ; bc_inten];   %includes all baseline correction line
intensities into one array

end

%   Now the last intensity data point is added to the basline intensity matrix.

t_bc_inten = [t_bc_inten ; bc(n_i_pts,2)];

%   The next section creates the baseline curve and removes it from the pattern.

co_inten = d_inten - t_bc_inten;
co_spec(:,1) = o_deg;             %places baseline corrected and filtered
co_spec(:,2) = co_inten;           %data into one array

plot(o_deg,co_inten,'b')          %plots corrected and average pattern
title('Pattern Analysis')
xlabel('2 Theta (degrees)')
```

```
ylabel('Intensity')
title('Pattern Analysis:Plate38Wells456')


%+++++++++++++++++++++++++++++++++++++++++++++++++++++++++++++++++
++++++++++++++++++++++++++++++++
%   At this point, the baseline curve has been created and subtracted from the
%   pattern to correct for the background.  Next, the peak intensity
%   values and their corresponding 2 Theta values are found.
n_cdp = max(size(peaks_cd));

for I4 = 1:n_cdp;

   if I4 == 1
        tol = 7e-6;
        np = 15;
    else if I4 == 2
        tol = 2e-5;
        np = 9;
    else if I4 == 3
        tol = 5e-6;
        np = 9;
        %else if I4 == 4
        %tol = 2e-4;
       % np = 15;
        %      else if I4 == 5
        %tol = 2e-4;
        %np = 15;
        % else if I4 == 6
        %tol = 2e-5;
        %np = 13;
        %else if I4 == 7
        %tol = 1e-3;
        %np = 15;
        %else if I4 == 8
        %tol = 8e-4;
        %np = 15;

    else

    end
    end
    %end
    %end
    %end
    %end
```

```
    %end
  end

  diff3 = abs(o_deg - peaks_cd(l4) * ones(size(o_deg)));
  min_diff3 = min(diff3);                    %finds the index where specific
  index3(l4,1) = find(diff3 == min_diff3);    %peak occurs

  range2_d = o_deg((index3(l4)-5):(index3(l4)+5));   %isolates the part of the
data
  range2_i = co_inten((index3(l4)-5):(index3(l4)+5)); %for the specific peak

  %   The maximum intensity value over this range of intensities is not always at
  %   the 2 Theta position stated, so a new range of values is found that is
centered on
  %   the maximum intensity.

  mrange_i = max(range2_i);
  ipeak(l4,1) = find(co_inten == mrange_i);

  range3_d = o_deg((ipeak(l4)-np):(ipeak(l4)+np));
  range3_i = co_inten((ipeak(l4)-np):(ipeak(l4)+np));

  xdata = range3_d;
  ydata = range3_i;

  %   Now a spline curve will be fitted around the peaks of interest.
  %   The splines have different stiffness'  and numbers of points used
  %   to adjust for the best-fit curve.

  cs=csapi(xdata,ydata);
  splinevalues = fnval(cs,xdata);
  scs = spaps(xdata,splinevalues,tol);
  xdata2 = xdata(1):0.1:xdata(np*2+1);
  splinevalues = fnval(scs,xdata2);
  %plot(xdata,ydata,'r.');
  %plot(xdata2,splinevalues,'k:');

  mx_i = max(splinevalues);
  pk_idx = find(splinevalues == mx_i);
  pi = mx_i;                %peak intensity
  pf = xdata2(pk_idx);       %peak 2 Theta position
  peaks(l4,1) = pf;
  peaks(l4,2) = pi;

end
```

```
%
++++++++++++++++++++++++++++++++++++++++++++++++++++++++++++++++++++++++++++++++
%   This section will determine the half-max of the 002 peak.

P002_ends = [25.5 26.5];
n002_pts = max(size(P002_ends));

for J4 = 1:n002_pts;

   diff4 = abs(o_deg - P002_ends(J4) * ones(size(o_deg)));
   min_diff4 = min(diff4);                  %locates the index of 25.5
   index4(J4,1) = find(diff4 == min_diff4);    %and 26.5 2 Theta values

   range4_d = o_deg((index4(J4)-15):(index4(J4)+15));     %isolates the data
containing
   range4_i = co_inten((index4(J4)-15):(index4(J4)+15));   %2 Theta values
between 25.5 and 26.5

   min_r4i = min(range4_i);               %finds the minimum intensity
   index5 = find(range4_i == min_r4i);     %indexes the minimum intensity

   P002LinePts(J4,1) = range4_d(index5);    %places 2 Theta values and
intensities
   P002LinePts(J4,2) = range4_i(index5);    %at 25.5 and 26.5 into an array

end

%   The peak intensity and corresponding 2 Theta values from the spline-fit.
P002Pk_i = peaks(1,2);
P002Pk_d = peaks(1,1);

hmi(1) = P002Pk_i/2;            %  The half-max from the global baseline

%   The FWHM is determined below.
FWHMPks = [peaks(1,1)];
n_FWHMPks = max(size(FWHMPks));

for J5 = 1:n_FWHMPks;

   diff6 = abs(o_deg - FWHMPks(J5) * ones(size(o_deg)));   %finds the index of
the max
   min_diff6 = min(diff6);                          %at the 002 peak
   index8(J5,1) = find(diff6 == min_diff6);
```

```
   RSrange_d = o_deg((index8(J5)):(index8(J5)+30));       %range of 2 Theta
values and intensities to
   RSrange_i = co_inten((index8(J5)):(index8(J5)+30));     %the right side of the
peak
   RSdiff = abs(RSrange_i - hmi(J5));
   RSmindiff = min(RSdiff);                  %finds and indexes the 1/2 max intensity
   RSPtId(J5) = find(RSdiff == RSmindiff);

   LSrange_d = o_deg((index8(J5)-30):(index8(J5)));       %range of 2 Theta
values and intensities to
   LSrange_i = co_inten((index8(J5)-30):(index8(J5)));     %the left side of the
peak
   LSdiff = abs(LSrange_i - hmi(J5));
   LSmindiff = min(LSdiff);               %finds and indexes the 1/2 max intensity
   LSPtId(J5) = find(LSdiff == LSmindiff);

   RSdeg(J5,1) = RSrange_d(RSPtId);
   LSdeg(J5,1) = LSrange_d(LSPtId);

   P002FWHM(J5,1) = RSdeg(J5,1) - LSdeg(J5,1);     %FWHM

end

%
++++++++++++++++++++++++++++++++++++++++++++++++++++++++++++++++++++++++++++++++
%   This section will determine the half-max of the 130 peak.

P130_ends = [38 42];
n130_pts = max(size(P130_ends));

for J4 = 1:n130_pts;

   diff4 = abs(o_deg - P130_ends(J4) * ones(size(o_deg)));
   min_diff4 = min(diff4);                   %locates the index of 38
   index4(J4,1) = find(diff4 == min_diff4);    %and 42 2 Theta values

   range4_d = o_deg((index4(J4)-15):(index4(J4)+15));     %isolates the data
containing
   range4_i = co_inten((index4(J4)-15):(index4(J4)+15));   %2 Theta values
between 38 and 42

   min_r4i = min(range4_i);               %finds the minimum intensity
   index5 = find(range4_i == min_r4i);     %indexes the minimum intensity
```

```
   P130LinePts(J4,1) = range4_d(index5);    %places 2 Theta values and
intensities
   P130LinePts(J4,2) = range4_i(index5);    %at 38 and 42 into an array

end

%   The peak intensity and corresponding 2 Theta values from the spline-fit.
P130Pk_i = peaks(2,2);
P130Pk_d = peaks(2,1);

hmi(1) = P130Pk_i/2;            %  The half-max from the global baseline

%   The FWHM is determined below.
FWHMPks = [peaks(2,1)];
n_FWHMPks = max(size(FWHMPks));

for J5 = 1:n_FWHMPks;

   diff6 = abs(o_deg - FWHMPks(J5) * ones(size(o_deg)));   %finds the index of
the max
   min_diff6 = min(diff6);                          %at the 130 peak
   index8(J5,1) = find(diff6 == min_diff6);

   RSrange_d = o_deg((index8(J5)):(index8(J5)+150));       %range of 2 Theta
values and intensities to
   RSrange_i = co_inten((index8(J5)):(index8(J5)+150));     %the right side of the
peak
   RSdiff = abs(RSrange_i - hmi(J5));
   RSmindiff = min(RSdiff);                  %finds and indexes the 1/2 max intensity
   RSPtId(J5) = find(RSdiff == RSmindiff);

   LSrange_d = o_deg((index8(J5)-150):(index8(J5)));       %range of 2 Theta
values and intensities to
   LSrange_i = co_inten((index8(J5)-150):(index8(J5)));     %the left side of the
peak
   LSdiff = abs(LSrange_i - hmi(J5));
   LSmindiff = min(LSdiff);              %finds and indexes the 1/2 max intensity
   LSPtId(J5) = find(LSdiff == LSmindiff);

   RSdeg(J5,1) = RSrange_d(RSPtId);
   LSdeg(J5,1) = LSrange_d(LSPtId);

   P130FWHM(J5,1) = RSdeg(J5,1) - LSdeg(J5,1);     %FWHM

end
```

```
%
++++++++++++++++++++++++++++++++++++++++++++++++++++++++++++++++++++++++++++++++
%   This section will determine the FWHM of the 004 peak.

P004_ends = [53 54.5];
n004_pts = max(size(P004_ends));

for J4 = 1:n004_pts;

   diff4 = abs(o_deg - P004_ends(J4) * ones(size(o_deg)));
   min_diff4 = min(diff4);                  %locates the index of 53
   index4(J4,1) = find(diff4 == min_diff4);    %and 54.5 2 Theta values

   range4_d = o_deg((index4(J4)-15):(index4(J4)+15));     %isolates the data
containing
   range4_i = co_inten((index4(J4)-15):(index4(J4)+15));   %2 Theta values
between 53 and 54.5

   min_r4i = min(range4_i);               %finds the minimum intensity
   index5 = find(range4_i == min_r4i);     %indexes the minimum intensity

   P004LinePts(J4,1) = range4_d(index5);    %places 2 Theta values and
intensities
   P004LinePts(J4,2) = range4_i(index5);    %at 53 and 54.5 into an array

end

%   The peak intensity and corresponding 2 Theta values from the spline-fit.
P004Pk_i = peaks(3,2);
P004Pk_d = peaks(3,1);

hmi(1) = P004Pk_i/2;            %  The half-max from the global baseline

%   The FWHM is determined below.
FWHMPks = [peaks(3,1)];
n_FWHMPks = max(size(FWHMPks));

for J5 = 1:n_FWHMPks;

   diff6 = abs(o_deg - FWHMPks(J5) * ones(size(o_deg)));   %finds the index of
the max
   min_diff6 = min(diff6);                          %at the 004 peak
   index8(J5,1) = find(diff6 == min_diff6);
```

```
   RSrange_d = o_deg((index8(J5)):(index8(J5)+70));       %range of 2 Theta
values and intensities to
   RSrange_i = co_inten((index8(J5)):(index8(J5)+70));     %the right side of the
peak
   RSdiff = abs(RSrange_i - hmi(J5));
   RSmindiff = min(RSdiff);                  %finds and indexes the 1/2 max intensity
   RSPtId(J5) = find(RSdiff == RSmindiff);

   LSrange_d = o_deg((index8(J5)-70):(index8(J5)));       %range of 2 Theta
values and intensities to
   LSrange_i = co_inten((index8(J5)-70):(index8(J5)));     %the left side of the
peak
   LSdiff = abs(LSrange_i - hmi(J5));
   LSmindiff = min(LSdiff);               %finds and indexes the 1/2 max intensity
   LSPtId(J5) = find(LSdiff == LSmindiff);

   RSdeg(J5,1) = RSrange_d(RSPtId);
   LSdeg(J5,1) = LSrange_d(LSPtId);

   P004FWHM(J5,1) = RSdeg(J5,1) - LSdeg(J5,1);     %FWHM

end

%Convert peak positions and FWHMs degrees to radians

clear pi;
peaks_r=peaks(:,1)*(pi/180);
P002FWHM_r=P002FWHM*(pi/180);
P130FWHM_r=P130FWHM*(pi/180);
P004FWHM_r=P004FWHM*(pi/180);

%Corrects the FWHM with respect to the calibration data for LaB6

P002r=peaks_r(1,1);
P130r=peaks_r(2,1);
P004r=peaks_r(3,1);

cP002FWHM_r=P002FWHM_r-((0.0026*(P002r^3))-
(0.0053*(P002r^2))+(0.0026*P002r)+0.0015);
cP130FWHM_r=P130FWHM_r-((0.0026*(P130r^3))-
(0.0053*(P130r^2))+(0.0026*P130r)+0.0015);
cP004FWHM_r=P004FWHM_r-((0.0026*(P004r^3))-
(0.0053*(P004r^2))+(0.0026*P004r)+0.0015);

%Find length of crystals in specified plane
```

```
L002=(0.9*0.15406)/(cP002FWHM_r*cos(peaks_r(1,1)));
L130=(0.9*0.15406)/(cP130FWHM_r*cos(peaks_r(2,1)));
L004=(0.9*0.15406)/(cP004FWHM_r*cos(peaks_r(3,1)));

fprintf(ana_pattern,'%s %g %g %g %g %g %g %g %g %g %g %g %g %g %g %g
%g %g %g %g %g %g %g %g %g %g %g %g %g %g %g %g %g %g %g %g %g
%g %g %g %g %g %g %g %g %g %g %g %g %g %g %g %g %g %g %g %g %g
%g %g %g %g %g %g %g %g %g %g %g %g %g
\n',sfilename,peaks(1,1),peaks_r(1,1),peaks(1,2),P002FWHM,P002FWHM_r,pea
ks(2,1),peaks_r(2,1),peaks(2,2),P130FWHM,P130FWHM_r,peaks(3,1),peaks_r(
3,1),peaks(3,2),P004FWHM,P004FWHM_r,L002,L130,L004);

fclose(ana_pattern);
```

Appendix K: Pattern Analysis Software Output Variables

variables ending in ‘d‘ are 2θ positions in degrees; variable ending in ‘r’ are 2θ positions in radians; variables ending in ‘i’ are intensities

Variable	Definition
002p_d	~26.1°, peak for the 002 reflection (degrees)
002p_r	~0.456, peak for the 002 reflection (radians)
002i	intensity of the 002 peak
002FWHM_d	002 peak full-width half-max in degrees
002FWHM_r	002 peak full-width half-max in radians
130p_d	~39.8°, peak for the 130 reflection (degrees)
130p_r	~0.695, peak for the 130 reflection (radians)
130i	intensity of the 130 peak
130FWHM_d	130 peak full-width half-max in degrees
130FWHM_r	130 peak full-width half-max in radians
004p_d	~53.6°, peak for the 004 reflection (degrees)
004p_r	~0.935, peak for the 004 reflection (radians)
004i	intensity of the 004 peak
004FWHM_d	004 peak full-width half-max in degrees
004FWHM_r	004 peak full-width half-max in radians
L002	crystal length along the 002 direction (nm)
L130	crystal length along the 130 direction (nm)
L004	crystal length along the 004 direction (nm)

Appendix L: XRD Data

Treatment	Control						PLA						PLG					
Plate	31	31	31	32	Avg	STD	32	33	33	33	Avg	STD	34	34	34	35	Avg	STD
Wells	123	123-2	456	123			456	123	456	456-2			123	123-2	456	123		
002p_d	26.18	26.07	26.19	26.14	26.15	0.05	26.11	26.24	26.14	26.14	26.16	0.06	26.24	26.24	26.22	26.24	26.24	0.01
002p_r	0.46	0.46	0.46	0.46	0.46	0.00	0.46	0.46	0.46	0.46	0.46	0.00	0.46	0.46	0.46	0.46	0.46	0.00
002i	386.68	468.37	846.56	793.22	623.71	230.01	775.80	731.12	911.75	593.71	753.09	131.12	1101.92	732.65	1467.33	1030.47	1083.09	301.98
002FWHM_d	0.45	0.57	0.58	0.58	0.55	0.06	0.57	0.58	0.57	0.55	0.57	0.01	0.57	0.64	0.58	0.62	0.60	0.03
002FWHM_r	0.01	0.01	0.01	0.01	0.01	0.00	0.01	0.01	0.01	0.01	0.01	0.00	0.01	0.01	0.01	0.01	0.01	0.00
130p_d	39.78	39.76	39.88	39.83	39.81	0.05	39.86	39.88	39.76	40.11	39.90	0.15	39.78	40.01	39.94	39.76	39.87	0.12
130p_r	0.69	0.69	0.70	0.70	0.69	0.00	0.70	0.70	0.69	0.70	0.70	0.00	0.69	0.70	0.70	0.69	0.70	0.00
130i	55.57	158.63	209.41	213.09	159.18	73.40	185.98	196.72	288.24	140.52	202.87	61.91	302.95	151.61	308.20	288.53	262.82	74.61
130FWHM_d	1.50	1.62	1.74	1.55	1.60	0.10	1.67	1.82	1.65	1.59	1.68	0.10	1.69	1.94	2.07	1.79	1.87	0.17
130FWHM_r	0.03	0.03	0.03	0.03	0.03	0.00	0.03	0.03	0.03	0.03	0.03	0.00	0.03	0.03	0.04	0.03	0.03	0.00
004p_d	53.64	53.45	53.63	53.61	53.58	0.09	53.66	53.63	53.55	53.48	53.58	0.08	53.65	53.71	53.63	53.70	53.67	0.04
004p_r	0.94	0.93	0.94	0.94	0.94	0.00	0.94	0.94	0.93	0.93	0.94	0.00	0.94	0.94	0.94	0.94	0.94	0.00
004i	60.23	186.75	290.08	253.87	197.73	101.17	275.25	280.20	354.01	174.43	270.97	73.75	425.80	308.33	497.40	427.02	414.64	78.38
004FWHM_d	0.87	0.87	0.84	0.85	0.86	0.02	0.74	0.75	0.75	0.80	0.76	0.03	0.79	0.72	0.70	0.77	0.74	0.04
004FWHM_r	0.02	0.02	0.01	0.01	0.01	0.00	0.01	0.01	0.01	0.01	0.01	0.00	0.01	0.01	0.01	0.01	0.01	0.00
L002	16.99	17.95	18.05	17.85	17.71	0.49	19.74	19.15	19.46	19.10	19.36	0.30	19.02	18.83	19.96	18.33	19.03	0.68
L130	7.34	6.78	6.31	7.10	6.88	0.45	6.57	6.00	6.63	6.96	6.54	0.40	6.50	5.63	5.24	6.11	5.87	0.55
L002/L130	2.31	2.65	2.86	2.51	2.58	0.23	3.00	3.19	2.93	2.74	2.97	0.18	2.93	3.34	3.81	3.00	3.27	0.40

Treatment	PLL						SC					
Plate	35	36	36	36	Avg	STD	38	39	39	39	Avg	STD
Wells	456	123	123-2	456			456	123	123-2	456		
002p_d	26.22	26.24	26.22	26.14	26.21	0.05	26.24	26.24	26.24	26.14	26.22	0.05
002p_r	0.46	0.46	0.46	0.46	0.46	0.00	0.46	0.46	0.46	0.46	0.46	0.00
002i	762.56	1173.93	628.31	531.61	774.10	282.87	1284.46	704.65	910.95	700.22	900.07	274.47
002FWHM_d	0.58	0.58	0.57	0.60	0.58	0.01	0.58	0.57	0.64	0.52	0.58	0.05
002FWHM_r	0.01	0.01	0.01	0.01	0.01	0.00	0.01	0.01	0.01	0.01	0.01	0.00
130p_d	39.78	39.99	39.91	39.96	39.91	0.10	39.79	39.78	39.98	39.78	39.83	0.10
130p_r	0.69	0.70	0.70	0.70	0.70	0.00	0.69	0.69	0.70	0.69	0.70	0.00
130i	164.66	354.18	163.30	111.92	198.52	106.64	321.44	226.72	251.39	179.18	244.68	59.30
130FWHM_d	1.25	2.04	1.87	2.49	1.91	0.51	1.94	1.80	1.75	1.64	1.78	0.12
130FWHM_r	0.02	0.04	0.03	0.04	0.03	0.01	0.03	0.03	0.03	0.03	0.03	0.00
004p_d	53.71	53.53	53.48	53.63	53.59	0.10	53.73	53.65	53.73	53.60	53.68	0.07
004p_r	0.94	0.93	0.93	0.94	0.94	0.00	0.94	0.94	0.94	0.94	0.94	0.00
004i	219.94	435.84	205.49	175.72	259.25	119.16	427.46	252.10	343.70	267.85	322.77	80.43
004FWHM_d	1.00	0.85	0.82	0.77	0.86	0.10	0.77	0.84	0.82	0.80	0.81	0.03
004FWHM_r	0.02	0.01	0.01	0.01	0.02	0.00	0.01	0.01	0.01	0.01	0.01	0.00
L002	16.46	17.84	18.55	18.60	17.86	1.00	18.94	18.38	17.41	19.92	18.66	1.05
L130	8.94	5.34	5.83	4.33	6.11	1.99	5.61	6.05	6.25	6.71	6.16	0.45
L002/L130	1.84	3.34	3.18	4.29	3.16	1.01	3.38	3.04	2.78	2.97	3.04	0.25

Appendix M: Typical X-Ray Diffraction Patterns

Control

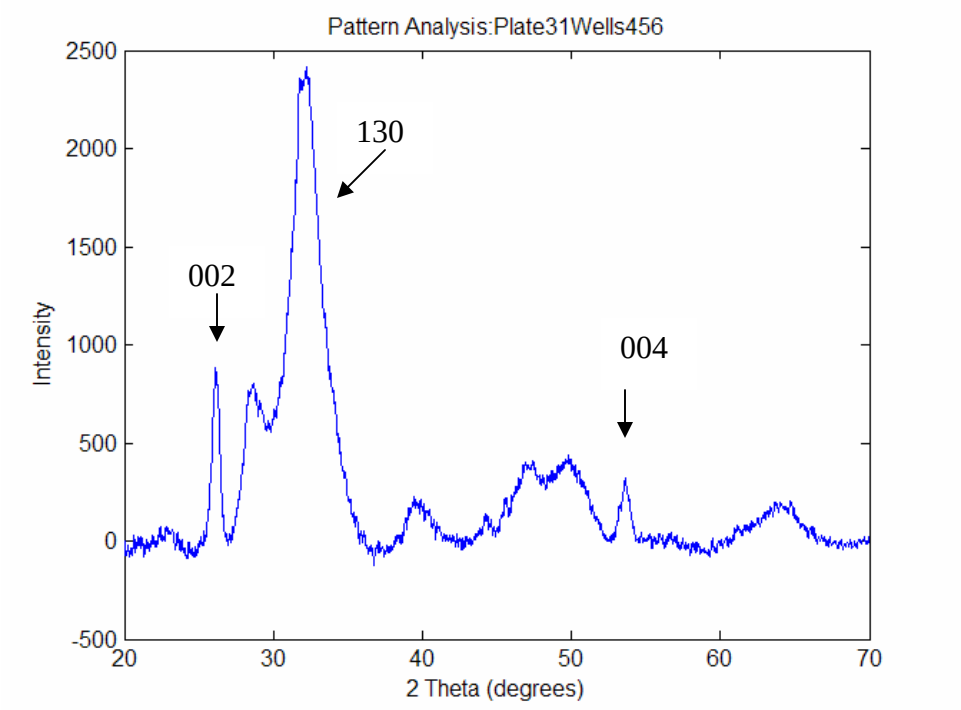

PLA

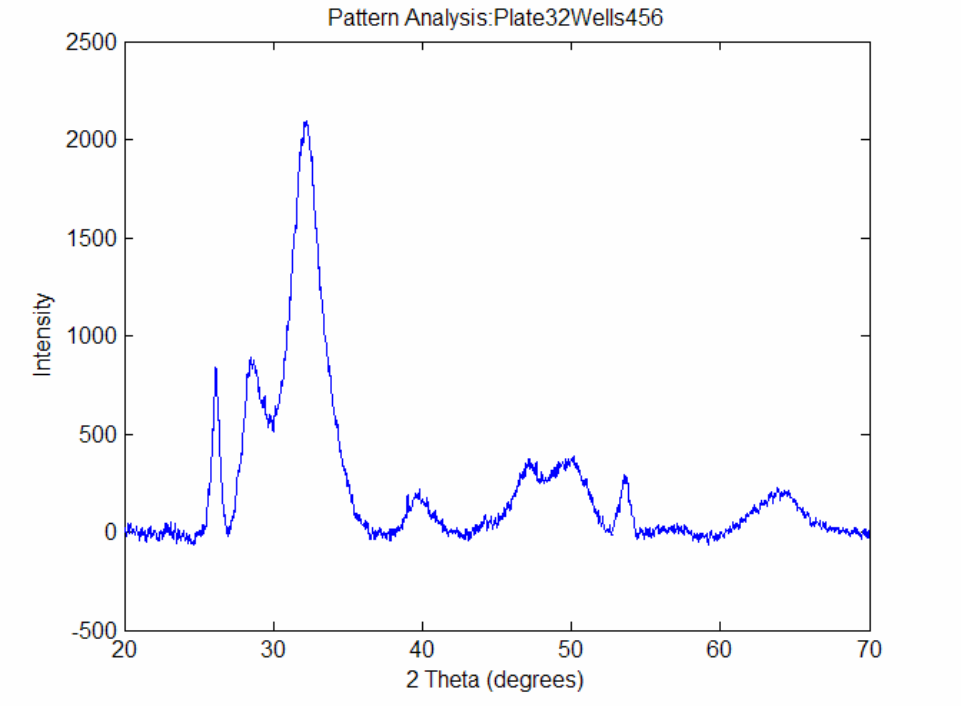

PLG

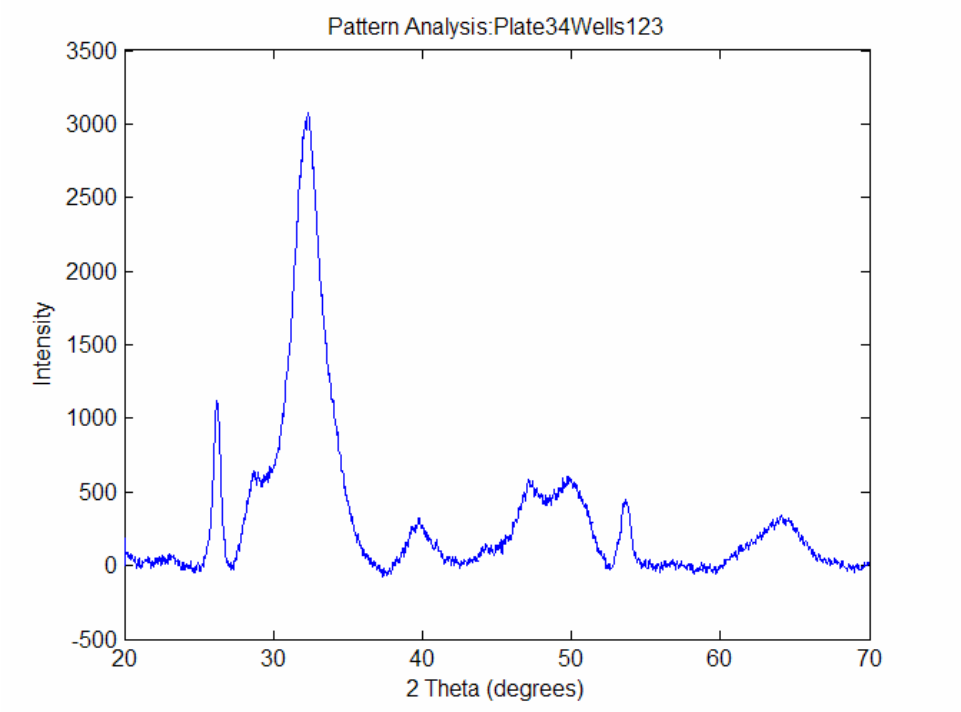
Pattern Analysis:Plate34Wells123
Intensity
2 Theta (degrees)
3500
3000
2500
2000
1500
1000
500
0
-500
20
30
40
50
60
70

PLL

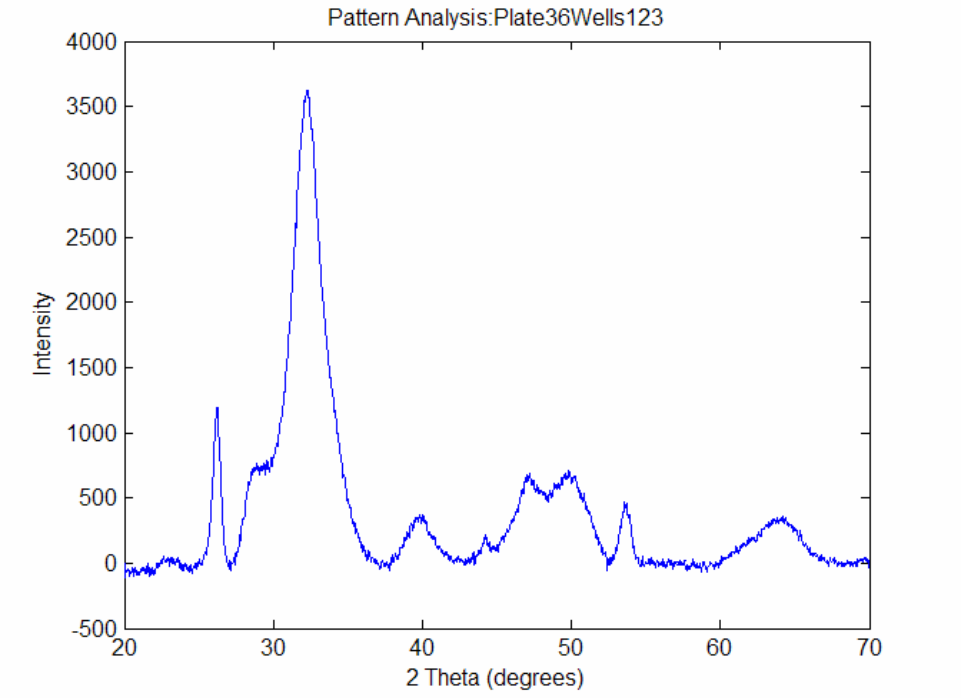
Pattern Analysis:Plate36Wells123
Intensity
2 Theta (degrees)
4000
3500
3000
2500
2000
1500
1000
500
0
-500
20
30
40
50
60
70

PSS

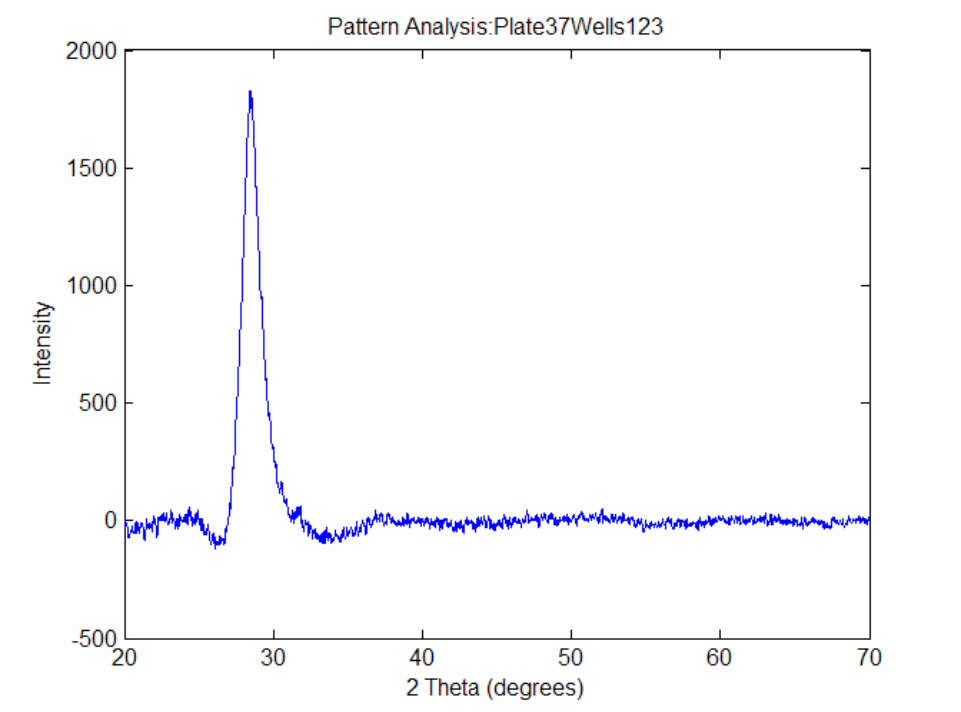
Pattern Analysis:Plate37Wells123
Intensity
2 Theta (degrees)
2000
1500
1000
500
0
-500
20
30
40
50
60
70

SC

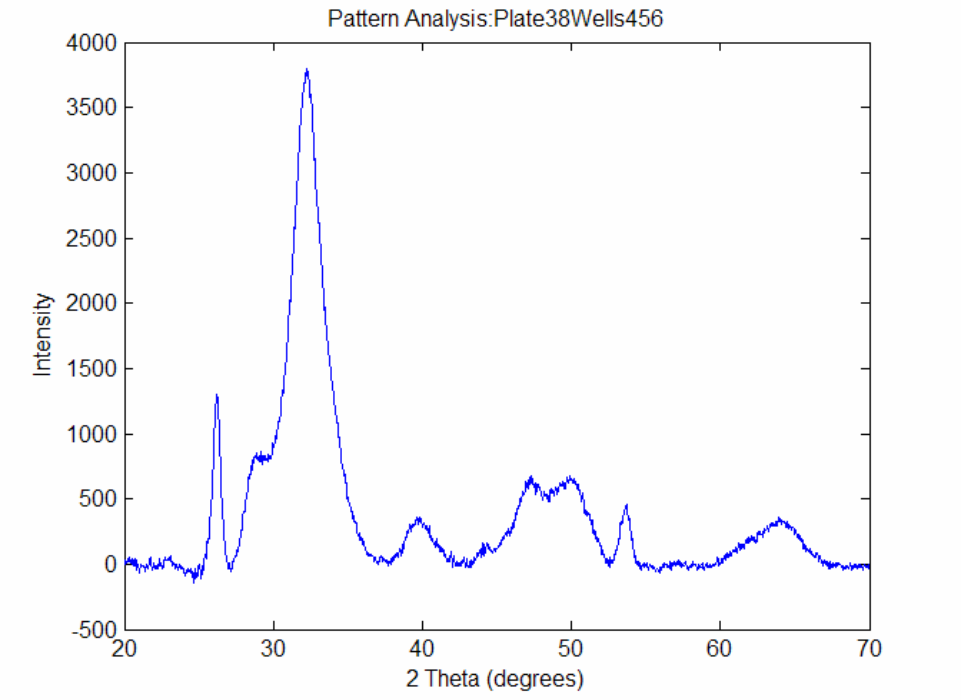
Pattern Analysis:Plate38Wells456
Intensity
2 Theta (degrees)
4000
3500
3000
2500
2000
1500
1000
500
0
-500
20
30
40
50
60
70

Appendix N: Vickers Microhardness Data

Control

				Microhardness			
Plate	Well	Section	Nodule	Reading 1	Reading 2	Reading 3	Average Reading
31	1	4	1-1	63.6	59.7	61.4	61.6
31	1	4	1-2	63.8	59.9	61.6	61.8
31	1	5	1-1	59.1	63.9	63	62.0
31	1	6	1-1	51	48.1	47.1	48.7
31	1	6	1-2	46.4	46.5	46.3	46.4
31	1	11	1-1	58.3	52.6	54.7	55.2
31	1	11	1-2	57.6	52.4	57.4	55.8
32	3	5	1-1	55.2	50.6	51.6	52.5
32	3	5	1-2	51.6	57.5	54	54.4
32	3	8	1-1	48.1	50.6	54.8	51.2
32	3	8	1-2	57.2	56.2	53.8	55.7
32	3	8	2-1	49.1	48.9	52.1	50.0
32	3	8	2-2	60.4	57.8	57.4	58.5
32	3	9	1-1	48.2	52.1	54.8	51.7
32	3	9	1-2	48	49.8	46.3	48.0
32	3	9	2-1	53	58.7	54.1	55.3
32	3	9	2-2	52.2	59.1	56	55.8
32	3	9	3-1	52.8	53.8	53.7	53.4
32	3	9	3-2	49.7	50.3	49.7	49.9
32	3	10	1-1	48.9	55.7	48.7	51.1
32	3	10	1-2	49.1	54	55.6	52.9
31	3	2	1-1	51.7	55.4	56.8	54.6
31	3	2	1-2	64.4	65	63	64.1
31	3	2	2-1	59.6	55	60.5	58.4
31	3	2	2-2	55.1	50.6	52.4	52.7
31	3	3	1-1	58.5	62.2	59.4	60.0
31	3	3	1-2	51.1	52.9	49	51.0
						Average	54.5
						STD	4.6

PLA

				Microhardness			
Plate	Well	Section	Nodule	Reading 1	Reading 2	Reading 3	Average Reading
32	4	8	1-1	53.6	55.9	52.5	54.0
32	4	8	1-2	55.7	52.8	55.4	54.6
32	4	8	2-1	51.5	55.1	50.7	52.4
32	4	8	2-2	56.8	62.4	60.6	59.9
32	4	10	1-1	54.2	59.5	59.8	57.8
32	5	5	1-1	60.8	60.2	60.6	60.5
32	5	5	1-2	50.8	55.9	51	52.6
32	5	5	2-1	61.6	62.5	58.8	61.0
32	5	5	2-2	60.6	63.2	59	60.9
32	5	6	1-1	56.8	57.5	52.5	55.6
32	5	6	1-2	52.3	52.5	50.1	51.6
32	5	6	2-1	52.3	58.9	53.6	54.9
32	5	6	2-2	59.2	58	54.9	57.4
32	5	7	1-1	64.7	61.1	61.6	62.5
32	5	7	1-2	69.4	67.8	65.9	67.7
32	5	7	2-1	51.7	58.8	55.5	55.3
32	5	7	2-2	51.4	52.8	56.5	53.6
32	5	8	1-1	54.2	52.3	55.4	54.0
32	5	8	1-2	51.1	50.8	52.7	51.5
32	5	8	2-1	65.2	66.6	63.4	65.1
32	5	8	2-2	47.5	53.7	52.4	51.2
32	5	9	1-1	63.9	66.2	60.8	63.6
32	5	9	1-2	65.8	64.3	65.9	65.3
33	4	6	1-1	49.4	49.4	49.5	49.4
33	4	6	1-2	49	52.1	50.5	50.5
33	4	7	1-1	51.2	53	49.2	51.1
33	4	7	1-2	62.4	66.7	56.7	61.9
33	4	13	1-1	55.6	55.5	60.7	57.3
33	4	13	1-2	66.2	62.2	61	63.1
						Average	57.1
						STD	5.2

PLG

				Microhardness			
Plate	Well	Section	Nodule	Reading 1	Reading 2	Reading 3	Average Reading
34	1	7	1-1	61.1	63.5	60.3	61.6
35	1	5	1-1	48.4	54.2	50.1	50.9
35	1	5	1-2	55.4	48.5	60.6	54.8
35	1	6	1-1	49.8	48.9	46.7	48.5
35	1	6	1-2	54	57.8	50.7	54.2
35	1	7	1-1	57.6	52.5	57.1	55.7
35	1	7	1-2	53.6	54	56.8	54.8
34	2	9	1-1	54.7	59.7	59	57.8
34	2	9	1-2	60.7	61.9	54	58.9
						Average	55.2
						STD	4.0

PLL

				Microhardness			
Plate	Well	Section	Nodule	Reading 1	Reading 2	Reading 3	Average Reading
35	5	4	1-1	50.3	50.5	55.5	52.1
35	5	4	1-2	52.8	51.2	51.3	51.8
35	5	4	2-1	50.4	54.5	50.9	51.9
35	5	4	2-2	50.3	48.6	51.7	50.2
35	5	5	1-1	54.8	55.8	52.9	54.5
35	5	5	1-2	51.8	52.3	55.3	53.1
35	5	12	1-1	56.1	58.1	58.7	57.6
35	5	12	1-2	50	49.1	48.6	49.2
35	5	13	1-1	57.9	52.7	58.6	56.4
35	5	13	1-2	52	51.9	52.9	52.3
35	5	13	2-1	49.8	49.5	50.1	49.8
35	5	13	2-2	51.2	50.5	48	49.9
35	5	14	1-1	56.5	58.7	58.4	57.9
35	5	14	1-2	55.2	53.3	55.4	54.6
35	5	14	2-1	51.5	55.2	54.7	53.8
35	5	14	2-2	52.4	53.1	53.5	53.0
35	5	15	1-1	55.4	50.9	52.6	53.0
35	5	15	1-2	51.9	52.6	52.7	52.4
36	1	3	1-1	58.6	55.4	58.4	57.5
36	1	3	1-2	50.6	54.6	55	53.4
36	1	3	2-1	60.1	63.8	60.5	61.5
36	1	3	2-2	61.6	60.7	59.5	60.6
36	1	7	1-1	54.7	58.4	56.2	56.4
36	1	7	1-2	54.6	60.1	54.2	56.3
36	1	7	2-1	57.2	57	58.2	57.5
36	1	7	2-2	54.8	53.4	55.9	54.7
36	1	7	3-1	61.6	62.5	56.4	60.2
36	1	7	3-2	49.9	57.2	53.9	53.7
36	1	9	1-1	61.9	61.2	61.9	61.7
36	1	9	1-2	50.3	51.3	57.5	53.0
35	6	4	1-1	57.4	59.1	56.7	57.7
35	6	4	1-2	60.7	62.1	63.1	62.0
35	6	6	1-1	63.7	59.8	56.6	60.0
35	6	6	1-2	51.2	51.3	47.6	50.0
35	6	7	1-1	53.8	57	55.7	55.5
35	6	7	1-2	51.3	52.6	51.3	51.7
						Average	54.9
						STD	3.7

PSS

				Microhardness			
Plate	Well	Section	Nodule	Reading 1	Reading 2	Reading 3	Average Reading
37	1	3	1-1	52.5	54	50	52.2
37	1	3	1-2	55.8	57	55.6	56.1
37	1	10	1-1	47.3	48	48.4	47.9
37	1	10	1-2	57.5	56.3	55.9	56.6
38	2	1	1-1	53.5	51	51.7	52.1
38	2	6	1-1	58.6	62.2	57	59.3
37	5	7	1-1	56.5	55.6	52.7	54.9
						Average	54.1
						STD	3.7

SC

				Microhardness			
Plate	Well	Section	Nodule	Reading 1	Reading 2	Reading 3	Average Reading
38	4	2	1-1	54.5	60.2	58.1	57.6
38	4	2	1-2	55	57.9	55	56
38	4	3	1-1	52	50	56.8	52.9
38	4	3	1-2	51	54	51	52
38	4	4	1-1	52.9	48	51.5	50.8
38	4	4	1-2	62.9	58.5	59.2	60.2
38	4	4	2-1	56.2	53.1	51.3	53.5
38	4	4	2-2	56	55.1	51.5	54.2
38	4	4	3-1	54.1	53.3	53.6	53.7
38	4	4	3-2	55.8	53.3	54.8	54.6
39	4	2	1-1	52	50.5	55.2	52.6
39	4	2	1-2	49.5	49.9	51.7	50.4
39	4	2	2-1	53.7	56.1	53.6	54.5
39	4	2	2-2	58.1	53.4	54.3	55.3
39	4	3	1-1	51	56.2	54.3	53.8
39	4	3	1-2	53.2	58.7	54.5	55.5
39	4	6	1-1	56	56.2	58.1	56.8
39	4	6	1-2	53.5	52.3	55.5	53.8
39	4	6	2-1	51.4	59.5	52.8	54.6
39	4	6	2-2	51.2	51.5	50.4	51
39	4	7	1-1	57.1	55.8	54.7	55.9
39	4	7	1-2	54.7	56.1	58.3	56.4
39	4	7	2-1	49.2	52.5	48.9	50.2
39	4	7	2-2	49.3	54.2	51.5	51.7
39	4	8	1-1	48.5	55.4	52.8	52.2
39	4	8	1-2	58.3	55.8	57.2	57.1
39	4	8	2-1	51.5	56.9	53.6	54
39	4	8	2-2	49.7	53.2	52.2	51.7
39	4	9	1-1	57	51.5	50.8	53.1
39	4	9	1-2	50	52.6	52.3	51.6
39	4	9	2-1	57.9	58.1	53.2	56.4
39	4	9	2-2	48.5	54.9	53.8	52.4
39	4	10	1-1	48.9	49.6	49.1	49.2
39	4	10	1-2	50.6	52	51.6	51.4
39	6	1	1-1	62.1	61	66.6	63.2
39	6	1	1-2	61.5	66.8	68.5	65.6
39	6	2	1-1	52.7	51.7	49.3	51.2
39	6	2	1-2	58.2	61.6	60	59.9
39	6	2	2-1	64.1	63.5	61.6	63.1
39	6	2	2-2	50.9	55.6	50.3	52.3
39	6	3	1-1	56.5	50.3	52.5	53.1
39	6	3	1-2	55.9	53.1	53.5	54.2
39	6	3	2-1	64	62.7	66.6	64.4
39	6	3	2-2	61.5	61.4	60.4	61.1
39	6	4	1-1	56.8	59.2	57.5	57.8
39	6	4	1-2	67.7	64	65	65.6
39	6	4	2-1	58.6	58.3	57.5	58.1
39	6	4	2-2	55.5	62.9	58.5	59
						Average	55.3
						STD	4.2

Literature Cited

[1] Akkus, O., F. Adar, and M.B. Schaffler, *Age-related changes in physicochemical properties of mineral crystals are related to impaired mechanical function of cortical bone.* Bone, 2004. **34**(3):

[2] Landis, W.J., *The strength of a calcified tissue depends in part on the molecular structure and organization of its constituent mineral crystals in their organic matrix.* Bone, 1995. **16**(5): p. 533-44.

[3] Akkus, O., *Elastic deformation of mineralized collagen fibrils: an equivalent inclusion based composite model.* J Biomech Eng, 2005. **127**(3): p. 383-90.

[4] Jager, I. and P. Fratzl, *Mineralized collagen fibrils: a mechanical model with a staggered arrangement of mineral particles.* Biophys J, 2000. **79**(4): p. 1737-46.

[5] Eanes, E.D. and A.W. Hailer, *Anionic effects on the size and shape of apatite crystals grown from physiological solutions.* Calcif Tissue Int, 2000. **66**(6): p. 449-55.

[6] Furedi-Milhofer, H., et al., *Control of Calcium Phosphate Crystal Nucleation, Growth and Morphology by Polyelectrolytes.* Key Engineering Materials, 2004. **254-256**: p. 11-14.

[7] Bar-Yosef Ofir, P., et al., *The Influence of Polyelectrolytes on the Formation and Phase Transformation of Amorphous Calcium Phosphate.* Crystal Growth & Design, 2004. **4**(1): p. 177-183.

[8] Romberg, R.W., et al., *Inhibition of hydroxyapatite crystal growth by bone-specific and other calcium-binding proteins.* Biochemistry, 1986. **25**(5): p. 1176-80.

[9] Jee, W.S.S., *Integrated Bone Tissue Physiology: Anatomy and Physiology*, in *Bone Biomechanics*.

[10] Hall, B.K. The Osteoblast and Osteocyte. CRC Press. 1990.

[11] Eisenberg, H. Biological Macromolecules and Polyelectrolytes in Solution. Clarendon Press, Oxford, 1976.

[12] National Institutes of Health. http://www.nih.gov/

[13] National Osteoporosis Foundation. http://www.nof.org/

[14] Shepherd, A.J., *An overview of osteoporosis.* Altern Ther Health Med, 2004. **10**(2): p. 26-33; quiz 34, 92.

[15] Bell, N.H., *Advances in the treatment of osteoporosis.* Curr Drug Targets Immune Endocr Metabol Disord, 2001. **1**(1): p. 93-102.

[16] Epstein, S., *The roles of bone mineral density, bone turnover, and other properties in reducing fracture risk during antiresorptive therapy.* Mayo Clin Proc, 2005. **80**(3): p. 379-88.

[17] Bouxsein, M.L., *Mechanisms of osteoporosis therapy: a bone strength perspective.* Clin Cornerstone, 2003. **Suppl 2**: p. S13-21.
[18] Prestwood, K.M. and L.G. Raisz, *Prevention and treatment of osteoporosis.* Clin Cornerstone, 2002. **4**(6): p. 31-41.
[19] Qin, L., L.J. Raggatt, and N.C. Partridge, *Parathyroid hormone: a double-edged sword for bone metabolism.* Trends Endocrinol Metab, 2004. **15**(2): p. 60-5.
[20] Garrett, I.R. and G.R. Mundy, *The role of statins as potential targets for bone formation.* Arthritis Res, 2002. **4**(4): p. 237-40.
[21] Cowles EA, et al., *Mineralization and the Expression of Matrix Proteins During in vivo Bone Development.* Calcif Tis Int, 1998. **62**(1): p. 74-82.
[22] Holden JL., et al., *Age and Temperature Related Changes to the Ultrastructure and Composition of Human Bone Mineral.* J Bone Miner Res, 1995. **10**(9): p. 1400-1409.
[23] Nagahata, M., et al., *The response of normal human osteoblasts to anionic polysaccharide polyelectrolyte complexes.* Biomaterials, 2005. **26**(25): p. 5138-44.
[24] Tryoen-Toth, P., et al., *Viability, adhesion, and bone phenotype of osteoblast-like cells on polyelectrolyte multilayer films.* J Biomed Mater Res, 2002. **60**(4): p. 657-67.
[25] Torricelli, P., et al., *Human osteopenic bone-derived osteoblasts: essential amino acids treatment effects.* Artif Cells Blood Substit Immobil Biotechnol, 2003. **31**(1): p. 35-46.
[26] Torricelli, P., et al., *L-arginine and L-lysine stimulation on cultured human osteoblasts.* Biomed Pharmacother, 2002. **56**(10): p. 492-7.
[27] Fini, M., et al., *Effect of L-lysine and L-arginine on primary osteoblast cultures from normal and osteopenic rats.* Biomed Pharmacother, 2001. **55**(4): p. 213-20.
[28] Bigi, A., et al., *Interaction of acidic poly-amino acids with octacalcium phosphate.* J Inorg Biochem, 2003. **95**(4): p. 291-6.
[29] Torricelli, P., et al., *Bone tissue cultures: an in vitro model for the evaluation of bone defect healing after L-arginine and L-lysine administration.* Artif Cells Blood Substit Immobil Biotechnol, 2001.